

A STUDY ON THE
FIRST-PASSAGE RELIABILITY PROBLEM
AND ITS APPLICATION IN
EARTHQUAKE ENGINEERING

A Thesis

Submitted to the Graduate Faculty of the
Louisiana State University and
Agricultural and Mechanical College
in partial fulfillment of the
requirements for the degree of
Master of Science in Civil Engineering

in

The Department of Civil and Environmental Engineering

by
Sara Ghazizadeh
B.S., Shiraz University, Iran, 2008
December, 2011

This work is sincerely dedicated to my parents.

ACKNOWLEDGMENTS

I would like to express my sincere appreciation to my advisor, Dr. Michele Barbato for his enormous help and guidance through the process of learning and performing this research. Undoubtedly, this work would have not been possible without such help. I would also like to thank my graduate committee members, Dr. Ayman Okeil and Dr. Steve Cai, for their support and technical guidance in the development of this thesis. My special appreciation goes to Dr. Enrico Tubaldi for all his great help in writing the codes and preparing the journal papers.

My genuine gratitude goes to my mother for all her love, support and prayers over the years and for always encouraging me in my studies. I would also like to thank my cousins and awesome friends for bearing with me through all the difficulties and their love and support when I needed them the most.

I would also like to thank the funding sources of this research (1) the Louisiana Board of Regents (LA BoR) through the Pilot Funding for New Research (Pfund) Program of the National Science Foundation (NSF) Experimental Program to Stimulate Competitive Research (EPSCoR) under Award No. LEQSF(2011)-PFUND-225; (2) the LA BoR through the Louisiana Board of Regents Research and Development Program, Research Competitiveness (RCS) subprogram, under Award No. LESQSF(2010-13)-RD-A-01; (3) the Longwell's Family Foundation through the Fund for Innovation in Engineering Research (FIER) Program; and (4) the LSU Council on Research through the 2009-2010 Faculty Research Grant Program.

TABLE OF CONTENTS

ACKNOWLEDGMENTS	iii
LIST OF TABLES	viii
LIST OF FIGURES	xii
ABSTRACT	xv
1 INTRODUCTION	1
1.1 Motivation	1
1.2 Stochastic Dynamic Analysis of Linear Systems.....	2
1.2.1 Statistical Moment and Covariance Functions of Stochastic Processes	2
1.2.2 Stationarity and Nonstationarity of Stochastic Processes.....	3
1.2.3 Modal Analysis	5
1.2.3.1 Real-valued (Classical) Modal Analysis	7
1.2.3.2 Complex-valued (Non-classical) Modal Analysis.....	7
1.2.4 Spectral Characteristics of Linear Oscillators Subjected to Random Processes.....	10
1.2.4.1 Geometric Spectral Characteristics of Stationary Processes	10
1.2.4.2 Geometric Spectral Characteristics of Nonstationary Processes	11
1.2.4.3 Non-geometric Spectral Characteristics of Real-valued Nonstationary Processes	12
1.2.4.4 Non-geometric Spectral Characteristics of Complex-valued Nonstationary Processes	14
1.2.4.5 Use of Modal Analysis in Seismic Engineering.....	17
1.2.5 First-passage Reliability Problem.....	18
1.2.5.1 Poisson's Approximation for FFPF	20
1.2.5.2 Vanmarcke's Approximations for FFPF	21
1.2.5.3 Monte Carlo Simulation for FFPF.....	22
1.2.5.4 ISEE Method for FFPF.....	22
1.3 Objectives and Organization of the Thesis	23
2 NEW ANALYTICAL APPROXIMATION OF THE FFPF FOR LINEAR SDOF SYSTEMS	25
2.1 Introduction and Previous Work	25
2.2 Hazard Function for Linear SDOF Systems Subjected to WN Excitation from At-rest Initial Conditions.....	26
2.3 Modifications of the Hazard Function Needed to Account for Time-modulation and Non-white Spectra	32
2.4 Parametric Study to Evaluate the Accuracy of the Existing and the Newly Proposed Analytical Approximations.....	34
2.4.1 Input Excitation Models.....	35
2.4.2 Results for Linear SDOF Systems Subjected to WN Excitation from At-rest Initial Conditions.....	36
2.4.3 Results for Linear SDOF Systems Subjected to WN Excitation Modulated in Time by a Shinozuka-Sato Function.....	39

2.4.4	Results for Linear SDOF Systems Subjected to KT Excitation from At-rest Initial Conditions	41
2.4.5	Results for Linear SDOF Systems Subjected to KT Excitation Modulated in Time by a Shinozuka-Sato Function	44
2.5	FPPF Dependency on Normalized Time.....	47
2.6	Conclusions	49
3	FPPF FOR LINEAR MDOF OSCILLATORS	51
3.1	Introduction	51
3.2	Use of Modal Truncation in FPPF of Linear MDOF Oscillators.....	51
3.2.1	Response Variance Computed Using Real-valued Modal Analysis.....	51
3.2.2	Response Variance Computed Using Complex-valued Modal Analysis	52
3.3	Extension of the Newly Proposed Analytical Approximation to MDOF Systems	52
3.4	Application Examples	54
3.4.1	Multi-story Shear-type Buildings	54
3.4.1.1	Input Excitation Models	55
3.4.1.2	Stochastic Dynamic Analysis Results	56
3.4.1.2.1	Two-story Shear-type Building	58
3.4.1.2.2	Three-story Shear-type Building	60
3.4.1.2.3	Eight-story Shear-type Building.....	61
3.4.1.2.4	20-story Shear-type Building.....	64
3.4.1.3	Discussion of the Results.....	64
3.4.1.3.1	Displacement and Velocity Variances.....	64
3.4.1.3.2	Mean Out-crossing Rate and Hazard Functions.....	65
3.4.1.3.3	Time-variant FPPF	68
3.4.1.3.4	Accuracy of the Analytical Approximations	69
3.4.2	Welded Steel 13-Story Building.....	70
3.4.2.1	Analysis Results	71
3.4.2.2	Stochastic Dynamic Analysis Results	73
3.4.2.2.1	Displacement and Velocity Variances.....	74
3.4.2.2.2	Mean out-crossing Rate and Hazard Function	74
3.4.2.2.3	Time-variant FPPF	77
3.4.2.2.4	Accuracy of the Analytical Approximations	77
3.4.3	Pounding of Adjacent Buildings.....	78
3.4.3.1	Computation of the Pounding Probability.....	79
3.4.3.2	Description of the Input Excitation and FE Model.....	81
3.4.3.3	Analysis Results	81
3.5	Conclusions	83
4	CONCLUSIONS AND RECOMMENDATIONS FOR FUTURE WORK.....	86
	REFERENCES	89
	APPENDIX A : CALCULATION OF HAZARD FUNCTION VALUES FROM ISEE.....	91

APPENDIX B : PROPOSED HAZARD FUNCTIONS FOR FPDF OF SDOF SYSTEMS SUBJECTED TO WN EXCITATION FROM AT-REST INITIAL CONDITIONS	94
B.1 Proposed #1	94
B.2 Proposed #2	95
B.3 Proposed #3	96
B.4 Proposed #4	98
B.5 Proposed #5	100
B.6 Proposed #6	101

APPENDIX C : PARAMETRIC STUDY RESULTS OF LINEAR SDOF SYSTEMS SUBJECTED TO WN EXCITATION FROM AT-REST INITIAL CONDITIONS	104
C.1 Proposed #1	104
C.2 Proposed #3	107
C.3 Proposed #4	110
C.4 Proposed #5	113
C.5 Proposed #6 (New)	116

APPENDIX D : PARAMETRIC STUDY RESULTS OF LINEAR SDOF SYSTEMS SUBJECTED TO TIME-MODULATED WHITE OR COLORED NOISE EXCITATIONS ..	119
D.1 Proposed #5	119
D.1.1 White Noise and Shinozuka-Sato Time-modulating Function, $T = 1.0s$	119
D.1.2 Kanai-Tajimi and Unit-step Time-modulating Function, $T = 0.1s$	122
D.1.3 Kanai-Tajimi and Unit-step Time-modulating Function, $T = 0.5s$	125
D.1.4 Kanai-Tajimi and Unit-step Time-modulating Function, $T = 1.0s$	128
D.1.5 Kanai-Tajimi and Shinozuka-Sato Time-modulating Function, $T = 0.1s$	131
D.1.6 Kanai-Tajimi and Shinozuka-Sato Time-modulating Function, $T = 0.5s$	134
D.1.7 Kanai-Tajimi and Shinozuka-Sato Time-modulating Function, $T = 1.0s$	137
D.2 Proposed #6- Without the Proposed Modifications	140
D.2.1 White Noise and Shinozuka-Sato Time-modulating Function, $T = 1.0s$	140
D.2.2 Kanai-Tajimi and Unit-step Time-modulating Function, $T = 0.1 s$	143
D.2.3 Kanai-Tajimi and Unit-step Time-modulating Function, $T = 0.5s$	146
D.2.4 Kanai-Tajimi and Unit-step Time-modulating Function, $T = 1.0s$	149
D.2.5 Kanai-Tajimi and Shinozuka-Sato Time-modulating Function, $T = 0.1s$	152
D.2.6 Kanai-Tajimi and Shinozuka-Sato Time-modulating Function, $T = 0.5s$	155
D.2.7 Kanai-Tajimi and Shinozuka-Sato Time-modulating Function, $T = 1.0s$	158
D.3 Comparison of the Proposed #5 and #6 NM	160
D.4 Newly Proposed Approximation	162
D.4.1 White noise and Shinozuka-Sato Time-modulating Function, $T = 1.0s$	162
D.4.2 Kanai-Tajimi and Unit-step Time-modulating Function, $T = 0.1s$	165
D.4.3 Kanai-Tajimi and Unit-step Time-modulating Function, $T = 0.5s$	168
D.4.4 Kanai-Tajimi and Unit-step Time-modulating Function, $T = 1.0s$	171
D.4.5 Kanai-Tajimi and Shinozuka-Sato Time-modulating Function, $T = 0.1s$	174
D.4.6 Kanai-Tajimi and Shinozuka-Sato Time-modulating Function, $T = 0.5s$	177
D.4.7 Kanai-Tajimi and Shinozuka-Sato Time-modulating Function, $T = 1.0s$	180
D.4.8 Summary of the Time-variant FPDF Obtained Using the New Proposed Hazard Function	183

APPENDIX E : INPUT PSD FUNCTIONS OF SHEAR-TYPE BUILDINGS	184
VITA	186

LIST OF TABLES

Table 2.1 - Coefficients of the polynomial representation of $C_{i,\infty}$ ($i=1,2$) given in Eq. (2.4). ..	30
Table 2.2 - Time-variant FPDF ($t_0 = 10$) for linear elastic SDOF systems subjected to WN base excitation from at-rest initial conditions (i.e., with unit step time-modulating function).....	37
Table 2.3 - Time-variant FPDF for linear elastic SDOF systems subjected to WN base excitation from at-rest initial conditions for $\zeta = 5$ and different values of normalized time t_0	38
Table 2.4 - Time-variant FPDF computed at $t = 20$ s for linear elastic SDOF systems with $T = 1.0$ s subjected to WN base excitation time modulated by a Shinozuka-Sato function.	40
Table 2.5 - Time-variant FPDF computed at $t = 1.0$ s for linear elastic SDOF system with $T = 0.1$ s subjected to KT base excitation from at-rest initial conditions.	42
Table 2.6 - Time-variant FPDF computed at $t = 5.0$ s for linear elastic SDOF system with	42
Table 2.7 - Time-variant FPDF computed at $t = 10.0$ s for linear elastic SDOF system with $T = 1.0$ s subjected to KT base excitation from at-rest initial conditions.	43
Table 2.8 - FPDF computed at $t = 20.0$ s for linear elastic SDOF system with $T = 0.1$ s subjected to KT base excitation time modulated by a Shinozuka-Sato function.....	45
Table 2.9 - FPDF computed at $t = 20.0$ s for linear elastic SDOF system with $T = 0.5$ s subjected to KT base excitation time modulated by a Shinozuka-Sato function.....	45
Table 2.10 - FPDF computed at $t = 20.0$ s for linear elastic SDOF system with $T = 1.0$ s subjected to KT base excitation time modulated by a Shinozuka-Sato function.....	46
Table 3.1 - Modeling properties of the shear-type buildings.....	54
Table 3.2- Modal analysis results for shear-type buildings.	57
Table 3.3 -Stochastic dynamic analysis results for the horizontal roof drift response of the two-story building subjected to stationary input.	58
Table 3.4 - Stochastic dynamic analysis results for the horizontal roof drift response of the two-story building subjected to nonstationary input.	59
Table 3.5 - Stochastic dynamic analysis results for the horizontal roof drift response of the three-story building subjected to stationary input.	60
Table 3.6 - Stochastic dynamic analysis results for the horizontal roof drift response of the three-story building subjected to nonstationary input.	61
Table 3.7 - Stochastic dynamic analysis results for the horizontal roof drift response of the eight-story building subjected to stationary input.	62

Table 3.8 - Stochastic dynamic analysis results for the horizontal roof drift response of the eight-story building subjected to nonstationary input.	63
Table 3.9 - Stochastic dynamic analysis results for the horizontal roof drift response of the 20-story building subjected to stationary input.	66
Table 3.10 - Stochastic dynamic analysis results for the horizontal roof drift response of the 20-story building subjected to nonstationary input.	67
Table 3.11 - Comparison of FPDF of different approximations subjected to stationary input.	69
Table 3.12 - Comparison of FPDF of different approximations subjected to nonstationary input.....	70
Table 3.13 - Modal properties of the 13-story building.....	72
Table 3.14 - Stochastic dynamic analysis for the 13-story building.....	75
Table 3.15 - Comparison of the analytical and ISEE estimates of FPDF for the 13-story building.....	78
Table A.1 - Numerical estimation of the hazard function values computed at time $t = 0.5s$ for a linear SDOF system subjected to a WN excitation from at-rest initial conditions ($T = 1.0s$; $\xi = 0.1$; $\zeta = 4$).....	92
Table B.1 - Proposed #1: Coefficients of the polynomial representation of $C(\xi, \zeta)$	94
Table B.2 - Proposed #3: Coefficients of the polynomial representation of $C_{1,\infty}(\xi, \zeta)$ and $C_{2,\infty}(\xi, \zeta)$	98
Table B.3 - Proposed #5: Coefficients of the polynomial fitted to $C_{1,\infty}(\xi, \zeta)$	100
Table C.1 - Proposed #1: Time-variant FPDF ($t_0 = 10$)	104
Table C.2 - Proposed #3: Time-variant FPDF ($t_0 = 10$)	107
Table C.3 - Proposed #4: Time-variant FPDF ($t_0 = 10$)	110
Table C.4 - Proposed #5: Time-variant FPDF ($t_0 = 10$).	113
Table C.5 - New: Time-variant FPDF ($t_0 = 10$).....	116
Table D.1 - Proposed #5: Time-variant FPDF computed at $t = 20s$ for linear elastic SDOF systems with $T = 1.0s$ subjected to WN base excitation time modulated by a Shinozuka-Sato function.	119
Table D.2 - Proposed #5: Time-variant FPDF computed at $t = 1.0s$ for linear elastic SDOF system with $T = 0.1s$ subjected to KT base excitation from at-rest initial conditions....	122

Table D.3 - Proposed #5: Time-variant FFPF computed at $t = 5.0s$ for linear elastic SDOF system with $T = 0.5s$ subjected to KT base excitation from at-rest initial conditions.	125
Table D.4 - Proposed #5: Time-variant FFPF computed at $t = 10.0s$ for linear elastic SDOF system with $T = 1.0s$ subjected to KT base excitation from at-rest initial conditions.	128
Table D.5 - Proposed #5: Time-variant FFPF computed at $t = 20s$ for linear elastic SDOF system with $T = 0.1s$ subjected to KT base excitation time modulated by a Shinozuka-Sato function.	131
Table D.6 - Proposed #5: Time-variant FFPF computed at $t = 20s$ for linear elastic SDOF system with $T = 0.5s$ subjected to KT base excitation time modulated by a Shinozuka-Sato function.	134
Table D.7 - Proposed #5: Time-variant FFPF computed at $t = 20s$ for linear elastic SDOF system with $T = 1.0s$ subjected to KT base excitation time modulated by a Shinozuka-Sato function.	137
Table D.8 - Proposed #6 NM: Time-variant FFPF computed at $t = 20s$ for linear elastic SDOF systems with $T = 1.0s$ subjected to WN base excitation time modulated by a Shinozuka-Sato function.	140
Table D.9 - Proposed #6 NM: Time-variant FFPF computed at $t = 1.0s$ for linear elastic SDOF system with $T = 0.1s$ subjected to KT base excitation from at-rest initial conditions.	143
Table D.10 - Proposed #6 NM: Time-variant FFPF computed at $t = 5.0s$ for linear elastic SDOF system with $T = 0.5s$ subjected to KT base excitation from at-rest initial conditions.	146
Table D.11 - Proposed #6 NM: Time-variant FFPF computed at $t = 10s$ for linear elastic SDOF system with $T = 1.0s$ subjected to KT base excitation from at-rest initial conditions.	149
Table D.12 - Proposed #6 NM: FFPF computed at $t = 20s$ for linear elastic SDOF system with $T = 0.1s$ subjected to KT base excitation time modulated by a Shinozuka-Sato function.	152
Table D.13 - Proposed #6 NM: Time-variant FFPF computed at $t = 20s$ for linear elastic SDOF system with $T = 0.5s$ subjected to KT base excitation time modulated by a Shinozuka-Sato function.	155
Table D.14 - Proposed #6 NM: Time-variant FFPF computed at $t = 20s$ for linear elastic SDOF system with $T = 1.0s$ subjected to KT base excitation time modulated by a Shinozuka-Sato function.	158
Table D.15 - Summary of time-variant FFPF obtained using the Proposed #5 and #6 NM.	161
Table D.16 - New: Time-variant FFPF computed at $t = 20s$ for SDOF systems with $T = 1.0s$ subjected to WN base excitation time modulated by a Shinozuka-Sato function.	162

Table D.17 - New: Time-variant FPDF computed at $t = 1.0s$ for linear elastic SDOF system with $T = 0.1s$ subjected to KT base excitation from at-rest initial conditions.	165
Table D.18 - New: Time-variant FPDF computed at $t = 1.0s$ for linear elastic SDOF system with $T = 0.5s$ subjected to KT base excitation from at-rest initial conditions.	168
Table D.19 - New: Time-variant FPDF computed at $t = 1.0s$ for linear elastic SDOF system with $T = 1.0s$ subjected to KT base excitation from at-rest initial conditions.	171
Table D.20 - New: FPDF computed at $t = 20s$ for linear elastic SDOF system with $T = 0.1s$ subjected to KT base excitation time modulated by a Shinozuka-Sato function.	174
Table D.21 - New: FPDF computed at $t = 20s$ for linear elastic SDOF system with $T = 0.5s$ subjected to KT base excitation time modulated by a Shinozuka-Sato function.	177
Table D.22 - FPDF computed at $t = 20s$ for linear elastic SDOF system with $T = 1.0s$ subjected to KT base excitation time modulated by a Shinozuka-Sato function.	180
Table D.23 - Summary of FPDF obtained using the New Proposed Hazard Function.	183

LIST OF FIGURES

Figure 1.1- Variation of Rayleigh damping ratios with circular frequency.....	6
Figure 2.1 - Computation of $\bar{C}_{1,\infty}$ and $\bar{C}_{2,\infty}$: SDOF system subjected to WN base excitation from at-rest initial conditions ($\bar{\xi} = 0.2$; $\bar{\zeta} = 3$).....	29
Figure 2.2 - Comparison between the interpolation surface $C_{1,\infty}$ (Surf) and values $\bar{C}_{1,\infty}$ obtained through least-square fitting (LSF).....	31
Figure 2.3 - Comparison between the interpolation surface $C_{2,\infty}$ (Surf) and values $\bar{C}_{2,\infty}$ obtained through least-square fitting (LSF).	31
Figure 2.4 - Time-modulating functions: (1) unit-step function, and (2) Shinozuka-Sato with $B_1 = 0.20\text{s}^{-1}$ and $B_2 = 0.25 \text{ s}^{-1}$	34
Figure 2.5 - FPDF for a linear elastic SDOF system subjected to WN base excitation from at-rest initial conditions ($\xi = 0.23$; $\zeta = 4.87$).....	39
Figure 2.6 - FPDF for a linear elastic SDOF system with $T = 1.0\text{s}$ subjected to WN base excitation with Shinozuka-Sato modulating function ($\xi = 0.42$; $\zeta = 3.5$).....	41
Figure 2.7 - FPDF for a linear elastic SDOF system with $T = 0.1\text{s}$ subjected to KT base excitation from at-rest initial conditions ($\xi = 0.035$; $\zeta = 3$).....	43
Figure 2.8 - FPDF for a linear elastic SDOF system with $T = 1.0\text{s}$ subjected to KT base excitation with Shinozuka-Sato modulating function ($\xi = 0.22$; $\zeta = 2.2$).....	46
Figure 2.9 - Comparison of FPDF for linear elastic SDOF with $T = 1.0\text{s}$ and $T = 0.5\text{s}$ subjected to WN base excitation from at-rest initial conditions.....	47
Figure 3.1- Types of PSD functions.	55
Figure 3.2 - Input PSD function for the two-story building.	59
Figure 3.3 - Estimates of the roof displacement variance of the eight-story building obtained using modal truncation (nonstationary input).	64
Figure 3.4 - Estimates of the roof velocity variance of the eight-story building obtained using modal truncation (nonstationary input).	65
Figure 3.5 - Estimates of the roof hazard functions of the eight-story building obtained using modal truncation (nonstationary input).	68
Figure 3.6 - Estimates of the roof FPDF of the eight-story building obtained using modal truncation (nonstationary input).....	69

Figure 3.7 - Frame elevation and member sizes (adapted from [29]).....	71
Figure 3.8- Input PSD function for the 13-story building.	73
Figure 3.9- Estimates of the roof displacement variance of the 13-story building obtained using modal truncation $p = 1, 2, 5$	74
Figure 3.10 - Estimates of the roof velocity variance of the 13-story building obtained using modal truncation $p = 1, 2, 5$	76
Figure 3.11 - Hazard functions for the roof horizontal drift of the 13-story building by including the first two and five modes.....	76
Figure 3.12 - FPDF for the roof horizontal drift of the 13-story building by including the first two and five modes.....	77
Figure 3.13 - Geometric description of the pounding problem between adjacent buildings.....	79
Figure 3.14 - FPDF for two SDOF models of adjacent buildings with $T_A = 1.0s$ and $T_B = 0.5s$	82
Figure 3.15 - FPDF for two SDOF models of adjacent buildings with $T_A = 1.0s$ and $T_B = 0.9s$	83
Figure A.1- Dependency of the hazard function numerical estimates on the time interval Δt computed at time $t = 0.5s$ for a linear SDOF system subjected to a WN excitation from at-rest initial conditions ($T = 1.0s$; $\xi = 0.1$; $\zeta = 4$).....	93
Figure B.1 - Proposed #1: Fitted surface for $C(\xi, \zeta)$ for Proposed#1.....	95
Figure B.2 - Proposed #2: Plot of sum of squared residuals of the error vs. C_1 and C_2 for linear SDOF system with $T = 1.0s$; $\xi = 0.1$; $\zeta = 4$	96
Figure B.3 - Proposed #3: (a) FPDF for the linear SDOF system with $T = 0.1s$; $\xi = 0.05$; $\zeta = 2$ (b) $C(\xi, \zeta, t)$ plotted as a function of the normalized time for the same SDOF system.....	97
Figure B.4 - Proposed #3: FPDF for a linear SDOF system with $T = 0.1s$ subjected to WN base excitation from at-rest initial conditions ($\xi = 0.05$; $\zeta = 2$).	98
Figure B.5 - Proposed #4: (a) FPDF for the linear SDOF system with $T = 0.1s$; $\xi = 0.05$; $\zeta = 2$ (b) $C(\xi, \zeta, t)$ plotted as a function of the normalized time for the same SDOF system.....	99
Figure B.6 - Proposed #4: FPDF for a linear SDOF system with $T = 0.1s$ subjected to WN base excitation from at-rest initial conditions ($\xi = 0.05$; $\zeta = 2$).	100

Figure B.7 - Proposed #5: FPDF obtained through least-square fitting of the ISEE results and the corresponding P and VM approximations for linear SDOF system ($\xi = 0.2 ; \zeta = 3$).	101
Figure B.8 - Proposed #5: Comparison between the interpolation surface $C_{1,\infty}$ (Surf) and values $\bar{C}_{1,\infty}$ obtained through least-square fitting (LSF) versus damping ratio.	102
Figure B.9 - Proposed #5: Comparison between the interpolation surface $C_{1,\infty}$ (Surf) and values $\bar{C}_{1,\infty}$ obtained through least-square fitting (LSF) versus the normalized threshold level.	102
Figure B.10 - Proposed #5: FPDF for a linear SDOF system with $T = 0.1s$ subjected to WN base excitation from at-rest initial conditions ($\xi = 0.05, \zeta = 2$).	103
Figure B.11 - Proposed #5: FPDF for a linear SDOF system with $T = 0.1s$ subjected to WN base excitation from at-rest initial conditions ($\xi = 0.05, \zeta = 4.5$).	103
Figure E.1-Input PSD function for the three-story building.	184
Figure E.2- Input PSD function for the eight-story building.	184
Figure E.3- Input PSD function for the 20-story building.	185

ABSTRACT

The research presented in this thesis focuses on analytical approximations for the time-variant first-passage failure probability (FPFP) of linear elastic models of structural systems subjected to stochastic excitations. The FPFP is defined as the probability that a response quantity of an engineering system subjected to a dynamic stochastic loading outcrosses a specified threshold within a given exposure time. The FPFP is an important and useful quantity for many structural engineering applications.

The classical first-passage reliability problem is studied for linear elastic single-degree-of-freedom (SDOF) and multi-degrees-of-freedom (MDOF) systems subjected to stationary and nonstationary Gaussian excitations. The absolute and relative accuracy of several analytical approximations available in the literature (i.e., the Poisson's (P), classical Vanmarcke's (cVM), and modified Vanmarcke's (mVM) approximations) are studied through an extensive parametric study for SDOF systems. In addition, a new analytical approximation for the FPFP of linear SDOF systems is developed. The new proposed approximation is verified by comparing its analytical estimates of the failure probability with the corresponding results obtained using existing analytical approximations and the importance sampling using elementary events (ISEE) method for a wide range of oscillator properties and different types of input excitations. It is found that the newly developed analytical approximation provides estimates of the time-variant FPFP of SDOF systems that are significantly more accurate than the estimates obtained using the P, cVM, and mVM approximations.

Real-valued and complex-valued modal analysis with modal truncation is used to study the time-variant FPFP of MDOF subjected to stationary and nonstationary stochastic excitations. The absolute and relative accuracy of the P, cVM, and mVM approximations as well as of the newly developed approximation are studied for a select number of case studies. It is found that the

newly proposed analytical approximation cannot be directly extended to the computation of the FPDF of MDOF systems, while the mVM approximation appears to be more accurate than the other existing analytical approximations.

1 INTRODUCTION

1.1 MOTIVATION

Dynamic engineering systems are characterized by significant uncertainty in their properties and randomness in their loading environment. Stochastic dynamics is a well-developed and challenging research subject that continues to draw notable interest in many engineering areas. A classical result sought in stochastic dynamics is the failure probability for the first-passage reliability problem, commonly referred to as first-passage failure probability (FPFP). The FPFP is defined as the probability that a response quantity of an engineering system subjected to a dynamic stochastic loading outcrosses a specified threshold within a given exposure time. The FPFP is an important and useful quantity for many structural engineering applications.

Many analytical and numerical studies have been devoted to the computation of the FPFP [1-6]. However, to date, no exact closed-form solution of the FPFP is available even for the simplest case, i.e., a single-degree-of-freedom (SDOF) linear oscillator subjected to Gaussian white noise (WN) excitation with a deterministic failure threshold [3, 7, 8].

Analytical approximations, such as the Poisson (P), classical Vanmarcke (cVM), and modified Vanmarcke (mVM) approximations, are commonly used for the estimation of the FPFP. Although these analytical approximations generally provide a good compromise between accuracy and computational effort, they also present some deficiencies [4, 5]. In addition, very little information is available on the accuracy of these analytical approximations for the case of nonstationary processes [8]. Therefore, improvements of the analytical approximations of the FPFP for a wide range of different conditions commonly encountered in structural engineering problems are needed.

1.2 STOCHASTIC DYNAMIC ANALYSIS OF LINEAR SYSTEMS

The response of a structural system subjected to a ground motion excitation is, in general, an uncertain quantity, since there is uncertainty in the input produced by the seismic event and in the properties of the structure. In order to model this uncertainty, the concept of stochastic process is very useful. In particular, the dynamic response of the structure at one instant of time t can be modeled as a random variable, while the uncertain history of the response over a range of time values can be modeled as a stochastic process [9]. Thus, a stochastic process is a family of random variables and can be presented in terms of its possible time histories. Each time history represents a single observation of the random process.

In order to have a complete description of a stochastic process, the joint probability distribution for every set of the random variables at any different value of time has to be known. This level of information is practically never available for the response of structural systems subjected to uncertain excitations. Thus, simpler descriptions of a stochastic process (requiring less information) are usually adopted, e.g., statistical moments and covariance functions.

1.2.1 Statistical Moment and Covariance Functions of Stochastic Processes

The statistical moment functions of a stochastic process are functions of time defined so that their value at a given instant of time is equal to the corresponding statistical moment of the random variable at that instant of time [9]. Knowledge of all statistical moment functions of any order corresponds to a complete description of the stochastic process. However, usually only the statistical moments of lower order are known. In particular, the mean function of a stochastic process is given as [9]:

$$\mu_X(t) \equiv E[X(t)] = \int_{-\infty}^{\infty} u \cdot p_{X(t)}(u) \cdot du \quad (1.1)$$

where $p_{X(t)}(u)$ = probability density function (PDF) of the random variable defined at time t and belonging to the family of random variables constituting the random process $X(t)$, and $E[...]$ = expectation value operator.

The cross-correlation function of processes $X(t)$ and $Y(t)$ is given as:

$$\phi_{XY}(t, s) \equiv E[X(t) \cdot Y(s)] = \int_{-\infty}^{\infty} \int_{-\infty}^{\infty} u \cdot v \cdot p_{X(t)Y(s)}(u, v) \cdot du \cdot dv \quad (1.2)$$

where $p_{X(t)Y(s)}(u, v)$ = joint PDF of random variables $X(u)$ and $Y(v)$.

The cross-covariance function between processes $X(t)$ and $Y(t)$ is defined as:

$$K_{XY}(t, s) \equiv E([X(t) - \mu_X(t)] \cdot [Y(s) - \mu_Y(s)]) \quad (1.3)$$

It is noticed here that the auto-correlation and the auto-covariance of process $X(t)$ can be obtained as special cases of the cross-correlation and cross-covariance functions given in Eqs. (1.2) and (1.3), respectively, by substituting $Y(s)$ with $X(s)$.

1.2.2 Stationarity and Nonstationarity of Stochastic Processes

A random process is stationary in a strict sense if its complete probability description is independent of a shift of the parametric origin. Lower order stationarity properties can also be defined. The simplest type of stationarity is mean value stationarity, for which $\mu_X(t) = \mu_X$. Second moment stationarity is obtained when, in addition to mean value stationarity, the auto-correlation (and auto-covariance) function is invariant under a time shift. By defining the time shift as $\tau = t - s$, the auto-covariance function can be written as:

$$R_{XX}(\tau) = \phi_{XX}(t + \tau, t) \equiv E[X(t + \tau) \cdot X(t)] \quad (1.4)$$

Similar relationships can be obtained for higher order moments, i.e., j -th order stationarity implies that the j -th moment function is invariant under a time shift.

In this study, all the processes considered are assumed to be zero-mean Gaussian processes. The PDFs of the family of Gaussian variables constituting the stochastic process at hand are symmetric about their mean value and as a result, all the odd central moments are zero and the even moments can be written as functions of the variance alone [9]. Therefore, processes that are second moment stationary are also stationary in a strict sense.

The power spectral density (PSD) function of a stationary process $X_S(t)$ is defined as the distribution of its mean square value with frequency and is given by the Fourier transform of the auto-covariance function:

$$G_{X_S X_S}(\omega) = \frac{1}{2\pi} \cdot \int_{-\infty}^{\infty} R_{X_S X_S}(\tau) \cdot e^{-i\omega\tau} \cdot d\tau \quad (1.5)$$

This implies that the inverse Fourier transform of the PSD function gives the auto-covariance function, i.e.:

$$R_{X_S X_S}(\tau) = \int_{-\infty}^{\infty} G_{X_S X_S}(\omega) \cdot e^{i\omega\tau} \cdot d\omega \quad (1.6)$$

While the PSD is the only spectrum used in the literature to describe stationary random processes, for nonstationary random processes several different descriptions are possible [10, 11]. Among the different spectra developed for nonstationary random processes, the Priestley's evolutionary power spectral density (EPSD) function is the most commonly used and is considered in this study [12].

The EPSD function of a nonstationary random process $X(t)$ is defined as [13]:

$$G_{XX}(\omega, t) = |A(\omega, t)|^2 \cdot G_{X_s X_s}(\omega) \quad (1.7)$$

where $A(\omega, t)$ = complex-valued deterministic amplitude modulating function. For the process $X(t)$ to be real, the complex modulating function must satisfy the condition $A(-\omega, t) = A^*(\omega, t)$, where the superscript $(\dots)^*$ denotes the complex-conjugate operator [13].

1.2.3 Modal Analysis

The equation of motion for a linear multi-degrees-of-freedom (MDOF) system with n degrees-of-freedom (DOFs) can be expressed as:

$$\mathbf{m} \cdot \ddot{\mathbf{u}}(t) + \mathbf{c} \cdot \dot{\mathbf{u}}(t) + \mathbf{k} \cdot \mathbf{u}(t) = \mathbf{p}(t) \quad (1.8)$$

where \mathbf{m} , \mathbf{c} , and \mathbf{k} = mass, damping, and the stiffness matrices, respectively; $\mathbf{u}(t)$, $\dot{\mathbf{u}}(t)$, and $\ddot{\mathbf{u}}(t)$ = nodal displacement, velocity, and the acceleration vectors, respectively; and $\mathbf{p}(t) = \mathbf{p} \cdot F(t)$, where \mathbf{p} = distribution vector of length n , and $F(t)$ = scalar function describing the time-history of the external loading modeled as random process. This matrix equation is constituted by a set of n coupled ordinary differential equations. The modal analysis method can be applied to transform this matrix equation into a set of uncoupled ordinary differential equations in order to solve for the structural response quantities. Natural frequencies and modes of vibration of the system are the solution of the eigenvalue problem defined by $\det[\mathbf{k} - \omega_i^2 \cdot \mathbf{m}] = 0$ [14]. Solving this equation gives the n natural frequencies, ω_i , and the corresponding n independent eigenvectors, ϕ_i (also known as natural mode shapes of vibration), with $i = 1, 2, \dots, n$. There are two general modal analysis methods: (1) real-valued (classical) modal analysis, which is used for systems with classical damping (i.e., damping matrix

proportional to mass and stiffness matrices); and (2) complex-valued (non-classical) modal analysis for non-classically damped systems.

Classical damping is an appropriate way to idealize the damping in buildings with similar structural systems and structural materials. A classical damping matrix can be constructed using the Rayleigh damping model, which is defined as follows:

$$\mathbf{c} = a_0 \cdot \mathbf{m} + a_1 \cdot \mathbf{k} \quad (1.9)$$

The damping ratio ξ_k for the k -th mode of vibration of a given system characterized by Rayleigh damping is:

$$\xi_k = \frac{a_0}{2} \cdot \frac{1}{\omega_k} + \frac{a_1}{2} \cdot \omega_k \quad (1.10)$$

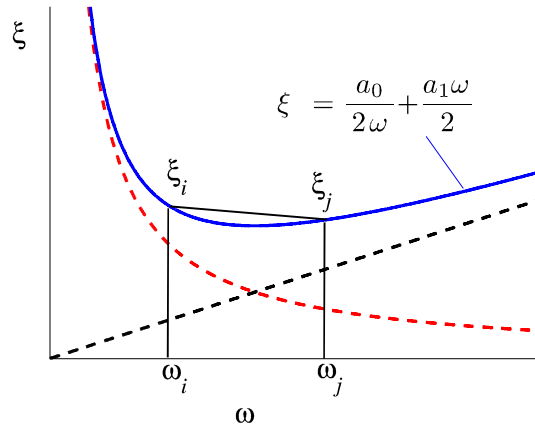


Figure 1.1- Variation of Rayleigh damping ratios with circular frequency.

Once the damping ratios ξ_i and ξ_j for the i -th and j -th modes are specified, the coefficients a_0 and a_1 are obtained as:

$$a_0 = \frac{2\omega_i \cdot \omega_j \cdot (\omega_j \cdot \xi_i - \omega_i \cdot \xi_j)}{(\omega_j^2 - \omega_i^2)} \quad a_1 = \frac{2\omega_j \cdot \xi_j - 2\omega_i \cdot \xi_i}{(\omega_j^2 - \omega_i^2)} \quad (1.11)$$

1.2.3.1 Real-valued (Classical) Modal Analysis

The displacement vector $\mathbf{u}(t)$ of a classically-damped MDOF system can be written in terms of modal contributions as:

$$\mathbf{u}(t) = \sum_{r=1}^n \boldsymbol{\phi}_r \cdot q_r(t) = \boldsymbol{\Phi} \cdot \mathbf{q}(t) \quad (1.12)$$

in which $\boldsymbol{\phi}_r$ = natural mode shape vector corresponding to the r -th DOF, $q_r(t)$ = scalar function called r -th modal coordinate, $\mathbf{q}(t) = [q_1(t), q_2(t), \dots, q_n(t)]^T$, and $\boldsymbol{\Phi}$ = modal matrix given as:

$$\boldsymbol{\Phi} = [\boldsymbol{\phi}_1, \boldsymbol{\phi}_2, \dots, \boldsymbol{\phi}_n] = \begin{bmatrix} \phi_{11} & \phi_{12} & \dots & \phi_{1n} \\ \phi_{21} & \phi_{22} & \vdots & \phi_{2n} \\ \vdots & \vdots & \ddots & \vdots \\ \phi_{n1} & \phi_{n2} & \dots & \phi_{nn} \end{bmatrix} \quad (1.13)$$

Using Eq. (1.12), the matrix equation of motion (Eq.(1.8)) can be written as follows:

$$\mathbf{M} \cdot \ddot{\mathbf{q}}(t) + \mathbf{C} \cdot \dot{\mathbf{q}}(t) + \mathbf{K} \cdot \mathbf{q}(t) = \mathbf{P}(t) \quad (1.14)$$

where

$$\mathbf{M} = \boldsymbol{\Phi}^T \cdot \mathbf{m} \cdot \boldsymbol{\Phi} ; \quad \mathbf{K} = \boldsymbol{\Phi}^T \cdot \mathbf{k} \cdot \boldsymbol{\Phi} ; \quad \mathbf{C} = \boldsymbol{\Phi}^T \cdot \mathbf{c} \cdot \boldsymbol{\Phi} ; \quad \mathbf{P}(t) = \boldsymbol{\Phi}^T \cdot \mathbf{p}(t) \quad (1.15)$$

Under the hypothesis of classical damping, matrices \mathbf{M} , \mathbf{K} , and \mathbf{C} are diagonal and, thus, the modal equations of motion (1.14) are uncoupled.

1.2.3.2 Complex-valued (Non-classical) Modal Analysis

Complex-valued modal analysis is particularly used for non-classically damped systems, for which the damping matrix is non-diagonal and the modal equations of motion (1.14) are coupled.

Using the state-space approach Eq. (1.8) can be rewritten as [15] :

$$\dot{\mathbf{Z}}(t) = \mathbf{G} \cdot \mathbf{Z}(t) + \tilde{\mathbf{P}} \cdot F(t) \quad (1.16)$$

where:

$$\mathbf{Z}(t) = \begin{bmatrix} \mathbf{u}(t) \\ \dot{\mathbf{u}}(t) \end{bmatrix}_{(2n \times 1)} \quad (1.17)$$

$$\mathbf{G} = \begin{bmatrix} \mathbf{0}_{(n \times n)} & \mathbf{I}_{(n \times n)} \\ (-\mathbf{m}^{-1} \cdot \mathbf{k}) & (-\mathbf{m}^{-1} \cdot \mathbf{c}) \end{bmatrix}_{(2n \times 2n)} \quad (1.18)$$

$$\tilde{\mathbf{P}} = \begin{bmatrix} \mathbf{0}_{(n \times 1)} \\ \mathbf{m}^{-1} \cdot \mathbf{p} \end{bmatrix}_{(2n \times 1)} \quad (1.19)$$

Solving the eigenvalue problem for matrix \mathbf{G} gives a diagonal matrix \mathbf{D} of eigenvalues and a complex modal matrix \mathbf{T} whose columns are the corresponding eigenvectors, so that $\mathbf{G} \cdot \mathbf{T} = \mathbf{T} \cdot \mathbf{D}$. Matrix \mathbf{D} is a diagonal matrix containing the $2n$ complex eigenvalues of the system matrix \mathbf{G} :

$$\mathbf{T}^{-1} \cdot \mathbf{G} \cdot \mathbf{T} = \mathbf{D} = \text{diag}[\lambda_1, \lambda_2, \dots, \lambda_{2n}] \quad (1.20)$$

The complex modal matrix, \mathbf{T} , can be used as an appropriate transformation matrix to decouple the first-order matrix equations. The transformed state vector $\mathbf{V}(t)$ of the complex modal coordinates is introduced as $\mathbf{Z}(t) = \mathbf{T} \cdot \mathbf{V}(t)$.

The complex-valued modal participation factors are defined as:

$$\mathbf{T}^{-1} \cdot \tilde{\mathbf{P}} = [\Gamma_1, \Gamma_2, \dots, \Gamma_{2n}]^T \quad (1.21)$$

in which Γ_i is the i -th modal participation factor. The normalized complex modal equations are obtained as:

$$\dot{S}_i(t) = \lambda_i \cdot S_i(t) + F(t) \quad i = 1, 2, \dots, 2n \quad (1.22)$$

where the normalized complex modal responses, $S_i(t)$, are given as:

$$S_i(t) = \frac{1}{\Gamma_i} \cdot V_i(t) \quad i = 1, 2, \dots, 2n \quad (1.23)$$

For a system with at-rest initial conditions, the normalized modal responses can be obtained by using the Duhamel integral:

$$S_i(t) = \int_0^t e^{\lambda_i(t-\tau)} \cdot F(\tau) \cdot d\tau \quad i = 1, 2, \dots, 2n \quad (1.24)$$

The normalized complex modal responses are given by:

$$S_i(t) = \int_{-\infty}^{\infty} A_{S_i}(\omega, t) \cdot e^{j\omega t} \cdot dZ(\omega) \quad i = 1, 2, \dots, 2n \quad (1.25)$$

where

$$A_{S_i}(\omega, t) = \int_0^t \left\{ e^{\lambda_i(t-\tau)} \cdot A_F(\omega, \tau) \cdot e^{j\omega(t-\tau)} \right\} \cdot d\tau \quad i = 1, 2, \dots, 2n \quad (1.26)$$

Finally, the state vector is obtained as:

$$\mathbf{Z}(t) = \mathbf{T} \cdot \mathbf{V}(t) = \mathbf{T} \cdot \mathbf{\Gamma} \cdot \mathbf{S}(t) = \tilde{\mathbf{T}} \cdot \mathbf{S}(t) \quad (1.27)$$

in which $\mathbf{\Gamma}$ is the diagonal matrix containing the $2n$ modal participation factors, $\tilde{\mathbf{T}} = \mathbf{T} \cdot \mathbf{\Gamma}$ is the effective modal participation matrix, and $\mathbf{S} = [S_1(t), S_2(t), \dots, S_{2n}(t)]^T$ is the normalized complex modal response vector.

It is worth mentioning that all variables involved in the classically-damped analysis are real-valued and the modal equations are second-order differential equations. In contrast, the variables in the non-classically damped analysis are, in general, complex-valued and the modal equations

are first-order differential equations. It has been shown that the complex-valued modal analysis can also be used for classically damped systems, since it provides the same results as the one obtained using real-valued modal analysis [16].

1.2.4 Spectral Characteristics of Linear Oscillators Subjected to Random Processes

Stochastic processes can be described using the so-called spectral characteristics, which are obtained from the properties of the process in the frequency domain.

1.2.4.1 Geometric Spectral Characteristics of Stationary Processes

A real-valued stationary process, $X_S(t)$, has the following spectral decomposition form [15]:

$$X_S(t) = \int_{-\infty}^{\infty} e^{j\omega t} \cdot dZ(\omega) \quad (1.28)$$

in which, t = time, ω = frequency parameter, $j = \sqrt{-1}$, and $dZ(\omega)$ = zero-mean orthogonal increment process defined so that $E[dZ^*(\omega_1) \cdot dZ(\omega_2)] = G_{X_S X_S}(\omega_1) \cdot \delta(\omega_1 - \omega_2) \cdot d\omega_1 \cdot d\omega_2$, where $G_{X_S X_S}(\omega)$ = PSD function of the stationary process $X_S(t)$, and $\delta(\dots)$ = Dirac delta function.

The n -th spectral moment of $G_{X_S X_S}(\omega)$ is given by:

$$\lambda_n = 2 \cdot \int_0^{\infty} \omega^n \cdot G_{X_S X_S}(\omega) \cdot d\omega = \int_{-\infty}^{\infty} |\omega|^n \cdot G_{X_S X_S}(\omega) \cdot d\omega \quad (1.29)$$

where $|\dots|$ = absolute value operator of a real-valued variable (or modulus of a complex-valued variable). Eq. (1.29) utilizes the property that the PSD $G_{X_S X_S}(\omega)$ of a stationary process $X_S(t)$ is an even function of ω .

The spectral moments are used to obtain several useful quantities for reliability analysis. In particular, the variances of the i -th time derivative of process $X_S(t)$, $X_S^{(i)}(t)$ (provided that this i -th time derivative process exists in the mean-square sense), is obtained as:

$$\sigma_{X_S^{(i)}}^2 = \lambda_{2i} \quad (i = 0, 1, \dots) \quad (1.30)$$

the central frequency of process $X_S(t)$, ω_{c, X_S} , is given as:

$$\omega_{c, X_S} = \frac{\lambda_1}{\lambda_0} \quad (1.31)$$

and the bandwidth parameter of process $X_S(t)$, q_{X_S} , is:

$$q_{X_S} = \left(1 - \frac{\lambda_1^2}{\lambda_0 \cdot \lambda_2} \right)^{1/2} \quad (1.32)$$

1.2.4.2 Geometric Spectral Characteristics of Nonstationary Processes

A real-valued nonstationary process $X(t)$ can be decomposed as:

$$X(t) = \int_{-\infty}^{\infty} A_X(\omega, t) \cdot e^{j\omega t} \cdot dZ(\omega) \quad (1.33)$$

An embedded stationary process $X_S(t)$ with PSD function $G_{X_S, X_S}(\omega)$ is associated to the real-valued nonstationary process $X(t)$. The transient spectral moments of an evolutionary process can be obtained in a similar way to the geometric spectral moments of stationary processes, i.e.,

$$\lambda_n(t) = 2 \int_0^{\infty} \omega^n \cdot G_{XX}(\omega, t) \cdot d\omega = \int_{-\infty}^{\infty} |\omega|^n \cdot G_{XX}(\omega, t) \cdot d\omega \quad (1.34)$$

Although there is no theoretical obstacle in applying the geometric definition of spectral characteristics to the nonstationary random processes, they have been proven to present some difficulties in application [4, 13]. In particular, the following major problems exist in using the geometric spectral characteristics for nonstationary stochastic processes:

- (1) the variance of the i -th time derivative of the process $X(t)$ is not equal to the $2i$ -th spectral moment; and
- (2) the i -th nonstationary geometric spectral moment can be divergent even when the variance of the i -th time derivative of the process is finite.

In this last case, the central frequency and bandwidth parameter given in Eqs. (1.31) and (1.32) in terms of geometric spectral moments cannot be computed.

1.2.4.3 Non-geometric Spectral Characteristics of Real-valued Nonstationary Processes

In order to avoid the problems related to the use of nonstationary geometric spectral moments, the so-called non-geometric spectral characteristics (NGSCs) have been introduced. Following Michaelov et al. [13], the NGSCs of process $X(t)$ are defined as:

$$c_{ik}(t) = 2 \cdot (-1)^k \cdot j^{i+k} \cdot \int_0^\infty G_{X^{(i)}X^{(k)}}(\omega, t) \cdot d\omega \quad i, k = 0, 1, \dots \quad (1.35)$$

where $G_{X^{(i)}X^{(k)}}(\omega, t) =$ evolutionary cross-PSD function of the time-derivatives of order i and k of process $X(t)$, i.e.,

$$G_{X^{(i)}X^{(k)}}(\omega, t) = A_{X^{(i)}}^*(\omega, t) \cdot G_{XX}(\omega) \cdot A_{X^{(k)}}(\omega, t) \quad i, k = 0, 1, \dots \quad (1.36)$$

in which $X^{(m)}(t) = d^m X(t) / dt^m$ ($m = i, k$), provided that $X^{(m)}(t)$ exists in the mean-square sense, and the modulating function $A_{X^{(m)}}(\omega, t)$ is obtained recursively [13].

If the process $Y(t)$ is defined as the modulation (with modulating function $A_X(\omega, t)$) of the stationary process $Y_s(t)$ defined as the Hilbert transform of the embedded stationary process $X_s(t)$, then $Y(t)$ is given as:

$$Y(t) = -j \cdot \int_{-\infty}^{\infty} \text{sign}(\omega) \cdot A_X(\omega, t) \cdot e^{j\omega t} \cdot dZ(\omega) \quad (1.37)$$

Thus, the non-geometric spectral characteristic $c_{01}(t)$ is obtained as:

$$c_{01}(t) = c_{10}^*(t) = -2 \cdot j \cdot \int_0^{\infty} G_{XX}(\omega, t) \cdot d\omega = \sigma_{XY}(t) - j \cdot \sigma_{X\dot{X}}(t) \quad (1.38)$$

where $\sigma_{X\dot{X}}(t)$ = cross-covariance of $X(t)$ and $\dot{X}(t)$, and $\sigma_{XY}(t)$ = cross-covariance of $X(t)$ and $\dot{Y}(t)$. Using Eq. (1.35) for NGSCs and Eq. (1.37), the central frequency and the bandwidth parameter are obtained as:

$$\omega_{c,X}(t) = \frac{\text{Re}[c_{01}(t)]}{c_{00}(t)} = \frac{\sigma_{XY}(t)}{\sigma_X^2(t)} \quad (1.39)$$

$$q_X(t) = \left(1 - \frac{(\text{Re}[c_{01}(t)])^2}{c_{00}(t) \cdot c_{11}(t)} \right)^{1/2} = \left(1 - \frac{\sigma_{XY}^2(t)}{\sigma_X^2(t) \cdot \sigma_{\dot{X}}^2(t)} \right)^{1/2} \quad (1.40)$$

where $\text{Re}[\dots]$ = real part of the quantity in square brackets.

The NGSC have been employed in structural reliability applications to compute in closed-form the time-variant central frequency and bandwidth parameter of the response process of SDOF and both classically and non-classically damped MDOF linear elastic systems subjected to white noise Gaussian excitation from at-rest initial conditions [15].

1.2.4.4 Non-geometric Spectral Characteristics of Complex-valued Nonstationary Processes

Barbato and Conte [15] extended the NGSCs for the complex-valued nonstationary (CVNS) random processes. For each CVNS process $X(t)$, two sets of NGSCs are defined as follows:

$$\begin{cases} c_{ik,XX}(t) = \int_{-\infty}^{\infty} G_{X^{(i)}X^{(k)}}(\omega, t) \cdot d\omega = \sigma_{X^{(i)}X^{(k)}}(t) \\ c_{ik,XY}(t) = \int_{-\infty}^{\infty} G_{X^{(i)}Y^{(k)}}(\omega, t) \cdot d\omega = \sigma_{X^{(i)}Y^{(k)}}(t) \end{cases} \quad i, k = 0, 1, \dots \quad (1.41)$$

where $\sigma_{X^{(i)}X^{(k)}}(t)$ = cross-covariance of the random processes $X^{(i)}(t)$ and $X^{(k)}(t)$, and $\sigma_{X^{(i)}Y^{(k)}}(t)$ = cross-covariance of random processes $X^{(i)}(t)$ and $Y^{(k)}(t) = d^k Y(t) / dt^k$. The process $Y(t)$ is defined by Eq. (1.37) and the evolutionary cross-PSD function $G_{X^{(i)}W^{(k)}}(\omega, t)$ ($W = X, Y$ and $i, k = 0, 1, \dots$) is given by:

$$G_{X^{(i)}X^{(k)}}(\omega, t) = A_{X^{(i)}}^*(\omega, t) \cdot G_{X_S X_S}(\omega) \cdot A_{W^{(k)}}(\omega, t); \quad W = X, Y; \quad i = 0, 1, \dots \quad (1.42)$$

where the modulating function is defined as [17]:

$$A_{W^{(i)}}(\omega, t) = e^{-j\omega t} \cdot \frac{\partial^i}{\partial t^i} [A_W(\omega, t) \cdot e^{j\omega t}]; \quad W = X, Y; \quad i = 0, 1, \dots \quad (1.43)$$

These NGSCs are used in the definition of the time-variant central frequency, $\omega_{c,X}(t)$, and bandwidth parameter, $q_X(t)$, of the CVNS process $X(t)$ as:

$$\omega_{c,X}(t) = \frac{c_{01,XY}(t)}{c_{00,XX}(t)} = \frac{\sigma_{XY}(t)}{\sigma_X^2(t)} \quad (1.44)$$

$$q_X(t) = \left(1 - \frac{[c_{01,XY}(t)]^2}{\sigma_X^2(t) \cdot \sigma_X^2(t)} \right)^{1/2} = \left(1 - \frac{\sigma_{XY}^2(t)}{\sigma_X^2(t) \cdot \sigma_X^2(t)} \right)^{1/2} \quad (1.45)$$

It is noted that for the CVNS processes, complex-valued central frequency and bandwidth parameter lose the simple physical interpretation of RVNS processes. If only Gaussian inputs are included (which is the case in this study), only few spectral characteristics are needed to fully describe the response process of linear elastic SDOF and MDOF systems. In particular, if $U_i(t)$ denotes the i -th DOF displacement response of a MDOF linear system subjected to Gaussian excitation, the only spectral characteristics required for reliability applications are:

$$\begin{cases} c_{00,U_i U_i}(t) = \sigma_{U_i}^2(t) \\ c_{11,U_i U_i}(t) = \sigma_{\dot{U}_i}^2(t) \\ c_{01,U_i U_i}(t) = \sigma_{U_i \dot{U}_i}^2(t) \\ c_{01,U_i \dot{Y}_i}(t) = \sigma_{U_i \dot{Y}_i}^2(t) \end{cases} \quad i = 1, 2, \dots, n \quad (1.46)$$

where $\dot{Y}_i(t)$ denotes the first time derivative of the process $Y_i(t)$ which is defined as:

$$Y_i(t) = -j \cdot \int_{-\infty}^{\infty} \text{sign}(\omega) \cdot A_{U_i}(\omega, t) \cdot e^{j\omega t} \cdot dZ(\omega) \quad i = 1, 2, \dots, n \quad (1.47)$$

and $A_{U_i}(\omega, t)$ denotes the time-frequency modulating function of process $U_i(t)$. The process $Y_i(t)$ is the modulation of the Hilbert transform of the stationary process embedded in the process $U_i(t)$.

An auxiliary state vector process can be defined as:

$$\Xi(t) = \begin{bmatrix} Y(t) \\ \dot{Y}(t) \end{bmatrix}_{(2n \times 1)} \quad (1.48)$$

Using the complex-valued modal decomposition, the cross-variance matrices of the response processes and the auxiliary processes can be computed as:

$$E[\mathbf{Z}(t) \cdot \mathbf{Z}^T(t)] = E \begin{bmatrix} \mathbf{U}(t) \cdot \mathbf{U}^T(t) & \mathbf{U}(t) \cdot \dot{\mathbf{U}}^T(t) \\ \dot{\mathbf{U}}(t) \cdot \mathbf{U}^T(t) & \dot{\mathbf{U}}(t) \cdot \dot{\mathbf{U}}^T(t) \end{bmatrix} = \tilde{\mathbf{T}}^* \cdot E[\mathbf{S}^*(t) \cdot \mathbf{S}^T(t)] \cdot \tilde{\mathbf{T}}^T \quad (1.49)$$

$$E[\mathbf{Z}(t) \cdot \boldsymbol{\Xi}^T(t)] = E \begin{bmatrix} \mathbf{U}(t) \cdot \boldsymbol{\Upsilon}(t) & \mathbf{U}(t) \cdot \dot{\boldsymbol{\Upsilon}}^T(t) \\ \dot{\mathbf{U}}(t) \cdot \boldsymbol{\Upsilon}^T(t) & \dot{\mathbf{U}}(t) \cdot \dot{\boldsymbol{\Upsilon}}^T(t) \end{bmatrix} = \tilde{\mathbf{T}}^* \cdot E[\mathbf{S}^*(t) \cdot \boldsymbol{\Sigma}^T(t)] \cdot \tilde{\mathbf{T}}^T \quad (1.50)$$

where the components of the vector process $\boldsymbol{\Sigma} = [\Sigma_1(t), \Sigma_2(t), \dots, \Sigma_{2n}(t)]^T$ are defined as

$$\Sigma_i(t) = -j \cdot \int_{-\infty}^{\infty} \text{sign}(\omega) \cdot A_{S_i}(\omega, t) \cdot e^{j\omega t} \cdot dZ(\omega); \quad i = 1, 2, \dots, 2n. \quad (1.51)$$

Eqs. (1.49) and (1.50) show that all quantities in Eq. (1.46) can be computed using the following spectral characteristics of the complex-valued nonstationary processes [15]:

$$\begin{cases} E[S_i^*(t) \cdot S_m(t)] = \sigma_{S_i S_m}(t) \\ E[S_i^*(t) \cdot \Sigma_m(t)] = \sigma_{S_i \Sigma_m}(t) \end{cases} \quad i, m = 1, 2, \dots, 2n. \quad (1.52)$$

It is noted that Eq. (1.52) allows the computation of the zeroth- to second-order spectral characteristics of the components of any response vector $\mathbf{Q}(t)$ linearly related to the displacement response vector $\mathbf{U}(t)$, i.e., $\mathbf{Q}(t) = \mathbf{B} \cdot \mathbf{U}(t)$, where \mathbf{B} = constant matrix.

The cross-correlation function is given as:

$$\rho_{U_i \dot{U}_i}(t) = \frac{\sigma_{U_i \dot{U}_i}(t)}{\sigma_{U_i}(t) \cdot \sigma_{\dot{U}_i}(t)} \quad (1.53)$$

The bandwidth parameter is also calculated from the non-geometric spectral characteristics as:

$$q_{U_i}(t) = \left(1 - \frac{\sigma_{U_i \dot{U}_i}^2(t)}{\sigma_{U_i}^2(t) \cdot \sigma_{\dot{U}_i}^2(t)} \right)^{1/2} \quad (1.54)$$

where $\sigma_{U_i}(t)$, $\sigma_{\dot{U}_i}(t)$ and $\sigma_{U_i \dot{U}_i}(t)$ are calculated using Eq. (1.46).

1.2.4.5 Use of Modal Analysis in Seismic Engineering

For design purposes, it is often sufficient to estimate the maximum value of some structural response quantities under the effects of ground motion excitation. Modal analysis can be efficiently used for this purpose in combination with modal truncation. Modal truncation consists in approximating the structural response by using only a limited number of the modes of the MDOF structural system under consideration. Modal combination rules (e.g., the square-root-of-the-sum-of-the-squares (SRSS) and the complete quadratic combination (CQC) rules [18]) can be then applied to estimate the maxima of the response quantities of interest.

The major advantage of the modal truncation method is that the size of the problem can be drastically reduced without compromising the accuracy of the results. Larger amount of energy is required to excite the higher modes (with higher modal frequencies) and, in general, the energy contents of the seismic excitation at higher frequencies are low [16]. As a result, higher modes contribute less to the response values. Modal truncation is performed by including only the contribution of the first few modes for which sufficiently accurate results are provided. In classical modal analysis, only the contributions of the first p modes ($p < n$, $n =$ number of DOFs) are considered. The equation of motion is then reduced to p differential equations. The response of the structure in the classical modal analysis is obtained by superposing the modal contributions up to the p -th mode as:

$$\mathbf{u}(t) \approx \sum_{r=1}^p \boldsymbol{\phi}_r \cdot q_r(t) = \boldsymbol{\Phi}_{(p)} \cdot \mathbf{q}_{(p)}(t) \quad (1.55)$$

in which $\boldsymbol{\Phi}_{(p)}$ is extracted from the modal matrix $\boldsymbol{\Phi}$ (Eq.(1.13)) and only includes the first p modal vectors (eigenvectors), and $\mathbf{q}_{(p)}(t) = [q_1(t), q_2(t), \dots, q_p(t)]^T$.

In the complex-valued modal analysis using the state-space approach, modal truncation is applied in similar manner. The state vector for the first p modes ($p < n$) is given as:

$$\mathbf{Z}(t) \approx \tilde{\mathbf{T}}_{2n \times 2p} \cdot \mathbf{S}_{2p \times 1}(t) \quad (1.56)$$

in which $\tilde{\mathbf{T}}_{2n \times 2p} = \mathbf{T}_{2n \times 2p} \cdot \mathbf{\Gamma}_{2p \times 2p}$, $\mathbf{T}_{2n \times 2p}$ = complex modal matrix including only the first p vectors and the $n+1$ to $n+p$ vectors, $\mathbf{\Gamma}_{2p \times 2p} = \text{diag}[\Gamma_1, \Gamma_2, \dots, \Gamma_p, \Gamma_{n+1}, \Gamma_{n+2}, \dots, \Gamma_{n+p}]$, and $\mathbf{S}_{2p \times 1}(t) = [S_1(t), S_2(t), \dots, S_p(t), S_{n+1}(t), S_{n+2}(t), \dots, S_{n+p}(t)]^T$.

1.2.5 First-passage Reliability Problem

The classical first-passage reliability problem consists in computing the probability that a specific response quantity of an engineering system subjected to dynamic stochastic loading outcrosses a given threshold level within a given exposure time. In this study, the failure probability for the first-passage reliability problem is called the first-passage failure probability (FPFP).

The first-passage reliability problem can be defined as the reliability of a system for a defined limit state function, $g[X(t)]$, in which $X(t)$ is the response vector of the system. The probability of failure in terms of limit state crossing is given by:

$$P_{f,|X|} = P[g[X(t)] \leq 0] \quad 0 \leq t \leq T \quad (1.57)$$

where T = duration of the input motion and $g[X(t)] = x_{\text{lim}} - |X(t)|$. This failure probability can also be presented in forms of the threshold x_{lim} crossing (double-barrier) as:

$$P_{f,|X|} = P[|X(t)| > x_{\text{lim}}] \quad 0 \leq t \leq T \quad (1.58)$$

Two types of barriers are considered in this study: (1) single barrier: $X(t) = x_{lim}$ or $X(t) = -x_{lim}$ and (2) symmetric double barrier that consists of a pair of lines, $X(t) = x_{lim}$ and $X(t) = -x_{lim}$.

The FPDF depends, in a complicated manner, on the characteristics of the dynamic system, initial conditions, input excitation and the threshold value. It has been shown that the early portion of the first-crossing density highly depends on the initial conditions and the dependence decreases exponentially as T increases [19].

The time-variant FPDF, $P_{f,|X|}$, corresponding to the out-crossing of a failure threshold level, x_{lim} , by the absolute value of the random process $X(t)$ (symmetric double-barrier problem), can be written in the following form [8]:

$$P_{f,|X|}(x_{lim}, t) = 1 - P[|X(t=0)| < x_{lim}] \cdot \exp\left\{-\int_0^t h_{|X|}(x_{lim}, \tau) \cdot d\tau\right\} \quad (1.59)$$

where $t = \text{time}$, $P[|X(t=0)| < x_{lim}] = \text{probability that the systems starts from the safe region at time } t=0$, and $h_{|X|}(x_{lim}, t) = \text{time-variant hazard function for the symmetric double-barrier problem}$. For at-rest initial conditions, $P[|X(t=0)| < x_{lim}] = 1$. In this thesis, the process $X(t)$ denotes the displacement response of a structural system subjected to a stationary and/or nonstationary input excitation. It is noteworthy that, once the hazard function is known, the FPDF can be obtained through Eq.(1.59). To the best of the writer's knowledge, no exact analytical solution is available for $h_{|X|}$ to date.

The FPDF can be estimated using two different approaches, i.e., analytical and numerical. The Poisson's (P), classical Vanmarcke's (cVM), and modified Vanmarcke's (mVM) are the most

commonly used analytical approximations for the hazard function. Monte Carlo simulation and the importance sampling using elementary events (ISEE) method are the numerical approaches considered in this research.

1.2.5.1 Poisson's Approximation for FFPF

The P approximation is the simplest approximation for the FFPF, which assumes that the occurrences of out-crossings are statistically independent events. In this approximation, the time-variant hazard function, introduced in Eq. (1.59), is assumed to be equal to the mean out-crossing rate function of process $X(t)$:

$$h_{p,|x|}(x_{lim}, t) = \nu_{|x|}(x_{lim}, t) = E \left[\frac{dN(t)}{dt} \right] \quad (1.60)$$

where $N(t)$ = number of out-crossing events in the time interval $[0, t]$. The mean out-crossing rate, $\nu_{|x|}(x_{lim}, t)$, for linear elastic systems subjected to Gaussian processes is known in exact closed-form, which is derived by using the Rice's formula [1, 2, 9].

Studies on the accuracy of the P approximation show that, for practical levels of barrier, the error produced by the use of this process strongly depends on the bandwidth of the process [5]. The P approximation becomes conservative for narrow-band processes and low failure thresholds and underestimates the failure probability for wide-band processes [20]. This is due to the fact that in wide-band processes, the P approximation does not take into account the time that the process spends in the safe region; however, for the case of narrow-band process the dependence correlation between subsequent out-crossings becomes important. The P approximation becomes more accurate as the response threshold level and the bandwidth of the response process increase [8].

1.2.5.2 Vanmarcke's Approximations for FPF

The cVM and mVM approximate solutions for the FPF have been introduced by Vanmarcke [5]. These two improved approximations are based on the two-state Markov process and use the envelope defined by Cramer and Leadbetter [21]. The cVM approximation assumes the following analytical expression for the time-variant hazard function [5] :

$$h_{\text{cVM},|X|}(x_{\text{lim}}, t) = \nu_{|X|}(x_{\text{lim}}, t) \cdot \frac{1 - \exp\left[-\sqrt{\pi/2} \cdot q_X(t) \cdot \frac{x_{\text{lim}}}{\sigma_X(t)}\right]}{1 - \exp\left\{-\frac{1}{2} \cdot \left[\frac{x_{\text{lim}}}{\sigma_X(t)}\right]^2\right\}} \quad (1.61)$$

where $\nu_{|X|}(x_{\text{lim}}, t)$ = mean out-crossing rate of the double-barrier process, $\sigma_X(t)$ = time-variant standard deviation of process $X(t)$, x_{lim} = threshold for the double-barrier problem, and $q_X(t)$ = time-variant bandwidth parameter (TVBP) of process $X(t)$. The cVM approximation takes into account the fraction of time that the envelope process spends above or below the failure threshold level, and considers the fact that that the out-crossings of the envelope process are not always associated with one or more out-crossings of the actual process [4, 5]. The former consideration is more useful for low failure threshold levels while the latter becomes more important for high failure threshold levels.

The mVM approximation heuristically accounts for super-clumping effects [4, 5] by introducing an exponent equal to 1.2 for the TVBP in the approximate hazard function equation:

$$h_{\text{mVM},|X|}(x_{\text{lim}}, t) = \nu_{|X|}(x_{\text{lim}}, t) \cdot \frac{1 - \exp\left\{-\sqrt{\pi/2} \cdot [q_X(t)]^{1.2} \cdot \frac{x_{\text{lim}}}{\sigma_X(t)}\right\}}{1 - \exp\left\{-\frac{1}{2} \cdot \left[\frac{x_{\text{lim}}}{\sigma_X(t)}\right]^2\right\}} \quad (1.62)$$

The P, cVM, and mVM hazard functions for the single-barrier FFPF are obtained from Eqs. (1.60), (1.61) and (1.62) respectively, by substituting (1) x_{lim} with x_{lim}^+ = threshold for the single-barrier problem, (2) $\nu_{|x|}(x_{lim}, t)$ with $\nu_x(x_{lim}^+, t)$ = mean up-crossing rate of x_{lim}^+ by process $X(t)$, and (3) $\sqrt{\pi/2}$ with $\sqrt{2\pi}$.

Vanmarcke's approximations, in general, provide more accurate results than the P approximation. However, they are characterized by inconsistent levels of accuracy for different structural systems and failure thresholds [4, 5]. The study performed by Barbato and Conte [8] shows that the accuracy of the mVM approximation improve with increasing exposure time to the white noise excitation and the accuracy of the two Vanmarcke's approximations in estimating the failure probability depends on both the order of magnitude of the failure probability and the damping ratio. It was found that for the failure probabilities smaller than $P_f < 1e-4$ the cVM is more accurate than the mVM.

1.2.5.3 Monte Carlo Simulation for FFPF

Monte Carlo (MC) simulation is a general and robust numerical method for calculating the FFPF. It can account for stationary and nonstationary behavior, linear and nonlinear structural behavior, and randomness in the structural parameters. However, in cases in which the FFPF is very small, MC simulation is computationally expensive if not prohibitive. In fact, the number of samples required to achieve a desired accuracy in the estimation of the FFPF is inversely proportional to the value of the FFPF. Thus, a large number of samples is required for computing small failure probabilities [22].

1.2.5.4 ISEE Method for FFPF

The ISEE method is a numerical method developed specifically to estimate the FFPF for

deterministic linear elastic structural models subjected to Gaussian excitation [22]. In order to improve the simulation efficiency compared to MC simulation, the ISEE method employs an importance sampling density with values larger than zero only in the failure region defined in the standard normal space of the random variables used to discretize the stochastic input. It has been shown that the ISEE method can accurately estimate even very small values of FPDF at a computational cost that is only a small fraction of the computational cost required by MC simulation [22].

1.3 OBJECTIVES AND ORGANIZATION OF THE THESIS

The research presented in this thesis focuses on the analytical estimation of the FPDF for linear SDOF and MDOF systems subjected to stationary and nonstationary random excitations.

This thesis consists of two main components. The first component is a detailed study of the time-variant FPDF for linear SDOF systems subjected to a seismic input modeled as a: (1) Gaussian white noise (WN) from at-rest initial conditions (stationary random processes), (2) white/colored noise input excitation and modulated in time (nonstationary random processes). The second component is a study of the time-variant FPDF for linear MDOF systems subjected to stationary and/or nonstationary random excitations.

The main objectives of this research are:

- (1) investigating the absolute and relative accuracy of existing analytical approximations (i.e., P, cVM, and mVM approximation) of the time-variant FPDF for linear SDOF systems subjected to stationary and/or nonstationary Gaussian excitations;
- (2) deriving an improved analytical approximate solution for the time-variant FPDF; and
- (3) evaluating the absolute and relative accuracy of the P, cVM, and mVM, as well as of the newly developed analytical approximation for linear elastic MDOF systems subjected to stationary and/or nonstationary Gaussian excitations.

The first aim is achieved by evaluating, via an extensive parametric study, the accuracy of the considered analytical estimates of the time-variant FPDF for a wide range of SDOF oscillator's properties (i.e., natural periods and damping ratios), failure threshold levels, and seismic input models. This evaluation is based on the comparison of the analytical results with the corresponding simulation results obtained using the importance ISEE method [22], which are assumed as the reference solution.

The second goal is achieved by proposing a new analytical approximation of the time-variant FPDF for linear SDOF systems subjected to stationary and/or nonstationary Gaussian excitations. First, a new hazard function is derived for the case of linear SDOF systems subjected to WN excitation from at-rest initial conditions. Then, appropriate modifications are derived to account for time-modulation and non-white spectra of the input loading. The accuracy in estimating the time-variant FPDF of this new analytical approximation is also examined in detail. The newly proposed hazard function provides significantly more accurate results when compared with the available analytical approximations.

The third objective is achieved by studying the FPDF of linear MDOF systems subjected to the stochastic loadings and applying modal truncation in the computation of the time-variant statistics needed in the analytical approximations of the FPDF. Several MDOF systems, subjected to both stationary and nonstationary Gaussian excitations, are investigated, including shear-type frames with varying number of DOFs, a linear elastic model of an actual 13-story welded steel building, and the system consisting of two adjacent building subjected to seismic pounding hazard.

2 NEW ANALYTICAL APPROXIMATION OF THE FPDF FOR LINEAR SDOF SYSTEMS

2.1 INTRODUCTION AND PREVIOUS WORK

To date, no exact closed-form solution of the FPDF is available even for the simplest case, i.e., a SDOF linear oscillator subjected to Gaussian WN excitation with a deterministic failure threshold [3, 7, 8]. Thus, several analytical approximations or numerical methods are used to compute the FPDF of linear SDOF systems.

Among the numerical methods used to compute the FPDF, MC simulation is the most general and robust, but is also computationally expensive or even prohibitive for low probability events. For linear elastic systems subjected to Gaussian random loading, the ISEE method has been proven to be an extremely efficient simulation method for computing the FPDF [22].

Among the various analytical approximations proposed to estimate the FPDF, the P, cVM, and mVM approximations are the most widely employed. Both the cVM and the mVM approximations require computing the bandwidth parameter of the response process of interest. However, only recently an appropriate definition of the TVBP of a nonstationary process was given based on the concept of non-geometric spectral characteristics [13, 23]. Currently, the exact closed-form of the TVBP are available for the displacement response processes (and for any response quantity linearly related to the displacement response) of linear SDOF systems, as well as of classically and non-classically damped MDOF systems, subjected (1) to Gaussian WN excitation from at-rest initial conditions [15], and (2) to time-modulated non-white noise excitation [24]. These exact solutions have been employed (1) to compute the cVM and mVM approximations of the time-variant FPDF for different linear structural systems subjected to different types of loading, and (2) to evaluate the absolute and relative accuracy of these analytical approximations when compared with the corresponding ISEE results [8].

In this chapter the absolute and relative accuracy of existing analytical approximations (i.e., P, cVM, and mVM approximation) of the time-variant FPDF for linear SDOF systems subjected to stationary and/or non-stationary Gaussian excitations modeled as separable non-stationary processes (i.e., stochastic processes defined as the product of a deterministic time modulating function and a stationary process) are investigated and an improved analytical approximate solution for the time-variant FPDF is proposed.

The new analytical hazard function for the displacement response $X(t)$ of a linear SDOF system is proposed to obtain improved estimates of $P_f(t)$ when compared to those obtained using the P, cVM, and mVM approximations. First, a new hazard function is derived for the case of linear SDOF systems subjected to WN excitation from at-rest initial conditions. Then, appropriate modifications are derived to account for time-modulation and non-white spectra of the input loading. The new approximation is proposed based on an extensive parametric study of the time-variant FPDF of linear SDOF systems with different damping ratios and normalized failure thresholds. Six hazard functions are proposed in total (see Appendix B) and their relative accuracy in computing the FPDF is evaluated (see Appendices C and D). The best approximation among the ones developed in this research is illustrated in this chapter. It is noted that the same procedure discussed here to derive the proposed approximation is followed for each of the proposed functions presented in the Appendix B.

2.2 HAZARD FUNCTION FOR LINEAR SDOF SYSTEMS SUBJECTED TO WN EXCITATION FROM AT-REST INITIAL CONDITIONS

The time-variant FPDF for linear SDOF systems subjected to WN excitation from at-rest initial conditions (i.e., with unit step time-modulating function) was investigated in Barbato and Conte [8]. It was found that the relative accuracy of the cVM and mVM approximations varies with the damping ratio, exposure time, and threshold level. In addition, for several cases it was

noted that the ISEE results shift progressively away from the cVM to the mVM approximation results as time elapses. This observation suggests that a better approximation of the FFP could be achieved (1) by considering a time-dependent exponent of the time-variant bandwidth parameter that increases with time until it reaches a stationary value, (2) by multiplying the mean out-crossing rate by a time-dependent factor (with values larger or equal to 1) that decreases with time until it reaches a stationary value equal to 1.

On the basis of these observed trends, a new hazard function for the double-barrier first-passage problem is proposed as follows:

$$h_{\text{New},|X|}(x_{\text{lim}}, t) = \nu_{|X|}(x_{\text{lim}}, t) \cdot \exp[C_2(\xi, \zeta, t)] \cdot \frac{1 - \exp\left\{-\sqrt{\pi/2} \cdot [q_X(t)]^{C_1(\xi, \zeta, t)} \cdot \frac{x_{\text{lim}}}{\sigma_X(t)}\right\}}{1 - \exp\left\{-\frac{1}{2} \cdot \left[\frac{x_{\text{lim}}}{\sigma_X(t)}\right]^2\right\}} \quad (2.1)$$

in which

$$C_1(\xi, \zeta, t) = C_{1,\infty}(\xi, \zeta) \cdot \exp\left\{-[q_X(t) - q_{X,\infty}^{(WN)}]\right\} \quad (2.2)$$

$$C_2(\xi, \zeta, t) = C_{2,\infty}(\xi, \zeta) \cdot [q_X(t) - q_{X,\infty}^{(WN)}] \quad (2.3)$$

where $\xi = \text{damping ratio}$, $\zeta = x_{\text{lim}}/\sigma_{X,\infty}^{(WN)} = x_{\text{lim}}/\sigma_{X,\text{max}}$ = normalized failure threshold level, $\sigma_{X,\infty}^{(WN)}$ = stationary value of the standard deviation of process $X(t)$ when the input process is a WN time modulated by a unit step function, $\sigma_{X,\text{max}} = \max_{t \geq 0}[\sigma_X(t)]$, $q_{X,\infty}^{(WN)}$ = stationary value of the time-variant bandwidth parameter of process $X(t)$ when the input process is a WN time modulated by a unit step function [15], and $C_{1,\infty}(\xi, \zeta)$, $C_{2,\infty}(\xi, \zeta)$ = stationary values of the time-variant functions $C_1(\xi, \zeta, t)$ and $C_2(\xi, \zeta, t)$, respectively. The hazard function for the single-barrier first-passage problem is obtained via the same substitutions described in Chapter 1 of this thesis for the P, cVM, and mVM approximations.

The time-dependent exponential term in Eq. (2.2), $\exp\left\{-\left[q_X(t)-q_{X,\infty}^{(WN)}\right]\right\}$, is introduced to account for the time-dependence of the exponent of the time-variant bandwidth parameter [15], since it always assumes positive values smaller than 1 and increases with time until it reaches a stationary value equal to 1. The stationary part $C_{1,\infty}(\xi,\zeta)$ of function $C_1(\xi,\zeta,t)$ accounts for the dependency on damping ratio and normalized failure threshold of the super-clumping effects identified in the literature [4, 5]. The time-dependent term in Eq. (2.3) reflects the effect of the sudden application of the input loading corresponding to a unit step time-modulating function. It is noteworthy that the time-variant PFP for a linear SDOF system subjected to WN excitation can be expressed as a function of normalized time $t_0 = t/T$ (i.e., the time t divided by the natural period T of the SDOF system, see Section 0). Thus, the stationary values $C_{1,\infty}(\xi,\zeta)$ and $C_{2,\infty}(\xi,\zeta)$ are independent of T .

In this research, a closed-form expression for $C_1(\xi,\zeta,t)$ and $C_2(\xi,\zeta,t)$ is obtained by deriving an analytical expression for the stationary values $C_{1,\infty}(\xi,\zeta)$ and $C_{2,\infty}(\xi,\zeta)$ as follows. First, the ISEE method is repeatedly applied to evaluate the time history of the time-variant PFP, $P_f(t)$ for different combinations of the damping ratio ($\bar{\xi} = 0.01, 0.02, 0.05, 0.10, 0.20, 0.30, 0.40,$ and 0.50) and of the normalized failure threshold level ($\bar{\zeta} = 1.5, 2, 3, 4,$ and 5). Closely spaced values of t_0 are considered from $t_0 = 0$ to a value of t_0 sufficiently large to reach stationarity. For each of these $8 \times 5 = 40$ time histories, the values of $\bar{C}_{1,\infty}(\bar{\xi},\bar{\zeta})$ and $\bar{C}_{2,\infty}(\bar{\xi},\bar{\zeta})$ are obtained through least-square fitting, using the Matlab function *lsqcurvefit* [25]. These values correspond to the best fit between the analytical estimates of $P_f(t_0)$, computed using Eqs. (1.59) and (2.1), and the ISEE results. The ISEE results used to estimate $\bar{C}_{1,\infty}(\bar{\xi},\bar{\zeta})$ and $\bar{C}_{2,\infty}(\bar{\xi},\bar{\zeta})$ are obtained imposing a very low target coefficient of variation (c.o.v. = 0.001), in

order to ensure a high accuracy in the estimates of $P_f(t_0)$ and to minimize the sensitivity of $\bar{C}_{1,\infty}(\bar{\xi}, \bar{\zeta})$ and $\bar{C}_{2,\infty}(\bar{\xi}, \bar{\zeta})$ to the variability of the simulation results.

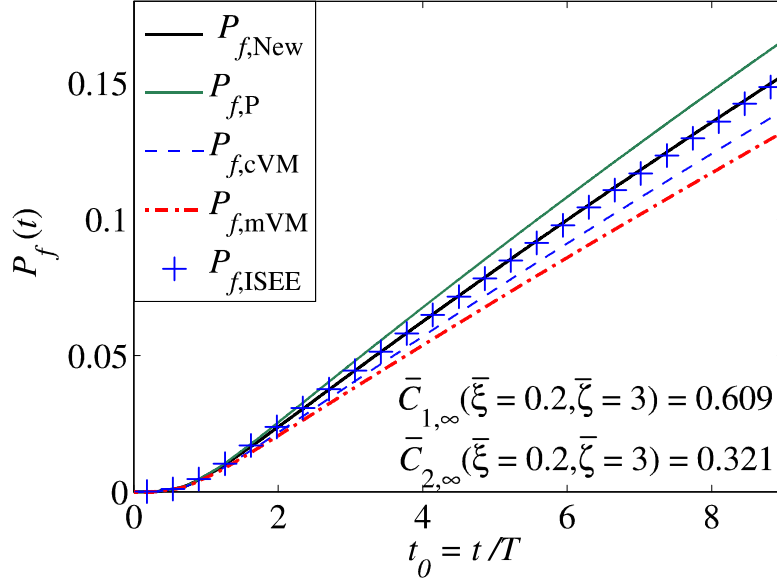


Figure 2.1 - Computation of $\bar{C}_{1,\infty}$ and $\bar{C}_{2,\infty}$: SDOF system subjected to WN base excitation from at-rest initial conditions ($\bar{\xi} = 0.2$; $\bar{\zeta} = 3$).

Figure 2.1 compares the values of $P_f(t_0)$ computed using (1) the ISEE method, (2) the P, cVM, and mVM approximations of the hazard function, and (3) the newly proposed analytical approximation of the hazard function given in Eq. (2.1) and based on the fitted values of $\bar{C}_{1,\infty}(\bar{\xi}, \bar{\zeta})$ and $\bar{C}_{2,\infty}(\bar{\xi}, \bar{\zeta})$, for the case corresponding to $T = 0.1s$, $\xi = 0.2$ and $\zeta = 3.0$. The hazard function built using the optimized values $\bar{C}_{1,\infty}(\bar{\xi}, \bar{\zeta})$ and $\bar{C}_{2,\infty}(\bar{\xi}, \bar{\zeta})$ is able to reproduce the simulation results with extremely high accuracy over the entire time history of $P_f(t_0)$. Similar results are obtained for all the combinations of $\bar{\xi}$ and $\bar{\zeta}$ considered here, thus validating the analytical expressions assumed for the time-variant hazard function in Eqs. (2.1) through (2.3). It is noted here that the functions $\bar{C}_{1,\infty}(\bar{\xi}, \bar{\zeta})$ and $\bar{C}_{2,\infty}(\bar{\xi}, \bar{\zeta})$ are obtained from the simulated estimates of the FPDF because the estimation of the hazard function from direct simulation is not

feasible, as shown in Appendix A.

Two polynomial surfaces $C_{1,\infty}(\xi, \zeta)$ and $C_{2,\infty}(\xi, \zeta)$ (expressed as functions of the damping ratio ξ and of the normalized threshold ζ) are fitted to the values $\bar{C}_{1,\infty}(\bar{\xi}, \bar{\zeta})$ and $\bar{C}_{2,\infty}(\bar{\xi}, \bar{\zeta})$ obtained via least-square fitting by using the *sftool* Matlab toolbox [25]. This fitting is performed in order to extend the proposed expression of the hazard function to values of ξ and ζ for which simulation results are not available. The order of the polynomials is kept as small as possible (equal to 5 for the damping ratio and to 4 for the normalized threshold), in order to balance the contrasting requirements of accuracy and simplicity. The following polynomial representations are suggested for $C_{1,\infty}(\xi, \zeta)$ and $C_{2,\infty}(\xi, \zeta)$:

$$C_{i,\infty}(\xi, \zeta) = \sum_{l=0}^5 \sum_{m=0}^4 (P_{lm}^{(i)} \cdot \xi^l \cdot \zeta^m); \quad i=1,2; \quad 0.01 \leq \xi \leq 0.50; \quad 1.5 \leq \zeta \leq 5.0 \quad (2.4)$$

in which the coefficients $P_{lm}^{(i)}$ ($i=1,2$; $l=0,1,2,3,4,5$; and $m=0,1,2,3,4$) obtained from the surface fitting are given in Table 2.1 .

Table 2.1 - Coefficients of the polynomial representation of $C_{i,\infty}$ ($i=1,2$) given in Eq. (2.4).

i	$P_{00}^{(i)}$	$P_{10}^{(i)}$	$P_{01}^{(i)}$	$P_{20}^{(i)}$	$P_{11}^{(i)}$	$P_{02}^{(i)}$	$P_{30}^{(i)}$	$P_{21}^{(i)}$	$P_{12}^{(i)}$	$P_{03}^{(i)}$
1	1.566	-22.23	-0.091	99.95	16.26	0.07	-252.3	-52.57	-5.714	-0.027
2	-5.319	29.07	6.734	39.89	-48.47	-1.639	-711.7	162	7.3	0.12
i	$P_{40}^{(i)}$	$P_{31}^{(i)}$	$P_{22}^{(i)}$	$P_{13}^{(i)}$	$P_{04}^{(i)}$	$P_{50}^{(i)}$	$P_{41}^{(i)}$	$P_{32}^{(i)}$	$P_{23}^{(i)}$	$P_{14}^{(i)}$
1	367.9	67.92	10.16	0.88	0.003	-214	-39.94	-4.476	-0.654	-0.052
2	1712	-181.5	-23.96	0.192	0.001	-1304	80.33	11.93	1.218	-0.081

For values of the damping ratio ξ and of the normalized threshold ζ that are outside the domain in which the two surfaces described above are fitted, Eq. (2.4) is computed using the values of ξ and ζ along the boundaries of the fitting domain (e.g., for damping ratios smaller

than 0.01, Eq. (2.4) is computed using $\xi = 0.01$). Figure 2.2 and Figure 2.3 plot the isocurves of $C_{1,\infty}(\xi, \zeta)$ and $C_{2,\infty}(\xi, \zeta)$, respectively, for discrete values of ζ as functions of ξ . These polynomial surfaces provide an accurate fit to the values $\bar{C}_{1,\infty}(\bar{\xi}, \bar{\zeta})$ and $\bar{C}_{2,\infty}(\bar{\xi}, \bar{\zeta})$ obtained through least-square fitting.

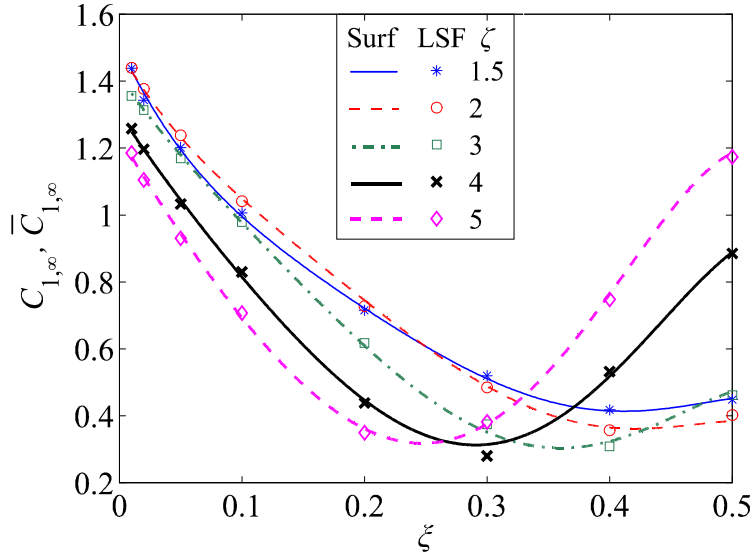


Figure 2.2 - Comparison between the interpolation surface $C_{1,\infty}$ (Surf) and values $\bar{C}_{1,\infty}$ obtained through least-square fitting (LSF).

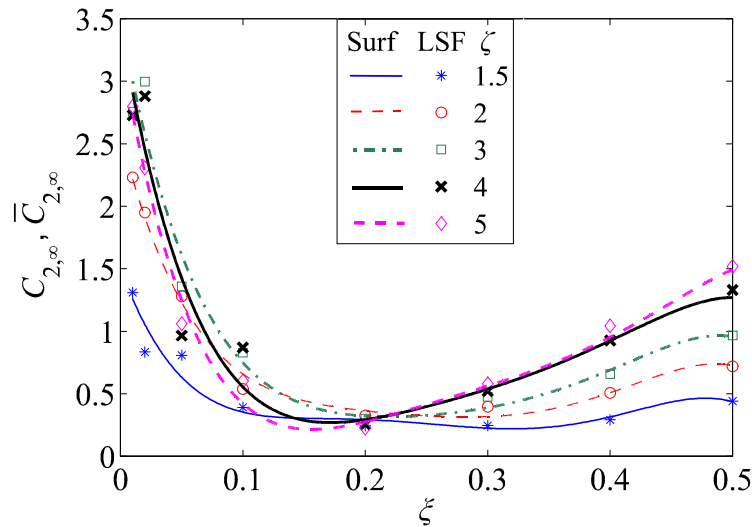


Figure 2.3 - Comparison between the interpolation surface $C_{2,\infty}$ (Surf) and values $\bar{C}_{2,\infty}$ obtained through least-square fitting (LSF).

2.3 MODIFICATIONS OF THE HAZARD FUNCTION NEEDED TO ACCOUNT FOR TIME-MODULATION AND NON-WHITE SPECTRA

When the input process is time-modulated (with time-modulating function $A(t)$) and/or characterized by a non-white spectrum (i.e., the excitation is a colored noise), the results obtained considering SDOF systems subjected to WN excitation from at-rest initial conditions can be still used by modifying Eqs. (2.2) and (2.3) as follows:

- (1) The functions in Eqs. (2.2) and (2.3) are computed using an equivalent damping ratio, $\tilde{\xi}$, and an equivalent time-variant normalized threshold level, $\tilde{\zeta}(t)$, i.e.,

$$C_1(\tilde{\xi}, \tilde{\zeta}(t), t) = C_{1,\infty}(\tilde{\xi}, \tilde{\zeta}(t)) \cdot \exp\left\{\min\left\{-[q_X(t) - q_{X,\infty}], 0\right\}\right\} \quad (2.5)$$

$$C_2(\tilde{\xi}, \tilde{\zeta}(t), t) = C_{2,\infty}(\tilde{\xi}, \tilde{\zeta}(t)) \cdot \max\left\{[q_X(t) - q_{X,\infty}], 0\right\} \quad (2.6)$$

in which $q_{X,\infty}$ = stationary value of the TVBP of process $X(t)$ computed using the unit step function as time-modulating function. The min and max operators are introduced because the quantity $[q_X(t) - q_{X,\infty}]$ can become negative for general non-stationary excitations, while the quantity $[q_X(t) - q_{X,\infty}^{(WN)}]$ is always positive for WN excitation and at-rest initial conditions.

- (2) The equivalent damping ratio, $\tilde{\xi}$, is taken as the value of the damping ratio that would provide the same stationary value of the TVBP obtained from the colored noise excitation if the SDOF system were subjected to a WN excitation. This equivalent damping ratio can be found using the closed-form expression of the time-variant bandwidth parameter [15] as follows:

$$\tilde{\xi} = \text{zero} \left\{ q_{X,\infty} - \left[1 - \frac{4 \cdot \left[\arctan \left(\sqrt{1 - \xi^2} / \xi \right) \right]^2}{\pi^2 \cdot (1 - \xi^2)} \right]^{\frac{1}{2}} \right\} \quad (2.7)$$

in which the operator “zero” denotes the root of the quantity in parentheses. Since the time-variant bandwidth parameter is a monotonically increasing continuous function of ξ , the solution $\tilde{\xi}$ of the transcendental Eq. (2.7) exists and is unique for any $0 \leq q_{X,\infty} < 1$.

(3) The equivalent normalized failure threshold, $\tilde{\zeta}(t)$, is computed as follows:

$$\tilde{\zeta}(t) = \frac{x_{\text{lim}}}{\sigma_{X,\text{max}} \cdot A(t)} \cdot \frac{G_{X_s X_s}(\omega_0)}{S_0} \quad (2.8)$$

in which $G_{X_s X_s}(\omega_0)$ = power spectral density of the colored noise excitation computed at $\omega_0 = 2 \cdot \pi / T$ = natural circular frequency of the SDOF system, and $S_0 = 1 \text{m}^2/\text{s}^3$ is a normalization factor.

(4) If $A(t)$ does not present a discontinuity for $t=0\text{s}$ (i.e., the time-modulating function increases gradually from zero to its maximum value), it is assumed that $C_2(\tilde{\xi}, \tilde{\zeta}(t), t) = 0$.

Otherwise, $C_2(\tilde{\xi}, \tilde{\zeta}(t), t)$ is computed according to Eq. (2.6).

The time-modulating function, $A(t)$, is scaled here so that its maximum value in time is equal to 1 (i.e., $\max_{t \geq 0} [A(t)] = 1$, see Figure 2.4). It is noteworthy that the equivalent damping ratio $\tilde{\xi}$ and the equivalent normalized threshold level $\tilde{\zeta}(t)$ reduce to the actual damping ratio ξ and normalized threshold level ζ for the case of SDOF systems subjected to WN excitation from at-rest initial conditions, i.e., Eqs. (2.2) and (2.3) can be regarded as special cases of

Eqs. (2.5) and (2.6).

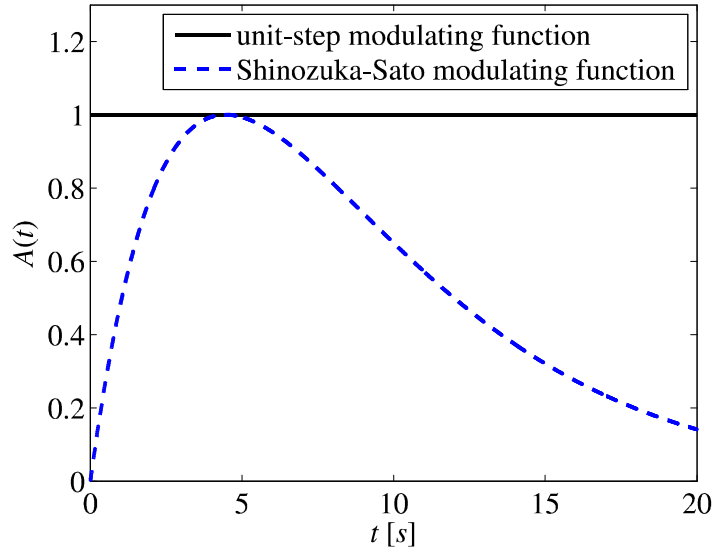


Figure 2.4 - Time-modulating functions: (1) unit-step function, and (2) Shinozuka-Sato with $B_1 = 0.20\text{s}^{-1}$ and $B_2 = 0.25\text{ s}^{-1}$.

2.4 PARAMETRIC STUDY TO EVALUATE THE ACCURACY OF THE EXISTING AND THE NEWLY PROPOSED ANALYTICAL APPROXIMATIONS

The results of an extensive parametric study are presented here in order to evaluate the absolute and relative accuracy of the P, cVM, and mVM approximations, as well as the accuracy of the newly proposed analytical approximation (denoted as “New”). This parametric study considers a wide range of natural periods, damping ratios, and threshold levels, as well as different input spectra and time-modulating functions. The time-variant FFPF results obtained from the analytical approximations are compared with the corresponding results obtained using the ISEE method with a target c.o.v. = 0.01, which is considered as the reference solution. The value of c.o.v. = 0.01 used for this parametric study is chosen because it provides sufficiently accurate estimates of the FFPF at a feasible computational cost (several times smaller than the computational effort required to obtain the value c.o.v. = 0.001 used to calibrate the analytical approximation denoted as New). The comparison between analytical approximations and ISEE

results is based on the percent error $\varepsilon = 100 \cdot (P_{f,i} - P_{f,ISEE}) / P_{f,ISEE}$ ($i = P, cVM, mVM, New$). For each type of input loading considered, synoptic results are also provided including the maximum (ε_{\max}) and minimum (ε_{\min}) percent errors, as well as the mean of the absolute values of the percent errors ($\mu_{|\varepsilon|}$) computed for the different damping ratios and normalized threshold levels considered. These synoptic results indicate whether a given approximate analytical solution tends to overestimate (ε_{\max}) or to underestimate (ε_{\min}) the FFPF. They also provide information regarding the average value of the error corresponding to a specific analytical solution for a given loading condition ($\mu_{|\varepsilon|}$). Only selected results are presented in this chapter and additional results can be found in Appendices C and D. It is worth mentioning that the different analytical approximations involve a similar computational cost, which can be several orders of magnitude smaller than the computational cost associated with the ISEE method.

2.4.1 Input Excitation Models

Two types of random excitations are considered in this study: (1) a WN excitation, represented by a constant PSD function (i.e., $G_{X_s X_s}(\omega) = S_0$, in which $\omega =$ circular frequency, and $S_0 = 1\text{m}^2/\text{s}^3$), and (2) a non-white excitation, modeled by using a Kanai-Tajimi (KT) PSD function. The KT PSD function is given by:

$$G_{X_s X_s}(\omega) = \frac{1 + 4 \cdot \xi_g^2 \cdot (\omega/\omega_g)^2}{\left[1 - (\omega/\omega_g)^2\right]^2 + (2 \cdot \xi_g \cdot \omega/\omega_g)^2} \cdot S_0 \quad (2.9)$$

in which $\xi_g =$ predominant ground damping ratio, and $\omega_g =$ ground natural circular frequency. In this study, $\xi_g = 0.6$ and $\omega_g = 9\pi$ rad/s are used [26].

Two time-modulating functions are considered in this thesis: (1) a unit step function, $H(t)$, and (2) a Shinozuka-Sato modulating function [27]. The latter modulating function is defined as:

$$A(t) = C \cdot [e^{-B_1 t} - e^{-B_2 t}] \cdot H(t) \quad (2.9)$$

where

$$C = \left(\frac{B_1}{B_2 - B_1} \right) \cdot \exp \left[\frac{B_2}{B_2 - B_1} \log \left(\frac{B_2}{B_1} \right) \right] \quad (2.10)$$

in which B_1 and $B_2 =$ constants defining the shape of the time-modulating function, and $C =$ normalizing constant. In this study, the following values are assumed for these constants: $B_1 = 0.20\text{s}^{-1}$, $B_2 = 0.25\text{s}^{-1}$, and $C = 12.207$. The two modulating functions considered are shown in Figure 2.4.

2.4.2 Results for Linear SDOF Systems Subjected to WN Excitation from At-rest Initial Conditions

For linear SDOF systems subjected to WN excitation from at-rest initial conditions, it can be shown that the time-variant FPDF depends on the time t and the natural period of the system T only through the normalized time $t_0 = t/T$ (see Section 0). Thus, the results are presented here as a function of the normalized time, the damping ratio, and the normalized threshold, and are valid for any natural period of the system. Table 2.2 shows the estimates of the FPDF corresponding to $t_0 = 10$, normalized thresholds $\zeta = 2, 3, 4$ and damping ratios $\xi = 0.01, 0.05, 0.10, 0.50$, computed using the ISEE method, as well as using the P, cVM, mVM, and New approximations. The FPDF values range from a maximum value of 0.932 to a minimum value of $2.24 \cdot 10^{-5}$. Table 2.2 also provides the percent error ε , as well as the minimum percent error, maximum percent error, and the mean of the absolute value of the percent error for each of the considered analytical

approximations. As expected, the P approximation consistently overestimates the FPDF, sometimes even by a large factor. The cVM and mVM approximations produce similar results and are more accurate than the P approximation. The cVM approximation tends to overestimate the FPDF, particularly for small damping, while the mVM approximation tends to underestimate the FPDF, particularly for large thresholds. The New approximation is overall significantly more accurate than all other analytical approximations, with a slight tendency to underestimate the FPDF. It presents the smallest value of the maximum error ($\varepsilon_{\max} = 1.07\%$) and of the mean of the absolute values of the errors ($\mu_{|e|} = 1.90\%$), which are more than 4 times smaller than the corresponding quantities for the second best approximation (i.e., in this case, the mVM approximation).

Table 2.2 - Time-variant FPDF ($t_0 = 10$) for linear elastic SDOF systems subjected to WN base excitation from at-rest initial conditions (i.e., with unit step time-modulating function).

ζ	ξ	ISEE	P	ε [%]	cVM	ε [%]	mVM	ε [%]	New	ε [%]	
2	0.01	1.23E-01	3.39E-01	176.24	1.66E-01	35.26	1.29E-01	4.87	1.20E-01	-2.29	
	0.05	6.15E-01	8.68E-01	41.22	6.78E-01	10.25	6.07E-01	-1.37	6.11E-01	-0.59	
	0.10	7.84E-01	9.07E-01	15.77	7.98E-01	1.85	7.52E-01	-4.03	7.92E-01	1.07	
	0.50	9.32E-01	9.29E-01	-0.35	9.13E-01	-2.04	9.05E-01	-2.90	9.33E-01	0.04	
3	0.01	3.49E-03	7.66E-03	119.47	4.07E-03	16.64	3.14E-03	-10.01	3.20E-03	-8.35	
	0.05	7.79E-02	1.34E-01	71.73	8.67E-02	11.26	7.35E-02	-5.60	7.71E-02	-1.05	
	0.10	1.28E-01	1.68E-01	31.41	1.26E-01	-0.96	1.14E-01	-10.83	1.29E-01	0.82	
	0.50	1.91E-01	1.93E-01	1.05	1.79E-01	-6.22	1.76E-01	-8.13	1.88E-01	-2.00	
4	0.01	2.24E-05	3.82E-05	70.60	2.37E-05	5.55	1.86E-05	-16.96	2.15E-05	-4.19	
	0.05	2.72E-03	3.79E-03	39.36	2.75E-03	0.89	2.37E-03	-13.03	2.70E-03	-0.58	
	0.10	4.60E-03	5.25E-03	14.04	4.31E-03	-6.23	3.94E-03	-14.25	4.62E-03	0.47	
	0.50	6.31E-03	6.41E-03	0.02	6.16E-03	-2.36	6.08E-03	-3.65	6.21E-03	-1.43	
				ε_{\max} %	176.24	ε_{\max} %	35.26	ε_{\max} %	4.87	ε_{\max} %	1.07
				ε_{\min} %	-0.35	ε_{\min} %	-6.23	ε_{\min} %	-16.96	ε_{\min} %	-8.35
				$\mu_{ e }$ %	48.44	$\mu_{ e }$ %	8.29	$\mu_{ e }$ %	7.97	$\mu_{ e }$ %	1.90

Table 2.3 provides the FPDF estimates for linear SDOF systems subjected to WN excitation from at-rest initial conditions with given normalized threshold $\zeta = 5$ and varying normalized time $t_0 = 10, 20$, and 50. The FPDF values range from a maximum value of $3.72 \cdot 10^{-4}$ to a minimum value of $3.53 \cdot 10^{-8}$. Also in this case, it is observed that the P approximation overestimates the FPDF, the cVM approximation tends to overestimate the FPDF, while the mVM approximation tends to underestimate the FPDF. The New approximation is very accurate under all combinations of damping ratios and normalized times, with $\mu_{|\varepsilon|} = 1.73\%$.

Table 2.3 - Time-variant FPDF for linear elastic SDOF systems subjected to WN base excitation from at-rest initial conditions for $\zeta = 5$ and different values of normalized time t_0 .

t_0	ζ	ISEE	P	ε [%]	cVM	ε [%]	mVM	ε [%]	New	ε [%]	
10	0.01	3.53E-08	5.00E-08	41.56	3.46E-08	-2.12	2.78E-08	-21.38	3.42E-08	-3.27	
	0.05	3.16E-05	3.74E-05	18.20	2.98E-05	-5.91	2.62E-05	-17.18	3.10E-05	-2.07	
	0.10	5.28E-05	5.59E-05	5.97	4.94E-05	-6.44	4.60E-05	-12.82	5.32E-05	0.75	
	0.50	6.97E-05	7.09E-05	1.83	6.97E-05	-0.02	6.91E-05	-0.77	6.93E-05	-0.48	
20	0.01	4.69E-06	9.74E-06	107.75	5.57E-06	18.78	4.18E-06	-10.74	4.66E-06	-0.63	
	0.05	9.29E-05	1.12E-04	20.17	8.81E-05	-5.18	7.72E-05	-16.86	9.12E-05	-1.82	
	0.10	1.24E-04	1.30E-04	5.59	1.15E-04	-6.94	1.07E-04	-13.36	1.24E-04	0.23	
	0.50	1.44E-04	1.45E-04	0.83	1.43E-04	-1.01	1.42E-04	-1.76	1.42E-04	-1.57	
50	0.01	7.01E-05	1.86E-04	165.23	9.60E-05	37.03	6.99E-05	-0.26	7.40E-05	5.61	
	0.05	2.75E-04	3.35E-04	22.10	2.64E-04	-3.95	2.31E-04	-15.90	2.73E-04	-0.73	
	0.10	3.37E-04	3.54E-04	4.99	3.12E-04	-7.55	2.90E-04	-13.97	3.36E-04	-0.42	
	0.50	3.72E-04	3.69E-04	-0.78	3.62E-04	-2.60	3.60E-04	-3.34	3.60E-04	-3.23	
				ε_{\max} %	165.23	ε_{\max} %	37.03	ε_{\max} %	-0.26	ε_{\max} %	5.61
				ε_{\min} %	-0.78	ε_{\min} %	-7.55	ε_{\min} %	-21.38	ε_{\min} %	-3.27
				$\mu_{ \varepsilon }$ %	32.92	$\mu_{ \varepsilon }$ %	8.13	$\mu_{ \varepsilon }$ %	10.70	$\mu_{ \varepsilon }$ %	1.73

Figure 2.5 plots the comparison of the FPDF estimates obtained using the ISEE method and the P, cVM, mVM, and New approximations for a linear SDOF system with damping ratio $\xi = 0.023$ for a normalized threshold $\zeta = 4.87$.

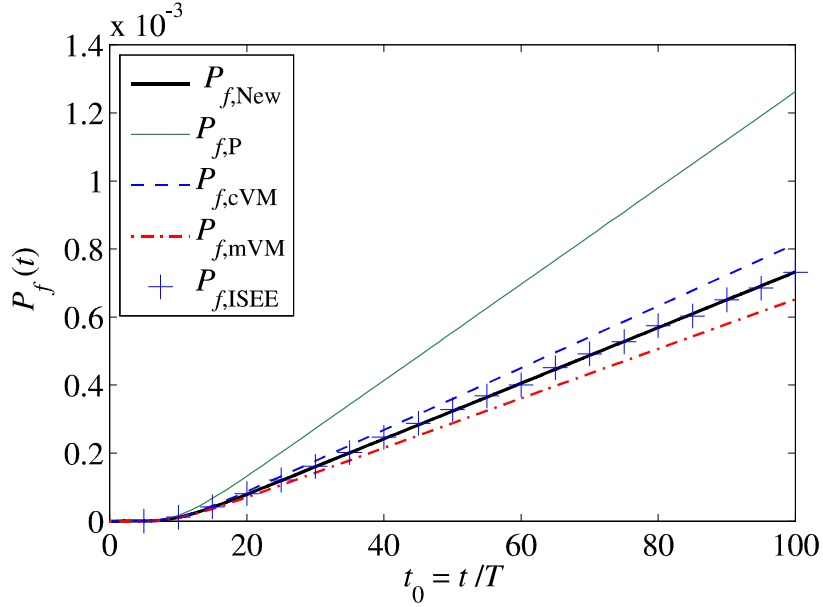


Figure 2.5 - FFPF for a linear elastic SDOF system subjected to WN base excitation from at-rest initial conditions ($\xi = 0.23$; $\zeta = 4.87$).

It is noteworthy that the damping ratio and the normalized threshold values used in this example are not included among the values used to define the functions $C_{1,\infty}(\xi, \zeta)$ and $C_{2,\infty}(\xi, \zeta)$. The agreement between the results obtained using the ISEE method and the New approximation is excellent over the entire range of normalized time, clearly showing that the New approximation is superior to all other considered analytical approximations for this input loading case.

2.4.3 Results for Linear SDOF Systems Subjected to WN Excitation Modulated in Time by a Shinozuka-Sato Function

For linear SDOF systems subjected to time-modulated WN excitation, the time-variant FFPF depends on both the time, t , and the natural period of the system, T . Table 2.4 presents the FFPF values obtained using the ISEE method and the four analytical approximations considered for SDOF oscillators with $T = 1.0s$ and with different damping ratios at $t = 20s$. The FFPF values range from a maximum value of 0.750 to a minimum value of $1.33 \cdot 10^{-3}$. Also in this case, the P

approximation largely overestimates the FPDF, the cVM approximation tends to overestimate the FPDF (particularly for small damping ratios), and the mVM approximation underestimates the FPDF (particularly for high thresholds). The New approximation is the most accurate among the analytical approximations (with $\mu_{|\varepsilon|} = 5.69\%$), even if it underestimates the FPDF for small damping ratios.

Table 2.4 - Time-variant FPDF computed at $t = 20\text{s}$ for linear elastic SDOF systems with $T = 1.0\text{s}$ subjected to WN base excitation time modulated by a Shinozuka-Sato function.

ζ	ξ	ISEE	P	ε [%]	cVM	ε [%]	mVM	ε [%]	New	ε [%]	
2	0.01	3.90E-01	9.21E-01	136.15	5.00E-01	28.16	3.77E-01	-3.38	3.21E-01	-17.62	
	0.05	4.99E-01	7.83E-01	56.83	5.61E-01	12.37	4.88E-01	-2.24	4.87E-01	-2.48	
	0.10	5.95E-01	7.53E-01	26.53	6.07E-01	2.02	5.56E-01	-6.47	5.99E-01	0.69	
	0.50	7.50E-01	7.41E-01	-1.23	7.09E-01	-5.43	6.97E-01	-7.11	7.40E-01	-1.30	
3	0.01	4.01E-02	1.37E-01	240.73	4.94E-02	23.33	3.46E-02	-13.59	3.36E-02	-16.12	
	0.05	4.95E-02	8.47E-02	71.03	5.36E-02	8.21	4.50E-02	-9.12	4.84E-02	-2.38	
	0.10	5.87E-02	7.76E-02	32.32	5.81E-02	-0.91	5.21E-02	-11.15	5.99E-02	2.07	
	0.50	7.43E-02	7.52E-02	1.27	6.98E-02	-6.00	6.84E-02	-7.93	7.25E-02	-2.33	
4	0.01	1.33E-03	3.38E-03	154.94	1.45E-03	9.36	1.03E-03	-22.39	1.09E-03	-17.68	
	0.05	1.51E-03	2.05E-03	36.22	1.47E-03	-2.32	1.26E-03	-16.25	1.48E-03	-1.95	
	0.10	1.65E-03	1.87E-03	13.42	1.55E-03	-6.40	1.41E-03	-14.41	1.67E-03	0.90	
	0.50	1.80E-03	1.81E-03	0.62	1.74E-03	-3.12	1.72E-03	-4.35	1.75E-03	-2.78	
				ε_{\max} %	240.73	ε_{\max} %	28.16	ε_{\max} %	-2.24	ε_{\max} %	2.07
				ε_{\min} %	-1.23	ε_{\min} %	-6.40	ε_{\min} %	-22.39	ε_{\min} %	-17.68
				$\mu_{ \varepsilon }$ %	64.27	$\mu_{ \varepsilon }$ %	8.97	$\mu_{ \varepsilon }$ %	9.87	$\mu_{ \varepsilon }$ %	5.69

Figure 2.6 plots the comparison of the FPDF estimates obtained using the ISEE method and the P, cVM, mVM, and New approximations for a linear SDOF system with $T = 1.0\text{s}$ and $\xi = 0.42$ for a normalized threshold value $\zeta = 3.5$. The New approximation provides the best agreement with the ISEE results among all analytical approximations considered here.

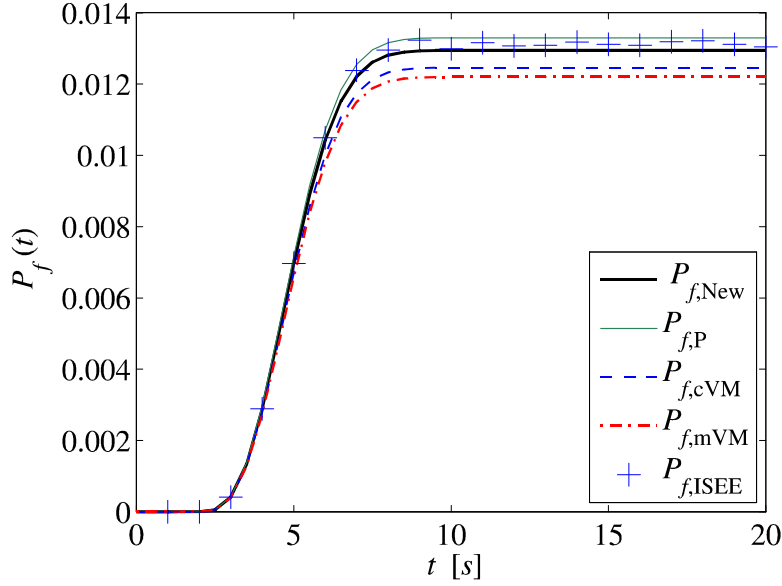


Figure 2.6 - FPF for a linear elastic SDOF system with $T = 1.0\text{s}$ subjected to WN base excitation with Shinozuka-Sato modulating function ($\xi = 0.42$; $\zeta = 3.5$).

2.4.4 Results for Linear SDOF Systems Subjected to KT Excitation from At-rest Initial Conditions

For linear SDOF systems subjected to non-white excitation, the time-variant FPF depends on the time, t , and the natural period of the system, T . Table 2.5 through Table 2.7 compare the FPF values computed using the ISEE method and the four analytical approximations considered in this thesis for linear SDOF systems with $T = 0.1\text{s}$, $T = 0.5\text{s}$ and $T = 1.0\text{s}$, respectively, subjected to a KT excitation from at-rest initial conditions.

The following observations are made: (1) the P approximation largely overestimates the FPF, with very large errors for small values of the damping ratio; (2) the cVM approximation tends to overestimate the FPF, particularly for low damping ratios and low thresholds; and (3) the mVM tends to underestimate the FPF. Again, the New approximation is more accurate than the other analytical approximations, particularly in the case of $T = 1.0\text{s}$, in which the New approximation presents an accuracy similar to the one achieved in the case of linear SDOF systems subjected to WN excitation from at-rest initial conditions.

Table 2.5 - Time-variant FFPF computed at $t = 1.0s$ for linear elastic SDOF system with $T = 0.1s$ subjected to KT base excitation from at-rest initial conditions.

ζ	ξ	ISEE	P	ε [%]	cVM	ε [%]	mVM	ε [%]	New	ε [%]
2	0.01	1.60E-01	3.74E-01	133.71	2.18E-01	36.11	1.79E-01	12.05	1.78E-01	11.16
	0.05	6.84E-01	8.55E-01	25.04	7.06E-01	3.26	6.50E-01	-5.01	6.92E-01	1.12
	0.10	8.05E-01	8.72E-01	8.31	7.71E-01	-4.22	7.30E-01	-9.25	7.90E-01	-1.86
	0.50	7.97E-01	7.84E-01	-1.56	7.32E-01	-8.17	7.10E-01	-10.88	7.75E-01	-2.71
3	0.01	5.02E-03	9.68E-03	93.05	6.00E-03	19.73	4.92E-03	-1.89	4.75E-03	-5.33
	0.05	9.30E-02	1.30E-01	39.45	9.27E-02	-0.27	8.18E-02	-12.05	8.93E-02	-4.00
	0.10	1.29E-01	1.49E-01	15.32	1.17E-01	-9.19	1.07E-01	-16.74	1.22E-01	-5.61
	0.50	1.12E-01	1.17E-01	4.40	1.04E-01	-7.68	9.98E-02	-11.23	1.12E-01	-0.76
4	0.01	3.44E-05	5.60E-05	62.90	3.96E-05	15.26	3.31E-05	-3.62	3.17E-05	-7.69
	0.05	3.13E-03	3.71E-03	18.32	2.92E-03	-6.72	2.62E-03	-16.41	2.82E-03	-10.00
	0.10	4.35E-03	4.65E-03	6.90	3.97E-03	-8.72	3.69E-03	-14.98	4.09E-03	-5.97
	0.50	3.56E-03	3.75E-03	5.37	3.49E-03	-1.72	3.40E-03	-4.35	3.65E-03	2.78
			ε_{\max} %	133.71	ε_{\max} %	36.11	ε_{\max} %	12.05	ε_{\max} %	11.16
			ε_{\min} %	-1.56	ε_{\min} %	-9.19	ε_{\min} %	-16.74	ε_{\min} %	-10.00
			$\mu_{ \varepsilon }$ %	34.53	$\mu_{ \varepsilon }$ %	10.09	$\mu_{ \varepsilon }$ %	9.87	$\mu_{ \varepsilon }$ %	4.91

Table 2.6 - Time-variant FFPF computed at $t = 5.0s$ for linear elastic SDOF system with $T = 0.5s$ subjected to KT base excitation from at-rest initial conditions.

ζ	ξ	ISEE	P	ε [%]	cVM	ε [%]	mVM	ε [%]	New	ε [%]
2	0.01	1.20E-01	3.39E-01	182.15	1.49E-01	24.35	1.12E-01	-6.92	1.09E-01	-9.49
	0.05	5.94E-01	8.69E-01	46.43	6.39E-01	7.66	5.56E-01	-6.37	6.31E-01	6.30
	0.10	7.91E-01	9.09E-01	14.92	7.68E-01	-2.92	7.09E-01	-10.40	7.41E-01	-6.29
	0.50	9.23E-01	9.29E-01	0.63	8.99E-01	-2.61	8.85E-01	-4.09	9.31E-01	0.80
3	0.01	3.34E-03	7.66E-03	129.25	3.67E-03	9.85	2.73E-03	-18.30	3.20E-03	-4.38
	0.05	7.56E-02	1.34E-01	77.18	7.94E-02	4.97	6.51E-02	-13.87	8.89E-02	17.49
	0.10	1.26E-01	1.69E-01	34.14	1.18E-01	-6.12	1.03E-01	-17.93	1.25E-01	-0.92
	0.50	1.92E-01	1.93E-01	0.75	1.73E-01	-9.80	1.67E-01	-12.88	1.87E-01	-2.32
4	0.01	2.21E-05	3.83E-05	73.04	2.16E-05	-2.46	1.64E-05	-26.13	2.02E-05	-8.59
	0.05	2.65E-03	3.80E-03	43.07	2.54E-03	-4.31	2.12E-03	-20.28	2.97E-03	12.02
	0.10	4.48E-03	5.28E-03	18.06	4.08E-03	-8.80	3.63E-03	-19.00	4.44E-03	-0.71
	0.50	6.33E-03	6.41E-03	1.37	6.01E-03	-4.96	5.87E-03	-7.27	6.29E-03	-0.55
			ε_{\max} %	182.15	ε_{\max} %	24.35	ε_{\max} %	-4.09	ε_{\max} %	17.49
			ε_{\min} %	0.63	ε_{\min} %	-9.80	ε_{\min} %	-26.13	ε_{\min} %	-9.49
			$\mu_{ \varepsilon }$ %	51.75	$\mu_{ \varepsilon }$ %	7.40	$\mu_{ \varepsilon }$ %	13.62	$\mu_{ \varepsilon }$ %	5.82

Table 2.7 - Time-variant FFPF computed at $t = 10.0s$ for linear elastic SDOF system with $T = 1.0s$ subjected to KT base excitation from at-rest initial conditions.

ζ	ξ	ISEE	P	ε [%]	cVM	ε [%]	mVM	ε [%]	New	ε [%]	
2	0.01	1.22E-01	3.42E-01	180.89	1.66E-01	36.11	1.28E-01	5.15	1.21E-01	-0.56	
	0.05	6.12E-01	8.71E-01	42.32	6.76E-01	10.55	6.03E-01	-1.37	6.06E-01	-0.95	
	0.10	8.00E-01	9.10E-01	13.76	7.98E-01	-0.23	7.51E-01	-6.17	7.89E-01	-1.47	
	0.50	9.50E-01	9.36E-01	-1.46	9.19E-01	-3.34	9.10E-01	-4.27	9.40E-01	-1.09	
3	0.01	3.55E-03	7.80E-03	119.71	4.10E-03	15.43	3.15E-03	-11.30	3.32E-03	-6.41	
	0.05	7.83E-02	1.35E-01	72.10	8.64E-02	10.35	7.30E-02	-6.75	7.85E-02	0.16	
	0.10	1.31E-01	1.70E-01	29.23	1.27E-01	-3.54	1.14E-01	-13.50	1.31E-01	-0.53	
	0.50	1.99E-01	2.00E-01	0.69	1.85E-01	-7.30	1.80E-01	-9.47	1.94E-01	-2.42	
4	0.01	2.32E-05	3.94E-05	69.97	2.41E-05	4.08	1.89E-05	-18.46	2.27E-05	-2.11	
	0.05	2.71E-03	3.82E-03	41.17	2.74E-03	1.26	2.35E-03	-13.07	2.78E-03	2.51	
	0.10	4.67E-03	5.32E-03	14.03	4.34E-03	-7.02	3.95E-03	-15.30	4.72E-03	1.09	
	0.50	6.65E-03	6.68E-03	0.38	6.38E-03	-4.13	6.28E-03	-5.64	6.46E-03	-2.82	
				ε_{\max} %	180.89	ε_{\max} %	36.11	ε_{\max} %	5.15	ε_{\max} %	2.51
				ε_{\min} %	-1.46	ε_{\min} %	-7.30	ε_{\min} %	-18.46	ε_{\min} %	-6.41
				$\mu_{ \varepsilon }$ %	48.81	$\mu_{ \varepsilon }$ %	8.61	$\mu_{ \varepsilon }$ %	9.20	$\mu_{ \varepsilon }$ %	1.84

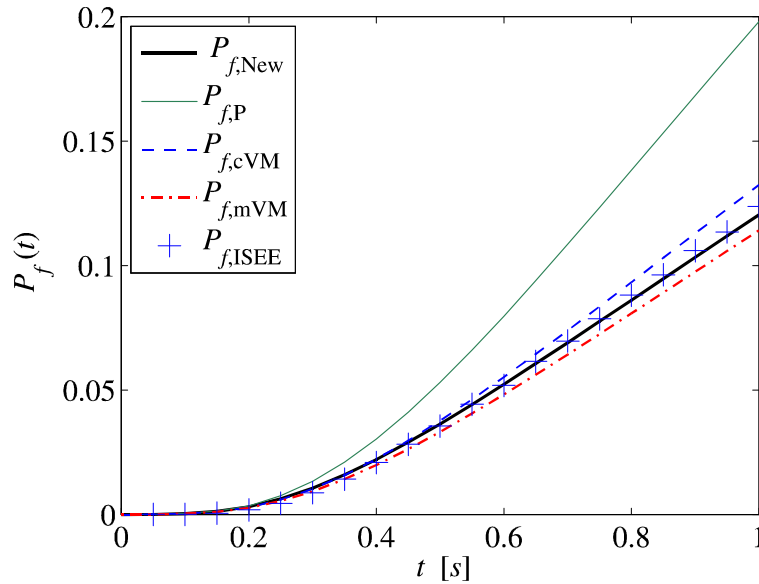


Figure 2.7 - FFPF for a linear elastic SDOF system with $T = 0.1s$ subjected to KT base excitation from at-rest initial conditions ($\xi = 0.035$; $\zeta = 3$).

Figure 2.7 plots the comparison of the FPDF estimates obtained using the ISEE method and the P, cVM, mVM, and New approximations for a linear SDOF system with $T = 0.1s$ and $\xi = 0.035$, for a normalized threshold value $\zeta = 3.0$. It is observed that the P approximation significantly overestimates the FPDF, the two Vanmarcke's approximations provide an upper and a lower bound of the FPDF, and the New approximation is in very good agreement with the ISEE results.

2.4.5 Results for Linear SDOF Systems Subjected to KT Excitation Modulated in Time by a Shinozuka-Sato Function

Table 2.8 through Table 2.10 compare the FPDF values computed using the ISEE method and the four analytical approximations considered in this thesis for linear SDOF systems with $T = 0.1s$, $T = 0.5s$, and $T = 1.0s$, respectively, subjected to a KT excitation modulated in time by a Shinozuka-Sato function.

The observations regarding the absolute and relative accuracy of the analytical approximations are very similar to the observations made in the previous cases. In particular, the New approximation is much more accurate than the P approximation and significantly more accurate than both the cVM and mVM approximations.

Figure 2.8 plots the comparison of the FPDF estimates obtained using the ISEE method and the P, cVM, mVM, and New approximations for a linear SDOF system with $T = 1.0s$ and $\xi = 0.22$, for a normalized threshold value $\zeta = 2.2$. In this case, the P and cVM approximations provide an upper and a lower bound, respectively, for the FPDF, while the New approximation is in excellent agreement with the ISEE results.

Table 2.8 - FPDF computed at $t = 20.0s$ for linear elastic SDOF system with $T = 0.1s$ subjected to KT base excitation time modulated by a Shinozuka-Sato function.

ζ	ξ	ISEE	P	ε [%]	cVM	ε [%]	mVM	ε [%]	New	ε [%]
2	0.01	8.74E-01	1	14.45	9.93E-01	13.67	9.73E-01	11.35	9.31E-01	6.52
	0.05	9.92E-01	1	0.80	9.99E-01	0.75	9.98E-01	0.62	9.99E-01	0.71
	0.10	9.90E-01	1	1.05	1	1.02	9.99E-01	0.97	1	1.03
	0.50	9.93E-01	1	0.64	9.99E-01	0.55	9.98E-01	0.49	9.99E-01	0.63
3	0.01	1.67E-01	5.46E-01	226.13	2.94E-01	75.81	2.28E-01	36.07	1.76E-01	5.23
	0.05	3.86E-01	5.04E-01	30.35	3.85E-01	-0.50	3.45E-01	-10.85	3.68E-01	-4.91
	0.10	4.45E-01	4.74E-01	6.51	3.94E-01	-11.59	3.66E-01	-17.74	4.05E-01	-9.08
	0.50	3.59E-01	3.63E-01	1.01	3.29E-01	-8.45	3.18E-01	-11.37	3.48E-01	-3.04
4	0.01	6.87E-03	1.81E-02	163.96	9.66E-03	40.61	7.34E-03	6.85	5.58E-03	-18.83
	0.05	1.40E-02	1.61E-02	15.02	1.26E-02	-9.87	1.13E-02	-19.60	1.20E-02	-14.10
	0.10	1.44E-02	1.48E-02	3.12	1.27E-02	-11.61	1.18E-02	-17.67	1.30E-02	-9.28
	0.50	1.03E-02	1.04E-02	0.52	9.74E-03	-5.81	9.48E-03	-8.24	1.01E-02	-1.82
			ε_{\max} %	226.13	ε_{\max} %	75.81	ε_{\max} %	36.07	ε_{\max} %	5.23
			ε_{\min} %	0.52	ε_{\min} %	-11.61	ε_{\min} %	-19.60	ε_{\min} %	-18.83
			$\mu_{ \varepsilon }$ %	38.63	$\mu_{ \varepsilon }$ %	15.02	$\mu_{ \varepsilon }$ %	11.82	$\mu_{ \varepsilon }$ %	6.27

Table 2.9 - FPDF computed at $t = 20.0s$ for linear elastic SDOF system with $T = 0.5s$ subjected to KT base excitation time modulated by a Shinozuka-Sato function.

ζ	ξ	ISEE	P	ε [%]	cVM	ε [%]	mVM	ε [%]	New	ε [%]
2	0.01	4.56E-01	9.80E-01	114.93	6.23E-01	36.55	4.73E-01	3.74	4.19E-01	-8.12
	0.05	6.80E-01	9.40E-01	38.16	7.44E-01	9.35	6.57E-01	-3.37	6.43E-01	-5.45
	0.10	8.12E-01	9.36E-01	15.23	8.11E-01	-0.14	7.55E-01	-7.08	7.90E-01	-2.72
	0.50	9.45E-01	9.33E-01	-1.36	9.02E-01	-4.58	8.89E-01	-5.94	9.31E-01	-1.52
3	0.01	4.83E-02	2.03E-01	319.65	6.84E-02	41.54	4.64E-02	-4.05	4.86E-02	0.47
	0.05	8.21E-02	1.50E-01	82.93	8.82E-02	7.39	7.18E-02	-12.50	8.00E-02	-2.57
	0.10	1.09E-01	1.47E-01	35.21	1.03E-01	-5.02	9.01E-02	-17.09	1.10E-01	1.12
	0.50	1.45E-01	1.45E-01	-0.47	1.30E-01	-10.54	1.26E-01	-13.55	1.40E-01	-3.71
4	0.01	1.68E-03	5.25E-03	212.60	2.04E-03	21.30	1.39E-03	-17.13	1.48E-03	-11.54
	0.05	2.58E-03	3.77E-03	46.12	2.50E-03	-3.21	2.07E-03	-19.82	2.36E-03	-8.43
	0.10	3.17E-03	3.68E-03	16.13	2.86E-03	-9.89	2.54E-03	-19.97	3.10E-03	-2.20
	0.50	3.60E-03	3.61E-03	0.44	3.40E-03	-5.46	3.32E-03	-7.69	3.55E-03	-1.45
			ε_{\max} %	319.65	ε_{\max} %	41.54	ε_{\max} %	-4.05	ε_{\max} %	1.12
			ε_{\min} %	-0.47	ε_{\min} %	-10.54	ε_{\min} %	-19.97	ε_{\min} %	-11.54
			$\mu_{ \varepsilon }$ %	73.60	$\mu_{ \varepsilon }$ %	12.91	$\mu_{ \varepsilon }$ %	10.99	$\mu_{ \varepsilon }$ %	4.11

Table 2.10 - FFPF computed at $t = 20.0s$ for linear elastic SDOF system with $T = 1.0s$ subjected to KT base excitation time modulated by a Shinozuka-Sato function.

ζ	ξ	ISEE	P	ϵ [%]	cVM	ϵ [%]	mVM	ϵ [%]	New	ϵ [%]	
2	0.01	3.94E-01	9.21E-01	133.80	4.96E-01	25.79	3.72E-01	-5.54	3.26E-01	-17.28	
	0.05	4.94E-01	7.85E-01	58.96	5.59E-01	13.11	4.85E-01	-1.92	4.85E-01	-1.87	
	0.10	6.03E-01	7.57E-01	25.52	6.07E-01	0.59	5.55E-01	-8.05	5.97E-01	-1.04	
	0.50	7.64E-01	7.54E-01	-1.25	7.18E-01	-6.00	7.04E-01	-7.86	7.54E-01	-1.30	
3	0.01	4.00E-02	1.37E-01	242.28	4.89E-02	22.37	3.41E-02	-14.59	3.44E-02	-13.94	
	0.05	4.89E-02	8.53E-02	74.40	5.34E-02	9.16	4.47E-02	-8.70	4.95E-02	1.20	
	0.10	6.02E-02	7.86E-02	30.57	5.83E-02	-3.21	5.21E-02	-13.57	6.10E-02	1.27	
	0.50	7.82E-02	7.80E-02	-0.14	7.18E-02	-8.07	7.01E-02	-10.26	7.52E-02	-3.79	
4	0.01	1.34E-03	3.39E-03	153.24	1.44E-03	7.35	1.02E-03	-24.13	1.08E-03	-18.98	
	0.05	1.51E-03	2.07E-03	37.03	1.47E-03	-2.66	1.25E-03	-16.89	1.50E-03	-0.46	
	0.10	1.69E-03	1.90E-03	12.40	1.55E-03	-8.00	1.41E-03	-16.20	1.70E-03	0.46	
	0.50	1.84E-03	1.88E-03	2.34	1.80E-03	-1.97	1.78E-03	-3.44	1.82E-03	-1.19	
				ϵ_{\max} %	242.28	ϵ_{\max} %	22.37	ϵ_{\max} %	-3.44	ϵ_{\max} %	1.27
				ϵ_{\min} %	-0.14	ϵ_{\min} %	-8.07	ϵ_{\min} %	-24.13	ϵ_{\min} %	-18.98
				$\mu_{ \epsilon }$ %	64.33	$\mu_{ \epsilon }$ %	9.02	$\mu_{ \epsilon }$ %	10.93	$\mu_{ \epsilon }$ %	5.23

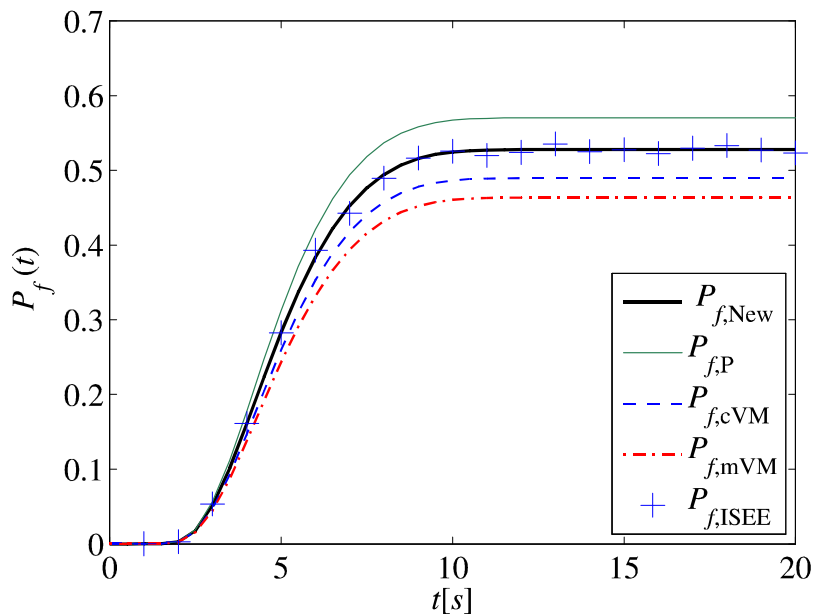


Figure 2.8 - FFPF for a linear elastic SDOF system with $T = 1.0s$ subjected to KT base excitation with Shinozuka-Sato modulating function ($\xi = 0.22$; $\zeta = 2.2$).

2.5 FFPF DEPENDENCY ON NORMALIZED TIME

The time-variant FFPF for a linear SDOF system subjected to a WN excitation from at-rest initial conditions can be expressed as a function of normalized time, normalized threshold, and damping ratio only. This fact can be shown by comparing the ISEE results for the FFPF obtained for SDOF systems with different natural periods, see Figure 2.9, and can be expressed mathematically as:

$$P_{f,|x|}(x_{\text{lim}}, t) = 1 - \exp\left\{-\int_0^t h_{|x|}(x_{\text{lim}}, \tau) \cdot d\tau\right\} = 1 - \exp\left\{-\int_0^{t_0} \bar{h}_{|x|}(\zeta, \tau_0) \cdot d\tau_0\right\} = \bar{P}_{f,|x|}(\zeta, t_0) \quad (2.11)$$

A superposed bar indicates a function that depends on time and natural period only through the normalized time t_0 . Eq. (2.11) implies that, for any natural period T , the following relation holds:

$$h_{|x|}(x_{\text{lim}}, t) = \frac{1}{T} \cdot \bar{h}_{|x|}(\zeta, t_0) \quad (2.12)$$

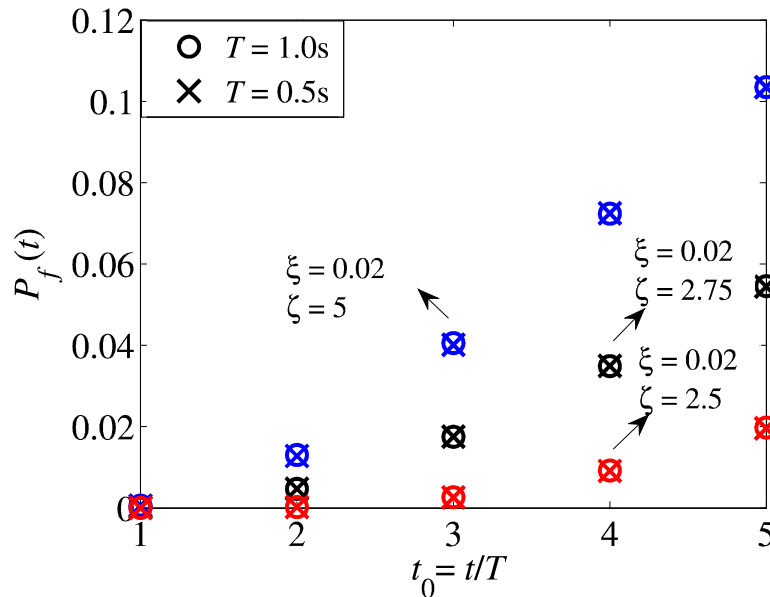


Figure 2.9 - Comparison of FFPF for linear elastic SDOF with $T = 1.0s$ and $T = 0.5s$ subjected to WN base excitation from at-rest initial conditions.

It can be demonstrated that the analytical approximations of the hazard functions of P, cVM and mVM satisfy Eq. (2.12). It is sufficient to prove that Eq. (2.12) is satisfied by the newly proposed hazard function given in Eq. (2.1). It has been shown that the bandwidth parameter can be expressed as a function of the normalized time, i.e., $q_X(t) = \bar{q}_X(t_0)$ [15]. This relation also implies that $C_1(\xi, \zeta, t) = \bar{C}_1(\xi, \zeta, t_0)$ and $C_2(\xi, \zeta, t) = \bar{C}_2(\xi, \zeta, t_0)$. From the closed-form solutions for the second-order statistics of the displacement and velocity response of a linear SDOF system subjected to a WN excitation with at-rest initial conditions [9], it can be also shown that

$$\sigma_X^2(t) = \sigma_{X\infty}^2 \cdot \bar{\sigma}_X^2(t_0) \quad (2.13)$$

$$\sigma_{\dot{X}}^2(t) = \frac{\sigma_{\dot{X}\infty}^2}{T^2} \cdot \bar{\sigma}_{\dot{X}}^2(t_0) \quad (2.14)$$

$$K_{X\dot{X}}(t) = \frac{\sigma_{X\infty}^2}{T} \cdot \bar{K}_{X\dot{X}}(t_0) \quad (2.15)$$

in which $K_{X\dot{X}}(t)$ = cross-covariance of the displacement and velocity responses of the linear SDOF system. The relation $\omega_0 \cdot t = 2 \cdot \pi \cdot t_0$ is used in Eqs. (2.13) through (2.15). Thus, the following relations are also valid:

$$\rho_{X\dot{X}}(t) = \frac{K_{X\dot{X}}(t)}{\sigma_X(t) \cdot \sigma_{\dot{X}}(t)} = \frac{\frac{\sigma_{X\infty}^2}{T} \cdot \bar{K}_{X\dot{X}}(t_0)}{\frac{\sigma_{X\infty}^2}{T} \cdot \sqrt{\bar{\sigma}_X(t_0) \cdot \bar{\sigma}_{\dot{X}}(t_0)}} = \bar{\rho}_{X\dot{X}}(t_0) \quad (2.16)$$

$$r(t) = \frac{\rho_{X\dot{X}}(t)}{\sqrt{2 \cdot [1 - \rho_{X\dot{X}}^2(t)]}} \cdot \left[\frac{x_{\text{lim}}}{\sigma_X(t)} \right] = \frac{\bar{\rho}_{X\dot{X}}(t_0)}{\sqrt{2 \cdot [1 - \bar{\rho}_{X\dot{X}}^2(t_0)]}} \cdot \left[\frac{\zeta}{\bar{\sigma}_X(t_0)} \right] = \bar{r}(t_0) \quad (2.17)$$

$$\begin{aligned}
v_{|X|}(x_{\text{lim}}, t) &= \frac{\sigma_{\dot{X}}(t) \cdot \sqrt{1 - \rho_{\dot{X}\dot{X}}^2(t)}}{\pi \cdot \sigma_X(t)} \cdot \exp\left(-\frac{r(t)}{\rho_{\dot{X}\dot{X}}^2(t)}\right) \cdot \left\{1 + \sqrt{\pi} \cdot r(t) \cdot \exp[r^2(t)] \cdot \text{erfc}(-r(t))\right\} \\
&= \frac{\bar{\sigma}_{\dot{X}}(t_0) \cdot \sqrt{1 - \bar{\rho}_{\dot{X}\dot{X}}^2(t_0)}}{T \cdot \pi \cdot \bar{\sigma}_X(t_0)} \cdot \exp\left(-\frac{\bar{r}(t_0)}{\bar{\rho}_{\dot{X}\dot{X}}^2(t_0)}\right) \cdot \left\{1 + \sqrt{\pi} \cdot \bar{r}(t_0) \cdot \exp[\bar{r}^2(t_0)] \cdot \text{erfc}(-\bar{r}(t_0))\right\} \quad (2.18) \\
&= \frac{1}{T} \cdot \bar{v}_{|X|}(\zeta, t_0)
\end{aligned}$$

Finally, the following relation is obtained:

$$\begin{aligned}
h_{\text{New}, |X|}(x_{\text{lim}}, t) &= v_{|X|}(x_{\text{lim}}, t) \cdot \exp[C_2(\xi, \zeta, t)] \cdot \frac{1 - \exp\left\{-\sqrt{\pi/2} \cdot [q_X(t)]^{C_1(\xi, \zeta, t)} \cdot \frac{x_{\text{lim}}}{\sigma_X(t)}\right\}}{1 - \exp\left\{-\frac{1}{2} \cdot \left[\frac{x_{\text{lim}}}{\sigma_X(t)}\right]^2\right\}} \\
&= \frac{1}{T} \bar{v}_{|X|}(\zeta, t_0) \cdot \exp[\bar{C}_2(\xi, \zeta, t_0)] \cdot \frac{1 - \exp\left\{-\sqrt{\pi/2} \cdot [\bar{q}_X(t_0)]^{\bar{C}_1(\xi, \zeta, t_0)} \cdot \frac{\zeta}{\bar{\sigma}_X(t_0)}\right\}}{1 - \exp\left\{-\frac{1}{2} \cdot \left[\frac{\zeta}{\bar{\sigma}_X(t_0)}\right]^2\right\}} \quad (2.19) \\
&= \frac{1}{T} \cdot \bar{h}_{\text{New}, |X|}(\zeta, t_0)
\end{aligned}$$

2.6 CONCLUSIONS

This chapter explores the classical first-passage reliability problem for linear elastic SDOF oscillators subjected to stationary and/or non-stationary Gaussian excitations modeled as separable non-stationary processes. Existing analytical approximations (i.e., the P, cVM, and mVM approximations) are reviewed and compared in terms of absolute and relative accuracy in estimating the time-variant FPDF.

A new analytical approximation of the FPDF for linear SDOF systems is proposed by modifying the cVM hazard function. This new approximation is verified by comparing its analytical estimates of the FPDF with the corresponding results obtained using existing analytical

approximations and the ISEE method for a wide range of damping ratios, natural periods, and threshold levels. Different types of stochastic input excitations are considered, including white and non-white spectra, with a sudden application of the loads (i.e., with a unit step time-modulating function) or with a load modulated in time by using a Shinozuka-Sato function. It is found that (1) the P approximation generally overestimates (sometimes by a large factor) the FPDF, (2) the two Vanmarcke's approximations are significantly more accurate than the P approximation, (3) the cVM approximation tends to overestimate the FPDF, (4) the mVM approximation tends to underestimate the FPDF, (5) the relative accuracy of the two Vanmarcke's approximation is different on a case-by-case basis, and (6) the newly proposed analytical approximation of the hazard function yields significantly improved estimates of the FPDF when compared with P, cVM, and mVM approximations.

3 FPDF FOR LINEAR MDOF OSCILLATORS

3.1 INTRODUCTION

This chapter presents the results of the research performed to gain a better insight into the first-passage reliability problem of MDOF systems subjected to stationary and/or nonstationary excitations. The use of the real-valued and complex-valued modal analysis methods in the context of stochastic dynamics is illustrated. Several application examples are used to study the convergence rate of spectral characteristics and analytical failure probability estimates obtained using modal truncation with increasing number of modes. These application examples include the analysis of: (1) the roof displacement response of four shear-type MDOF systems subjected to both stationary and nonstationary random excitations, (2) the roof displacement response of a finite element (FE) model of an actual 13-story welded steel building, and (3) the relative displacement response of two adjacent buildings modeled as SDOF systems subjected to seismic pounding hazard.

3.2 USE OF MODAL TRUNCATION IN FPDF OF LINEAR MDOF OSCILLATORS

The application of modal truncation for the FPDF of MDOF linear oscillators requires the use of the spectral characteristics which are obtained from the truncated modal response values. The response values are calculated considering only the contributions of the first p modes ($p < n$, $n =$ total number of DOFs of the system).

3.2.1 Response Variance Computed Using Real-valued Modal Analysis

The spectral characteristics for computation of the FPDF of the response of MDOF systems are discussed in Chapter 1. The auto-covariance matrix function corresponding to the truncated modal response is obtained as:

$$E[\mathbf{u}(t) \cdot \mathbf{u}^T(t)] \approx E\left[\left(\sum_{r=1}^p \boldsymbol{\phi}_r \cdot q_r(t)\right) \cdot \left(\sum_{s=1}^p \boldsymbol{\phi}_s \cdot q_s(t)\right)\right] = \boldsymbol{\Phi}_{(p)} \cdot E[\mathbf{q}_{(p)}(t) \cdot \mathbf{q}_{(p)}^T(t)] \cdot \boldsymbol{\Phi}_{(p)}^T \quad (3.1)$$

3.2.2 Response Variance Computed Using Complex-valued Modal Analysis

In stochastic dynamic analysis of complex-valued nonstationary random processes, the normalized complex modal response vectors are obtained using the equations discussed in Chapter 1. The auto-covariance matrix function using the modal truncation for the contributions of the first $2p$ complex modes is given as:

$$E[\mathbf{Z}(t) \cdot \mathbf{Z}^T(t)] \approx \tilde{\mathbf{T}}_{2n \times 2p}^* \cdot E[\mathbf{S}_{2p \times 1}^*(t) \cdot \mathbf{S}_{1 \times 2p}^T(t)] \cdot \tilde{\mathbf{T}}_{2p \times 2n}^T \quad (3.2)$$

where $\tilde{\mathbf{T}}_{2n \times 2p}$ = effective modal participation factor which includes the contributions of the first $2p$ complex modes. The cross-covariance matrix function between the response vector $\mathbf{Z}(t)$ and the auxiliary process vector $\boldsymbol{\Xi}(t)$ using modal truncation is computed as:

$$E[\mathbf{Z}(t) \cdot \boldsymbol{\Xi}^T(t)] \approx \tilde{\mathbf{T}}_{2n \times 2p}^* \cdot E[\mathbf{S}_{2p \times 1}^*(t) \cdot \boldsymbol{\Sigma}_{1 \times 2p}^T(t)] \cdot \tilde{\mathbf{T}}_{2p \times 2n}^T \quad (3.3)$$

where

$$\boldsymbol{\Sigma}_{2p \times 1}(t) = [\Sigma_1(t), \Sigma_2(t), \dots, \Sigma_p(t), \Sigma_{n+1}(t), \Sigma_{n+2}(t), \dots, \Sigma_{n+p}(t)]^T \quad (3.4)$$

3.3 EXTENSION OF THE NEWLY PROPOSED ANALYTICAL APPROXIMATION TO MDOF SYSTEMS

The newly proposed hazard function for SDOF systems subjected to both stationary and nonstationary random processes is used here to find the FPDF of linear MDOF systems as well.

The proposed hazard function for SDOF systems is defined as:

$$h_{\text{New},|X|}(x_{\text{lim}}, t) = v_{|X|}(x_{\text{lim}}, t) \cdot \exp[C_2(\xi, \zeta, t)] \cdot \frac{1 - \exp\left\{-\sqrt{\pi/2} \cdot [q_X(t)]^{C_1(\xi, \zeta, t)} \cdot \frac{x_{\text{lim}}}{\sigma_X(t)}\right\}}{1 - \exp\left\{-\frac{1}{2} \cdot \left[\frac{x_{\text{lim}}}{\sigma_X(t)}\right]^2\right\}} \quad (3.5)$$

where, $C_1(\xi, \zeta, t)$ and $C_2(\xi, \zeta, t)$ are found using Eqs. (2.2) and (2.3).

In this study, the MDOF systems are subjected to both stationary (white noise excitation from at-rest initial conditions) and nonstationary random excitations. The nonstationary random input has the PSD function of Kanai-Tajimi modified by Clough and Penzien (KT-CP) and is modulated in time with the Shinozuka-Sato modulating function. Several modifications for the hazard function corresponding to nonstationary input processes are proposed in Chapter 2. Two forms of the newly proposed hazard function (differing only in the computation of the equivalent normalized threshold and damping ratio to be used in Eqs. (2.5) and (2.6)) are evaluated for accuracy in this section. The first form of the newly proposed hazard function, referred to as New1, is characterized by the following equivalent damping ratio and normalized threshold:

$$\tilde{\xi} = \xi_1 \quad (3.6)$$

$$\tilde{\zeta}(t) = \frac{x_{\text{lim}}}{\sigma_X(t)} \quad (3.7)$$

where $\xi_1 =$ damping ratio of the first mode of vibration of the MDOF system.

The second form of the newly proposed hazard function, referred to as New2, is characterized by the following equivalent damping ratio and normalized threshold:

$$\xi_{\infty} = \text{zero} \left\{ q_{X,\infty} - \left\{ 1 - \frac{4 \cdot \left[\arctan \left(\sqrt{1 - \xi_1^2} / \xi_1 \right) \right]^2}{\pi^2 \cdot (1 - \xi_1^2)} \right\}^{\frac{1}{2}} \right\} \quad (3.8)$$

$$\tilde{\zeta}(t) = \frac{x_{\text{lim}}}{\sigma_{X,\text{max}} \cdot A(t)} \cdot \frac{G_{X_s X_s}(\omega_1)}{S_0} \quad (3.9)$$

where ω_1 = natural frequency of the MDOF system.

3.4 APPLICATION EXAMPLES

Three application examples are discussed in this section. In the first and second examples, the FPDF for the roof displacement of the MDOF systems are studied using modal truncation. In each case, the convergence rate of the spectral characteristics and the stochastic dynamic results are studied for an increasing number of modes used in the modal truncation. The third example considers the pounding problem of two adjacent buildings, modeled as two SDOF systems for two cases of close and well separated natural periods, and includes the evaluation of the accuracy of analytical FPDF approximations.

3.4.1 Multi-story Shear-type Buildings

Four shear-type buildings with different number of stories (i.e., DOFs) are studied using modal analysis. The material properties and damping coefficients of these systems are presented in Table 3.1.

Table 3.1 - Modeling properties of the shear-type buildings.

# of DOFs	Mass/Floor (ton)	Stiffness (kN/m)	Damping Ratio
2	45	30000	2%
3	28.8	40561.52344	2%
8	454.454	628801	2%
20	454.454	827490.234	2%

3.4.1.1 Input Excitation Models

Two types of excitations are considered in this chapter: (1) a WN excitation, represented by a constant PSD function (i.e., $G_{X_s X_s}(\omega) = S_0$, in which ω = circular frequency, and $S_0 = 1\text{m}^2/\text{s}^3$), and (2) a non-white excitation, modeled using a KT PSD function modified by Clough and Penzien (KT-CP) with the function given as:

$$G_{X_s X_s}(\omega) = \frac{1 + 4 \cdot \xi_g^2 \cdot (\omega/\omega_g)^2}{\left[1 - (\omega/\omega_g)^2\right]^2 + (2 \cdot \xi_g \cdot \omega/\omega_g)^2} \cdot \frac{(\omega/\omega_f)^2}{\left[1 - (\omega/\omega_f)^2\right]^2 + (2 \xi_f \cdot \omega/\omega_f)^2} \cdot S_0 \quad (3.10)$$

where ξ_f and ω_f = damping ratio and the natural frequency of the Clough-Penzien filter. In this study the parameters of the Kanai-Tajimi filter are assumed equal to $\omega_g = 12.5\text{rad/s}$ and $\xi_g = 0.6$, and the parameters of the Clough-Penzien filter are $\omega_f = 2.0\text{rad/s}$ and $\xi_f = 0.7$.

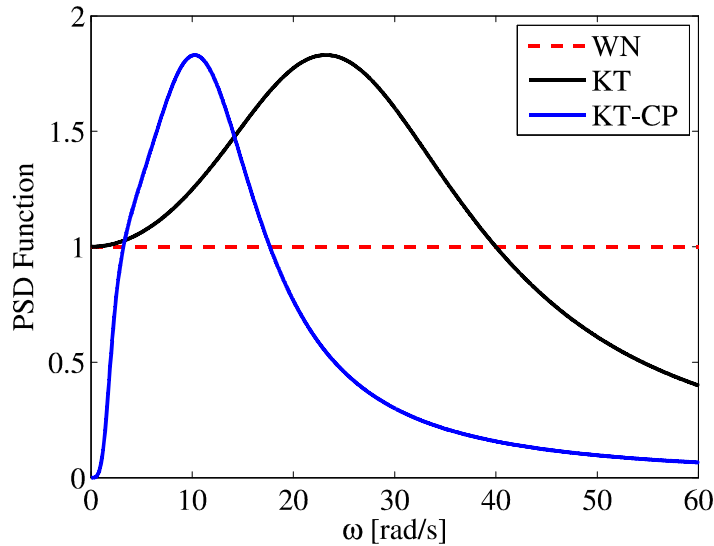


Figure 3.1- Types of PSD functions.

The unit step and Shinozuka-Sato (with parameters $B_1 = 0.2\text{s}^{-1}$; $B_2 = 0.25\text{s}^{-1}$) time-modulating functions are considered in this example. The shear-type buildings are studied subjected to both stationary (WN and unit step time-modulating function) and nonstationary

(KT-CP and Shinozuka-Sato time-modulating function).

The spectral characteristics of the roof displacement response are computed using modal truncation. These spectral characteristics are used to estimate the FPDF of the roof displacement for a given threshold. The time-variant FPDF is calculated for a double-barrier problem with normalized failure threshold level of $\zeta = 4$ using the P, cVM, and mVM analytical approximations, as well as the newly proposed New1 and New2 hazard functions. The convergence rate of results obtained using spectral characteristics computed via modal truncation for each p ($1 \leq p < n$) to the results obtained using the spectral characteristics computed including all modes is studied. Table 3.2 presents the modal analysis results of the four shear-type buildings, including modal periods, T_i , modal circular frequencies, ω_i , modal damping ratios, ξ_i , modal participation factors, Γ_i , and cumulative modal participation factors, $\Gamma_{cum,i}$ ($i = 1, 2, \dots, n$ where $n =$ number of DOFs). The MDOF systems are all classically damped and the classical damping matrix is obtained using the Rayleigh damping model by assuming that the damping ratios correspond to the first and the last mode of vibration of each system are equal to 2%.

3.4.1.2 Stochastic Dynamic Analysis Results

The stochastic dynamic analysis is performed on all four shear-type buildings subjected to stationary and nonstationary random processes and the results are presented in separate tables for each building. These results include the maximum values of displacement variance ($\sigma_{u_{Roof}}^2(t)$), velocity variance ($\sigma_{\dot{u}_{Roof}}^2(t)$), hazard functions based on P ($U_{|u_{Roof}|}(x_{lim}, t)$), cVM ($h_{cVM}(x_{lim}, t)$), mVM ($h_{mVM}(x_{lim}, t)$), New1 ($h_{New1}(x_{lim}, t)$), and New2 ($h_{New2}(x_{lim}, t)$)(for nonstationary cases) approximations, and the corresponding failure probabilities (P, cVM, mVM, New1 and New2).

Table 3.2- Modal analysis results for shear-type buildings.

Mode (<i>i</i>)	T_i [s]	ω_i [rad/s]	ξ_i	Γ_i [%]	$\Gamma_{cum,i}$ [%]
2-story shear-type building					
1	0.3937	15.9576	0.0200	94.7214	94.7214
2	0.1504	41.7775	0.0200	5.2786	100
3-story shear-type building					
1	0.3762	16.7017	0.0200	91.4079	91.4079
2	0.1343	46.7972	0.0168	7.4877	98.8956
3	0.0929	67.6240	0.0200	1.1044	100.0000
8-story shear-type building					
1	0.9154	6.8636	0.0200	85.6332	85.6332
2	0.3086	20.3570	0.0113	9.0828	94.7161
3	0.1895	33.1572	0.0121	2.9656	97.6816
4	0.1402	44.8283	0.0140	1.2894	98.9710
5	0.1143	54.9728	0.0160	0.6111	99.5821
6	0.0993	63.2453	0.0178	0.2819	99.8640
7	0.0906	69.3640	0.0192	0.1104	99.9743
8	0.0859	73.1206	0.0200	0.0257	100
20-story shear-type building					
1	1.9223	3.2685	0.0200	83.0021	83.0021
2	0.6420	9.7864	0.0086	9.1503	92.1524
3	0.3867	16.2469	0.0076	3.2423	95.3947
4	0.2779	22.6120	0.0079	1.6149	97.0096
5	0.2178	28.8444	0.0087	0.9454	97.9550
6	0.1800	34.9075	0.0097	0.6068	98.5618
7	0.1541	40.7658	0.0108	0.4124	98.9742
8	0.1355	46.3849	0.0119	0.2908	99.2650
9	0.1215	51.7317	0.0129	0.2099	99.4749
10	0.1107	56.7750	0.0140	0.1535	99.6284
11	0.1022	61.4851	0.0149	0.1130	99.7414
12	0.0954	65.8344	0.0159	0.0829	99.8243
13	0.0900	69.7973	0.0167	0.0603	99.8847
14	0.0857	73.3507	0.0175	0.0431	99.9278
15	0.0822	76.4735	0.0181	0.0299	99.9577
16	0.0794	79.1477	0.0187	0.0198	99.9775
17	0.0772	81.3573	0.0192	0.0122	99.9897
18	0.0756	83.0895	0.0196	0.0067	99.9964
19	0.0745	84.3341	0.0198	0.0029	99.9993
20	0.0738	85.0838	0.0200	0.0007	100

The results obtained using the modal truncation for each $p < n$ (R_p) are also compared with the results obtained when the contribution of all modes are considered in the response (R_n). These

differences are denoted as error, $\varepsilon[\%] = \frac{R_p - R_n}{R_n} \times 100$.

3.4.1.2.1 Two-story Shear-type Building

As observed from Table 3.2, the first mode of the two-story building contains almost 94.7% of the total mass of the system in the horizontal direction. For the case of stationary random process (Table 3.3), including only the first mode gives a maximum error value of 2.5% for all the reliability measures while it is less than 1% the for the nonstationary case (Table 3.4).

Table 3.3 -Stochastic dynamic analysis results for the horizontal roof drift response of the two-story building subjected to stationary input.

Modes included	#1 to #2	#1	ε [%]
$\max(\sigma_{u_{Roof}}^2(t))$	2.6524E-02	2.6495E-02	-0.1087
$\max(\sigma_{\dot{u}_{Roof}}^2(t))$	6.8000E+00	6.7469E+00	-0.7811
$\max(\nu_{ u_{Roof} }(x_{lim}, t))$	1.7097E-03	1.6892E-03	-1.2007
$\max(h_{cVM}(x_{lim}, t))$	9.4248E-04	9.2421E-04	-1.9391
$\max(h_{mVM}(x_{lim}, t))$	7.2841E-04	7.1222E-04	-2.2226
$\max(h_{New1}(x_{lim}, t))$	7.3861E-04	7.2000E-04	-2.5203
P	2.6457E-02	2.6137E-02	-1.2079
cVM	1.4820E-02	1.4534E-02	-1.9326
mVM	1.1511E-02	1.1256E-02	-2.2129
New1	1.1756E-02	1.1463E-02	-2.4998

It is observed that the error values for the nonstationary case are significantly lower than for the stationary case. This observation can be explained based on the differences in the PSD functions of the inputs.

Table 3.4 - Stochastic dynamic analysis results for the horizontal roof drift response of the two-story building subjected to nonstationary input.

Modes included	#1 to #2	#1	ε [%]
$\max(\sigma_{u_{Roof}}^2(t))$	2.5670E-04	2.5701E-04	0.1199
$\max(\sigma_{u_{Roof}}^2(t))$	6.3364E-02	6.3259E-02	-0.1655
$\max(u_{ u_{Roof} }(x_{lim}, t))$	1.6777E-03	1.6914E-03	0.8177
$\max(h_{cVM}(x_{lim}, t))$	7.5158E-04	7.5394E-04	0.3137
$\max(h_{mVM}(x_{lim}, t))$	5.3951E-04	5.4033E-04	0.1520
$\max(h_{New1}(x_{lim}, t))$	6.2600E-04	6.2686E-04	0.1362
$\max(h_{New2}(x_{lim}, t))$	3.5914E-04	3.5846E-04	-0.1903
P	7.1944E-03	7.2571E-03	0.8714
cVM	3.2863E-03	3.2986E-03	0.3743
mVM	2.3641E-03	2.3691E-03	0.2125
New1	2.7503E-03	2.7565E-03	0.2261
New2	1.5836E-03	1.5829E-03	-0.0489

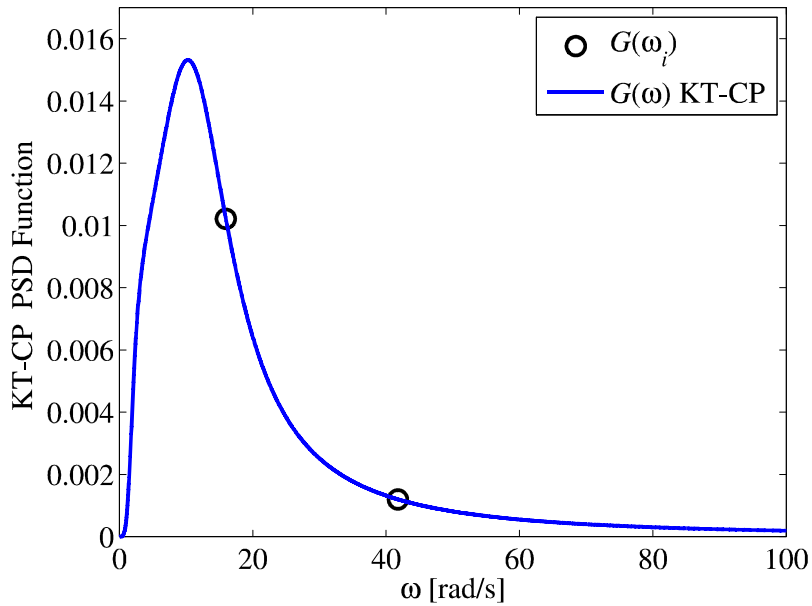


Figure 3.2 - Input PSD function for the two-story building.

Figure 3.2 shows the PSD function of the nonstationary input excitation and the modal circular frequencies of the 2-DOF system. The frequency content of the input in correspondence of the circular frequency of the first mode is almost 10 times larger than the frequency content of the input in correspondence of the circular frequency of the second mode. Thus, the first mode of vibration contributes to the structural response relatively more for the nonstationary case than for the white noise excitation case, in which the input frequency content is constant for all modes.

3.4.1.2.2 Three-story Shear-type Building

In the three-story building, the first mode contributes 91% of the total mass and the first two modes contribute 98% of the total mass of the system in the horizontal direction (Table 3.2). The maximum value of error for the FFP estimates is 14.14 % for the stationary cases (Table 3.5) and is 1.28% for the nonstationary case (Table 3.6) when considering only one mode in the modal truncation.

Table 3.5 - Stochastic dynamic analysis results for the horizontal roof drift response of the three-story building subjected to stationary input.

Modes included	#1 to #3	#1	ε [%]	#1 to #2	ε [%]
$\max(\sigma_{u_{Roof}}^2(t))$	2.5178E-02	2.5108E-02	-0.2771	2.5177E-02	-0.0036
$\max(\sigma_{\dot{u}_{Roof}}^2(t))$	7.1621E+00	7.0039E+00	-2.2083	7.1582E+00	-0.0537
$\max(u_{ u_{Roof} }(x_{lim}, t))$	1.8010E-03	1.7442E-03	-3.1499	1.8000E-03	-0.0541
$\max(h_{cVM}(x_{lim}, t))$	1.0556E-03	9.5483E-04	-9.5470	1.0478E-03	-0.7409
$\max(h_{mVM}(x_{lim}, t))$	8.3519E-04	7.3588E-04	-11.8906	8.2679E-04	-1.0059
$\max(h_{New1}(x_{lim}, t))$	9.0147E-04	7.7394E-04	-14.1460	8.9019E-04	-1.2513
P	2.8191E-02	2.7300E-02	-3.1611	2.8176E-02	-0.0542
cVM	1.6763E-02	1.5183E-02	-9.4211	1.6641E-02	-0.7253
mVM	1.3323E-02	1.1759E-02	-11.7394	1.3191E-02	-0.9870
New1	1.4462E-02	1.2449E-02	-13.9164	1.4285E-02	-1.2233

Inclusion of the first two modes in the modal truncation decreases the maximum error values to 1.25% and 0.28% for the stationary and nonstationary cases, respectively. The difference between the stationary and nonstationary cases has an explanation similar to the one presented for the two-story building problem (see Appendix E).

Table 3.6 - Stochastic dynamic analysis results for the horizontal roof drift response of the three-story building subjected to nonstationary input.

Modes included	#1 to #3	#1	ε [%]	#1 to #2	ε [%]
$\max(\sigma_{u_{Roof}}^2(t))$	2.2557E-04	2.2597E-04	0.1731	2.2553E-04	-0.0214
$\max(\sigma_{\dot{u}_{Roof}}^2(t))$	6.0816E-02	6.0701E-02	-0.1887	6.0820E-02	0.0068
$\max(u_{ u_{Roof} }(x_{lim}, t))$	1.7533E-03	1.7745E-03	1.2082	1.7506E-03	-0.1568
$\max(h_{cVM}(x_{lim}, t))$	8.0586E-04	8.1074E-04	0.6050	8.0415E-04	-0.2123
$\max(h_{mVM}(x_{lim}, t))$	5.8357E-04	5.8598E-04	0.4121	5.8221E-04	-0.2332
$\max(h_{New1}(x_{lim}, t))$	6.7454E-04	6.7732E-04	0.4123	6.7290E-04	-0.2435
$\max(h_{New2}(x_{lim}, t))$	3.9647E-04	3.9666E-04	0.0474	3.9535E-04	-0.2840
P	7.4785E-03	7.5746E-03	1.2848	7.4661E-03	-0.1661
cVM	3.5046E-03	3.5289E-03	0.6927	3.4968E-03	-0.2217
mVM	2.5437E-03	2.5564E-03	0.4997	2.5375E-03	-0.2427
New1	2.9474E-03	2.9626E-03	0.5146	2.9403E-03	-0.2422
New2	1.7389E-03	1.7423E-03	0.1910	1.7341E-03	-0.2786

3.4.1.2.3 Eight-story Shear-type Building

For the eight-story building, the cumulative mass participation factor by including one, two, and three modes are 85.6%, 94.7%, and 97.7%, respectively (see Table 3.2). By including the first two modes, the maximum value of the error for the reliability measures is 7.8% and 2.5% for stationary and nonstationary input excitations, respectively (Table 3.7 and Table 3.8). Inclusion of the third mode in the analysis reduces the corresponding error values in the two cases considered to 1.37% and 0.59% , respectively.

Table 3.7 - Stochastic dynamic analysis results for the horizontal roof drift response of the eight-story building subjected to stationary input.

Modes included	#1 to #8	#1	ε [%]	#1 to #2	ε [%]	#1 to #3	ε [%]	#1 to #4	ε [%]	#1 to #5	ε [%]
$\max(\sigma_{u_{Roof}}^2(t))$	3.8940E-01	3.8664E-01	-0.7097	3.8922E-01	-0.0466	3.8938E-01	-0.0055	3.8940E-01	-0.0009	3.8940E-01	-0.0001
$\max(\sigma_{\dot{u}_{Roof}}^2(t))$	1.9512E+01	1.8211E+01	-6.6663	1.9289E+01	-1.1413	1.9464E+01	-0.2462	1.9501E+01	-0.0540	1.9510E+01	-0.0091
$\max(u_{ u_{Roof} }(x_{lim}, t))$	7.5627E-04	6.9252E-04	-8.4304	7.4932E-04	-0.9191	7.5503E-04	-0.1644	7.5602E-04	-0.0335	7.5623E-04	-0.0053
$\max(h_{cVM}(x_{lim}, t))$	5.1577E-04	3.8055E-04	-26.2175	4.8944E-04	-5.1062	5.1116E-04	-0.8950	5.1429E-04	-0.2883	5.1569E-04	-0.0162
$\max(h_{mVM}(x_{lim}, t))$	4.3388E-04	2.9361E-04	-32.3281	4.0436E-04	-6.8041	4.2866E-04	-1.2020	4.3216E-04	-0.3958	4.3379E-04	-0.0208
$\max(h_{New1}(x_{lim}, t))$	5.5760E-04	3.5157E-04	-36.9492	5.1396E-04	-7.8266	5.4994E-04	-1.3727	5.5506E-04	-0.4548	5.5747E-04	-0.0234
P	7.8651E-03	7.1719E-03	-8.8132	7.7897E-03	-0.9584	7.8517E-03	-0.1706	7.8624E-03	-0.0347	7.8647E-03	-0.0055
cVM	5.4788E-03	4.0737E-03	-25.6460	5.2069E-03	-4.9621	5.4312E-03	-0.8688	5.4636E-03	-0.2784	5.4779E-03	-0.0158
mVM	4.6422E-03	3.1765E-03	-31.5739	4.3351E-03	-6.6165	4.5881E-03	-1.1674	4.6245E-03	-0.3831	4.6413E-03	-0.0203
New1	6.0517E-03	3.8864E-03	-35.7799	5.5963E-03	-7.5249	5.9720E-03	-1.3171	6.0254E-03	-0.4349	6.0504E-03	-0.0225

Table 3.8 - Stochastic dynamic analysis results for the horizontal roof drift response of the eight-story building subjected to nonstationary input.

Modes included	#1 to #8	#1	ε [%]	#1 to #2	ε [%]	#1 to #3	ε [%]	#1 to #4	ε [%]	#1 to #5	ε [%]
$\max(\sigma_{u_{Roof}}^2(t))$	4.0359E-03	4.0161E-03	-0.4907	4.0363E-03	0.0104	4.0357E-03	-0.0050	4.0360E-03	0.0016	4.0359E-03	-0.0006
$\max(\sigma_{\dot{u}_{Roof}}^2(t))$	1.9819E-01	1.9085E-01	-3.7050	1.9805E-01	-0.0712	1.9809E-01	-0.0514	1.9821E-01	0.0090	1.9818E-01	-0.0052
$\max(v_{ u_{Roof} }(x_{lim}, t))$	7.4845E-04	7.0779E-04	-5.4324	7.4877E-04	0.0426	7.4798E-04	-0.0634	7.4858E-04	0.0164	7.4840E-04	-0.0074
$\max(h_{cVM}(x_{lim}, t))$	4.1664E-04	3.0193E-04	-27.5329	4.1192E-04	-1.1323	4.1538E-04	-0.3029	4.1671E-04	0.0181	4.1654E-04	-0.0229
$\max(h_{mVM}(x_{lim}, t))$	3.2338E-04	2.1333E-04	-34.0326	3.1830E-04	-1.5696	3.2211E-04	-0.3936	3.2344E-04	0.0189	3.2329E-04	-0.0288
$\max(h_{New1}(x_{lim}, t))$	3.645E-04	2.490E-04	-31.702	3.581E-04	-1.7832	3.630E-04	-0.4401	3.646E-04	0.0198	3.644E-04	-0.0313
$\max(h_{New2}(x_{lim}, t))$	2.5938E-04	1.5704E-04	-39.4553	2.5291E-04	-2.4914	2.5786E-04	-0.5863	2.5943E-04	0.0206	2.5927E-04	-0.0413
P	3.7794E-03	3.5681E-03	-5.5902	3.7812E-03	0.0486	3.7769E-03	-0.0653	3.7800E-03	0.0171	3.7791E-03	-0.0077
cVM	2.1307E-03	1.5404E-03	-27.7077	2.1071E-03	-1.1081	2.1243E-03	-0.3007	2.1311E-03	0.0188	2.1302E-03	-0.0229
mVM	1.6553E-03	1.0879E-03	-34.2775	1.6298E-03	-1.5445	1.6488E-03	-0.3911	1.6556E-03	0.0196	1.6548E-03	-0.0288
New1	1.8688E-03	1.2702E-03	-32.0298	1.8396E-03	-1.5587	1.8613E-03	-0.3985	1.8691E-03	0.0197	1.8682E-03	-0.0293
New2	1.3311E-03	8.0015E-04	-39.8871	1.3018E-03	-2.2003	1.3240E-03	-0.5343	1.3314E-03	0.0209	1.3306E-03	-0.0382

3.4.1.2.4 20-story Shear-type Building

The first two, three, and four modes contribute 92%, 95%, and 97% of the total mass of the structure in the horizontal direction, respectively (see Table 3.2). Inclusion of the first three modes yields a maximum error value of 4.2% and 1.6% for the stationary (Table 3.9) and nonstationary (Table 3.10) input cases, respectively.

3.4.1.3 Discussion of the Results

3.4.1.3.1 Displacement and Velocity Variances

Study of the stochastic dynamic analysis of the four MDOF cases reveals that the displacement variances converge faster than the velocity variances.

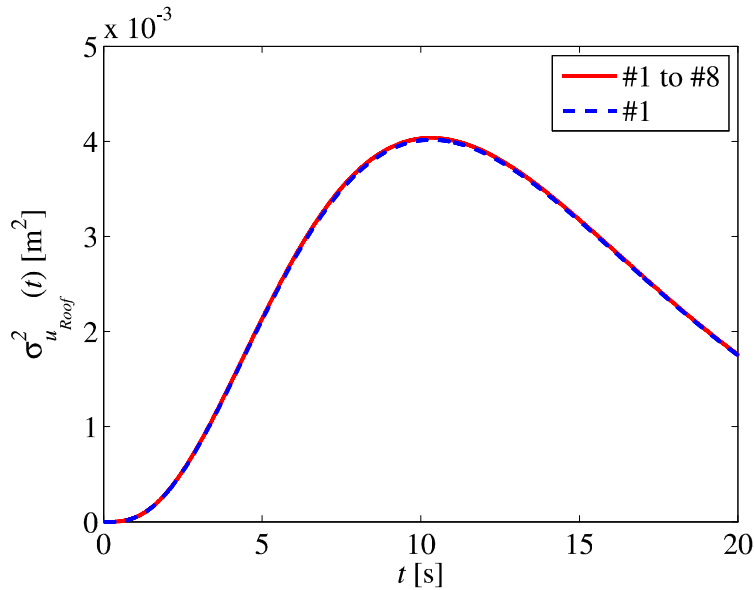


Figure 3.3 - Estimates of the roof displacement variance of the eight-story building obtained using modal truncation (nonstationary input).

Figure 3.3 and Figure 3.4 show the displacement and velocity variances, respectively, of the eight-story building model subjected to nonstationary input excitation for one and eight modes included in the modal truncation. It is observed that the displacement variance for the MDOF systems with higher number of DOFs (i.e., the eight- and 20-story buildings) presents a significantly smaller error compared to the one observed for the velocity variance. This error

reduces rapidly when more modes are included in the analysis. For the two- and three-story buildings, the errors of the displacement and velocity variances have the same order of magnitude.

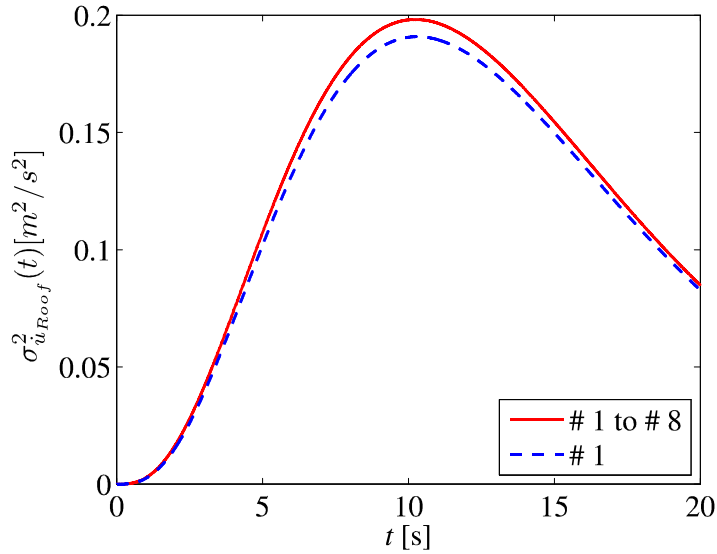


Figure 3.4 - Estimates of the roof velocity variance of the eight-story building obtained using modal truncation (nonstationary input).

3.4.1.3.2 Mean Out-crossing Rate and Hazard Functions

Based on the results presented in Table 3.3 through Table 3.10, the convergence error corresponding to the mean out-crossing rate (the Poisson's hazard function) obtained from modal truncation for the two- and three-story buildings is similar to the convergence error corresponding to the other analytical hazard approximations. However, for taller buildings, i.e., eight- and 20-story buildings, the mean out-crossing rate presents significantly smaller convergence error values compared to the other approximations. Including more modes in the analysis decreases the error values considerably. Figure 3.5 shows the different hazard function approximations for the eight-story buildings subjected to nonstationary input process when one mode is included in the modal truncation. It is noted that the mean out-crossing rate (denoted by h_p in the figure) presents a faster convergence error compared to the other approximations.

Table 3.9 - Stochastic dynamic analysis results for the horizontal roof drift response of the 20-story building subjected to stationary input.

Modes included	#1 to #20	#1	ε [%]	#1 to #2	ε [%]	#1 to #3	ε [%]	#1 to #4	ε [%]	#1 to #5	ε [%]
$\max(\sigma_{u_{Roof}}^2(t))$	3.413E+00	3.376E+00	-1.085	3.410E+00	-0.107	3.412E+00	-0.020	3.413E+00	-0.005	3.413E+00	-0.002
$\max(\sigma_{\dot{u}_{Roof}}^2(t))$	4.036E+01	3.596E+01	-10.902	3.914E+01	-3.031	3.992E+01	-1.099	4.017E+01	-0.467	4.027E+01	-0.216
$\max(\nu_{ u_{Roof} }(x_{lim}, t))$	3.686E-04	3.209E-04	-12.933	3.601E-04	-2.291	3.660E-04	-0.698	3.676E-04	-0.272	3.681E-04	-0.120
$\max(h_{cVM}(x_{lim}, t))$	2.778E-04	1.849E-04	-33.430	2.530E-04	-8.919	2.696E-04	-2.950	2.740E-04	-1.352	2.761E-04	-0.584
$\max(h_{mVM}(x_{lim}, t))$	2.441E-04	1.452E-04	-40.498	2.155E-04	-11.698	2.344E-04	-3.942	2.396E-04	-1.833	2.421E-04	-0.792
$\max(h_{New1}(x_{lim}, t))$	3.610E-04	2.004E-04	-44.475	3.157E-04	-12.558	3.460E-04	-4.161	3.540E-04	-1.927	3.580E-04	-0.829
P	2.056E-03	1.774E-03	-13.695	2.005E-03	-2.458	2.040E-03	-0.745	2.050E-03	-0.290	2.053E-03	-0.128
cVM	1.592E-03	1.080E-03	-32.187	1.454E-03	-8.664	1.546E-03	-2.868	1.571E-03	-1.310	1.583E-03	-0.565
mVM	1.412E-03	8.629E-04	-38.875	1.251E-03	-11.354	1.358E-03	-3.832	1.387E-03	-1.779	1.401E-03	-0.768
New1	2.127E-03	1.231E-03	-42.116	1.873E-03	-11.971	2.043E-03	-3.965	2.088E-03	-1.831	2.111E-03	-0.788

Table 3.10 - Stochastic dynamic analysis results for the horizontal roof drift response of the 20-story building subjected to nonstationary input.

Modes included	#1 to #20	#1	ε [%]	#1 to #2	ε [%]	#1 to #3	ε [%]	#1 to #4	ε [%]	#1 to #5	ε [%]
$\max(\sigma_{u_{Roof}}^2(t))$	1.9101E-02	1.8683E-02	-2.1886	1.9085E-02	-0.0844	1.9097E-02	-0.0241	1.9102E-02	0.0036	1.9101E-02	-0.0029
$\max(\sigma_{\dot{u}_{Roof}}^2(t))$	2.4680E-01	2.0519E-01	-16.8619	2.4002E-01	-2.7454	2.4533E-01	-0.5969	2.4657E-01	-0.0913	2.4666E-01	-0.0557
$\max(\nu_{ u_{Roof} }(x_{lim}, t))$	3.8395E-04	2.9609E-04	-22.8849	3.7631E-04	-1.9895	3.8214E-04	-0.4728	3.8389E-04	-0.0172	3.8376E-04	-0.0490
$\max(h_{cVM}(x_{lim}, t))$	2.9828E-04	1.4219E-04	-52.3320	2.7942E-04	-6.3245	2.9430E-04	-1.3365	2.9768E-04	-0.2034	2.9790E-04	-0.1277
$\max(h_{mVM}(x_{lim}, t))$	2.6577E-04	1.0470E-04	-60.6034	2.4391E-04	-8.2269	2.6117E-04	-1.7315	2.6500E-04	-0.2888	2.6533E-04	-0.1640
$\max(h_{New1}(x_{lim}, t))$	2.8014E-04	1.2003E-04	-57.1548	2.5947E-04	-7.3777	2.7579E-04	-1.5539	2.7944E-04	-0.2503	2.7973E-04	-0.1477
$\max(h_{New2}(x_{lim}, t))$	2.8884E-04	1.3023E-04	-54.9124	2.6900E-04	-6.8702	2.8466E-04	-1.4489	2.8819E-04	-0.2277	2.8844E-04	-0.1380
P	2.4274E-03	1.8588E-03	-23.4242	2.3795E-03	-1.9721	2.4159E-03	-0.4740	2.4271E-03	-0.0135	2.4262E-03	-0.0498
cVM	1.9015E-03	8.8932E-04	-53.2296	1.7842E-03	-6.1669	1.8767E-03	-1.2999	1.8978E-03	-0.1906	1.8991E-03	-0.1248
mVM	1.6963E-03	6.5173E-04	-61.5798	1.5599E-03	-8.0407	1.6678E-03	-1.6843	1.6917E-03	-0.2733	1.6936E-03	-0.1602
New1	1.7881E-03	7.4875E-04	-58.1268	1.6584E-03	-7.2544	1.7604E-03	-1.5518	1.7837E-03	-0.2489	1.7855E-03	-0.1505
New2	1.8429E-03	8.1345E-04	-55.8610	1.7185E-03	-6.7492	1.8163E-03	-1.4452	1.8388E-03	-0.2256	1.8403E-03	-0.1404

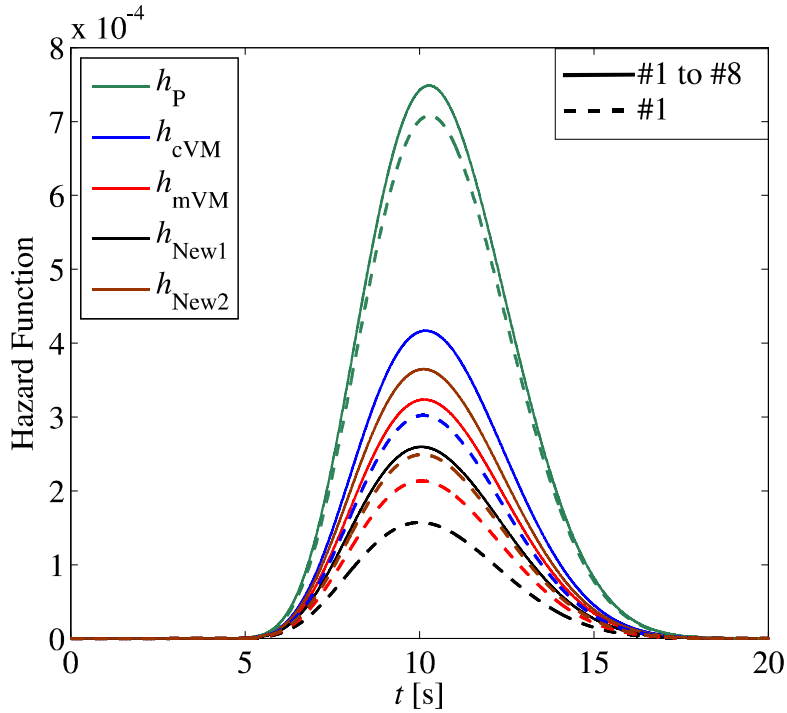


Figure 3.5 - Estimates of the roof hazard functions of the eight-story building obtained using modal truncation (nonstationary input).

3.4.1.3.3 Time-variant FFP

The time-variant FFP using the Poisson approximation shows a significantly faster convergence when compared to the other analytical approximations for the case of eight- and 20-story buildings. For the case of shorter buildings (i.e., two- and three-story buildings), the convergence error corresponding to P approximation is of the same order of magnitude of other approximations. The cVM, mVM, New1, and New2 show similar values of convergence error for the different shear-type buildings considered.

Figure 3.6 compares the analytical results obtained using modal truncation by including the first mode and including all modes for the eight-story building. It is observed that the proposed hazard function is not in a good agreement with the ISEE results. The ISEE results almost coincide with the FFP obtained using the mVM approximation with all modes included.

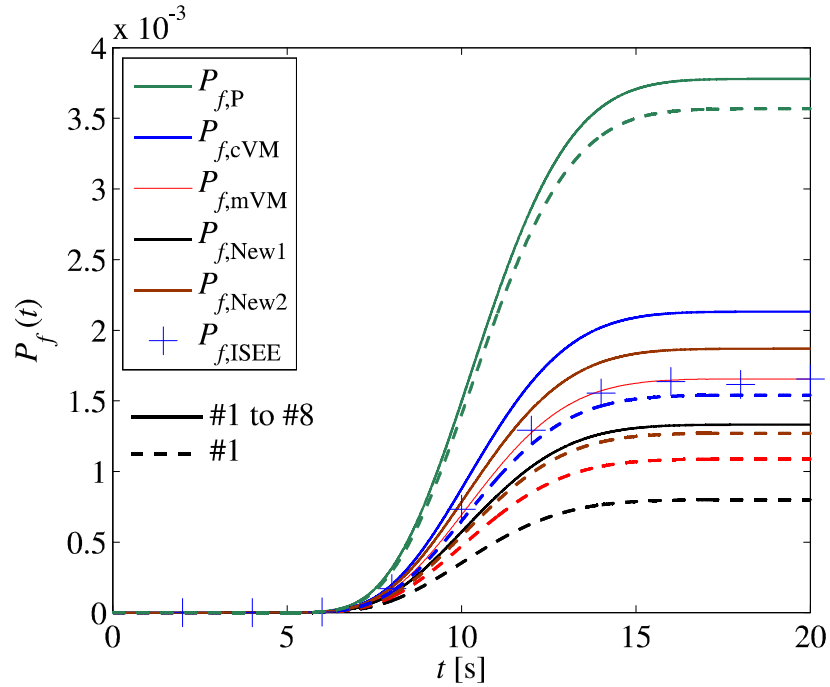


Figure 3.6 - Estimates of the roof FPDF of the eight-story building obtained using modal truncation (nonstationary input).

3.4.1.3.4 Accuracy of the Analytical Approximations

The FPDF values of stationary and nonstationary random processes are calculated using the P, cVM, mVM, and the newly proposed approximations. In general, the FPDF of the nonstationary cases present smaller error values compared with the stationary case. In the stationary case, the mVM approximation provides the most accurate results compared with other analytical approximations.

Table 3.11 - Comparison of FPDF of different approximations subjected to stationary input.

P_f \ # DOF	2-story	ϵ [%]	3-story	ϵ [%]	8-story	ϵ [%]	20-story	ϵ [%]
ISEE	1.1440E-02	-----	1.2239E-02	-----	3.6745E-03	-----	1.1073E-03	-----
P	2.6457E-02	131.27	2.8191E-02	130.35	7.8651E-03	114.05	2.0558E-03	85.66
cVM	1.4820E-02	29.55	1.6763E-02	36.97	5.4788E-03	49.11	1.5919E-03	43.77
mVM	1.1511E-02	0.62	1.3323E-02	8.86	4.6422E-03	26.34	1.4118E-03	27.50
New1	1.1756E-02	2.77	1.4462E-02	18.17	6.0517E-03	64.70	2.1274E-03	92.13
	ϵ_{\max}	131.27	ϵ_{\max}	130.35	ϵ_{\max}	114.05	ϵ_{\max}	92.13
	ϵ_{\min}	0.62	ϵ_{\min}	8.86	ϵ_{\min}	26.34	ϵ_{\min}	27.50
	$\mu_{ \epsilon }$	41.05	$\mu_{ \epsilon }$	48.58	$\mu_{ \epsilon }$	63.55	$\mu_{ \epsilon }$	62.26

In the nonstationary case, the cVM and New1 approximations provide the most accurate results for shorter buildings (two- and three-story), while the results are less accurate as the number of DOFs increases. For the taller buildings (eight- and 20-story), the best estimates of FFPF are given by the mVM approximation.

Table 3.12 - Comparison of FFPF of different approximations subjected to nonstationary input.

P_f \ # DOF	2-story	ϵ [%]	3-story	ϵ [%]	8-story	ϵ [%]	20-story	ϵ [%]
ISEE	3.0872E-03	-----	3.1942E-03	-----	1.6556E-03	-----	1.2376E-03	----
P	7.1944E-03	133.04	7.4785E-03	134.13	3.7794E-03	128.28	1.8790E-03	51.83
cVM	3.2863E-03	6.45	3.5046E-03	9.72	2.1307E-03	28.70	1.5034E-03	21.47
mVM	2.3641E-03	-23.42	2.5437E-03	-20.37	1.6553E-03	-0.02	1.3545E-03	9.44
New1	2.7503E-03	-10.91	2.9474E-03	-7.73	1.8688E-03	12.87	1.5457E-03	24.90
New2	1.5836E-03	-48.70	1.7389E-03	-45.56	1.3311E-03	-19.60	1.4649E-03	18.37
	ϵ_{\max}	133.04	ϵ_{\max}	134.13	ϵ_{\max}	128.28	ϵ_{\max}	51.83
	ϵ_{\min}	-48.70	ϵ_{\min}	-45.56	ϵ_{\min}	-19.60	ϵ_{\min}	9.44
	$\mu_{ \epsilon }$	52.90	$\mu_{ \epsilon }$	52.44	$\mu_{ \epsilon }$	44.15	$\mu_{ \epsilon }$	25.28

3.4.2 Welded Steel 13-Story Building

The Woodland Hills building is a 13-story welded steel moment frame (WSMF) building constructed in 1975 using the 1973 UBC and was damaged during the Northridge earthquake in 1994. This building is located in the southern San Fernando Valley, about 3 miles southwest of the Northridge earthquake epicenter.

The lateral loads are resisted by four identical steel frames along the building perimeter (two frames in each principal direction of the building). The typical story is square with side length of 160ft (48.77 m). The cross-sections used for the steel members are shown in Figure 3.7.

All the frame members are A36 steel. In this study, uniformly distributed dead load of 82.5 psf and 62.5 psf are used to calculate the reactive weights of the floors and roof, respectively. In addition, a 20 psf curtain wall weight is considered over the full building height [28].

The following conditions are assumed for the linear elastic analysis:

- (1) reactive weight equal to 10 psf partition load and no live load.
- (2) fixed beam columns at the ground level and infinitely stiff springs to prevent translation and plan rotation at the plaza level (i.e., plaza level is considered as fixed supports).
- (3) Rayleigh damping model with damping ratio of 5% for the 1st and 3rd of vibration.

More details on the characteristics of this building can be found in [28].

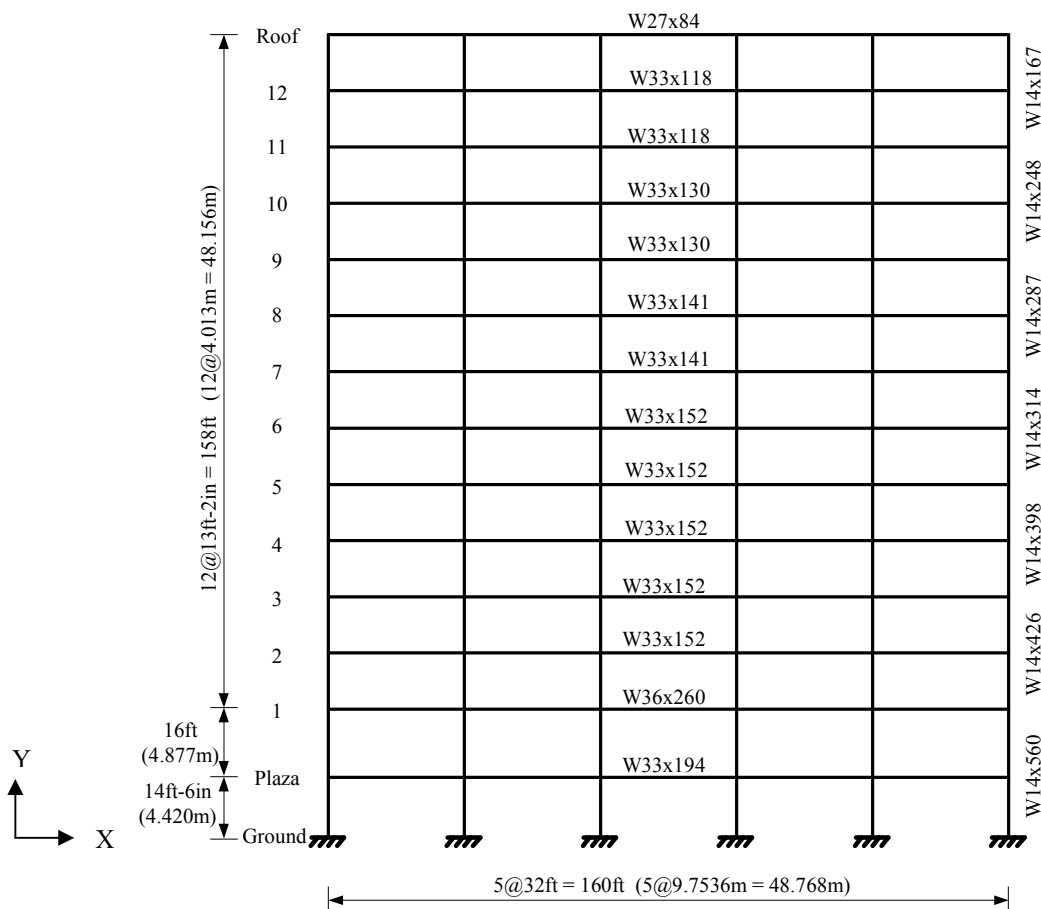


Figure 3.7 - Frame elevation and member sizes (adapted from [29]).

3.4.2.1 Analysis Results

This structure is modeled considering three DOFs (2 translational and one rotational) at each node, for a total of 270 DOF for the entire building. Using the static condensation procedure [14], the rotational DOFs, for which the assigned masses are zero, are eliminated from the

dynamic analysis. 12 nodes are assumed to be fixed at the ground and the plaza level. Thus, the total number of free DOFs is 156 for this problem. This building is analyzed using a Matlab toolbox called FEDEASLab [30]. Using modal analysis, the modal frequencies, modal periods, and mass participation ratios are calculated. In this study, the FPPF of the horizontal roof displacement is the response of the interest.

Table 3.13 - Modal properties of the 13-story building.

Mode (<i>i</i>)	T_i [s]	ω_i [rad / s]	ξ_i	Γ_{x_i} [%]	Γ_{cum-x_i} [%]	Γ_{y_i} [%]	Γ_{cum-y_i} [%]
1	3.0325	2.0720	0.0500	77.9029	77.9029	0	0
2	1.0779	5.8292	0.0394	11.0888	88.9917	0	0
3	0.6470	9.7119	0.0500	4.0787	93.0705	0	0
4	0.4583	13.7083	0.0644	2.2734	95.3438	0	0
5	0.3517	17.8634	0.0806	1.5260	96.8699	0	0
6	0.2989	21.0176	0.0932	0	96.8699	63.6738	63.6738
7	0.2863	21.9459	0.0970	0.0037	96.8736	0	63.6738
8	0.2841	22.1172	0.0977	0.9806	97.8542	0	63.6738
9	0.2680	23.4462	0.1031	0	97.8542	5.3961	69.0699
10	0.2502	25.1169	0.1100	0.0002	97.8544	0	69.0699
11	0.2401	26.1703	0.1143	0.5824	98.4368	0	69.0699
12	0.2062	30.4759	0.1321	0.3941	98.8308	0	69.0699
13	0.2046	30.7071	0.1331	0	98.8308	10.3555	79.4254
14	0.2034	30.8970	0.1339	0.1098	98.9407	0	79.4254
15	0.1792	35.0612	0.1512	0.3727	99.3134	0	79.4254
16	0.1571	39.9946	0.1718	0.2109	99.5243	0	79.4254
17	0.1571	40.0072	0.1719	0	99.5243	0.0025	79.4279
18	0.1498	41.9480	0.1800	0	99.5243	0.0001	79.4280
19	0.1445	43.4874	0.1865	0	99.5243	0.0002	79.4282
20	0.1408	44.6238	0.1913	0	99.5243	0.0003	79.4285

Table 3.13 shows the modal analysis results for the first 20 modes of the 13-story building. The modal participation factors are shown for both x- and y-directions. The first five modes contribute 96.9% of the total mass of the building in the x-direction. All higher modes contribute less than 1% to the modal mass of the building in the x-direction. The sixth mode contributes in the y-direction and accounts for 63.7% of the total mass in that direction. It is observed that the

modal contributions of x- and y-directions are well separated.

3.4.2.2 Stochastic Dynamic Analysis Results

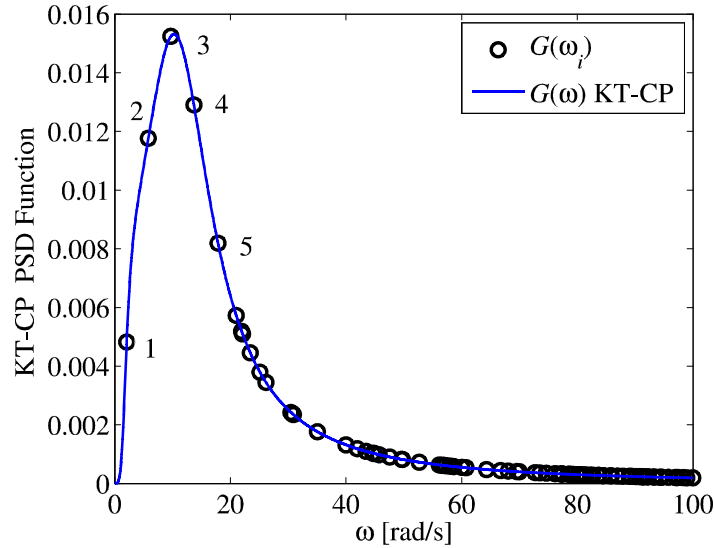


Figure 3.8- Input PSD function for the 13-story building.

The 13-story building model is subjected to an earthquake ground motion excitation modeled as a nonstationary random process with the same KT-CP PSD function used for the shear-type buildings (see Section 3.4.1.1) and modulated in time with the Shinozuka-Sato function. Figure 3.8 shows the PSD function of the nonstationary input excitation and the modal circular frequencies of the 13-story building. The frequency content of the input is largest in correspondence of the circular frequency of the first five modes which contribute 96.9% of the total mass of the system in the x-direction. Thus, the modal superposition of the first five modes is used as reference solution for this problem and the complex-valued spectral characteristics are calculated for the first five modes only and the modal truncation is performed for increasing number of modes $p < 5$. The error values corresponding to different numbers of modes included in the modal truncation are computed with respect to the results obtained from the modal superposition of the first five modes.

3.4.2.2.1 Displacement and Velocity Variances

Study of the displacement and velocity variances reveals that the displacement variance converges faster than the velocity variance. Figure 3.9 and Figure 3.10 present the displacement and velocity variances obtained using modal truncation with $p=1,2,5$, respectively. It is observed that the displacement variance is converged with $p=2$, while the velocity variance present larger error value. As it is seen in Table 3.14, with two modes included in the modal truncation, the error of the maximum displacement variance and velocity variance are 0.02% and 4.38%, respectively. Inclusion of the first four modes gives the error value of 0.29% for the maximum velocity variance.

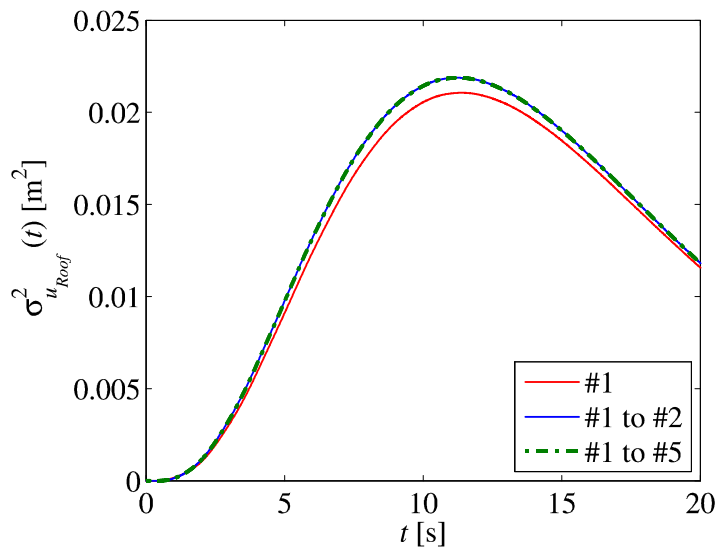


Figure 3.9- Estimates of the roof displacement variance of the 13-story building obtained using modal truncation $p = 1, 2, 5$.

3.4.2.2.2 Mean out-crossing Rate and Hazard Function

Inclusion of the first two modes in the modal truncation gives a convergence error value of 1.96% for the mean out-crossing rate (see Table 3.14). The cVM, mVM, New1, and New2 hazard functions present significantly larger values of convergence error compared to the mean out-crossing rate.

Table 3.14 - Stochastic dynamic analysis for the 13-story building.

Modes included	#1 to #5	#1	ε [%]	#1 to #2	ε [%]	#1 to #3	ε [%]	#1 to #4	ε [%]
$\max(\sigma_{u_{Roof}}^2(t))$	0.0218694	2.1056E-02	-3.7186	2.1873E-02	0.0182	2.1850E-02	-0.0886	2.1882E-02	0.0559
$\max(\sigma_{\dot{u}_{Roof}}^2(t))$	0.1309523	1.0596E-01	-19.0815	1.2521E-01	-4.3826	1.2967E-01	-0.9773	1.3134E-01	0.2927
$\max(u_{ u_{Roof} }(x_{lim}, t))$	0.0002604	1.7568E-04	-32.5245	2.5526E-04	-1.9603	2.5744E-04	-1.1230	2.6181E-04	0.5582
$\max(h_{cVM}(x_{lim}, t))$	0.0002122	1.2176E-04	-42.6235	1.9735E-04	-7.0068	2.0829E-04	-1.8524	2.1362E-04	0.6599
$\max(h_{mVM}(x_{lim}, t))$	0.0001934	1.0303E-04	-46.7252	1.7548E-04	-9.2646	1.8914E-04	-2.1988	1.9477E-04	0.7105
$\max(h_{New1}(x_{lim}, t))$	0.0002171	1.2695E-04	-41.5234	2.0314E-04	-6.4286	2.1326E-04	-1.7657	2.1850E-04	0.6472
$\max(h_{New2}(x_{lim}, t))$	0.0002239	1.3443E-04	-39.9618	2.1131E-04	-5.6260	2.2022E-04	-1.6464	2.2532E-04	0.6301
P	0.0014171	9.4443E-04	-33.3568	1.3904E-03	-1.8891	1.4008E-03	-1.1531	1.4254E-03	0.5825
cVM	0.0011614	6.5749E-04	-43.3862	1.0821E-03	-6.8235	1.1397E-03	-1.8644	1.1693E-03	0.6814
mVM	0.0010586	5.5565E-04	-47.5090	9.6255E-04	-9.0699	1.0352E-03	-2.2077	1.0663E-03	0.7316
New1	0.0011879	6.8563E-04	-42.2816	1.1137E-03	-6.2497	1.1668E-03	-1.7785	1.1958E-03	0.6690
New2	0.0012248	7.2615E-04	-40.7151	1.1580E-03	-5.4549	1.2045E-03	-1.6609	1.2328E-03	0.6521

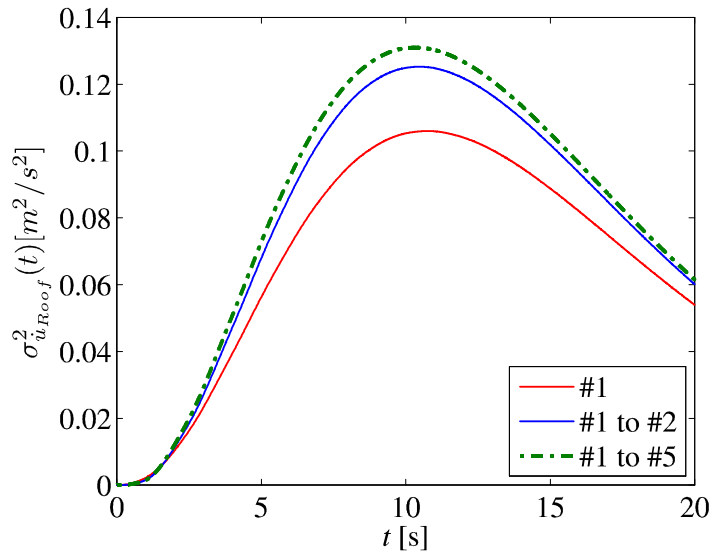


Figure 3.10 - Estimates of the roof velocity variance of the 13-story building obtained using modal truncation $p = 1, 2, 5$.

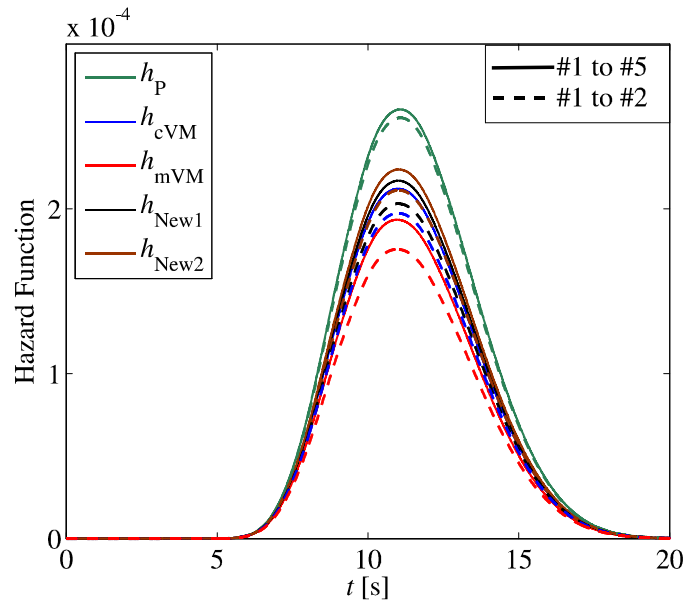


Figure 3.11 - Hazard functions for the roof horizontal drift of the 13-story building by including the first two and five modes.

Inclusion of the first three modes reduces the error values for all hazard functions to less than 2.2%. The mVM approximation shows the largest value of convergence error. Figure 3.11 presents the estimates of hazard functions for the case of two and five modes included in the modal truncation. It is observed that the mean out-crossing rate presents the smallest value of

error compared to the other hazard approximations.

3.4.2.2.3 Time-variant FFPF

Based on Table 3.14, inclusion of the first two modes in the modal truncation yields convergence error values of less than 10% in the FFPF approximations. By including the contribution of the third mode in the analysis, the corresponding convergence error values reduce to less than 2.2%. As it is seen in Figure 3.12, the mVM approximation for the FFPF presents, in general, the largest value of convergence error when modal truncation is used. By contrast, the P approximation presents the smallest value of convergence error among the analytical approximations.

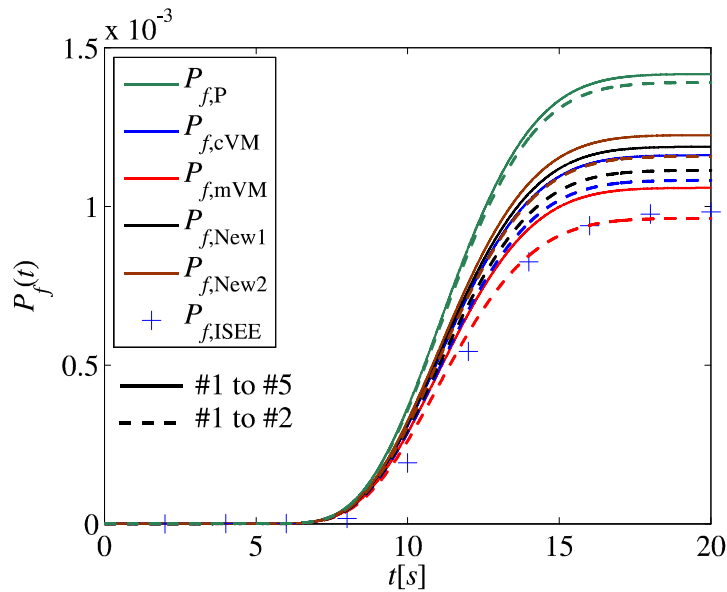


Figure 3.12 - FFPF for the roof horizontal drift of the 13-story building by including the first two and five modes.

3.4.2.2.4 Accuracy of the Analytical Approximations

Table 3.15 compares the FFPF values obtained by including the first five modes, with the exact ISEE results (which includes indirectly all modes of the structural model). It is observed that the mVM approximation gives the most accurate results among all analytical approximations

with an error of 7.7%. The results presented in Table 3.14 and Table 3.15 show that the mVM approximation is the most accurate analytical approximation; however, in order to reach this level of accuracy, a larger number of modes need to be included in the modal truncation compared to the P approximation.

Table 3.15 - Comparison of the analytical and ISEE estimates of FFP for the 13-story building.

P_f \ #Modes	5-modes	ϵ [%]
ISEE	9.8247E-04	-----
P	1.4171E-03	44.2419
cVM	1.1614E-03	18.2081
mVM	1.0586E-03	7.7438
New1	1.1879E-03	20.9080
New2	1.2248E-03	24.6699
	ϵ_{\max}	44.2419
	ϵ_{\min}	7.7438
	$\mu_{ \epsilon }$	23.1544

3.4.3 Pounding of Adjacent Buildings

Earthquake ground motion excitation can induce pounding in adjacent buildings with inadequate separation distance. The corresponding risk is particularly relevant in densely inhabited metropolitan areas, due to the usually limited separation distance between the adjacent buildings. In this section, two adjacent SDOF systems are studied for the pounding risk. These two SDOF are modeled as a 2-DOF system and the FFP is found for the specified threshold value for two sets of natural periods.

Pounding occurs when the separation distance between two adjacent buildings is insufficient to accommodate the motion of the two buildings subjected to seismic excitation. Pounding events can be analyzed as first-passage failure problems. The FFP in the case of pounding is defined as the probability that the relative displacement of the adjacent buildings subjected to

seismic loading, outcrosses the separation distance between the two buildings at-rest (see Figure 3.13).

Based on Eq. (1.59), a single-barrier time-variant pounding probability can be defined as:

$$P_p(t) = P\{U_{rel}(t) \geq u_{lim}\} \quad (3.11)$$

in which $U_{rel}(t) = U_A(t) - U_B(t)$, $U_A(t)$ and $U_B(t)$ = displacement response of the adjacent buildings A and B at the (most likely) pounding location, and u_{lim} = deterministic value of the building separation distance (see Figure 3.13).

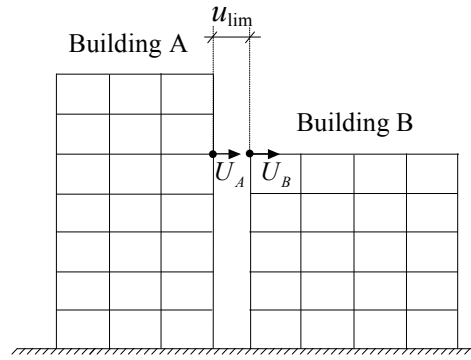


Figure 3.13 - Geometric description of the pounding problem between adjacent buildings.

3.4.3.1 Computation of the Pounding Probability

Under the hypotheses of deterministic linear elastic systems subjected to Gaussian loading processes and of deterministic threshold, the analytical approximations of $P_p(t)$ discussed previously in this thesis (i.e., P, cVM, mVM, and New approximations) can be used to estimate the pounding probability. Following the methodology described in Barbato et. al. [15], a state-space formulation of the equations of motion for the two buildings is employed to compute exactly and in closed-form the required spectral characteristics. The seismic input is modeled as a time-modulated Gaussian colored noise process. For this specific input ground motion process,

the spectral characteristics of the displacement processes (and of any response process obtained as a linear combination of the displacement processes) are available in exact closed-form for single-degree-of-freedom (SDOF) systems and both classically and non-classically damped MDOF systems [15].

The equations of motion for the linear system constituted by two non-connected adjacent buildings can be expressed as follows:

$$\mathbf{m} \cdot \ddot{\mathbf{U}}(t) + \mathbf{c} \cdot \dot{\mathbf{U}}(t) + \mathbf{k} \cdot \mathbf{U}(t) = \mathbf{p} \cdot F(t) \quad (3.12)$$

in which $\mathbf{m} = \begin{pmatrix} \mathbf{m}_A & \mathbf{0} \\ \mathbf{0} & \mathbf{m}_B \end{pmatrix}$, $\mathbf{c} = \begin{pmatrix} \mathbf{c}_A & \mathbf{0} \\ \mathbf{0} & \mathbf{c}_B \end{pmatrix}$, $\mathbf{k} = \begin{pmatrix} \mathbf{k}_A & \mathbf{0} \\ \mathbf{0} & \mathbf{k}_B \end{pmatrix}$, $\mathbf{U} = \begin{pmatrix} \mathbf{U}_A \\ \mathbf{U}_B \end{pmatrix}$; \mathbf{m}_i , \mathbf{k}_i , \mathbf{c}_i and \mathbf{U}_i = mass matrix, damping matrix, stiffness matrix, and vector of nodal displacements of building i , respectively ($i = A, B$); \mathbf{p} = load distribution vector; $F(t)$ = scalar function describing the time-history of the external loading (input random process); and a superposed dot denotes differentiation with respect to time. It is noteworthy that connections between the two buildings (e.g., damping devices interposed between the buildings to mitigate seismic pounding risk) can be easily modeled by introducing the appropriate terms in matrix \mathbf{c} . The response process $U_{rel}(t)$ can be related to the displacement response vector $\mathbf{U}(t)$ by means of a linear operator \mathbf{b} , i.e., $U_{rel}(t) = \mathbf{b} \cdot \mathbf{U}(t)$. The probability of pounding is given by:

$$P_p(t) = 1 - P[U_{rel}(t=0) < u_{lim}] \cdot \exp \left\{ - \int_0^{t_{max}} h_{U_{rel}}(u_{lim}, \tau) \cdot d\tau \right\} \quad (3.13)$$

in which $P[U_{rel}(t=0) < u_{lim}]$ = probability that the random process $U_{rel}(t)$ is below the threshold ξ at time $t = 0$ s, and $h_{U_{rel}}(u_{lim}, t)$ = time-variant hazard function, and t_{max} = duration

of the seismic excitation. For systems with at-rest initial conditions, $P[U_{rel}(t=0) < u_{lim}] = 1$. The $h_{U_{rel}}(u_{lim}, t)$ is calculated using Eqs. (1.60), (1.61) and (1.62) considering the changes for the single-barrier problem. In addition, for linear elastic systems subjected to Gaussian loading, P_p can be efficiently and accurately estimated by using the ISEE method [22].

3.4.3.2 Description of the Input Excitation and FE Model

For this problem, the input ground acceleration is modeled by a time-modulated Gaussian process, with the time-modulating function represented by the Shinozuka-Sato's function given by Eqs. (2.9) and (2.10) for which $B_1 = 0.045\pi \text{ s}^{-1}$, $B_2 = 0.050\pi \text{ s}^{-1}$, $C = 25.812$. A duration of $t_{max} = 30\text{s}$ is considered for the seismic excitation. The PSD of the embedded stationary process is described by the Kanai-Tajimi model, as modified by Clough and Penzien with the same parameter values used in the previous application example presented in Section 3.4.1.1.

The two adjacent buildings are modeled as deterministic linear elastic SDOF systems with periods T_A and T_B , and damping ratios $\xi_A = \xi_B = 5\%$. A deterministic separation distance between the buildings $u_{lim} = 0.1\text{m}$ is assumed. Two different combinations of the natural periods of the two systems are considered, i.e., (1) $T_A = 1.0\text{s}$ and $T_B = 0.5\text{s}$, referred to as well separated natural periods, and (2) $T_A = 1.0\text{s}$ and $T_B = 0.9\text{s}$, referred to as close natural periods.

3.4.3.3 Analysis Results

The probability of pounding, P_p , is calculated using the analytical approximations, P, cVM, mVM, New1, and New2. These results are compared with the corresponding ISEE results and are presented in Figure 3.14 for the case of well separated natural periods, and in Figure 3.15 for

the case of close natural periods.

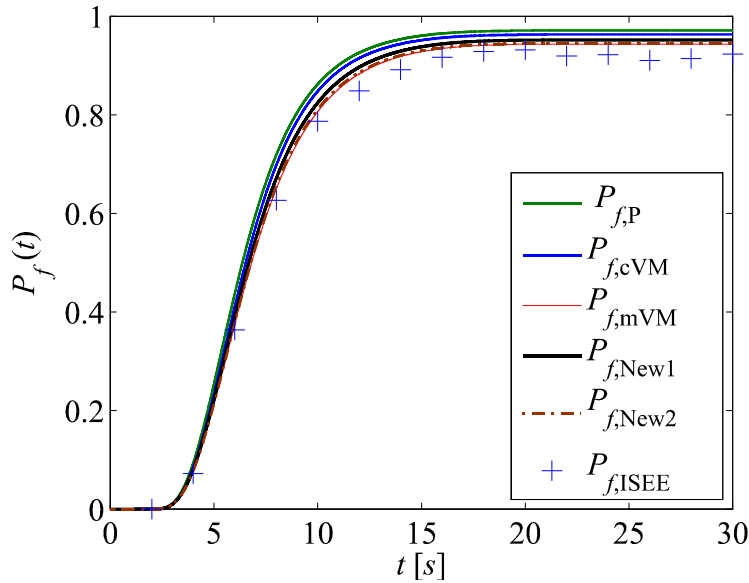


Figure 3.14 - FFPF for two SDOF models of adjacent buildings with $T_A = 1.0\text{s}$ and $T_B = 0.5\text{s}$.

Figure 3.14 shows that the time-variant pounding probability obtained using the P, cVM, mVM, New1, and New2 approximations are very similar and close to the ISEE results for the case of well separated natural periods. In Figure 3.15, it is observed that, for the case of close natural periods, the FFPF estimated with the approximate analytical methods show significant differences, and only the cVM approximation provides results that are close to the FFPF estimated using the ISEE method.

The observed results can be explained by recognizing that the relative displacement process $U_{rel}(t)$ can be interpreted as a response process of a 2-DOF system. This multi-modal characteristic of $U_{rel}(t)$ can significantly affect the accuracy of the different approximations of the time-variant hazard function $h_{U_{rel}}(u_{lim}, t)$. In the case of well separated natural periods, the contribution to $U_{rel}(t)$ of the vibration mode with higher period is significantly larger than the contribution of the vibration mode with lower period. By contrast, in

the case of close natural periods, both vibration modes provide a significant contribution to the response process. Therefore, it is found that the analytical approximations give relatively accurate results for the case of well separated natural periods; while for the case of close natural periods, the analytical approximations, with exception of the cVM approximation, are not in good agreement with the ISEE results.

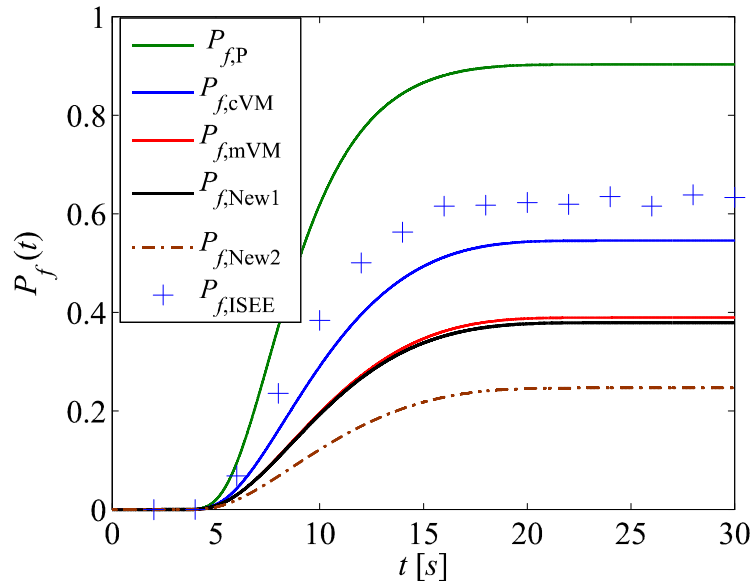


Figure 3.15 - FPDF for two SDOF models of adjacent buildings with $T_A = 1.0\text{s}$ and $T_B = 0.9\text{s}$.

It is also found that the P approximation of the time-variant hazard function always yields conservative results, while the mVM approximation underestimates the risk computed using the ISEE method for the case of close natural periods. Similar results have been documented for the first-passage reliability problem of SDOF and MDOF systems subjected to time-modulated white and colored noise excitations [8].

3.5 CONCLUSIONS

In this chapter, the accuracy of analytical approximations of the time-variant FPDF of linear MDOF systems is studied. Three application examples are considered: (1) a set of shear-type

buildings with different number of DOFs; (2) the linear elastic finite element model of a real-world moment resisting steel frame; and (3) two adjacent buildings modeled as SDOF systems and subjected to seismic pounding hazard.

In the first two examples, effects of modal truncation are studied. The modal properties of each system are obtained using classical modal analysis, and the response statistics and FPDF are computed using modal truncation. The stochastic dynamic analysis of the shear-type buildings reveals that, when the MDOF systems are subjected to stationary random excitations, a number of p modes such that their cumulative mass participation factor is at least 95% is needed to obtain accurate results (i.e., with errors smaller than 5% compared to the solutions obtained by considering all modes). However, for the case of nonstationary random input, accurate stochastic dynamic analysis results are obtained by including a number of modes for which the cumulative mass participation factor is more than 90%. It is also noted that the convergence errors produced by using the modal truncation in the displacement variances are usually smaller than for other quantities, while the hazard functions and the FPDFs present the largest convergence error values when the same number of modes are included in the modal truncation.

For the case of the 13-story building, including 90% of the total mass in the x-direction leads to acceptable results in the displacement variances. A larger number of modes is needed to obtain sufficiently accurate results in the hazard functions and FPDF. The mVM approximation is the most accurate approximation compared with the ISEE results, however its convergence for increasing number of modes included in the modal truncation is relatively slow compared to the P approximation.

In the pounding problem of two adjacent buildings, it is found that, for the case of close natural periods, the FPDF obtained from different analytical approximations do not present

similar results and are not in good agreement with the ISEE results. However, for the case of well separated natural periods, the analytical approximations give similar results and are close to the ISEE values.

In all cases considered as application examples, it is observed that the newly proposed analytical approximation of the hazard function becomes less accurate as the system considered becomes more different from a linear elastic SDOF system (i.e., for increasing number of DOFs in the shear-type buildings and for close natural periods in the pounding problem).

4 CONCLUSIONS AND RECOMMENDATIONS FOR FUTURE WORK

The research presented in this thesis focuses on the analytical approximation of the first-passage failure probability (FPFP). A new analytical approximation of the FPFP for linear SDOF systems is proposed by modifying the classical Vanmarcke's hazard function. This new approximation is verified by comparing its failure probability estimates with the results obtained using existing analytical approximations and the importance sampling using elementary events (ISEE) method for a wide range of oscillator properties, threshold levels, and types of input excitations. It is shown that the newly proposed analytical approximation of the hazard function yields significantly more accurate estimates the FPFP when compared with Poisson's, classical Vanmarcke's, and modified Vanmarcke's approximations.

The parametric study presented in this thesis provides an extensive comparison of the absolute and relative accuracy of the different analytical hazard rate approximations that are available in the literature. Although the proposed formulas are not obtained from analytical derivations, they closely reproduce the behaviour observed from accurate importance sampling (ISEE) simulations. The modifications to the hazard function approximation are based on known limitations of the existing analytical approximations and on additional observations available in the literature. It is worth-mentioning that the approach followed in this thesis to improve the analytical approximation of the hazard rate has conceptual similarities with techniques previously employed in the literature. The solution obtained in this study represents a clear advancement when compared with the heuristic constant value of the exponent of the bandwidth parameter, since it allows accounting for the major parameters affecting this exponent. It is noted here that the nonstationary response processes considered in the parametric study behave as narrow-band and wide-band processes at different instants of time, as shown by the values assumed by their time-varying bandwidth parameter. Thus, the proposed formula is found to be

accurate both for narrow-band or wide-band processes, as demonstrated by the results presented in the thesis.

The new analytical approximation of the time-variant FPDF developed in this study for linear elastic SDOF systems subjected to stationary and/or nonstationary Gaussian excitations provides an extremely valuable tool for validating, in the linear range, numerical methods used to estimate failure probabilities in more general cases, such as those involving nonlinear structural behavior and non-Gaussian excitations and pounding of adjacent buildings. The proposed analytical approximation is also very useful in applications requiring numerous repeated computations of the failure probability, such as parametric studies and design optimization, since its computational cost is only a very small fraction of the computational cost associated with simulation techniques. Finally, this new analytical approximation represents an important first step toward the development of a more general approximation of the time-variant FPDF for linear and nonlinear MDOF systems subjected to stationary and/or nonstationary excitations.

Based on the research work performed and presented herein, several research areas have been identified as open to and in need of future work:

- (1) Extension of the proposed approximation of the FPDF found in this thesis for the case of SDOF systems subjected to stationary and/or nonstationary random processes to MDOF systems. This extension would be very significant, since most of the real-world structures are modeled as MDOF systems and the estimation of the FPDF for these structures using simulation is even more computationally expensive than for SDOF systems.
- (2) Application of the proposed FPDF approximation to pounding of adjacent buildings and other structural engineering applications where the first-passage problem is the dominant failure mechanism.
- (3) Extension of the proposed improved approximation of the time-variant FPDF to linear

elastic systems subjected to more general fully nonstationary excitation models (e.g., processes with time-varying amplitude and frequency content obtained as the summation of separable nonstationary processes).

- (4) Extension of the proposed approximation of the FPDF to nonlinear systems. This extension is fundamental due to the fact that most structural systems exhibit a nonlinear structural behavior, particularly when subjected to strong excitations, such as earthquake ground motions.
- (5) Extension of the proposed approximation of the FPDF to structural systems characterized by uncertain properties.

REFERENCES

- [1] Rice SO. Mathematical Analysis of Random Noise. Bell System Technical Journal. 1944;23:282-332.
- [2] Rice SO. Mathematical analysis of random noise-conclusion. Bell Systems Technical Journal. 1945;24:46-156.
- [3] Crandall S. First-crossing probabilities of the linear oscillator. Journal of Sounds and Vibrations. 1970;12(3):285-99.
- [4] Corotis RB, Vanmarcke EH, Cornell CA. First passage of nonstationary random processes. Journal of the Engineering Mechanics Division. 1972;98(EM2):401-14.
- [5] Vanmarcke EH. On the distribution of the first-passage time for normal stationary random processes. Journal of Applied Mechanics, ASME 1975;42:215-20.
- [6] Beck A. The random barrier-crossing problem. Probabilistic Engineering Mechanics. 2008;23:134-45.
- [7] Naess A. Approximate first-passage and extremes of narrow-band Gaussian and non-Gaussian random vibrations. Journal of Sounds and Vibrations. 1990;138:365-80.
- [8] Barbato M, Conte J. Structural Reliability Applications of Nonstationary Spectral Characteristics. Journal of Engineering Mechanics, ASCE 2011;137:371-82.
- [9] Lutes LD, Sarkani S. Random vibrations: Analysis of structural and mechanical systems. Burlington (MA): Elsevier Butterworth-Heinemann; 2004.
- [10] Bendat JS, Piersol AG. Random data: analysis and measurement procedures. New York (NY): John Wiley & Sons, Inc.; 1986.
- [11] Priestley MB. Non-linear and non-stationary time series analysis. London (UK): Academic Press; 1988.
- [12] Priestley MB. Spectral analysis and time series. Volume 1: Univariate series. Volume 2: Multivariate series, prediction and control. London (UK): Academic Press; 1987 Fifth printing.
- [13] Michaelov G, Sarkani S, Lutes L. Spectral characteristics of nonstationary random processes — A critical review. Structural safety. 1999;21:223-44.
- [14] Chopra AK. Dynamics of structures: theory and applications to earthquake engineering. New Jersey : Prentice Hall Upper Saddle River; 1995.
- [15] Barbato M, Conte J. Spectral characteristics of non-stationary random processes: Theory and applications to linear structural models. Probabilistic Engineering Mechanics. 2008;23:416-26.

- [16] Datta TK. Seismic Analysis of Structures. Singapore: John Wiley & Sons (Asia) Pte LTD; 2010.
- [17] Peng B, Conte J. Closed-form solutions for the response of linear systems to fully nonstationary earthquake excitation. *Journal of Engineering Mechanics*, ASCE 1998;124(6):684-94.
- [18] Elnashai AS, Di Sarno L. Fundamentals of earthquake engineering: Wiley Online Library; 2008.
- [19] Crandall S. First-crossing probabilities of the linear oscillator. *Journal of Sounds and Vibrations*. 1970;12(3):285-99.
- [20] Crandall S, Chandiramani K, Cook R, Engineers ASOM. Some first-passage problems in random vibration. *Journal of Applied Mechanics*, ASME; 1966; 33: 532-38.
- [21] Leadbetter M, Cramér H. Stationary and related stochastic processes. New York : Wiley; 1967.
- [22] Au S, Beck J. First excursion probabilities for linear systems by very efficient importance sampling. *Probabilistic Engineering Mechanics*. 2001;16(3):193-207.
- [23] Di Paola M. Transient spectral moments of linear systems. *SM archives*. 1985;10:225-43.
- [24] Barbato M, Vasta M. Closed-form solutions for the time-variant spectral characteristics of non-stationary random processes. *Probabilistic Engineering Mechanics*. 2010;25(1):9-17.
- [25] MathWorks-Inc. Matlab—High performance numeric computation and visualization software User’s Guide. Natick, MA, USA: The MathWorks Inc; 1997.
- [26] Vanmarcke EH. Structural response to earthquakes. In Lomnitz C., and Rosenblueth E. (Eds.). *Seismic Risk and Engineering Descisions*; Amsterdam: Elsevier, 1976.
- [27] Shinozuka M, Sato Y. Simulation of nonstationary random processes. *Journal of the Engineering Mechanics Division*, ASCE. 1967;93:11-40.
- [28] Yu QS, Sadre A. Seismic response of an instrumented 13-story steel frame building damaged in the 1994 Northridge earthquake. *Earthquake spectra*. 1997;13:131.
- [29] Barbato M, Conte J. Simplified probabilistic dynamic response analysis of structural systems. Greece, 2007. p. 13–6.
- [30] Filippou F, Constandines M. FedeeasLab Getting Started Guide And Simulations Examples-Dpt of civil and env. Engng UC Berkeley. 2004.

APPENDIX A : CALCULATION OF HAZARD FUNCTION VALUES FROM ISEE

The time-variant FPDF, $P_{f,|X|}$, corresponding to the out-crossing of a failure threshold level, x_{lim} , by the absolute value of the random process $X(t)$ (symmetric double-barrier problem) from at-rest initial conditions, is commonly expressed as:

$$P_{f,|X|}(x_{lim}, t) = 1 - \exp \left\{ - \int_0^t h_{|X|}(x_{lim}, \tau) \cdot d\tau \right\} \quad (A.1)$$

where t = time, $h_{|X|}$ = time-variant hazard function for the symmetric double-barrier problem.

Taking the time derivative of Eq. (A.1) gives:

$$\frac{dP_{f,|X|}(x_{lim}, t)}{dt} = \left\{ - \int_0^t h_{|X|}(x_{lim}, \tau) \cdot d\tau \right\} \cdot h(t) \quad (A.2)$$

Combining Eqs. (A.1) and (A.2) provides the hazard function as:

$$h_{|X|}(x_{lim}, t) = \frac{dP_{f,|X|}(x_{lim}, t)}{dt} \cdot \frac{1}{1 - P_{f,|X|}(x_{lim}, t)} \quad (A.3)$$

in which the $P_{f,|X|}(x_{lim}, t)$ function is not known explicitly but can be evaluated for different values of x_{lim} and t by using the ISEE method.

Since $P_{f,|X|}(x_{lim}, t)$ is computed implicitly through simulation, the time derivative of the FPDF can be calculated using a numerical differentiation method. Finite difference (FD) is one of the commonly used methods and has the following three general forms:

$$\text{Backward FD: } h_{BW}(t) = \frac{P_f^{(ISEE)}(t) - P_f^{(ISEE)}(t - \Delta t)}{\Delta t} \cdot \frac{1}{1 - P_f^{(ISEE)}(t)} \quad (A.4)$$

Forward FD:
$$h_{FW}(t) = \frac{P_f^{(ISEE)}(t + \Delta t) - P_f^{(ISEE)}(t)}{\Delta t} \cdot \frac{1}{1 - P_f^{(ISEE)}(t)} \quad (A.5)$$

Central FD:
$$h_C(t) = \frac{P_f^{(ISEE)}(t + \Delta t) - P_f^{(ISEE)}(t - \Delta t)}{2 \cdot \Delta t} \cdot \frac{1}{1 - P_f^{(ISEE)}(t)} \quad (A.6)$$

in which Δt = small but finite time increment.

Several SDOF linear oscillators with different damping ratios and normalized failure thresholds are studied here and the values of the hazard function are obtained from the ISEE results using the three numerical differentiation forms given in Eqs. (A.4) through (A.6) for the following values of $\Delta t = [0.01, 0.02, \dots, 0.07]$ s. A coefficient of variation equal to 0.01 is used for estimating the FFP with the ISEE method.

Table A.1 - Numerical estimation of the hazard function values computed at time $t = 0.5$ s for a linear SDOF system subjected to a WN excitation from at-rest initial conditions ($T = 1.0$ s ; $\xi = 0.1$; $\zeta = 4$).

Δt	t	P_f	h_{BW}	h_C	h_{FW}
0.01	0.49	9.63E-09	7.68E-08	7.80E-08	7.92E-08
	0.5	1.04E-08			
	0.51	1.12E-08			
0.02	0.48	8.91E-09	7.57E-08	7.66E-08	7.75E-08
	0.5	1.04E-08			
	0.52	1.20E-08			
0.03	0.47	8.15E-09	7.49E-08	7.72E-08	7.95E-08
	0.5	1.04E-08			
	0.53	1.28E-08			
0.04	0.46	7.41E-09	7.52E-08	7.86E-08	8.21E-08
	0.5	1.04E-08			
	0.54	1.37E-08			
0.05	0.45	6.63E-09	7.58E-08	8.02E-08	8.46E-08
	0.5	1.04E-08			
	0.55	1.46E-08			
0.06	0.44	5.87E-09	7.57E-08	8.21E-08	8.86E-08
	0.5	1.04E-08			
	0.56	1.57E-08			
0.07	0.43	5.09E-09	7.61E-08	8.46E-08	9.32E-08
	0.5	1.04E-08			
	0.57	1.69E-08			

The results of this study relative to the hazard function computed at time $t = 0.5s$ for a linear SDOF system with $T = 1.0s$; $\xi = 0.1$; $\zeta = 4$ and subjected to a WN excitation from at-rest initial conditions are shown in Table A.1 and Figure A.1. The hazard function values are normalized with the value corresponding to $\Delta t = 0.01s$ and are plotted versus the values of Δt in Figure A.1. The results in Table A.1 and Figure A.1 show that the hazard function values are significantly sensitive to both the form of the numerical differentiation used and the value of Δt . Therefore, it is concluded that the estimation of the hazard function from direct simulation is not feasible because it is prone to numerical inaccuracies.

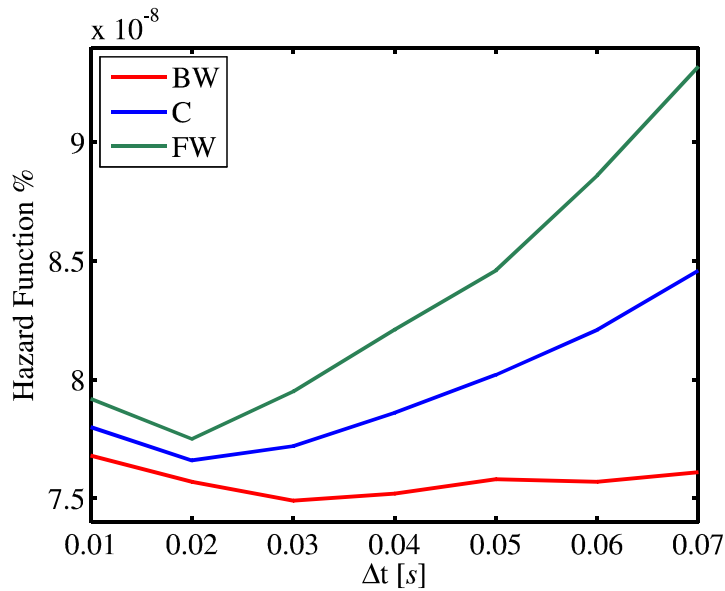


Figure A.1- Dependency of the hazard function numerical estimates on the time interval Δt computed at time $t = 0.5s$ for a linear SDOF system subjected to a WN excitation from at-rest initial conditions ($T = 1.0s$; $\xi = 0.1$; $\zeta = 4$).

APPENDIX B : PROPOSED HAZARD FUNCTIONS FOR FPDF OF SDOF SYSTEMS SUBJECTED TO WN EXCITATION FROM AT-REST INITIAL CONDITIONS

Six different hazard function approximations for linear elastic SDOF systems subjected to WN excitation from at-rest initial conditions are developed and studied in this research in order to determine the proposed improved analytical approximation presented in this thesis. In this appendix, these six hazard functions are presented and described in detail.

B.1 PROPOSED #1

The first proposed hazard function (referred to as Proposed #1) is given by Eq. (B.1) and is obtained by introducing a constant value for the exponent of the TVBP. This constant exponent is defined by a time independent function obtained as a polynomial surface (Eq. (B.2)) fitted to ISEE simulation results for different values of ξ and ζ (see Figure B.1). The coefficients of the polynomial function are given in Table B.1.

$$h_{1,|X|}(x_{\text{lim}}, t) = \nu_{|X|}(x_{\text{lim}}, t) \cdot \frac{1 - \exp\left\{-\sqrt{\pi/2} \cdot [q_X(t)]^{C(\xi, \zeta)} \cdot \frac{x_{\text{lim}}}{\sigma_X(t)}\right\}}{1 - \exp\left\{-\frac{1}{2} \left[\frac{x_{\text{lim}}}{\sigma_X(t)}\right]^2\right\}} \quad (\text{B.1})$$

$$C(\xi, \zeta) = \sum_{l=0}^5 \sum_{m=0}^4 (P_{lm}^{(i)} \cdot \xi^l \cdot \zeta^m) \quad ; \quad 0.01 \leq \xi \leq 0.50 \quad ; \quad 1.5 \leq \zeta \leq 5.0 \quad (\text{B.2})$$

Table B.1 - Proposed #1: Coefficients of the polynomial representation of $C(\xi, \zeta)$.

$P_{00}^{(i)}$	$P_{10}^{(i)}$	$P_{01}^{(i)}$	$P_{20}^{(i)}$	$P_{11}^{(i)}$	$P_{02}^{(i)}$	$P_{30}^{(i)}$	$P_{21}^{(i)}$	$P_{12}^{(i)}$	$P_{03}^{(i)}$
1.676	-18.23	-0.1955	77.2	11.09	0.06903	-136.2	-47.33	-2.522	-0.01776
$P_{40}^{(i)}$	$P_{31}^{(i)}$	$P_{22}^{(i)}$	$P_{13}^{(i)}$	$P_{04}^{(i)}$	$P_{50}^{(i)}$	$P_{41}^{(i)}$	$P_{32}^{(i)}$	$P_{23}^{(i)}$	$P_{14}^{(i)}$
155.2	44.52	9.688	0.09391	0.001621	-84.81	-14.33	-4.609	-0.5489	0.01242

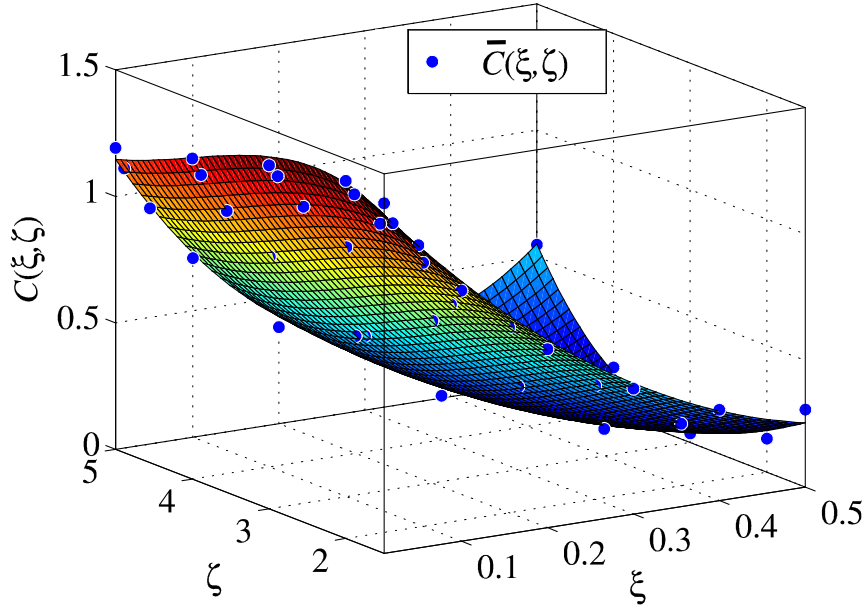


Figure B.1 - Proposed #1: Fitted surface for $C(\xi, \zeta)$ for Proposed#1.

B.2 PROPOSED #2

The second proposed hazard function (referred to as Proposed #2) is given by Eq. (B.3) and is obtained by introducing two constant values, one for the exponent of the TVBP and one as the coefficient of the TVBP. These two constant exponents are defined by time independent functions obtained as polynomial surfaces (Eq. (B.5)) fitted to ISEE simulation results for different values of ξ and ζ .

$$h_{2,|X|}(x_{\text{lim}}, t) = v_{|X|}(x_{\text{lim}}, t) \cdot \frac{1 - \exp \left\{ -\sqrt{\pi/2} \cdot [C_2(\xi, \zeta) \cdot q_X(t)]^{C_1(\xi, \zeta)} \cdot \frac{x_{\text{lim}}}{\sigma_X(t)} \right\}}{1 - \exp \left\{ -\frac{1}{2} \left[\frac{x_{\text{lim}}}{\sigma_X(t)} \right]^2 \right\}} \quad (\text{B.4})$$

where

$$C_i(\xi, \zeta) = \sum_{l=0}^5 \sum_{m=0}^4 (P_{lm}^{(i)} \cdot \xi^l \cdot \zeta^m) \quad ; \quad i = 1, 2 \quad ; \quad 0.01 \leq \xi \leq 0.50 \quad ; \quad 1.5 \leq \zeta \leq 5.0 \quad (\text{B.5})$$

It is observed that the function used in the least-square fitting procedure is not properly constrained, the obtained optimized values of $C_1(\xi, \zeta)$ and $C_2(\xi, \zeta)$ are not unique and depend on the starting point of the optimization procedure, and, thus, this proposed function is not applicable.

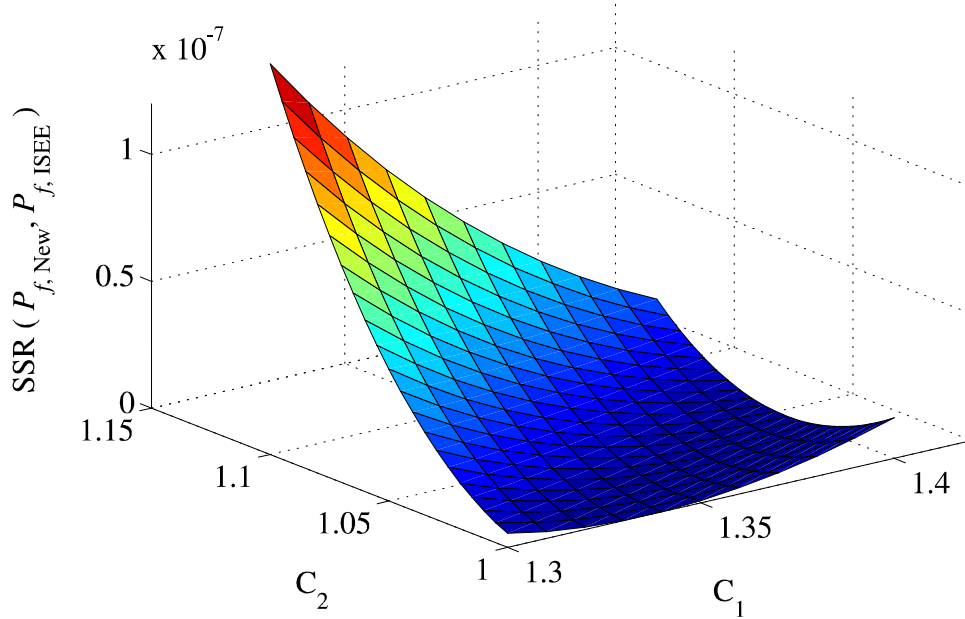


Figure B.2 - Proposed #2: Plot of sum of squared residuals of the error vs. C_1 and C_2 for linear SDOF system with $T = 1.0s$; $\xi = 0.1$; $\zeta = 4$.

Figure B.2 presents the sum of squared residuals of the FPDF using the proposed hazard function and the ISEE results (i.e., $\sum_{C_i=1}^{1.5} \sum_{C_j=1}^{1.5} [P_{f,New}^{(C_i, C_j)}(t) - P_{f,ISEE}(t)]^2$, in which C_i and C_j are chosen to be in the same range of $C_{1,2}(\bar{\xi}, \bar{\zeta})$ obtained from the optimization) for the case of $T = 1.0s$; $\xi = 0.1$; $\zeta = 4$. As it is seen, the sum of squared residuals lies along a line and does not have a unique minimum.

B.3 PROPOSED #3

On the basis of the observed trends (see Section 2.2), a hazard function for the double-barrier first-passage problem is proposed (see Figure B.3). This proposed hazard function (referred to as

Proposed #3) is given by Eq. (B.6) and is obtained by introducing a time-variant function for the exponent of the TVBP given by Eq. (B.7):

$$h_{\text{new},|X|}(x_{\text{lim}}, t) = v_{|X|}(x_{\text{lim}}, t) \cdot \frac{1 - \exp\left\{-\sqrt{\pi/2} \cdot [q_X(t)]^{C(\xi, \zeta, t)} \cdot \frac{x_{\text{lim}}}{\sigma_X(t)}\right\}}{1 - \exp\left\{-\frac{1}{2} \left[\frac{x_{\text{lim}}}{\sigma_X(t)}\right]^2\right\}} \quad (\text{B.6})$$

in which $C(\xi, \zeta, t) =$ time-variant function with two variables given as:

$$C(\xi, \zeta, t) = C_{1,\infty}(\xi, \zeta) \left(1 + C_{2,\infty}(\xi, \zeta) \cdot e^{-\frac{t}{T}}\right) \quad (\text{B.7})$$

where $C_{1,\infty}(\xi, \zeta)$ and $C_{2,\infty}(\xi, \zeta)$ are obtained from Eq. (B.8) with the coefficients given in Table B.2.

$$C_{i,\infty}(\xi, \zeta) = \sum_{l=0}^5 \sum_{m=0}^4 (P_{lm}^{(i)} \cdot \xi^l \cdot \zeta^m) \quad ; \quad i=1,2 \quad ; \quad 0.01 \leq \xi \leq 0.50 \quad ; \quad 1.5 \leq \zeta \leq 5.0 \quad (\text{B.8})$$

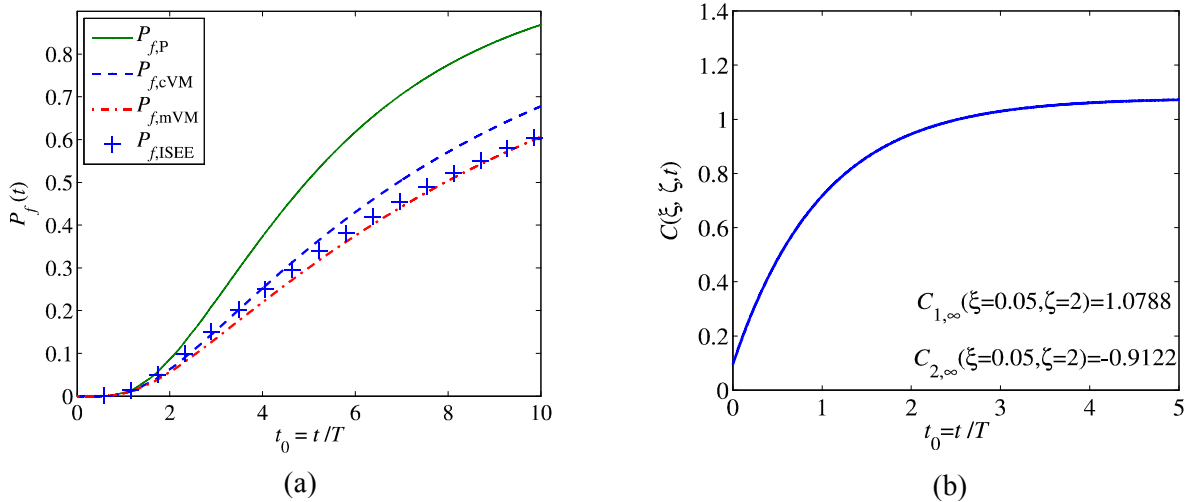


Figure B.3 - Proposed #3: (a) FPDF for the linear SDOF system with $T = 0.1\text{s}$; $\xi = 0.05$; $\zeta = 2$
(b) $C(\xi, \zeta, t)$ plotted as a function of the normalized time for the same SDOF system.

Table B.2 - Proposed #3: Coefficients of the polynomial representation of $C_{1,\infty}(\xi, \zeta)$ and $C_{2,\infty}(\xi, \zeta)$.

i	$P_{00}^{(i)}$	$P_{10}^{(i)}$	$P_{01}^{(i)}$	$P_{20}^{(i)}$	$P_{11}^{(i)}$	$P_{02}^{(i)}$	$P_{30}^{(i)}$	
1	0.7601	-4.065	0.526	15.4	-0.01364	-0.04164	-18.7	
2	-552.4	5668	400.5	-26800	-1535	-152.7	57850	
i	$P_{21}^{(i)}$	$P_{12}^{(i)}$	$P_{03}^{(i)}$	$P_{40}^{(i)}$	$P_{31}^{(i)}$	$P_{22}^{(i)}$	$P_{13}^{(i)}$	$P_{04}^{(i)}$
1	-7.129	0.06362	-0.03764	11.79	4.812	0.8123	-0.006323	0.005449
2	2710	238.8	26.92	-46710	-1080	-271.3	-7.619	-1.854

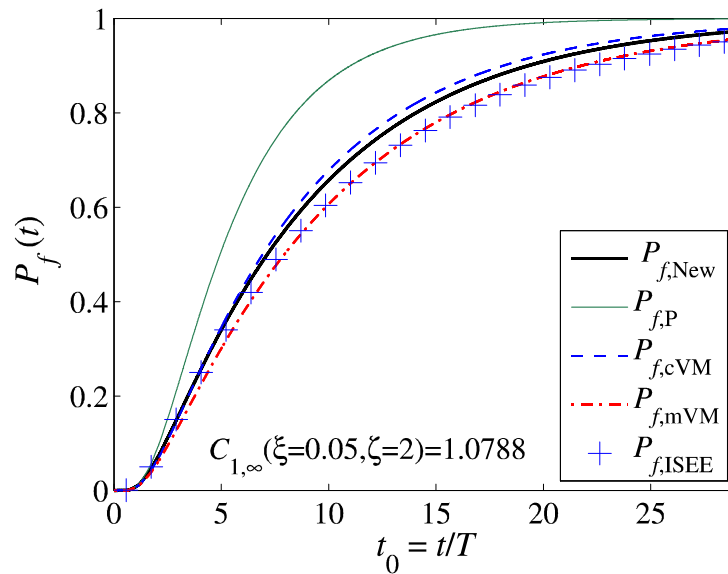


Figure B.4 - Proposed #3: FPDF for a linear SDOF system with $T = 0.1$ s subjected to WN base excitation from at-rest initial conditions ($\xi = 0.05$; $\zeta = 2$).

B.4 PROPOSED #4

Based on the observed trends and behavior of the ISEE results (see Section 2.2), the fourth hazard function (referred to as Proposed #4) is proposed by introducing a time-variant function with follows the same trend as discussed in Section 2.2 (see Figure B.5). This proposed hazard function is given by Eq. (B.9):

$$h_{\text{new},|X|}(x_{\text{lim}}, t) = \nu_{|X|}(x_{\text{lim}}, t) \cdot \frac{1 - \exp\left\{-\sqrt{\pi/2} \cdot [q_X(t)]^{C(\xi, \zeta, t)} \cdot \frac{x_{\text{lim}}}{\sigma_X(t)}\right\}}{1 - \exp\left\{-\frac{1}{2} \left[\frac{x_{\text{lim}}}{\sigma_X(t)}\right]^2\right\}} \quad (\text{B.9})$$

The time-variant function in Eq. (B.9) is given as:

$$C(\xi, \zeta, t) = C_{1,\infty}(\xi, \zeta) + C_{2,\infty}(\xi, \zeta) \cdot \left(1 - \exp[q(t) - q_{X,\infty}]\right) \quad (\text{B.10})$$

in which

$$q_{X,\infty} = \lim_{t \rightarrow \infty} q(t) = \left\{1 - \frac{4 \left[\text{arctg}(\sqrt{1 - \xi^2} / \xi)\right]^2}{\pi^2 (1 - \xi^2)}\right\}^{1/2} \quad (\text{B.11})$$

where $q_{X,\infty}$ = stationary value of the bandwidth parameter.

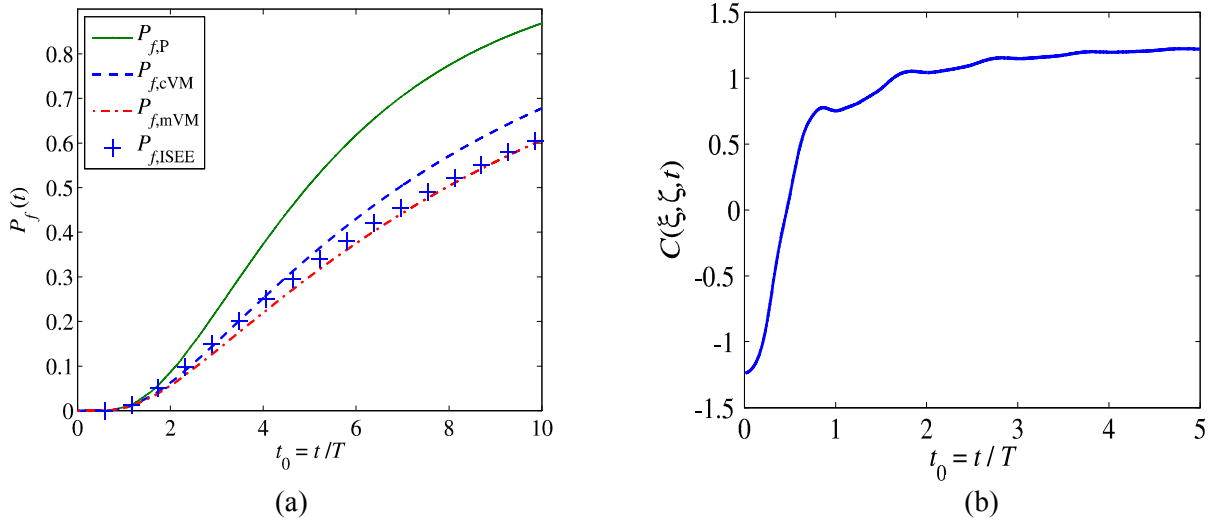


Figure B.5 - Proposed #4: (a) FPF for the linear SDOF system with $T = 0.1\text{s}$; $\xi = 0.05$; $\zeta = 2$
(b) $C(\xi, \zeta, t)$ plotted as a function of the normalized time for the same SDOF system.

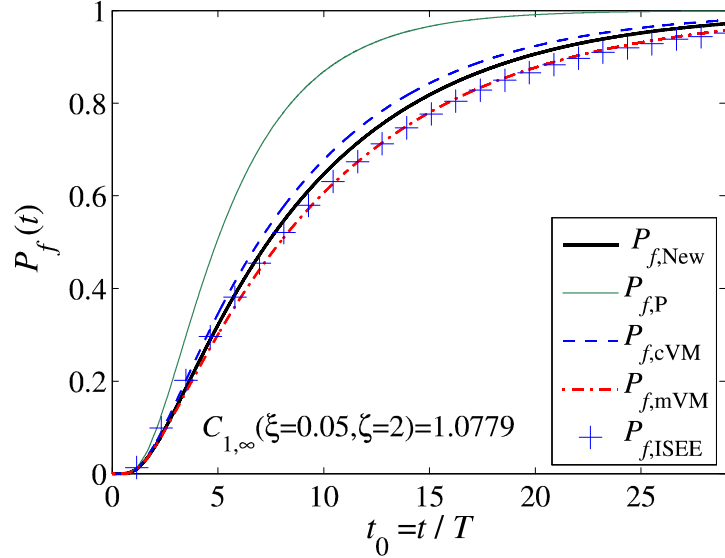


Figure B.6 - Proposed #4: FFPF for a linear SDOF system with $T = 0.1s$ subjected to WN base excitation from at-rest initial conditions ($\xi = 0.05$; $\zeta = 2$).

B.5 PROPOSED #5

The fifth proposed hazard function (referred to as Proposed #5) is given by Eq. (B.12) and is obtained by introducing a time-variant function for the exponent of the TVBP (Eq. (B.13)) which is calculated using Eq. (B.8) and coefficients presented in Table B.3:

$$h_{\text{new},|x|}(x_{\text{lim}}, t) = \nu_{|x|}(x_{\text{lim}}, t) \cdot \frac{1 - \exp\left\{-\sqrt{\pi/2} \cdot [q_X(t)]^{C_{\text{exp}}(\xi, \zeta, t)} \cdot \frac{x_{\text{lim}}}{\sigma_X(t)}\right\}}{1 - \exp\left\{-\frac{1}{2} \left[\frac{x_{\text{lim}}}{\sigma_X(t)}\right]^2\right\}} \quad (\text{B.12})$$

in which $C(\xi, \zeta, t) =$ time-variant exponent is defined as follows:

$$C(\xi, \zeta, t) = C_{1,\infty}(\xi, \zeta) \cdot e^{[-q_X(t) + q_{X,\infty}]} \quad (\text{B.13})$$

Table B.3 - Proposed #5: Coefficients of the polynomial fitted to $C_{1,\infty}(\xi, \zeta)$.

i	$P_{00}^{(i)}$	$P_{10}^{(i)}$	$P_{01}^{(i)}$	$P_{20}^{(i)}$	$P_{11}^{(i)}$	$P_{02}^{(i)}$	$P_{30}^{(i)}$	$P_{21}^{(i)}$	$P_{12}^{(i)}$	$P_{03}^{(i)}$
1	1.053	-13.31	0.5111	65.91	6.435	-0.2108	-142.6	-35.92	-1.199	0.03141
i	$P_{40}^{(i)}$	$P_{31}^{(i)}$	$P_{22}^{(i)}$	$P_{13}^{(i)}$	$P_{04}^{(i)}$	$P_{50}^{(i)}$	$P_{41}^{(i)}$	$P_{32}^{(i)}$	$P_{23}^{(i)}$	$P_{14}^{(i)}$
1	214.9	30.36	7.934	-0.07924	-0.001609	-145.1	-7.412	-3.666	-0.4575	0.02134

Figure B.7 shows the FFPF obtained from the analytical approximations and the proposed #5 obtained using the optimized value of $C(\xi, \zeta, t)$ are in a significantly good agreement with the ISEE results compared to the other analytical approximations.

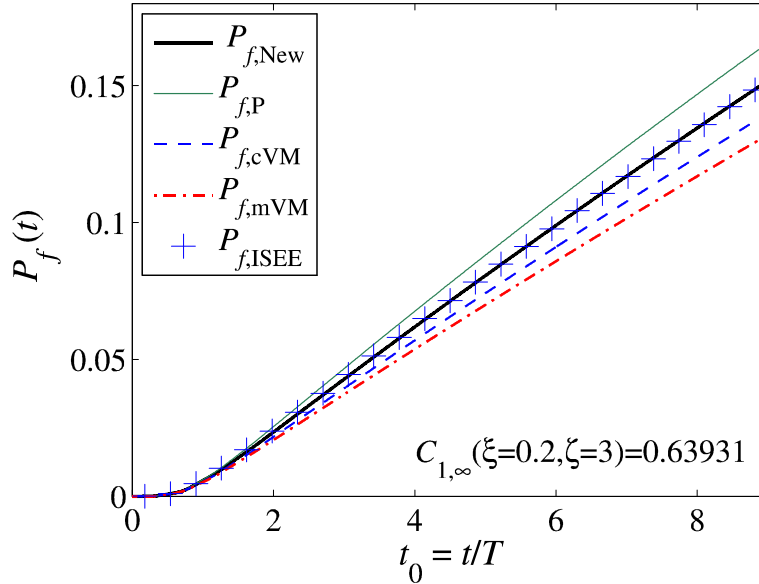


Figure B.7 - Proposed #5: FFPF obtained through least-square fitting of the ISEE results and the corresponding P and VM approximations for linear SDOF system ($\xi = 0.2$; $\zeta = 3$).

Figure B.8 and Figure B.9 plot the isocurves of $C_{1,\infty}(\xi, \zeta)$ as a function of damping ratio and normalized threshold level, respectively. It is observed that the surface fitted to the optimized values of $C_{1,\infty}(\xi, \zeta)$ is an accurate fit to the values obtained from the least-square fitting.

Figure B.10 and Figure B.11 show that the FFPF values obtained using the proposed #5 are in significantly better agreement with the ISEE results compared to the other analytical approximations.

B.6 PROPOSED #6

The sixth proposed function is introduced in Chapter 2 and referred to as newly proposed hazard function (New).

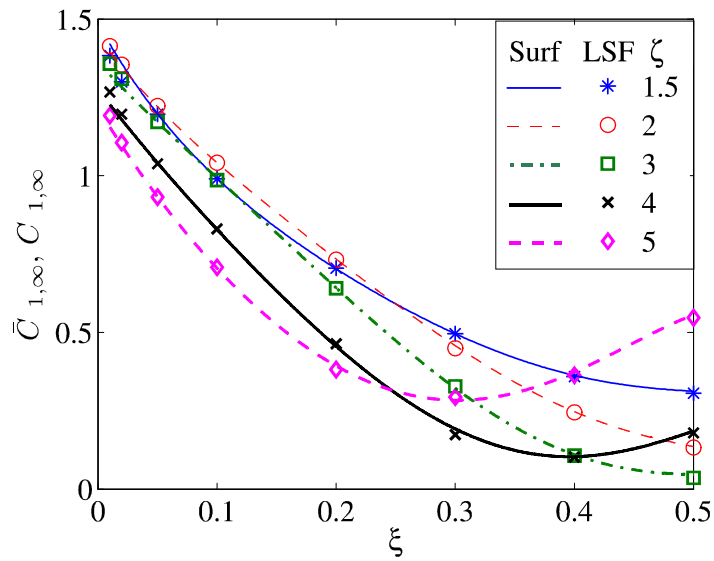


Figure B.8 - Proposed #5: Comparison between the interpolation surface $C_{1,\infty}$ (Surf) and values $\bar{C}_{1,\infty}$ obtained through least-square fitting (LSF) versus damping ratio.

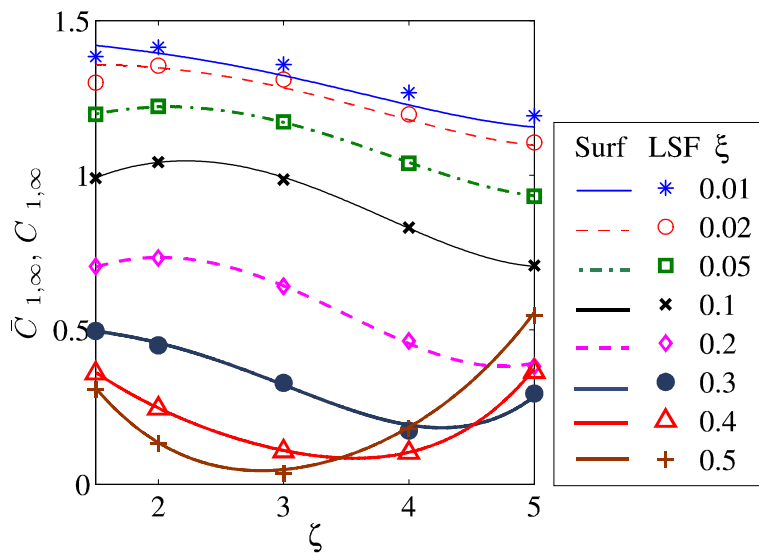


Figure B.9 - Proposed #5: Comparison between the interpolation surface $C_{1,\infty}$ (Surf) and values $\bar{C}_{1,\infty}$ obtained through least-square fitting (LSF) versus the normalized threshold level.

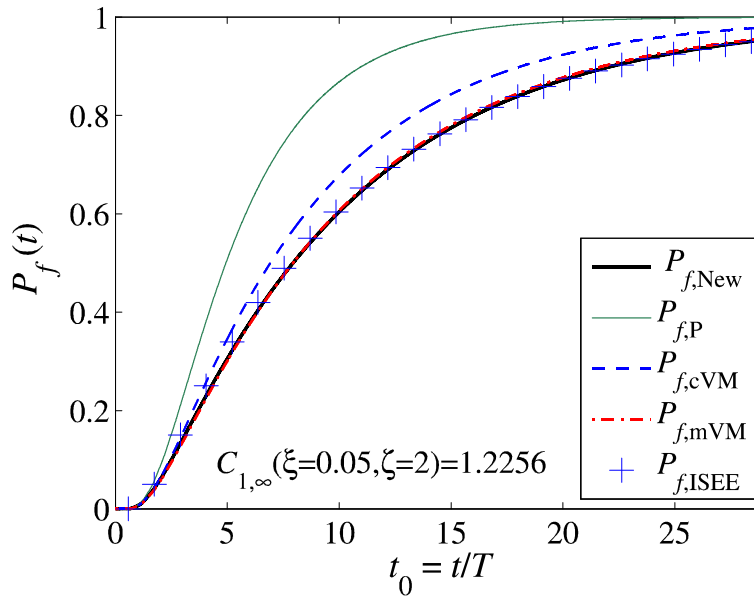


Figure B.10 - Proposed #5: FFPF for a linear SDOF system with $T = 0.1s$ subjected to WN base excitation from at-rest initial conditions ($\xi = 0.05, \zeta = 2$).

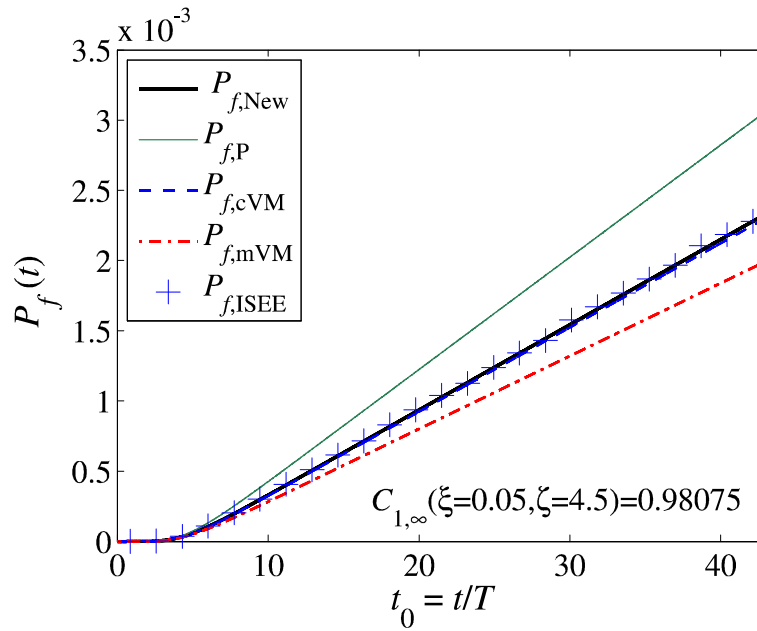


Figure B.11 - Proposed #5: FFPF for a linear SDOF system with $T = 0.1s$ subjected to WN base excitation from at-rest initial conditions ($\xi = 0.05, \zeta = 4.5$).

APPENDIX C : PARAMETRIC STUDY RESULTS OF LINEAR SDOF SYSTEMS SUBJECTED TO WN EXCITATION FROM AT-REST INITIAL CONDITIONS

In this appendix, the absolute and relative accuracy of the six proposed hazard functions (see Appendix B), for linear elastic SDOF systems subjected to WN base excitation from at-rest initial conditions, is evaluated, by comparing the obtained time-variant FPDF with the corresponding ISEE values for a wide range of damping ratios and normalized failure thresholds. It is noted here that the accuracy of the proposed hazard functions is verified indirectly, through comparison of FPDF results, due to the difficulty in obtaining the values of the hazard function directly from simulation, as shown in Appendix A.

C.1 PROPOSED #1

Table C.1 - Proposed #1: Time-variant FPDF ($t_0 = 10$) .

ζ	ξ	ISEE	P	ε [%]	cVM	ε [%]	mVM	ε [%]	#1	ε [%]
1.5	0.01	4.06E-01	8.44E-01	108.10	5.39E-01	32.81	4.42E-01	9.10	3.44E-01	-15.15
	0.02	6.83E-01	9.72E-01	42.30	8.05E-01	17.82	7.16E-01	4.85	6.38E-01	-6.62
	0.05	9.20E-01	9.95E-01	8.16	9.52E-01	3.53	9.16E-01	-0.42	9.16E-01	-0.38
	0.1	9.92E-01	9.97E-01	0.53	9.85E-01	-0.70	9.73E-01	-1.92	9.85E-01	-0.67
	0.15	9.98E-01	9.98E-01	-0.04	9.92E-01	-0.58	9.87E-01	-1.14	9.95E-01	-0.29
	0.2	9.84E-01	9.98E-01	1.43	9.95E-01	1.15	9.92E-01	0.83	9.98E-01	1.41
	0.25	9.95E-01	9.98E-01	0.35	9.97E-01	0.20	9.95E-01	0.00	9.99E-01	0.40
	0.3	1.00E+00	9.98E-01	-0.18	9.97E-01	-0.26	9.96E-01	-0.39	9.99E-01	-0.09
	0.35	1.00E+00	9.98E-01	-0.17	9.98E-01	-0.21	9.97E-01	-0.30	9.99E-01	-0.07
	0.4	9.81E-01	9.98E-01	1.73	9.98E-01	1.73	9.98E-01	1.65	9.99E-01	1.85
	0.45	9.98E-01	9.98E-01	0.05	9.98E-01	0.07	9.98E-01	0.01	9.99E-01	0.16
0.5	1.00E+00	9.98E-01	-0.17	9.99E-01	-0.13	9.98E-01	-0.18	1.00E+00	-0.05	
2	0.01	1.23E-01	3.39E-01	176.24	1.66E-01	35.26	1.29E-01	4.87	9.81E-02	-20.01
	0.02	3.16E-01	6.81E-01	115.15	4.08E-01	28.77	3.34E-01	5.44	2.83E-01	-10.53
	0.05	6.15E-01	8.68E-01	41.22	6.78E-01	10.25	6.07E-01	-1.37	5.99E-01	-2.60
	0.1	7.84E-01	9.07E-01	15.77	7.98E-01	1.85	7.52E-01	-4.03	7.89E-01	0.71
	0.15	8.47E-01	9.18E-01	8.34	8.44E-01	-0.37	8.12E-01	-4.16	8.60E-01	1.53
	0.2	8.94E-01	9.22E-01	3.15	8.68E-01	-2.91	8.44E-01	-5.58	8.93E-01	-0.07
	0.25	9.18E-01	9.25E-01	0.74	8.83E-01	-3.82	8.64E-01	-5.85	9.12E-01	-0.69
	0.3	9.26E-01	9.26E-01	0.02	8.93E-01	-3.58	8.78E-01	-5.21	9.23E-01	-0.40
	0.35	9.34E-01	9.27E-01	-0.69	9.00E-01	-3.59	8.88E-01	-4.93	9.29E-01	-0.50
	0.4	9.32E-01	9.28E-01	-0.44	9.06E-01	-2.84	8.95E-01	-3.98	9.33E-01	0.11
	0.45	9.29E-01	9.29E-01	-0.02	9.10E-01	-2.03	9.01E-01	-3.03	9.36E-01	0.74
0.5	9.32E-01	9.29E-01	-0.35	9.13E-01	-2.04	9.05E-01	-2.90	9.37E-01	0.53	

ζ	ξ	ISEE	P	ε [%]	cVM	ε [%]	mVM	ε [%]	#1	ε [%]
2.5	0.01	2.48E-02	6.43E-02	159.70	3.15E-02	27.38	2.42E-02	-2.25	1.92E-02	-22.63
	0.02	9.95E-02	2.45E-01	146.08	1.29E-01	29.50	1.02E-01	2.69	8.76E-02	-11.92
	0.05	2.61E-01	4.57E-01	74.65	3.01E-01	14.97	2.58E-01	-1.51	2.55E-01	-2.31
	0.1	4.03E-01	5.26E-01	30.42	4.04E-01	0.23	3.67E-01	-8.99	3.97E-01	-1.52
	0.15	4.74E-01	5.47E-01	15.43	4.51E-01	-4.82	4.21E-01	-11.16	4.69E-01	-1.13
	0.2	5.02E-01	5.58E-01	11.04	4.79E-01	-4.60	4.54E-01	-9.51	5.10E-01	1.56
	0.25	5.41E-01	5.64E-01	4.18	4.98E-01	-8.05	4.77E-01	-11.85	5.35E-01	-1.07
	0.3	5.57E-01	5.68E-01	1.98	5.11E-01	-8.24	4.93E-01	-11.38	5.51E-01	-0.97
	0.35	5.38E-01	5.70E-01	5.95	5.21E-01	-3.29	5.05E-01	-6.09	5.61E-01	4.26
	0.4	5.57E-01	5.72E-01	2.76	5.28E-01	-5.15	5.15E-01	-7.52	5.67E-01	1.90
	0.45	5.69E-01	5.73E-01	0.74	5.34E-01	-6.20	5.22E-01	-8.25	5.71E-01	0.31
0.5	5.60E-01	5.74E-01	2.54	5.39E-01	-3.84	5.28E-01	-5.69	5.73E-01	2.31	
3	0.01	3.49E-03	7.66E-03	119.47	4.07E-03	16.64	3.14E-03	-10.01	2.64E-03	-24.29
	0.02	2.30E-02	5.18E-02	125.54	2.81E-02	22.25	2.22E-02	-3.37	2.00E-02	-13.02
	0.05	7.79E-02	1.34E-01	71.73	8.66E-02	11.26	7.35E-02	-5.60	7.54E-02	-3.18
	0.1	1.27E-01	1.68E-01	31.41	1.26E-01	-0.96	1.14E-01	-10.83	1.27E-01	-0.63
	0.15	1.55E-01	1.79E-01	15.41	1.45E-01	-6.45	1.34E-01	-13.25	1.53E-01	-0.85
	0.2	1.70E-01	1.84E-01	8.30	1.56E-01	-8.35	1.47E-01	-13.49	1.69E-01	-0.71
	0.25	1.80E-01	1.87E-01	4.24	1.63E-01	-9.23	1.56E-01	-13.31	1.78E-01	-1.00
	0.3	1.83E-01	1.89E-01	3.49	1.68E-01	-8.04	1.62E-01	-11.45	1.83E-01	0.21
	0.35	1.86E-01	1.91E-01	2.85	1.72E-01	-7.22	1.67E-01	-10.11	1.87E-01	0.65
	0.4	1.85E-01	1.92E-01	4.03	1.75E-01	-5.05	1.71E-01	-7.59	1.89E-01	2.37
	0.45	1.90E-01	1.93E-01	1.67	1.78E-01	-6.35	1.73E-01	-8.52	1.90E-01	0.30
0.5	1.91E-01	1.93E-01	1.05	1.79E-01	-6.22	1.76E-01	-8.13	1.91E-01	-0.24	
3.5	0.01	3.37E-04	6.40E-04	90.15	3.69E-04	9.64	2.87E-04	-14.61	2.59E-04	-22.99
	0.02	3.94E-03	7.71E-03	95.55	4.48E-03	13.75	3.57E-03	-9.48	3.43E-03	-13.10
	0.05	1.69E-02	2.61E-02	54.11	1.78E-02	5.13	1.52E-02	-10.29	1.63E-02	-3.43
	0.1	2.80E-02	3.45E-02	23.17	2.71E-02	-3.38	2.45E-02	-12.49	2.81E-02	0.15
	0.15	3.37E-02	3.74E-02	10.77	3.13E-02	-7.15	2.92E-02	-13.39	3.37E-02	-0.07
	0.2	3.66E-02	3.88E-02	5.81	3.38E-02	-7.83	3.20E-02	-12.52	3.67E-02	0.11
	0.25	3.76E-02	3.96E-02	5.19	3.54E-02	-6.03	3.40E-02	-9.81	3.83E-02	1.86
	0.3	3.88E-02	4.02E-02	3.57	3.65E-02	-5.84	3.53E-02	-8.91	3.94E-02	1.45
	0.35	4.03E-02	4.06E-02	0.76	3.74E-02	-7.21	3.64E-02	-9.71	4.00E-02	-0.75
	0.4	4.03E-02	4.09E-02	1.36	3.80E-02	-5.73	3.71E-02	-7.88	4.04E-02	0.09
	0.45	4.14E-02	4.11E-02	-0.65	3.85E-02	-6.88	3.78E-02	-8.71	4.06E-02	-1.83
0.5	4.12E-02	4.12E-02	0.06	3.89E-02	-5.64	3.82E-02	-7.24	4.07E-02	-1.17	

ζ	ξ	ISEE	P	ε [%]	cVM	ε [%]	mVM	ε [%]	#1	ε [%]	
4	0.01	2.24E-05	3.82E-05	70.60	2.37E-05	5.55	1.86E-05	-16.96	1.80E-05	-19.87	
	0.02	4.95E-04	8.66E-04	74.75	5.40E-04	8.90	4.33E-04	-12.53	4.44E-04	-10.35	
	0.05	2.72E-03	3.79E-03	39.36	2.74E-03	0.89	2.37E-03	-13.03	2.67E-03	-1.93	
	0.1	4.60E-03	5.25E-03	14.04	4.31E-03	-6.23	3.94E-03	-14.25	4.59E-03	-0.25	
	0.15	5.36E-03	5.73E-03	6.92	5.00E-03	-6.82	4.70E-03	-12.33	5.40E-03	0.78	
	0.2	5.70E-03	5.98E-03	4.89	5.38E-03	-5.54	5.15E-03	-9.67	5.80E-03	1.84	
	0.25	6.00E-03	6.12E-03	1.96	5.63E-03	-6.24	5.44E-03	-9.40	6.02E-03	0.25	
	0.3	6.07E-03	6.22E-03	2.48	5.80E-03	-4.41	5.65E-03	-6.98	6.15E-03	1.33	
	0.35	6.27E-03	6.29E-03	0.34	5.93E-03	-5.43	5.80E-03	-7.50	6.23E-03	-0.55	
	0.4	6.33E-03	6.34E-03	0.16	6.03E-03	-4.86	5.92E-03	-6.60	6.29E-03	-0.66	
	0.45	6.34E-03	6.38E-03	0.69	6.10E-03	-3.79	6.01E-03	-5.27	6.33E-03	-0.17	
0.5	6.30E-03	6.41E-03	1.70	6.16E-03	-2.36	6.07E-03	-3.65	6.35E-03	0.74		
4.5	0.01	1.07E-06	1.64E-06	53.12	1.07E-06	0.59	8.54E-07	-20.04	8.71E-07	-18.43	
	0.02	4.78E-05	7.45E-05	55.86	4.93E-05	3.11	4.00E-05	-16.38	4.32E-05	-9.58	
	0.05	3.32E-04	4.26E-04	28.50	3.25E-04	-2.02	2.83E-04	-14.64	3.30E-04	-0.58	
	0.1	5.62E-04	6.14E-04	9.25	5.25E-04	-6.54	4.85E-04	-13.69	5.65E-04	0.58	
	0.15	6.45E-04	6.77E-04	4.95	6.09E-04	-5.57	5.78E-04	-10.41	6.55E-04	1.58	
	0.2	6.94E-04	7.08E-04	2.06	6.55E-04	-5.61	6.31E-04	-9.09	6.97E-04	0.47	
	0.25	7.14E-04	7.27E-04	1.86	6.84E-04	-4.18	6.65E-04	-6.84	7.20E-04	0.93	
	0.3	7.21E-04	7.40E-04	2.56	7.04E-04	-2.41	6.89E-04	-4.53	7.35E-04	1.88	
	0.35	7.52E-04	7.49E-04	-0.39	7.18E-04	-4.44	7.06E-04	-6.11	7.44E-04	-0.97	
	0.4	7.52E-04	7.56E-04	0.49	7.29E-04	-3.02	7.19E-04	-4.40	7.51E-04	-0.11	
	0.45	7.46E-04	7.61E-04	2.05	7.38E-04	-1.06	7.29E-04	-2.24	7.56E-04	1.37	
0.5	7.57E-04	7.65E-04	1.14	7.44E-04	-1.59	7.37E-04	-2.58	7.59E-04	0.36		
5	0.01	3.53E-08	5.00E-08	41.56	3.46E-08	-2.12	2.78E-08	-21.38	2.93E-08	-17.13	
	0.02	3.42E-06	4.92E-06	43.82	3.42E-06	0.12	2.80E-06	-18.00	3.13E-06	-8.60	
	0.05	3.16E-05	3.74E-05	18.20	2.98E-05	-5.91	2.62E-05	-17.18	3.08E-05	-2.48	
	0.1	5.28E-05	5.59E-05	5.97	4.94E-05	-6.44	4.60E-05	-12.82	5.30E-05	0.41	
	0.15	6.12E-05	6.22E-05	1.63	5.73E-05	-6.29	5.48E-05	-10.43	6.10E-05	-0.39	
	0.2	6.43E-05	6.53E-05	1.61	6.16E-05	-4.14	5.97E-05	-7.10	6.47E-05	0.60	
	0.25	6.77E-05	6.72E-05	-0.75	6.42E-05	-5.06	6.28E-05	-7.22	6.67E-05	-1.39	
	0.3	6.89E-05	6.84E-05	-0.70	6.60E-05	-4.15	6.49E-05	-5.82	6.80E-05	-1.22	
	0.35	6.94E-05	6.93E-05	-0.14	6.73E-05	-2.99	6.64E-05	-4.32	6.89E-05	-0.65	
	0.4	6.98E-05	7.00E-05	0.27	6.83E-05	-2.15	6.75E-05	-3.23	6.96E-05	-0.30	
	0.45	7.01E-05	7.05E-05	0.55	6.91E-05	-1.53	6.84E-05	-2.43	7.01E-05	-0.12	
	0.5	6.97E-05	7.09E-05	1.83	6.97E-05	-0.02	6.91E-05	-0.77	7.04E-05	1.07	
				μ_ε %	22.38	μ_ε %	-0.004	μ_ε %	-7.09	μ_ε %	-2.54
				σ_ε %	39.25	σ_ε %	9.45	σ_ε %	5.76	σ_ε %	6.25
				ε_{\max} %	176.24	ε_{\max} %	35.26	ε_{\max} %	9.10	ε_{\max} %	4.26
				ε_{\min} %	-0.75	ε_{\min} %	-9.23	ε_{\min} %	-21.38	ε_{\min} %	-24.29
				$\mu_{ \varepsilon }$ %	22.48	$\mu_{ \varepsilon }$ %	6.32	$\mu_{ \varepsilon }$ %	7.70	$\mu_{ \varepsilon }$ %	3.35

C.2 PROPOSED #3

Table C.2 - Proposed #3: Time-variant FPDF ($t_0 = 10$).

ζ	ξ	ISEE	P	ε [%]	cVM	ε [%]	mVM	ε [%]	#3	ε [%]
1.5	0.01	4.06E-01	8.44E-01	108.10	5.39E-01	32.81	4.42E-01	9.10	5.48E-01	35.22
	0.02	6.83E-01	9.72E-01	42.30	8.05E-01	17.82	7.16E-01	4.85	8.28E-01	21.26
	0.05	9.20E-01	9.95E-01	8.16	9.52E-01	3.53	9.16E-01	-0.42	9.70E-01	5.42
	0.1	9.92E-01	9.97E-01	0.53	9.85E-01	-0.70	9.73E-01	-1.92	9.93E-01	0.05
	0.15	9.98E-01	9.98E-01	-0.04	9.92E-01	-0.58	9.87E-01	-1.14	9.87E-01	-1.11
	0.2	9.84E-01	9.98E-01	1.43	9.95E-01	1.15	9.92E-01	0.83	9.97E-01	1.28
	0.25	9.95E-01	9.98E-01	0.35	9.97E-01	0.20	9.95E-01	0.00	9.99E-01	0.44
	0.3	1.00E+00	9.98E-01	-0.18	9.97E-01	-0.26	9.96E-01	-0.39	9.99E-01	-0.06
	0.35	1.00E+00	9.98E-01	-0.17	9.98E-01	-0.21	9.97E-01	-0.30	9.99E-01	-0.06
	0.4	9.81E-01	9.98E-01	1.73	9.98E-01	1.73	9.98E-01	1.65	9.99E-01	1.83
	0.45	9.98E-01	9.98E-01	0.05	9.98E-01	0.07	9.98E-01	0.01	9.99E-01	0.13
	0.5	1.00E+00	9.98E-01	-0.17	9.99E-01	-0.13	9.98E-01	-0.18	1.00E+00	-0.05
2	0.01	1.23E-01	3.39E-01	176.24	1.66E-01	35.26	1.29E-01	4.87	1.51E-01	23.08
	0.02	3.16E-01	6.81E-01	115.15	4.08E-01	28.77	3.34E-01	5.44	3.80E-01	20.13
	0.05	6.15E-01	8.68E-01	41.22	6.78E-01	10.25	6.07E-01	-1.37	6.57E-01	6.85
	0.1	7.84E-01	9.07E-01	15.77	7.98E-01	1.85	7.52E-01	-4.03	7.88E-01	0.61
	0.15	8.47E-01	9.18E-01	8.34	8.44E-01	-0.37	8.12E-01	-4.16	8.17E-01	-3.48
	0.2	8.94E-01	9.22E-01	3.15	8.68E-01	-2.91	8.44E-01	-5.58	9.03E-01	1.03
	0.25	9.18E-01	9.25E-01	0.74	8.83E-01	-3.82	8.64E-01	-5.85	9.24E-01	0.61
	0.3	9.26E-01	9.26E-01	0.02	8.93E-01	-3.58	8.78E-01	-5.21	9.31E-01	0.55
	0.35	9.34E-01	9.27E-01	-0.69	9.00E-01	-3.59	8.88E-01	-4.93	9.35E-01	0.08
	0.4	9.32E-01	9.28E-01	-0.44	9.06E-01	-2.84	8.95E-01	-3.98	9.34E-01	0.23
	0.45	9.29E-01	9.29E-01	-0.02	9.10E-01	-2.03	9.01E-01	-3.03	9.33E-01	0.41
	0.5	9.32E-01	9.29E-01	-0.35	9.13E-01	-2.04	9.05E-01	-2.90	9.37E-01	0.54
2.5	0.01	2.48E-02	6.43E-02	159.70	3.15E-02	27.38	2.42E-02	-2.25	2.86E-02	15.49
	0.02	9.95E-02	2.45E-01	146.08	1.29E-01	29.50	1.02E-01	2.69	1.20E-01	20.12
	0.05	2.61E-01	4.57E-01	74.65	3.01E-01	14.97	2.58E-01	-1.51	2.94E-01	12.35
	0.1	4.03E-01	5.26E-01	30.42	4.04E-01	0.23	3.67E-01	-8.99	4.07E-01	0.95
	0.15	4.74E-01	5.47E-01	15.43	4.51E-01	-4.82	4.21E-01	-11.16	4.76E-01	0.30
	0.2	5.02E-01	5.58E-01	11.04	4.79E-01	-4.60	4.54E-01	-9.51	5.28E-01	5.16
	0.25	5.41E-01	5.64E-01	4.18	4.98E-01	-8.05	4.77E-01	-11.85	5.50E-01	1.66
	0.3	5.57E-01	5.68E-01	1.98	5.11E-01	-8.24	4.93E-01	-11.38	5.62E-01	0.88
	0.35	5.38E-01	5.70E-01	5.95	5.21E-01	-3.29	5.05E-01	-6.09	5.68E-01	5.46
	0.4	5.57E-01	5.72E-01	2.76	5.28E-01	-5.15	5.15E-01	-7.52	5.70E-01	2.44
	0.45	5.69E-01	5.73E-01	0.74	5.34E-01	-6.20	5.22E-01	-8.25	5.71E-01	0.25
	0.5	5.60E-01	5.74E-01	2.54	5.39E-01	-3.84	5.28E-01	-5.69	5.73E-01	2.40

ζ	ξ	ISEE	P	ε [%]	cVM	ε [%]	mVM	ε [%]	#3	ε [%]
3	0.01	3.49E-03	7.66E-03	119.47	4.07E-03	16.64	3.14E-03	-10.01	3.96E-03	13.38
	0.02	2.30E-02	5.18E-02	125.54	2.81E-02	22.25	2.22E-02	-3.37	2.77E-02	20.78
	0.05	7.79E-02	1.34E-01	71.73	8.66E-02	11.26	7.35E-02	-5.60	8.95E-02	14.95
	0.1	1.27E-01	1.68E-01	31.41	1.26E-01	-0.96	1.14E-01	-10.83	1.33E-01	4.36
	0.15	1.55E-01	1.79E-01	15.41	1.45E-01	-6.45	1.34E-01	-13.25	1.59E-01	2.87
	0.2	1.70E-01	1.84E-01	8.30	1.56E-01	-8.35	1.47E-01	-13.49	1.74E-01	2.49
	0.25	1.80E-01	1.87E-01	4.24	1.63E-01	-9.23	1.56E-01	-13.31	1.82E-01	1.15
	0.3	1.83E-01	1.89E-01	3.49	1.68E-01	-8.04	1.62E-01	-11.45	1.86E-01	1.58
	0.35	1.86E-01	1.91E-01	2.85	1.72E-01	-7.22	1.67E-01	-10.11	1.88E-01	1.49
	0.4	1.85E-01	1.92E-01	4.03	1.75E-01	-5.05	1.71E-01	-7.59	1.90E-01	2.81
	0.45	1.90E-01	1.93E-01	1.67	1.78E-01	-6.35	1.73E-01	-8.52	1.90E-01	0.40
0.5	1.91E-01	1.93E-01	1.05	1.79E-01	-6.22	1.76E-01	-8.13	1.91E-01	-0.08	
3.5	0.01	3.37E-04	6.40E-04	90.15	3.69E-04	9.64	2.87E-04	-14.61	3.97E-04	18.07
	0.02	3.94E-03	7.71E-03	95.55	4.48E-03	13.75	3.57E-03	-9.48	4.85E-03	22.92
	0.05	1.69E-02	2.61E-02	54.11	1.78E-02	5.13	1.52E-02	-10.29	1.94E-02	14.63
	0.1	2.80E-02	3.45E-02	23.17	2.71E-02	-3.38	2.45E-02	-12.49	2.93E-02	4.64
	0.15	3.37E-02	3.74E-02	10.77	3.13E-02	-7.15	2.92E-02	-13.39	3.46E-02	2.64
	0.2	3.66E-02	3.88E-02	5.81	3.38E-02	-7.83	3.20E-02	-12.52	3.74E-02	1.99
	0.25	3.76E-02	3.96E-02	5.19	3.54E-02	-6.03	3.40E-02	-9.81	3.88E-02	3.04
	0.3	3.88E-02	4.02E-02	3.57	3.65E-02	-5.84	3.53E-02	-8.91	3.96E-02	2.16
	0.35	4.03E-02	4.06E-02	0.76	3.74E-02	-7.21	3.64E-02	-9.71	4.01E-02	-0.31
	0.4	4.03E-02	4.09E-02	1.36	3.80E-02	-5.73	3.71E-02	-7.88	4.05E-02	0.34
	0.45	4.14E-02	4.11E-02	-0.65	3.85E-02	-6.88	3.78E-02	-8.71	4.06E-02	-1.72
0.5	4.12E-02	4.12E-02	0.06	3.89E-02	-5.64	3.82E-02	-7.24	4.08E-02	-0.97	
4	0.01	2.24E-05	3.82E-05	70.60	2.37E-05	5.55	1.86E-05	-16.96	2.80E-05	24.83
	0.02	4.95E-04	8.66E-04	74.75	5.40E-04	8.90	4.33E-04	-12.53	6.33E-04	27.78
	0.05	2.72E-03	3.79E-03	39.36	2.74E-03	0.89	2.37E-03	-13.03	3.11E-03	14.46
	0.1	4.60E-03	5.25E-03	14.04	4.31E-03	-6.23	3.94E-03	-14.25	4.73E-03	2.79
	0.15	5.36E-03	5.73E-03	6.92	5.00E-03	-6.82	4.70E-03	-12.33	5.48E-03	2.19
	0.2	5.70E-03	5.98E-03	4.89	5.38E-03	-5.54	5.15E-03	-9.67	5.85E-03	2.72
	0.25	6.00E-03	6.12E-03	1.96	5.63E-03	-6.24	5.44E-03	-9.40	6.05E-03	0.77
	0.3	6.07E-03	6.22E-03	2.48	5.80E-03	-4.41	5.65E-03	-6.98	6.17E-03	1.66
	0.35	6.27E-03	6.29E-03	0.34	5.93E-03	-5.43	5.80E-03	-7.50	6.25E-03	-0.32
	0.4	6.33E-03	6.34E-03	0.16	6.03E-03	-4.86	5.92E-03	-6.60	6.30E-03	-0.51
	0.45	6.34E-03	6.38E-03	0.69	6.10E-03	-3.79	6.01E-03	-5.27	6.34E-03	-0.07
0.5	6.30E-03	6.41E-03	1.70	6.16E-03	-2.36	6.07E-03	-3.65	6.36E-03	0.93	

ζ	ξ	ISEE	P	ε [%]	cVM	ε [%]	mVM	ε [%]	#3	ε [%]
4.5	0.01	1.07E-06	1.64E-06	53.12	1.07E-06	0.59	8.54E-07	-20.04	1.34E-06	25.38
	0.02	4.78E-05	7.45E-05	55.86	4.93E-05	3.11	4.00E-05	-16.38	6.06E-05	26.80
	0.05	3.32E-04	4.26E-04	28.50	3.25E-04	-2.02	2.83E-04	-14.64	3.75E-04	13.05
	0.1	5.62E-04	6.14E-04	9.25	5.25E-04	-6.54	4.85E-04	-13.69	5.75E-04	2.35
	0.15	6.45E-04	6.77E-04	4.95	6.09E-04	-5.57	5.78E-04	-10.41	6.59E-04	2.12
	0.2	6.94E-04	7.08E-04	2.06	6.55E-04	-5.61	6.31E-04	-9.09	7.00E-04	0.83
	0.25	7.14E-04	7.27E-04	1.86	6.84E-04	-4.18	6.65E-04	-6.84	7.22E-04	1.17
	0.3	7.21E-04	7.40E-04	2.56	7.04E-04	-2.41	6.89E-04	-4.53	7.36E-04	2.06
	0.35	7.52E-04	7.49E-04	-0.39	7.18E-04	-4.44	7.06E-04	-6.11	7.46E-04	-0.82
	0.4	7.52E-04	7.56E-04	0.49	7.29E-04	-3.02	7.19E-04	-4.40	7.52E-04	0.01
	0.45	7.46E-04	7.61E-04	2.05	7.38E-04	-1.06	7.29E-04	-2.24	7.56E-04	1.37
0.5	7.57E-04	7.65E-04	1.14	7.44E-04	-1.59	7.37E-04	-2.58	7.60E-04	0.49	
5	0.01	3.53E-08	5.00E-08	41.56	3.46E-08	-2.12	2.78E-08	-21.38	4.31E-08	21.83
	0.02	3.42E-06	4.92E-06	43.82	3.42E-06	0.12	2.80E-06	-18.00	4.20E-06	22.92
	0.05	3.16E-05	3.74E-05	18.20	2.98E-05	-5.91	2.62E-05	-17.18	3.40E-05	7.59
	0.1	5.28E-05	5.59E-05	5.97	4.94E-05	-6.44	4.60E-05	-12.82	5.35E-05	1.29
	0.15	6.12E-05	6.22E-05	1.63	5.73E-05	-6.29	5.48E-05	-10.43	6.10E-05	-0.32
	0.2	6.43E-05	6.53E-05	1.61	6.16E-05	-4.14	5.97E-05	-7.10	6.48E-05	0.74
	0.25	6.77E-05	6.72E-05	-0.75	6.42E-05	-5.06	6.28E-05	-7.22	6.68E-05	-1.24
	0.3	6.89E-05	6.84E-05	-0.70	6.60E-05	-4.15	6.49E-05	-5.82	6.81E-05	-1.07
	0.35	6.94E-05	6.93E-05	-0.14	6.73E-05	-2.99	6.64E-05	-4.32	6.90E-05	-0.51
	0.4	6.98E-05	7.00E-05	0.27	6.83E-05	-2.15	6.75E-05	-3.23	6.96E-05	-0.27
	0.45	7.01E-05	7.05E-05	0.55	6.91E-05	-1.53	6.84E-05	-2.43	6.99E-05	-0.31
0.5	6.97E-05	7.09E-05	1.83	6.97E-05	-0.02	6.91E-05	-0.77	7.04E-05	1.07	
		μ_ε %	22.38	μ_ε %	-0.004	μ_ε %	-7.09	μ_ε %	5.42	
		σ_ε %	39.25	σ_ε %	9.45	σ_ε %	5.76	σ_ε %	8.60	
		ε_{\max} %	176.24	ε_{\max} %	35.26	ε_{\max} %	9.10	ε_{\max} %	35.22	
		ε_{\min} %	-0.75	ε_{\min} %	-9.23	ε_{\min} %	-21.38	ε_{\min} %	-3.48	
		$\mu_{ \varepsilon }$ %	22.48	$\mu_{ \varepsilon }$ %	6.32	$\mu_{ \varepsilon }$ %	7.70	$\mu_{ \varepsilon }$ %	5.89	

C.3 PROPOSED #4

Table C.3 - Proposed #4: Time-variant FPDF ($t_0 = 10$).

ζ	ξ	ISEE	P	ε [%]	cVM	ε [%]	mVM	ε [%]	#4	ε [%]
1.5	0.01	4.06E-01	8.44E-01	108.10	5.39E-01	32.81	4.42E-01	9.10	5.13E-01	26.57
	0.02	6.83E-01	9.72E-01	42.30	8.05E-01	17.82	7.16E-01	4.85	7.64E-01	11.81
	0.05	9.20E-01	9.95E-01	8.16	9.52E-01	3.53	9.16E-01	-0.42	9.18E-01	-0.20
	0.1	9.92E-01	9.97E-01	0.53	9.85E-01	-0.70	9.73E-01	-1.92	9.66E-01	-2.63
	0.15	9.98E-01	9.98E-01	-0.04	9.92E-01	-0.58	9.87E-01	-1.14	9.97E-01	-0.08
	0.2	9.84E-01	9.98E-01	1.43	9.95E-01	1.15	9.92E-01	0.83	9.98E-01	1.44
	0.25	9.95E-01	9.98E-01	0.35	9.97E-01	0.20	9.95E-01	0.00	9.97E-01	0.28
	0.3	1.00E+00	9.98E-01	-0.18	9.97E-01	-0.26	9.96E-01	-0.39	9.98E-01	-0.20
	0.35	1.00E+00	9.98E-01	-0.17	9.98E-01	-0.21	9.97E-01	-0.30	9.99E-01	-0.10
	0.4	9.81E-01	9.98E-01	1.73	9.98E-01	1.73	9.98E-01	1.65	1.00E+00	1.86
	0.45	9.98E-01	9.98E-01	0.05	9.98E-01	0.07	9.98E-01	0.01	1.00E+00	0.18
	0.5	1.00E+00	9.98E-01	-0.17	9.99E-01	-0.13	9.98E-01	-0.18	9.99E-01	-0.06
2	0.01	1.23E-01	3.39E-01	176.24	1.66E-01	35.26	1.29E-01	4.87	1.51E-01	23.16
	0.02	3.16E-01	6.81E-01	115.15	4.08E-01	28.77	3.34E-01	5.44	3.80E-01	20.11
	0.05	6.15E-01	8.68E-01	41.22	6.78E-01	10.25	6.07E-01	-1.37	6.56E-01	6.71
	0.1	7.84E-01	9.07E-01	15.77	7.98E-01	1.85	7.52E-01	-4.03	7.87E-01	0.47
	0.15	8.47E-01	9.18E-01	8.34	8.44E-01	-0.37	8.12E-01	-4.16	8.77E-01	3.60
	0.2	8.94E-01	9.22E-01	3.15	8.68E-01	-2.91	8.44E-01	-5.58	8.66E-01	-3.10
	0.25	9.18E-01	9.25E-01	0.74	8.83E-01	-3.82	8.64E-01	-5.85	8.59E-01	-6.39
	0.3	9.26E-01	9.26E-01	0.02	8.93E-01	-3.58	8.78E-01	-5.21	8.77E-01	-5.35
	0.35	9.34E-01	9.27E-01	-0.69	9.00E-01	-3.59	8.88E-01	-4.93	9.04E-01	-3.18
	0.4	9.32E-01	9.28E-01	-0.44	9.06E-01	-2.84	8.95E-01	-3.98	9.28E-01	-0.41
	0.45	9.29E-01	9.29E-01	-0.02	9.10E-01	-2.03	9.01E-01	-3.03	9.36E-01	0.79
	0.5	9.32E-01	9.29E-01	-0.35	9.13E-01	-2.04	9.05E-01	-2.90	9.35E-01	0.28
2.5	0.01	2.48E-02	6.43E-02	159.70	3.15E-02	27.38	2.42E-02	-2.25	2.84E-02	14.77
	0.02	9.95E-02	2.45E-01	146.08	1.29E-01	29.50	1.02E-01	2.69	1.17E-01	17.66
	0.05	2.61E-01	4.57E-01	74.65	3.01E-01	14.97	2.58E-01	-1.51	2.78E-01	6.49
	0.1	4.03E-01	5.26E-01	30.42	4.04E-01	0.23	3.67E-01	-8.99	3.80E-01	-5.70
	0.15	4.74E-01	5.47E-01	15.43	4.51E-01	-4.82	4.21E-01	-11.16	4.51E-01	-4.98
	0.2	5.02E-01	5.58E-01	11.04	4.79E-01	-4.60	4.54E-01	-9.51	4.37E-01	-12.96
	0.25	5.41E-01	5.64E-01	4.18	4.98E-01	-8.05	4.77E-01	-11.85	4.48E-01	-17.17
	0.3	5.57E-01	5.68E-01	1.98	5.11E-01	-8.24	4.93E-01	-11.38	4.74E-01	-14.90
	0.35	5.38E-01	5.70E-01	5.95	5.21E-01	-3.29	5.05E-01	-6.09	5.12E-01	-4.94
	0.4	5.57E-01	5.72E-01	2.76	5.28E-01	-5.15	5.15E-01	-7.52	5.53E-01	-0.75
	0.45	5.69E-01	5.73E-01	0.74	5.34E-01	-6.20	5.22E-01	-8.25	5.68E-01	-0.13
	0.5	5.60E-01	5.74E-01	2.54	5.39E-01	-3.84	5.28E-01	-5.69	5.70E-01	1.72

ζ	ξ	ISEE	P	ε [%]	cVM	ε [%]	mVM	ε [%]	#4	ε [%]
3	0.01	3.49E-03	7.66E-03	119.47	4.07E-03	16.64	3.14E-03	-10.01	3.91E-03	12.12
	0.02	2.30E-02	5.18E-02	125.54	2.81E-02	22.25	2.22E-02	-3.37	2.67E-02	16.46
	0.05	7.79E-02	1.34E-01	71.73	8.66E-02	11.26	7.35E-02	-5.60	7.98E-02	2.45
	0.1	1.27E-01	1.68E-01	31.41	1.26E-01	-0.96	1.14E-01	-10.83	1.13E-01	-11.69
	0.15	1.55E-01	1.79E-01	15.41	1.45E-01	-6.45	1.34E-01	-13.25	1.34E-01	-13.57
	0.2	1.70E-01	1.84E-01	8.30	1.56E-01	-8.35	1.47E-01	-13.49	1.36E-01	-19.77
	0.25	1.80E-01	1.87E-01	4.24	1.63E-01	-9.23	1.56E-01	-13.31	1.43E-01	-20.64
	0.3	1.83E-01	1.89E-01	3.49	1.68E-01	-8.04	1.62E-01	-11.45	1.53E-01	-16.29
	0.35	1.86E-01	1.91E-01	2.85	1.72E-01	-7.22	1.67E-01	-10.11	1.69E-01	-8.95
	0.4	1.85E-01	1.92E-01	4.03	1.75E-01	-5.05	1.71E-01	-7.59	1.85E-01	-0.03
	0.45	1.90E-01	1.93E-01	1.67	1.78E-01	-6.35	1.73E-01	-8.52	1.89E-01	-0.09
0.5	1.91E-01	1.93E-01	1.05	1.79E-01	-6.22	1.76E-01	-8.13	1.90E-01	-0.66	
3.5	0.01	3.37E-04	6.40E-04	90.15	3.69E-04	9.64	2.87E-04	-14.61	3.94E-04	16.99
	0.02	3.94E-03	7.71E-03	95.55	4.48E-03	13.75	3.57E-03	-9.48	4.71E-03	19.48
	0.05	1.69E-02	2.61E-02	54.11	1.78E-02	5.13	1.52E-02	-10.29	1.75E-02	3.22
	0.1	2.80E-02	3.45E-02	23.17	2.71E-02	-3.38	2.45E-02	-12.49	2.48E-02	-11.73
	0.15	3.37E-02	3.74E-02	10.77	3.13E-02	-7.15	2.92E-02	-13.39	2.93E-02	-13.16
	0.2	3.66E-02	3.88E-02	5.81	3.38E-02	-7.83	3.20E-02	-12.52	3.02E-02	-17.45
	0.25	3.76E-02	3.96E-02	5.19	3.54E-02	-6.03	3.40E-02	-9.81	3.17E-02	-15.79
	0.3	3.88E-02	4.02E-02	3.57	3.65E-02	-5.84	3.53E-02	-8.91	3.42E-02	-11.85
	0.35	4.03E-02	4.06E-02	0.76	3.74E-02	-7.21	3.64E-02	-9.71	3.77E-02	-6.50
	0.4	4.03E-02	4.09E-02	1.36	3.80E-02	-5.73	3.71E-02	-7.88	4.00E-02	-0.90
	0.45	4.14E-02	4.11E-02	-0.65	3.85E-02	-6.88	3.78E-02	-8.71	4.05E-02	-2.00
0.5	4.12E-02	4.12E-02	0.06	3.89E-02	-5.64	3.82E-02	-7.24	4.05E-02	-1.64	
4	0.01	2.24E-05	3.82E-05	70.60	2.37E-05	5.55	1.86E-05	-16.96	2.78E-05	24.10
	0.02	4.95E-04	8.66E-04	74.75	5.40E-04	8.90	4.33E-04	-12.53	6.23E-04	25.80
	0.05	2.72E-03	3.79E-03	39.36	2.74E-03	0.89	2.37E-03	-13.03	2.92E-03	7.23
	0.1	4.60E-03	5.25E-03	14.04	4.31E-03	-6.23	3.94E-03	-14.25	4.19E-03	-8.98
	0.15	5.36E-03	5.73E-03	6.92	5.00E-03	-6.82	4.70E-03	-12.33	4.95E-03	-7.75
	0.2	5.70E-03	5.98E-03	4.89	5.38E-03	-5.54	5.15E-03	-9.67	5.11E-03	-10.39
	0.25	6.00E-03	6.12E-03	1.96	5.63E-03	-6.24	5.44E-03	-9.40	5.32E-03	-11.37
	0.3	6.07E-03	6.22E-03	2.48	5.80E-03	-4.41	5.65E-03	-6.98	5.69E-03	-6.16
	0.35	6.27E-03	6.29E-03	0.34	5.93E-03	-5.43	5.80E-03	-7.50	6.09E-03	-2.81
	0.4	6.33E-03	6.34E-03	0.16	6.03E-03	-4.86	5.92E-03	-6.60	6.27E-03	-1.06
	0.45	6.34E-03	6.38E-03	0.69	6.10E-03	-3.79	6.01E-03	-5.27	6.32E-03	-0.29
0.5	6.30E-03	6.41E-03	1.70	6.16E-03	-2.36	6.07E-03	-3.65	6.27E-03	-0.63	

ζ	ξ	ISEE	P	ε [%]	cVM	ε [%]	mVM	ε [%]	#4	ε [%]
4.5	0.01	1.07E-06	1.64E-06	53.12	1.07E-06	0.59	8.54E-07	-20.04	1.34E-06	24.98
	0.02	4.78E-05	7.45E-05	55.86	4.93E-05	3.11	4.00E-05	-16.38	6.02E-05	25.87
	0.05	3.32E-04	4.26E-04	28.50	3.25E-04	-2.02	2.83E-04	-14.64	3.63E-04	9.45
	0.1	5.62E-04	6.14E-04	9.25	5.25E-04	-6.54	4.85E-04	-13.69	5.37E-04	-4.40
	0.15	6.45E-04	6.77E-04	4.95	6.09E-04	-5.57	5.78E-04	-10.41	6.39E-04	-0.95
	0.2	6.94E-04	7.08E-04	2.06	6.55E-04	-5.61	6.31E-04	-9.09	6.64E-04	-4.31
	0.25	7.14E-04	7.27E-04	1.86	6.84E-04	-4.18	6.65E-04	-6.84	6.84E-04	-4.20
	0.3	7.21E-04	7.40E-04	2.56	7.04E-04	-2.41	6.89E-04	-4.53	7.14E-04	-1.04
	0.35	7.52E-04	7.49E-04	-0.39	7.18E-04	-4.44	7.06E-04	-6.11	7.38E-04	-1.83
	0.4	7.52E-04	7.56E-04	0.49	7.29E-04	-3.02	7.19E-04	-4.40	7.50E-04	-0.27
	0.45	7.46E-04	7.61E-04	2.05	7.38E-04	-1.06	7.29E-04	-2.24	7.55E-04	1.28
0.5	7.57E-04	7.65E-04	1.14	7.44E-04	-1.59	7.37E-04	-2.58	7.15E-04	-5.47	
5	0.01	3.53E-08	5.00E-08	41.56	3.46E-08	-2.12	2.78E-08	-21.38	4.30E-08	21.65
	0.02	3.42E-06	4.92E-06	43.82	3.42E-06	0.12	2.80E-06	-18.00	4.19E-06	22.46
	0.05	3.16E-05	3.74E-05	18.20	2.98E-05	-5.91	2.62E-05	-17.18	3.34E-05	5.64
	0.1	5.28E-05	5.59E-05	5.97	4.94E-05	-6.44	4.60E-05	-12.82	5.14E-05	-2.70
	0.15	6.12E-05	6.22E-05	1.63	5.73E-05	-6.29	5.48E-05	-10.43	6.09E-05	-0.55
	0.2	6.43E-05	6.53E-05	1.61	6.16E-05	-4.14	5.97E-05	-7.10	6.44E-05	0.22
	0.25	6.77E-05	6.72E-05	-0.75	6.42E-05	-5.06	6.28E-05	-7.22	6.62E-05	-2.21
	0.3	6.89E-05	6.84E-05	-0.70	6.60E-05	-4.15	6.49E-05	-5.82	6.76E-05	-1.83
	0.35	6.94E-05	6.93E-05	-0.14	6.73E-05	-2.99	6.64E-05	-4.32	6.88E-05	-0.78
	0.4	6.98E-05	7.00E-05	0.27	6.83E-05	-2.15	6.75E-05	-3.23	6.96E-05	-0.24
	0.45	7.01E-05	7.05E-05	0.55	6.91E-05	-1.53	6.84E-05	-2.43	6.99E-05	-0.33
0.5	6.97E-05	7.09E-05	1.83	6.97E-05	-0.02	6.91E-05	-0.77	5.85E-05	-15.98	
		μ_ε %	22.38	μ_ε %	-0.004	μ_ε %	-7.09	μ_ε %	0.26	
		σ_ε %	39.25	σ_ε %	9.45	σ_ε %	5.76	σ_ε %	10.95	
		ε_{\max} %	176.24	ε_{\max} %	35.26	ε_{\max} %	9.10	ε_{\max} %	26.57	
		ε_{\min} %	-0.75	ε_{\min} %	-9.23	ε_{\min} %	-21.38	ε_{\min} %	-20.64	
		$\mu_{ \varepsilon }$ %	22.48	$\mu_{ \varepsilon }$ %	6.32	$\mu_{ \varepsilon }$ %	7.70	$\mu_{ \varepsilon }$ %	7.78	

C.4 PROPOSED #5

Table C.4 - Proposed #5: Time-variant FFP (t₀ = 10).

ζ	ξ	ISEE	P	ε [%]	cVM	ε [%]	mVM	ε [%]	#5	ε [%]
1.5	0.01	4.06E-01	8.44E-01	108.10	5.39E-01	32.81	4.42E-01	9.10	3.94E-01	-2.73
	0.02	6.83E-01	9.72E-01	42.30	8.05E-01	17.82	7.16E-01	4.85	6.80E-01	-0.48
	0.05	9.20E-01	9.95E-01	8.16	9.52E-01	3.53	9.16E-01	-0.42	9.26E-01	0.62
	0.1	9.92E-01	9.97E-01	0.53	9.85E-01	-0.70	9.73E-01	-1.92	9.86E-01	-0.59
	0.15	9.98E-01	9.98E-01	-0.04	9.92E-01	-0.58	9.87E-01	-1.14	9.95E-01	-0.28
	0.2	9.84E-01	9.98E-01	1.43	9.95E-01	1.15	9.92E-01	0.83	9.98E-01	1.41
	0.25	9.95E-01	9.98E-01	0.35	9.97E-01	0.20	9.95E-01	0.00	9.99E-01	0.41
	0.3	1.00E+00	9.98E-01	-0.18	9.97E-01	-0.26	9.96E-01	-0.39	9.99E-01	-0.09
	0.35	1.00E+00	9.98E-01	-0.17	9.98E-01	-0.21	9.97E-01	-0.30	9.99E-01	-0.07
	0.4	9.81E-01	9.98E-01	1.73	9.98E-01	1.73	9.98E-01	1.65	9.99E-01	1.85
	0.45	9.98E-01	9.98E-01	0.05	9.98E-01	0.07	9.98E-01	0.01	9.99E-01	0.17
	0.5	1.00E+00	9.98E-01	-0.17	9.99E-01	-0.13	9.98E-01	-0.18	1.00E+00	-0.05
2	0.01	1.23E-01	3.39E-01	176.24	1.66E-01	35.26	1.29E-01	4.87	1.08E-01	-11.61
	0.02	3.16E-01	6.81E-01	115.15	4.08E-01	28.77	3.34E-01	5.44	2.98E-01	-5.71
	0.05	6.15E-01	8.68E-01	41.22	6.78E-01	10.25	6.07E-01	-1.37	6.09E-01	-0.90
	0.1	7.84E-01	9.07E-01	15.77	7.98E-01	1.85	7.52E-01	-4.03	7.95E-01	1.47
	0.15	8.47E-01	9.18E-01	8.34	8.44E-01	-0.37	8.12E-01	-4.16	8.64E-01	2.01
	0.2	8.94E-01	9.22E-01	3.15	8.68E-01	-2.91	8.44E-01	-5.58	8.97E-01	0.32
	0.25	9.18E-01	9.25E-01	0.74	8.83E-01	-3.82	8.64E-01	-5.85	9.15E-01	-0.35
	0.3	9.26E-01	9.26E-01	0.02	8.93E-01	-3.58	8.78E-01	-5.21	9.25E-01	-0.12
	0.35	9.34E-01	9.27E-01	-0.69	9.00E-01	-3.59	8.88E-01	-4.93	9.31E-01	-0.29
	0.4	9.32E-01	9.28E-01	-0.44	9.06E-01	-2.84	8.95E-01	-3.98	9.35E-01	0.25
	0.45	9.29E-01	9.29E-01	-0.02	9.10E-01	-2.03	9.01E-01	-3.03	9.37E-01	0.82
	0.5	9.32E-01	9.29E-01	-0.35	9.13E-01	-2.04	9.05E-01	-2.90	9.38E-01	0.60
2.5	0.01	2.48E-02	6.43E-02	159.70	3.15E-02	27.38	2.42E-02	-2.25	2.08E-02	-15.90
	0.02	9.95E-02	2.45E-01	146.08	1.29E-01	29.50	1.02E-01	2.69	9.18E-02	-7.78
	0.05	2.61E-01	4.57E-01	74.65	3.01E-01	14.97	2.58E-01	-1.51	2.61E-01	-0.05
	0.1	4.03E-01	5.26E-01	30.42	4.04E-01	0.23	3.67E-01	-8.99	4.04E-01	0.07
	0.15	4.74E-01	5.47E-01	15.43	4.51E-01	-4.82	4.21E-01	-11.16	4.75E-01	0.08
	0.2	5.02E-01	5.58E-01	11.04	4.79E-01	-4.60	4.54E-01	-9.51	5.15E-01	2.59
	0.25	5.41E-01	5.64E-01	4.18	4.98E-01	-8.05	4.77E-01	-11.85	5.40E-01	-0.22
	0.3	5.57E-01	5.68E-01	1.98	5.11E-01	-8.24	4.93E-01	-11.38	5.55E-01	-0.29
	0.35	5.38E-01	5.70E-01	5.95	5.21E-01	-3.29	5.05E-01	-6.09	5.64E-01	4.78
	0.4	5.57E-01	5.72E-01	2.76	5.28E-01	-5.15	5.15E-01	-7.52	5.69E-01	2.24
	0.45	5.69E-01	5.73E-01	0.74	5.34E-01	-6.20	5.22E-01	-8.25	5.72E-01	0.52
	0.5	5.60E-01	5.74E-01	2.54	5.39E-01	-3.84	5.28E-01	-5.69	5.74E-01	2.51

ζ	ξ	ISEE	P	ε [%]	cVM	ε [%]	mVM	ε [%]	#5	ε [%]
3	0.01	3.49E-03	7.66E-03	119.47	4.07E-03	16.64	3.14E-03	-10.01	2.86E-03	-17.99
	0.02	2.30E-02	5.18E-02	125.54	2.81E-02	22.25	2.22E-02	-3.37	2.09E-02	-8.98
	0.05	7.79E-02	1.34E-01	71.73	8.66E-02	11.26	7.35E-02	-5.60	7.73E-02	-0.69
	0.1	1.27E-01	1.68E-01	31.41	1.26E-01	-0.96	1.14E-01	-10.83	1.29E-01	1.15
	0.15	1.55E-01	1.79E-01	15.41	1.45E-01	-6.45	1.34E-01	-13.25	1.55E-01	0.43
	0.2	1.70E-01	1.84E-01	8.30	1.56E-01	-8.35	1.47E-01	-13.49	1.70E-01	0.29
	0.25	1.80E-01	1.87E-01	4.24	1.63E-01	-9.23	1.56E-01	-13.31	1.79E-01	-0.21
	0.3	1.83E-01	1.89E-01	3.49	1.68E-01	-8.04	1.62E-01	-11.45	1.85E-01	0.83
	0.35	1.86E-01	1.91E-01	2.85	1.72E-01	-7.22	1.67E-01	-10.11	1.88E-01	1.12
	0.4	1.85E-01	1.92E-01	4.03	1.75E-01	-5.05	1.71E-01	-7.59	1.90E-01	2.71
	0.45	1.90E-01	1.93E-01	1.67	1.78E-01	-6.35	1.73E-01	-8.52	1.91E-01	0.54
0.5	1.91E-01	1.93E-01	1.05	1.79E-01	-6.22	1.76E-01	-8.13	1.91E-01	0.00	
3.5	0.01	3.37E-04	6.40E-04	90.15	3.69E-04	9.64	2.87E-04	-14.61	2.79E-04	-17.08
	0.02	3.94E-03	7.71E-03	95.55	4.48E-03	13.75	3.57E-03	-9.48	3.57E-03	-9.47
	0.05	1.69E-02	2.61E-02	54.11	1.78E-02	5.13	1.52E-02	-10.29	1.67E-02	-1.33
	0.1	2.80E-02	3.45E-02	23.17	2.71E-02	-3.38	2.45E-02	-12.49	2.85E-02	1.51
	0.15	3.37E-02	3.74E-02	10.77	3.13E-02	-7.15	2.92E-02	-13.39	3.40E-02	0.86
	0.2	3.66E-02	3.88E-02	5.81	3.38E-02	-7.83	3.20E-02	-12.52	3.69E-02	0.82
	0.25	3.76E-02	3.96E-02	5.19	3.54E-02	-6.03	3.40E-02	-9.81	3.86E-02	2.44
	0.3	3.88E-02	4.02E-02	3.57	3.65E-02	-5.84	3.53E-02	-8.91	3.95E-02	1.90
	0.35	4.03E-02	4.06E-02	0.76	3.74E-02	-7.21	3.64E-02	-9.71	4.01E-02	-0.39
	0.4	4.03E-02	4.09E-02	1.36	3.80E-02	-5.73	3.71E-02	-7.88	4.05E-02	0.38
	0.45	4.14E-02	4.11E-02	-0.65	3.85E-02	-6.88	3.78E-02	-8.71	4.07E-02	-1.58
0.5	4.12E-02	4.12E-02	0.06	3.89E-02	-5.64	3.82E-02	-7.24	4.08E-02	-0.90	
4	0.01	2.24E-05	3.82E-05	70.60	2.37E-05	5.55	1.86E-05	-16.96	1.91E-05	-14.84
	0.02	4.95E-04	8.66E-04	74.75	5.40E-04	8.90	4.33E-04	-12.53	4.58E-04	-7.65
	0.05	2.72E-03	3.79E-03	39.36	2.74E-03	0.89	2.37E-03	-13.03	2.70E-03	-0.61
	0.1	4.60E-03	5.25E-03	14.04	4.31E-03	-6.23	3.94E-03	-14.25	4.63E-03	0.56
	0.15	5.36E-03	5.73E-03	6.92	5.00E-03	-6.82	4.70E-03	-12.33	5.44E-03	1.35
	0.2	5.70E-03	5.98E-03	4.89	5.38E-03	-5.54	5.15E-03	-9.67	5.83E-03	2.31
	0.25	6.00E-03	6.12E-03	1.96	5.63E-03	-6.24	5.44E-03	-9.40	6.04E-03	0.64
	0.3	6.07E-03	6.22E-03	2.48	5.80E-03	-4.41	5.65E-03	-6.98	6.17E-03	1.66
	0.35	6.27E-03	6.29E-03	0.34	5.93E-03	-5.43	5.80E-03	-7.50	6.25E-03	-0.26
	0.4	6.33E-03	6.34E-03	0.16	6.03E-03	-4.86	5.92E-03	-6.60	6.31E-03	-0.40
	0.45	6.34E-03	6.38E-03	0.69	6.10E-03	-3.79	6.01E-03	-5.27	6.35E-03	0.09
0.5	6.30E-03	6.41E-03	1.70	6.16E-03	-2.36	6.07E-03	-3.65	6.37E-03	1.04	

ζ	ξ	ISEE	P	ε [%]	cVM	ε [%]	mVM	ε [%]	#5	ε [%]
4.5	0.01	1.07E-06	1.64E-06	53.12	1.07E-06	0.59	8.54E-07	-20.04	9.13E-07	-14.53
	0.02	4.78E-05	7.45E-05	55.86	4.93E-05	3.11	4.00E-05	-16.38	4.40E-05	-7.93
	0.05	3.32E-04	4.26E-04	28.50	3.25E-04	-2.02	2.83E-04	-14.64	3.32E-04	0.05
	0.1	5.62E-04	6.14E-04	9.25	5.25E-04	-6.54	4.85E-04	-13.69	5.68E-04	1.05
	0.15	6.45E-04	6.77E-04	4.95	6.09E-04	-5.57	5.78E-04	-10.41	6.58E-04	1.97
	0.2	6.94E-04	7.08E-04	2.06	6.55E-04	-5.61	6.31E-04	-9.09	7.00E-04	0.81
	0.25	7.14E-04	7.27E-04	1.86	6.84E-04	-4.18	6.65E-04	-6.84	7.23E-04	1.22
	0.3	7.21E-04	7.40E-04	2.56	7.04E-04	-2.41	6.89E-04	-4.53	7.37E-04	2.15
	0.35	7.52E-04	7.49E-04	-0.39	7.18E-04	-4.44	7.06E-04	-6.11	7.46E-04	-0.72
	0.4	7.52E-04	7.56E-04	0.49	7.29E-04	-3.02	7.19E-04	-4.40	7.53E-04	0.16
	0.45	7.46E-04	7.61E-04	2.05	7.38E-04	-1.06	7.29E-04	-2.24	7.58E-04	1.65
0.5	7.57E-04	7.65E-04	1.14	7.44E-04	-1.59	7.37E-04	-2.58	7.62E-04	0.68	
5	0.01	3.53E-08	5.00E-08	41.56	3.46E-08	-2.12	2.78E-08	-21.38	3.07E-08	-13.27
	0.02	3.42E-06	4.92E-06	43.82	3.42E-06	0.12	2.80E-06	-18.00	3.18E-06	-6.91
	0.05	3.16E-05	3.74E-05	18.20	2.98E-05	-5.91	2.62E-05	-17.18	3.10E-05	-1.84
	0.1	5.28E-05	5.59E-05	5.97	4.94E-05	-6.44	4.60E-05	-12.82	5.32E-05	0.86
	0.15	6.12E-05	6.22E-05	1.63	5.73E-05	-6.29	5.48E-05	-10.43	6.12E-05	-0.04
	0.2	6.43E-05	6.53E-05	1.61	6.16E-05	-4.14	5.97E-05	-7.10	6.49E-05	0.90
	0.25	6.77E-05	6.72E-05	-0.75	6.42E-05	-5.06	6.28E-05	-7.22	6.69E-05	-1.13
	0.3	6.89E-05	6.84E-05	-0.70	6.60E-05	-4.15	6.49E-05	-5.82	6.82E-05	-0.96
	0.35	6.94E-05	6.93E-05	-0.14	6.73E-05	-2.99	6.64E-05	-4.32	6.91E-05	-0.38
	0.4	6.98E-05	7.00E-05	0.27	6.83E-05	-2.15	6.75E-05	-3.23	6.98E-05	-0.01
	0.45	7.01E-05	7.05E-05	0.55	6.91E-05	-1.53	6.84E-05	-2.43	7.03E-05	0.20
0.5	6.97E-05	7.09E-05	1.83	6.97E-05	-0.02	6.91E-05	-0.77	7.06E-05	1.40	
		μ_ε %	22.38	μ_ε %	-0.004	μ_ε %	-7.09	μ_ε %	-1.24	
		σ_ε %	39.25	σ_ε %	9.45	σ_ε %	5.76	σ_ε %	4.62	
		ε_{\max} %	176.24	ε_{\max} %	35.26	ε_{\max} %	9.10	ε_{\max} %	4.78	
		ε_{\min} %	-0.75	ε_{\min} %	-9.23	ε_{\min} %	-21.38	ε_{\min} %	-17.99	
		$\mu_{ \varepsilon }$ %	22.48	$\mu_{ \varepsilon }$ %	6.32	$\mu_{ \varepsilon }$ %	7.70	$\mu_{ \varepsilon }$ %	2.58	

C.5 PROPOSED #6 (NEW)

Table C.5 - New: Time-variant FPDF ($t_0 = 10$).

ζ	ξ	ISEE	P	ε [%]	cVM	ε [%]	mVM	ε [%]	New	ε [%]
1.5	0.01	4.06E-01	8.44E-01	108.10	5.39E-01	32.81	4.42E-01	9.10	4.07E-01	0.36
	0.02	6.83E-01	9.72E-01	42.30	8.05E-01	17.82	7.16E-01	4.85	6.86E-01	0.46
	0.05	9.20E-01	9.95E-01	8.16	9.52E-01	3.53	9.16E-01	-0.42	9.26E-01	0.63
	0.1	9.92E-01	9.97E-01	0.53	9.85E-01	-0.70	9.73E-01	-1.92	9.86E-01	-0.60
	0.15	9.98E-01	9.98E-01	-0.04	9.92E-01	-0.58	9.87E-01	-1.14	9.95E-01	-0.29
	0.2	9.84E-01	9.98E-01	1.43	9.95E-01	1.15	9.92E-01	0.83	9.98E-01	1.40
	0.25	9.95E-01	9.98E-01	0.35	9.97E-01	0.20	9.95E-01	0.00	9.99E-01	0.40
	0.3	1.00E+00	9.98E-01	-0.18	9.97E-01	-0.26	9.96E-01	-0.39	9.99E-01	-0.09
	0.35	1.00E+00	9.98E-01	-0.17	9.98E-01	-0.21	9.97E-01	-0.30	9.99E-01	-0.07
	0.4	9.81E-01	9.98E-01	1.73	9.98E-01	1.73	9.98E-01	1.65	9.99E-01	1.84
	0.45	9.98E-01	9.98E-01	0.05	9.98E-01	0.07	9.98E-01	0.01	9.99E-01	0.16
0.5	1.00E+00	9.98E-01	-0.17	9.99E-01	-0.13	9.98E-01	-0.18	9.99E-01	-0.06	
2	0.01	1.23E-01	3.39E-01	176.24	1.66E-01	35.26	1.29E-01	4.87	1.20E-01	-2.29
	0.02	3.16E-01	6.81E-01	115.15	4.08E-01	28.77	3.34E-01	5.44	3.12E-01	-1.38
	0.05	6.15E-01	8.68E-01	41.22	6.78E-01	10.25	6.07E-01	-1.37	6.11E-01	-0.59
	0.1	7.84E-01	9.07E-01	15.77	7.98E-01	1.85	7.52E-01	-4.03	7.92E-01	1.07
	0.15	8.47E-01	9.18E-01	8.34	8.44E-01	-0.37	8.12E-01	-4.16	8.60E-01	1.59
	0.2	8.94E-01	9.22E-01	3.15	8.68E-01	-2.91	8.44E-01	-5.58	8.93E-01	-0.07
	0.25	9.18E-01	9.25E-01	0.74	8.83E-01	-3.82	8.64E-01	-5.85	9.11E-01	-0.72
	0.3	9.26E-01	9.26E-01	0.02	8.93E-01	-3.58	8.78E-01	-5.21	9.22E-01	-0.48
	0.35	9.34E-01	9.27E-01	-0.69	9.00E-01	-3.59	8.88E-01	-4.93	9.28E-01	-0.67
	0.4	9.32E-01	9.28E-01	-0.44	9.06E-01	-2.84	8.95E-01	-3.98	9.31E-01	-0.16
	0.45	9.29E-01	9.29E-01	-0.02	9.10E-01	-2.03	9.01E-01	-3.03	9.32E-01	0.34
0.5	9.32E-01	9.29E-01	-0.35	9.13E-01	-2.04	9.05E-01	-2.90	9.33E-01	0.04	
2.5	0.01	2.48E-02	6.43E-02	159.70	3.15E-02	27.38	2.42E-02	-2.25	2.34E-02	-5.63
	0.02	9.95E-02	2.45E-01	146.08	1.29E-01	29.50	1.02E-01	2.69	9.63E-02	-3.26
	0.05	2.61E-01	4.57E-01	74.65	3.01E-01	14.97	2.58E-01	-1.51	2.61E-01	-0.06
	0.1	4.03E-01	5.26E-01	30.42	4.04E-01	0.23	3.67E-01	-8.99	4.01E-01	-0.53
	0.15	4.74E-01	5.47E-01	15.43	4.51E-01	-4.82	4.21E-01	-11.16	4.72E-01	-0.46
	0.2	5.02E-01	5.58E-01	11.04	4.79E-01	-4.60	4.54E-01	-9.51	5.12E-01	2.03
	0.25	5.41E-01	5.64E-01	4.18	4.98E-01	-8.05	4.77E-01	-11.85	5.37E-01	-0.85
	0.3	5.57E-01	5.68E-01	1.98	5.11E-01	-8.24	4.93E-01	-11.38	5.51E-01	-1.05
	0.35	5.38E-01	5.70E-01	5.95	5.21E-01	-3.29	5.05E-01	-6.09	5.59E-01	3.83
	0.4	5.57E-01	5.72E-01	2.76	5.28E-01	-5.15	5.15E-01	-7.52	5.63E-01	1.12
	0.45	5.69E-01	5.73E-01	0.74	5.34E-01	-6.20	5.22E-01	-8.25	5.65E-01	-0.81
0.5	5.60E-01	5.74E-01	2.54	5.39E-01	-3.84	5.28E-01	-5.69	5.65E-01	0.90	

ζ	ξ	ISEE	P	ε [%]	cVM	ε [%]	mVM	ε [%]	New	ε [%]
3	0.01	3.49E-03	7.66E-03	119.47	4.07E-03	16.64	3.14E-03	-10.01	3.20E-03	-8.35
	0.02	2.30E-02	5.18E-02	125.54	2.81E-02	22.25	2.22E-02	-3.37	2.17E-02	-5.34
	0.05	7.79E-02	1.34E-01	71.73	8.66E-02	11.26	7.35E-02	-5.60	7.71E-02	-1.05
	0.1	1.27E-01	1.68E-01	31.41	1.26E-01	-0.96	1.14E-01	-10.83	1.29E-01	0.82
	0.15	1.55E-01	1.79E-01	15.41	1.45E-01	-6.45	1.34E-01	-13.25	1.55E-01	0.27
	0.2	1.70E-01	1.84E-01	8.30	1.56E-01	-8.35	1.47E-01	-13.49	1.70E-01	0.01
	0.25	1.80E-01	1.87E-01	4.24	1.63E-01	-9.23	1.56E-01	-13.31	1.78E-01	-0.70
	0.3	1.83E-01	1.89E-01	3.49	1.68E-01	-8.04	1.62E-01	-11.45	1.83E-01	0.09
	0.35	1.86E-01	1.91E-01	2.85	1.72E-01	-7.22	1.67E-01	-10.11	1.86E-01	0.12
	0.4	1.85E-01	1.92E-01	4.03	1.75E-01	-5.05	1.71E-01	-7.59	1.87E-01	1.39
	0.45	1.90E-01	1.93E-01	1.67	1.78E-01	-6.35	1.73E-01	-8.52	1.88E-01	-1.12
0.5	1.91E-01	1.93E-01	1.05	1.79E-01	-6.22	1.76E-01	-8.13	1.87E-01	-2.00	
3.5	0.01	3.37E-04	6.40E-04	90.15	3.69E-04	9.64	2.87E-04	-14.61	3.12E-04	-7.35
	0.02	3.94E-03	7.71E-03	95.55	4.48E-03	13.75	3.57E-03	-9.48	3.70E-03	-6.08
	0.05	1.69E-02	2.61E-02	54.11	1.78E-02	5.13	1.52E-02	-10.29	1.66E-02	-1.60
	0.1	2.80E-02	3.45E-02	23.17	2.71E-02	-3.38	2.45E-02	-12.49	2.84E-02	1.41
	0.15	3.37E-02	3.74E-02	10.77	3.13E-02	-7.15	2.92E-02	-13.39	3.40E-02	0.81
	0.2	3.66E-02	3.88E-02	5.81	3.38E-02	-7.83	3.20E-02	-12.52	3.68E-02	0.58
	0.25	3.76E-02	3.96E-02	5.19	3.54E-02	-6.03	3.40E-02	-9.81	3.84E-02	1.95
	0.3	3.88E-02	4.02E-02	3.57	3.65E-02	-5.84	3.53E-02	-8.91	3.92E-02	1.18
	0.35	4.03E-02	4.06E-02	0.76	3.74E-02	-7.21	3.64E-02	-9.71	3.97E-02	-1.36
	0.4	4.03E-02	4.09E-02	1.36	3.80E-02	-5.73	3.71E-02	-7.88	3.99E-02	-0.96
	0.45	4.14E-02	4.11E-02	-0.65	3.85E-02	-6.88	3.78E-02	-8.71	4.00E-02	-3.35
0.5	4.12E-02	4.12E-02	0.06	3.89E-02	-5.64	3.82E-02	-7.24	3.99E-02	-3.12	
4	0.01	2.24E-05	3.82E-05	70.60	2.37E-05	5.55	1.86E-05	-16.96	2.15E-05	-4.19
	0.02	4.95E-04	8.66E-04	74.75	5.40E-04	8.90	4.33E-04	-12.53	4.77E-04	-3.68
	0.05	2.72E-03	3.79E-03	39.36	2.74E-03	0.89	2.37E-03	-13.03	2.70E-03	-0.58
	0.1	4.60E-03	5.25E-03	14.04	4.31E-03	-6.23	3.94E-03	-14.25	4.62E-03	0.47
	0.15	5.36E-03	5.73E-03	6.92	5.00E-03	-6.82	4.70E-03	-12.33	5.43E-03	1.21
	0.2	5.70E-03	5.98E-03	4.89	5.38E-03	-5.54	5.15E-03	-9.67	5.81E-03	1.98
	0.25	6.00E-03	6.12E-03	1.96	5.63E-03	-6.24	5.44E-03	-9.40	6.01E-03	0.15
	0.3	6.07E-03	6.22E-03	2.48	5.80E-03	-4.41	5.65E-03	-6.98	6.13E-03	0.98
	0.35	6.27E-03	6.29E-03	0.34	5.93E-03	-5.43	5.80E-03	-7.50	6.19E-03	-1.19
	0.4	6.33E-03	6.34E-03	0.16	6.03E-03	-4.86	5.92E-03	-6.60	6.22E-03	-1.75
	0.45	6.34E-03	6.38E-03	0.69	6.10E-03	-3.79	6.01E-03	-5.27	6.22E-03	-1.83
0.5	6.30E-03	6.41E-03	1.70	6.16E-03	-2.36	6.07E-03	-3.65	6.21E-03	-1.43	

ζ	ξ	ISEE	P	ε [%]	cVM	ε [%]	mVM	ε [%]	New	ε [%]
4.5	0.01	1.07E-06	1.64E-06	53.12	1.07E-06	0.59	8.54E-07	-20.04	1.03E-06	-3.38
	0.02	4.78E-05	7.45E-05	55.86	4.93E-05	3.11	4.00E-05	-16.38	4.61E-05	-3.60
	0.05	3.32E-04	4.26E-04	28.50	3.25E-04	-2.02	2.83E-04	-14.64	3.33E-04	0.22
	0.1	5.62E-04	6.14E-04	9.25	5.25E-04	-6.54	4.85E-04	-13.69	5.67E-04	0.91
	0.15	6.45E-04	6.77E-04	4.95	6.09E-04	-5.57	5.78E-04	-10.41	6.57E-04	1.77
	0.2	6.94E-04	7.08E-04	2.06	6.55E-04	-5.61	6.31E-04	-9.09	6.98E-04	0.51
	0.25	7.14E-04	7.27E-04	1.86	6.84E-04	-4.18	6.65E-04	-6.84	7.20E-04	0.82
	0.3	7.21E-04	7.40E-04	2.56	7.04E-04	-2.41	6.89E-04	-4.53	7.33E-04	1.58
	0.35	7.52E-04	7.49E-04	-0.39	7.18E-04	-4.44	7.06E-04	-6.11	7.40E-04	-1.55
	0.4	7.52E-04	7.56E-04	0.49	7.29E-04	-3.02	7.19E-04	-4.40	7.43E-04	-1.15
	0.45	7.46E-04	7.61E-04	2.05	7.38E-04	-1.06	7.29E-04	-2.24	7.44E-04	-0.32
0.5	7.57E-04	7.65E-04	1.14	7.44E-04	-1.59	7.37E-04	-2.58	7.43E-04	-1.77	
5	0.01	3.53E-08	5.00E-08	41.56	3.46E-08	-2.12	2.78E-08	-21.38	3.42E-08	-3.27
	0.02	3.42E-06	4.92E-06	43.82	3.42E-06	0.12	2.80E-06	-18.00	3.29E-06	-3.67
	0.05	3.16E-05	3.74E-05	18.20	2.98E-05	-5.91	2.62E-05	-17.18	3.10E-05	-2.07
	0.1	5.28E-05	5.59E-05	5.97	4.94E-05	-6.44	4.60E-05	-12.82	5.32E-05	0.75
	0.15	6.12E-05	6.22E-05	1.63	5.73E-05	-6.29	5.48E-05	-10.43	6.11E-05	-0.13
	0.2	6.43E-05	6.53E-05	1.61	6.16E-05	-4.14	5.97E-05	-7.10	6.48E-05	0.76
	0.25	6.77E-05	6.72E-05	-0.75	6.42E-05	-5.06	6.28E-05	-7.22	6.68E-05	-1.35
	0.3	6.89E-05	6.84E-05	-0.70	6.60E-05	-4.15	6.49E-05	-5.82	6.80E-05	-1.33
	0.35	6.94E-05	6.93E-05	-0.14	6.73E-05	-2.99	6.64E-05	-4.32	6.87E-05	-1.01
	0.4	6.98E-05	7.00E-05	0.27	6.83E-05	-2.15	6.75E-05	-3.23	6.91E-05	-1.07
	0.45	7.01E-05	7.05E-05	0.55	6.91E-05	-1.53	6.84E-05	-2.43	6.92E-05	-1.37
	0.5	6.97E-05	7.09E-05	1.83	6.97E-05	-0.02	6.91E-05	-0.77	6.94E-05	-0.45
		μ_ε %	22.38	μ_ε %	-0.004	μ_ε %	-7.09	μ_ε %	-0.71	
		σ_ε %	39.25	σ_ε %	9.45	σ_ε %	5.76	σ_ε %	2.04	
		ε_{\max} %	176.24	ε_{\max} %	35.26	ε_{\max} %	9.10	ε_{\max} %	3.83	
		ε_{\min} %	-0.75	ε_{\min} %	-9.23	ε_{\min} %	-21.38	ε_{\min} %	-8.35	
		$\mu_{ \varepsilon }$ %	22.48	$\mu_{ \varepsilon }$ %	6.32	$\mu_{ \varepsilon }$ %	7.70	$\mu_{ \varepsilon }$ %	1.47	

APPENDIX D : PARAMETRIC STUDY RESULTS OF LINEAR SDOF SYSTEMS SUBJECTED TO TIME-MODULATED WHITE OR COLORED NOISE EXCITATIONS

This appendix presents the parametric study results of the FPDF of linear SDOF systems subjected to time-modulated white or non-white excitation. The proposed #5 (Appendix B) and the proposed #6 (denoted as New in the text) obtained with and without the proposed modifications (see Section 2.3) are evaluated for accuracy in estimating the time-variant FPDF of linear SDOF systems with different damping ratios and normalized threshold levels.

D.1 PROPOSED #5

D.1.1 White Noise and Shinozuka-Sato Time-modulating Function, $T=1.0s$

Table D.1 - Proposed #5: Time-variant FPDF computed at $t = 20s$ for linear elastic SDOF systems with $T = 1.0s$ subjected to WN base excitation time modulated by a Shinozuka-Sato function.

ζ	ξ	ISEE	P	ε [%]	cVM	ε [%]	mVM	ε [%]	#5	ε [%]
1.5	0.01	7.45E-01	9.99E-01	34.15	8.57E-01	15.04	7.33E-01	-1.62	6.20E-01	-16.84
	0.02	7.89E-01	9.97E-01	26.34	8.83E-01	11.81	7.89E-01	-0.04	7.29E-01	-7.65
	0.05	8.81E-01	9.90E-01	12.41	9.15E-01	3.89	8.61E-01	-2.21	8.73E-01	-0.90
	0.1	9.38E-01	9.85E-01	5.08	9.43E-01	0.59	9.14E-01	-2.47	9.46E-01	0.91
	0.15	9.71E-01	9.84E-01	1.30	9.58E-01	-1.40	9.40E-01	-3.25	9.69E-01	-0.21
	0.2	9.80E-01	9.83E-01	0.34	9.66E-01	-1.44	9.53E-01	-2.71	9.79E-01	-0.11
	0.25	9.80E-01	9.83E-01	0.35	9.71E-01	-0.87	9.62E-01	-1.80	9.84E-01	0.43
	0.3	9.60E-01	9.83E-01	2.40	9.75E-01	1.54	9.68E-01	0.80	9.87E-01	2.77
	0.35	9.70E-01	9.83E-01	1.30	9.77E-01	0.72	9.72E-01	0.13	9.88E-01	1.82
	0.4	9.90E-01	9.83E-01	-0.70	9.79E-01	-1.07	9.75E-01	-1.54	9.89E-01	-0.10
	0.45	9.84E-01	9.83E-01	-0.12	9.81E-01	-0.34	9.77E-01	-0.74	9.89E-01	0.52
0.5	9.92E-01	9.83E-01	-0.88	9.82E-01	-0.98	9.79E-01	-1.32	9.90E-01	-0.21	
2	0.01	3.90E-01	9.21E-01	136.15	5.00E-01	28.16	3.77E-01	-3.38	2.84E-01	-27.06
	0.02	4.13E-01	8.59E-01	108.08	5.22E-01	26.48	4.19E-01	1.55	3.57E-01	-13.48
	0.05	4.99E-01	7.83E-01	56.83	5.61E-01	12.37	4.88E-01	-2.24	4.89E-01	-2.05
	0.1	5.95E-01	7.53E-01	26.53	6.07E-01	2.02	5.56E-01	-6.47	6.03E-01	1.45
	0.15	6.46E-01	7.45E-01	15.38	6.37E-01	-1.35	5.99E-01	-7.29	6.63E-01	2.68
	0.2	6.92E-01	7.43E-01	7.36	6.58E-01	-4.91	6.28E-01	-9.34	6.99E-01	0.94
	0.25	7.26E-01	7.42E-01	2.16	6.73E-01	-7.35	6.48E-01	-10.83	7.20E-01	-0.82
	0.3	7.29E-01	7.42E-01	1.75	6.84E-01	-6.14	6.63E-01	-9.06	7.34E-01	0.71
	0.35	7.39E-01	7.41E-01	0.29	6.93E-01	-6.30	6.74E-01	-8.78	7.42E-01	0.39
	0.4	7.48E-01	7.41E-01	-0.88	6.99E-01	-6.47	6.83E-01	-8.61	7.47E-01	-0.16
	0.45	7.49E-01	7.41E-01	-1.09	7.05E-01	-5.91	6.91E-01	-7.80	7.49E-01	-0.02
0.5	7.50E-01	7.41E-01	-1.23	7.09E-01	-5.43	6.97E-01	-7.11	7.51E-01	0.09	

ζ	ξ	ISEE	P	ε [%]	cVM	ε [%]	mVM	ε [%]	#5	ε [%]
2.5	0.01	1.46E-01	4.95E-01	238.92	1.88E-01	28.78	1.34E-01	-8.49	1.01E-01	-30.93
	0.02	1.55E-01	4.09E-01	163.23	1.95E-01	25.72	1.49E-01	-3.78	1.28E-01	-17.88
	0.05	1.85E-01	3.37E-01	81.89	2.10E-01	13.45	1.77E-01	-4.53	1.79E-01	-3.25
	0.1	2.30E-01	3.13E-01	36.33	2.30E-01	0.30	2.06E-01	-10.17	2.30E-01	0.14
	0.15	2.56E-01	3.08E-01	20.24	2.45E-01	-4.35	2.26E-01	-11.70	2.60E-01	1.45
	0.2	2.72E-01	3.06E-01	12.49	2.55E-01	-6.25	2.40E-01	-11.88	2.78E-01	2.16
	0.25	2.86E-01	3.05E-01	6.73	2.62E-01	-8.24	2.50E-01	-12.70	2.89E-01	1.09
	0.3	2.96E-01	3.05E-01	3.16	2.68E-01	-9.32	2.57E-01	-12.99	2.96E-01	0.09
	0.35	2.93E-01	3.05E-01	4.17	2.72E-01	-6.88	2.63E-01	-10.09	3.00E-01	2.43
	0.4	2.98E-01	3.05E-01	2.17	2.76E-01	-7.48	2.68E-01	-10.23	3.02E-01	1.16
	0.45	2.99E-01	3.05E-01	1.89	2.79E-01	-6.76	2.71E-01	-9.19	3.03E-01	1.23
0.5	3.02E-01	3.05E-01	0.98	2.81E-01	-6.80	2.75E-01	-8.95	3.03E-01	0.55	
3	0.01	4.01E-02	1.37E-01	240.73	4.94E-02	23.33	3.46E-02	-13.59	2.80E-02	-30.08
	0.02	4.17E-02	1.07E-01	156.43	5.06E-02	21.32	3.84E-02	-7.91	3.48E-02	-16.72
	0.05	4.95E-02	8.47E-02	71.03	5.36E-02	8.21	4.50E-02	-9.12	4.74E-02	-4.26
	0.1	5.87E-02	7.76E-02	32.32	5.81E-02	-0.91	5.21E-02	-11.15	5.94E-02	1.33
	0.15	6.50E-02	7.61E-02	17.13	6.15E-02	-5.31	5.69E-02	-12.39	6.62E-02	1.87
	0.2	6.94E-02	7.56E-02	8.98	6.39E-02	-7.88	6.02E-02	-13.17	7.00E-02	0.95
	0.25	7.16E-02	7.54E-02	5.26	6.56E-02	-8.40	6.26E-02	-12.60	7.22E-02	0.79
	0.3	7.19E-02	7.53E-02	4.68	6.69E-02	-7.00	6.44E-02	-10.50	7.34E-02	2.00
	0.35	7.25E-02	7.53E-02	3.77	6.79E-02	-6.39	6.57E-02	-9.35	7.40E-02	2.00
	0.4	7.44E-02	7.52E-02	1.18	6.87E-02	-7.65	6.68E-02	-10.15	7.42E-02	-0.15
	0.45	7.32E-02	7.52E-02	2.78	6.93E-02	-5.31	6.77E-02	-7.53	7.43E-02	1.58
0.5	7.43E-02	7.52E-02	1.27	6.98E-02	-6.00	6.84E-02	-7.93	7.44E-02	0.16	
3.5	0.01	8.28E-03	2.48E-02	199.02	9.67E-03	16.77	6.80E-03	-17.86	6.02E-03	-27.36
	0.02	8.63E-03	1.92E-02	122.33	9.77E-03	13.16	7.46E-03	-13.52	7.27E-03	-15.80
	0.05	1.00E-02	1.51E-02	50.24	1.01E-02	1.17	8.59E-03	-14.26	9.48E-03	-5.39
	0.1	1.14E-02	1.37E-02	20.81	1.08E-02	-4.93	9.78E-03	-13.96	1.14E-02	-0.05
	0.15	1.23E-02	1.35E-02	8.97	1.13E-02	-8.18	1.06E-02	-14.32	1.23E-02	-0.36
	0.2	1.27E-02	1.34E-02	5.56	1.17E-02	-7.54	1.11E-02	-12.19	1.28E-02	0.88
	0.25	1.29E-02	1.33E-02	3.01	1.20E-02	-7.51	1.15E-02	-11.15	1.30E-02	0.50
	0.3	1.31E-02	1.33E-02	1.87	1.22E-02	-6.95	1.18E-02	-9.90	1.31E-02	0.36
	0.35	1.32E-02	1.33E-02	1.03	1.23E-02	-6.55	1.20E-02	-9.00	1.32E-02	-0.03
	0.4	1.30E-02	1.33E-02	2.24	1.24E-02	-4.52	1.21E-02	-6.63	1.32E-02	1.34
	0.45	1.31E-02	1.33E-02	1.53	1.25E-02	-4.48	1.23E-02	-6.29	1.32E-02	0.65
0.5	1.29E-02	1.33E-02	2.75	1.26E-02	-2.76	1.24E-02	-4.35	1.32E-02	1.84	

ζ	ξ	ISEE	P	ε [%]	cVM	ε [%]	mVM	ε [%]	#5	ε [%]
4	0.01	1.33E-03	3.38E-03	154.94	1.45E-03	9.36	1.03E-03	-22.39	9.88E-04	-25.57
	0.02	1.32E-03	2.62E-03	98.75	1.45E-03	9.73	1.12E-03	-15.24	1.16E-03	-11.75
	0.05	1.51E-03	2.05E-03	36.22	1.47E-03	-2.32	1.26E-03	-16.25	1.45E-03	-3.87
	0.1	1.65E-03	1.87E-03	13.42	1.55E-03	-6.40	1.41E-03	-14.41	1.66E-03	0.37
	0.15	1.74E-03	1.83E-03	5.25	1.61E-03	-7.83	1.51E-03	-13.21	1.74E-03	0.07
	0.2	1.79E-03	1.82E-03	1.72	1.65E-03	-7.96	1.58E-03	-11.90	1.78E-03	-0.60
	0.25	1.82E-03	1.82E-03	-0.21	1.68E-03	-7.84	1.62E-03	-10.86	1.80E-03	-1.39
	0.3	1.78E-03	1.81E-03	2.12	1.70E-03	-4.37	1.66E-03	-6.85	1.80E-03	1.38
	0.35	1.80E-03	1.81E-03	0.95	1.72E-03	-4.52	1.68E-03	-6.53	1.80E-03	0.40
	0.4	1.80E-03	1.81E-03	0.54	1.73E-03	-4.19	1.70E-03	-5.87	1.80E-03	0.04
	0.45	1.82E-03	1.81E-03	-0.41	1.74E-03	-4.55	1.71E-03	-5.96	1.80E-03	-0.93
0.5	1.80E-03	1.81E-03	0.62	1.74E-03	-3.12	1.72E-03	-4.35	1.80E-03	0.04	
4.5	0.01	1.61E-04	3.62E-04	124.53	1.69E-04	4.92	1.21E-04	-24.81	1.24E-04	-23.08
	0.02	1.60E-04	2.81E-04	75.51	1.67E-04	4.15	1.30E-04	-18.64	1.43E-04	-10.73
	0.05	1.72E-04	2.20E-04	27.58	1.66E-04	-3.49	1.44E-04	-16.31	1.70E-04	-1.40
	0.1	1.85E-04	2.00E-04	8.53	1.72E-04	-6.90	1.59E-04	-14.02	1.86E-04	0.63
	0.15	1.93E-04	1.96E-04	1.41	1.77E-04	-8.43	1.68E-04	-13.07	1.91E-04	-1.30
	0.2	1.94E-04	1.95E-04	0.22	1.81E-04	-7.00	1.74E-04	-10.35	1.93E-04	-0.91
	0.25	1.93E-04	1.94E-04	0.89	1.83E-04	-4.80	1.78E-04	-7.37	1.93E-04	0.31
	0.3	1.91E-04	1.94E-04	1.57	1.85E-04	-3.09	1.81E-04	-5.12	1.93E-04	1.20
	0.35	1.91E-04	1.94E-04	1.74	1.87E-04	-2.17	1.83E-04	-3.80	1.93E-04	1.44
	0.4	1.95E-04	1.94E-04	-0.55	1.88E-04	-3.81	1.85E-04	-5.13	1.93E-04	-0.85
	0.45	1.92E-04	1.94E-04	1.24	1.88E-04	-1.66	1.86E-04	-2.78	1.93E-04	0.88
0.5	1.93E-04	1.94E-04	0.65	1.89E-04	-1.89	1.87E-04	-2.84	1.93E-04	0.24	
5	0.01	1.53E-05	3.04E-05	99.11	1.53E-05	0.22	1.11E-05	-27.46	1.20E-05	-21.79
	0.02	1.50E-05	2.36E-05	57.34	1.49E-05	-0.67	1.18E-05	-21.54	1.34E-05	-10.50
	0.05	1.57E-05	1.85E-05	17.71	1.46E-05	-6.93	1.28E-05	-18.40	1.53E-05	-2.77
	0.1	1.63E-05	1.69E-05	3.22	1.49E-05	-8.69	1.39E-05	-14.91	1.61E-05	-1.61
	0.15	1.62E-05	1.65E-05	2.12	1.53E-05	-5.61	1.46E-05	-9.73	1.63E-05	0.53
	0.2	1.64E-05	1.64E-05	0.29	1.55E-05	-5.17	1.50E-05	-8.03	1.63E-05	-0.36
	0.25	1.61E-05	1.64E-05	1.31	1.57E-05	-2.89	1.53E-05	-5.04	1.63E-05	0.96
	0.3	1.63E-05	1.63E-05	0.25	1.58E-05	-3.06	1.55E-05	-4.69	1.63E-05	0.01
	0.35	1.63E-05	1.63E-05	0.11	1.59E-05	-2.60	1.57E-05	-3.89	1.63E-05	-0.12
	0.4	1.60E-05	1.63E-05	1.89	1.60E-05	-0.43	1.58E-05	-1.49	1.63E-05	1.63
	0.45	1.60E-05	1.63E-05	2.21	1.60E-05	0.21	1.59E-05	-0.66	1.63E-05	1.88
0.5	1.63E-05	1.63E-05	0.38	1.60E-05	-1.33	1.59E-05	-2.05	1.63E-05	-0.01	
		μ_ε %	28.27	μ_ε %	-0.673	μ_ε %	-8.81	μ_ε %	-3.02	
		σ_ε %	53.27	σ_ε %	8.93	σ_ε %	5.74	σ_ε %	7.97	
		ε_{\max} %	240.73	ε_{\max} %	28.78	ε_{\max} %	1.55	ε_{\max} %	2.77	
		ε_{\min} %	-1.23	ε_{\min} %	-9.32	ε_{\min} %	-27.46	ε_{\min} %	-30.93	
		$\mu_{ \varepsilon }$ %	28.39	$\mu_{ \varepsilon }$ %	6.58	$\mu_{ \varepsilon }$ %	8.86	$\mu_{ \varepsilon }$ %	4.09	

D.1.2 Kanai-Tajimi and Unit-step Time-modulating Function, $T = 0.1s$

Table D.2 - Proposed #5: Time-variant FFPF computed at $t = 1.0s$ for linear elastic SDOF system with $T = 0.1s$ subjected to KT base excitation from at-rest initial conditions.

ζ	ξ	ISEE	P	ε [%]	cVM	ε [%]	mVM	ε [%]	#5	ε [%]
1.5	0.01	5.15E-01	8.88E-01	72.41	6.71E-01	30.18	5.88E-01	14.16	5.71E-01	10.91
	0.02	8.17E-01	9.84E-01	20.54	9.01E-01	10.36	8.47E-01	3.72	8.44E-01	3.40
	0.05	9.76E-01	9.98E-01	2.25	9.86E-01	1.04	9.73E-01	-0.31	9.81E-01	0.49
	0.1	1.00E+00	9.99E-01	-0.08	9.97E-01	-0.26	9.94E-01	-0.56	9.98E-01	-0.20
	0.15	9.97E-01	9.99E-01	0.24	9.99E-01	0.21	9.98E-01	0.09	1.00E+00	0.26
	0.2	1.00E+00	9.99E-01	-0.05	1.00E+00	-0.05	9.99E-01	-0.10	1.00E+00	-0.01
	0.25	9.79E-01	1.00E+00	2.13	1.00E+00	2.15	9.99E-01	2.12	1.00E+00	2.18
	0.3	9.94E-01	9.99E-01	0.60	1.00E+00	0.64	1.00E+00	0.61	1.00E+00	0.65
	0.35	1.00E+00	9.99E-01	-0.05	1.00E+00	-0.01	1.00E+00	-0.03	1.00E+00	0.00
	0.4	1.00E+00	9.99E-01	-0.06	1.00E+00	-0.01	1.00E+00	-0.03	1.00E+00	0.00
	0.45	1.00E+00	9.99E-01	-0.06	1.00E+00	-0.01	1.00E+00	-0.02	1.00E+00	0.00
0.5	1.00E+00	9.99E-01	-0.06	1.00E+00	0.00	1.00E+00	-0.01	1.00E+00	0.00	
2	0.01	1.82E-01	4.17E-01	129.44	2.45E-01	34.90	2.02E-01	11.34	1.90E-01	4.63
	0.02	4.40E-01	7.73E-01	75.49	5.52E-01	25.38	4.81E-01	9.27	4.69E-01	6.49
	0.05	8.22E-01	9.43E-01	14.75	8.39E-01	2.03	7.89E-01	-4.05	8.07E-01	-1.79
	0.1	9.54E-01	9.78E-01	2.48	9.39E-01	-1.56	9.15E-01	-4.06	9.41E-01	-1.30
	0.15	9.93E-01	9.86E-01	-0.63	9.68E-01	-2.46	9.54E-01	-3.84	9.76E-01	-1.62
	0.2	9.99E-01	9.90E-01	-0.87	9.80E-01	-1.84	9.71E-01	-2.73	9.89E-01	-0.95
	0.25	9.92E-01	9.92E-01	-0.03	9.86E-01	-0.57	9.80E-01	-1.22	9.94E-01	0.25
	0.3	9.99E-01	9.93E-01	-0.66	9.90E-01	-0.95	9.85E-01	-1.44	9.97E-01	-0.23
	0.35	1.00E+00	9.93E-01	-0.68	9.92E-01	-0.82	9.88E-01	-1.22	9.98E-01	-0.20
	0.4	1.00E+00	9.93E-01	-0.65	9.93E-01	-0.69	9.90E-01	-1.02	9.99E-01	-0.14
	0.45	1.00E+00	9.94E-01	-0.64	9.94E-01	-0.60	9.91E-01	-0.89	9.99E-01	-0.11
0.5	1.00E+00	9.94E-01	-0.64	9.95E-01	-0.53	9.92E-01	-0.79	9.99E-01	-0.09	
2.5	0.01	4.14E-02	9.31E-02	124.83	5.36E-02	29.44	4.37E-02	5.44	4.16E-02	0.51
	0.02	1.71E-01	3.40E-01	98.60	2.10E-01	22.79	1.76E-01	3.18	1.73E-01	1.21
	0.05	4.85E-01	6.59E-01	35.96	4.99E-01	2.93	4.49E-01	-7.44	4.69E-01	-3.23
	0.1	7.33E-01	8.16E-01	11.35	7.03E-01	-4.04	6.62E-01	-9.74	7.10E-01	-3.14
	0.15	8.45E-01	8.79E-01	3.99	8.00E-01	-5.32	7.68E-01	-9.19	8.26E-01	-2.25
	0.2	9.17E-01	9.11E-01	-0.63	8.54E-01	-6.79	8.28E-01	-9.66	8.90E-01	-2.91
	0.25	9.38E-01	9.29E-01	-0.89	8.87E-01	-5.36	8.66E-01	-7.68	9.27E-01	-1.10
	0.3	9.53E-01	9.40E-01	-1.26	9.08E-01	-4.63	8.90E-01	-6.56	9.49E-01	-0.38
	0.35	9.45E-01	9.48E-01	0.30	9.23E-01	-2.34	9.07E-01	-4.04	9.62E-01	1.78
	0.4	9.67E-01	9.53E-01	-1.49	9.33E-01	-3.54	9.18E-01	-5.02	9.69E-01	0.24
	0.45	9.75E-01	9.56E-01	-1.99	9.40E-01	-3.62	9.27E-01	-4.95	9.74E-01	-0.13
0.5	9.76E-01	9.58E-01	-1.81	9.45E-01	-3.13	9.33E-01	-4.35	9.77E-01	0.15	

ζ	ξ	ISEE	P	ε [%]	cVM	ε [%]	mVM	ε [%]	#5	ε [%]
3	0.01	6.54E-03	1.30E-02	98.28	7.96E-03	21.77	6.52E-03	-0.33	6.47E-03	-1.13
	0.02	4.62E-02	8.76E-02	89.81	5.44E-02	17.76	4.54E-02	-1.69	4.61E-02	-0.27
	0.05	1.97E-01	2.81E-01	43.03	2.00E-01	1.56	1.76E-01	-10.33	1.90E-01	-3.25
	0.1	3.96E-01	4.70E-01	18.67	3.72E-01	-5.89	3.43E-01	-13.35	3.84E-01	-3.03
	0.15	5.44E-01	5.90E-01	8.34	4.95E-01	-9.12	4.64E-01	-14.67	5.27E-01	-3.13
	0.2	6.32E-01	6.70E-01	6.02	5.82E-01	-7.83	5.53E-01	-12.45	6.33E-01	0.15
	0.25	7.06E-01	7.24E-01	2.51	6.46E-01	-8.62	6.18E-01	-12.53	7.09E-01	0.38
	0.3	7.60E-01	7.62E-01	0.33	6.92E-01	-8.91	6.66E-01	-12.33	7.63E-01	0.43
	0.35	7.91E-01	7.89E-01	-0.20	7.27E-01	-8.12	7.02E-01	-11.22	8.00E-01	1.19
	0.4	8.25E-01	8.09E-01	-1.91	7.53E-01	-8.72	7.30E-01	-11.52	8.26E-01	0.16
	0.45	8.18E-01	8.24E-01	0.72	7.73E-01	-5.47	7.51E-01	-8.15	8.44E-01	3.23
0.5	8.50E-01	8.35E-01	-1.76	7.89E-01	-7.16	7.68E-01	-9.61	8.57E-01	0.93	
3.5	0.01	7.25E-04	1.28E-03	76.95	8.45E-04	16.64	6.98E-04	-3.64	7.23E-04	-0.22
	0.02	9.32E-03	1.59E-02	70.19	1.04E-02	11.60	8.73E-03	-6.33	9.22E-03	-1.06
	0.05	5.72E-02	7.94E-02	38.72	5.75E-02	0.46	5.08E-02	-11.30	5.66E-02	-1.12
	0.1	1.54E-01	1.81E-01	17.53	1.42E-01	-7.75	1.30E-01	-15.45	1.50E-01	-2.39
	0.15	2.47E-01	2.75E-01	11.45	2.25E-01	-9.09	2.09E-01	-15.26	2.46E-01	-0.38
	0.2	3.41E-01	3.57E-01	4.75	2.98E-01	-12.34	2.81E-01	-17.46	3.34E-01	-1.81
	0.25	4.13E-01	4.23E-01	2.61	3.61E-01	-12.44	3.42E-01	-17.00	4.10E-01	-0.59
	0.3	4.65E-01	4.77E-01	2.62	4.13E-01	-11.07	3.94E-01	-15.27	4.72E-01	1.56
	0.35	5.07E-01	5.20E-01	2.40	4.56E-01	-10.14	4.36E-01	-14.06	5.21E-01	2.65
	0.4	5.42E-01	5.54E-01	2.05	4.91E-01	-9.50	4.71E-01	-13.18	5.59E-01	3.03
	0.45	5.72E-01	5.81E-01	1.47	5.19E-01	-9.21	5.00E-01	-12.69	5.88E-01	2.78
0.5	6.16E-01	6.02E-01	-2.22	5.43E-01	-11.85	5.23E-01	-15.05	6.11E-01	-0.78	
4	0.01	5.59E-05	9.26E-05	65.64	6.49E-05	16.05	5.42E-05	-3.14	5.81E-05	3.88
	0.02	1.45E-03	2.19E-03	51.44	1.53E-03	5.35	1.29E-03	-10.80	1.41E-03	-2.45
	0.05	1.34E-02	1.68E-02	25.32	1.27E-02	-5.00	1.13E-02	-15.52	1.29E-02	-3.45
	0.1	4.58E-02	5.13E-02	11.88	4.14E-02	-9.64	3.81E-02	-16.82	4.47E-02	-2.46
	0.15	8.79E-02	9.49E-02	7.92	7.86E-02	-10.64	7.34E-02	-16.54	8.73E-02	-0.71
	0.2	1.32E-01	1.42E-01	6.90	1.19E-01	-10.16	1.12E-01	-15.39	1.35E-01	1.65
	0.25	1.76E-01	1.87E-01	5.97	1.59E-01	-9.95	1.50E-01	-14.72	1.81E-01	3.01
	0.3	2.18E-01	2.28E-01	4.71	1.96E-01	-10.21	1.86E-01	-14.62	2.25E-01	3.20
	0.35	2.51E-01	2.65E-01	5.54	2.29E-01	-8.80	2.18E-01	-13.01	2.63E-01	4.85
	0.4	2.86E-01	2.97E-01	3.66	2.58E-01	-9.82	2.47E-01	-13.77	2.96E-01	3.36
	0.45	3.15E-01	3.24E-01	2.84	2.84E-01	-9.99	2.72E-01	-13.75	3.23E-01	2.59
0.5	3.38E-01	3.47E-01	2.86	3.06E-01	-9.48	2.93E-01	-13.11	3.46E-01	2.54	

ζ	ξ	ISEE	P	ε [%]	cVM	ε [%]	mVM	ε [%]	#5	ε [%]
4.5	0.01	3.19E-06	4.91E-06	53.90	3.62E-06	13.48	3.05E-06	-4.31	3.35E-06	5.19
	0.02	1.68E-04	2.37E-04	41.20	1.74E-04	3.44	1.49E-04	-11.59	1.67E-04	-0.88
	0.05	2.44E-03	2.83E-03	16.26	2.25E-03	-7.78	2.02E-03	-17.25	2.34E-03	-4.11
	0.1	1.07E-02	1.16E-02	8.88	9.72E-03	-8.79	9.02E-03	-15.41	1.06E-02	-0.72
	0.15	2.44E-02	2.61E-02	6.73	2.23E-02	-8.97	2.09E-02	-14.48	2.47E-02	1.08
	0.2	4.17E-02	4.48E-02	7.53	3.86E-02	-7.46	3.65E-02	-12.45	4.34E-02	3.98
	0.25	6.27E-02	6.59E-02	4.98	5.70E-02	-9.14	5.42E-02	-13.65	6.45E-02	2.79
	0.3	8.37E-02	8.75E-02	4.53	7.61E-02	-9.14	7.25E-02	-13.37	8.63E-02	3.07
	0.35	1.01E-01	1.09E-01	7.39	9.48E-02	-6.31	9.06E-02	-10.45	1.08E-01	6.23
	0.4	1.23E-01	1.29E-01	4.85	1.13E-01	-8.24	1.08E-01	-12.12	1.27E-01	3.73
	0.45	1.39E-01	1.47E-01	5.67	1.29E-01	-7.24	1.24E-01	-11.02	1.45E-01	4.27
0.5	1.58E-01	1.63E-01	3.32	1.44E-01	-9.04	1.38E-01	-12.62	1.61E-01	1.59	
5	0.01	1.27E-07	1.90E-07	49.83	1.46E-07	15.32	1.25E-07	-1.77	1.40E-07	9.86
	0.02	1.50E-05	2.02E-05	34.95	1.55E-05	3.29	1.33E-05	-10.90	1.52E-05	1.52
	0.05	3.44E-04	3.88E-04	12.86	3.20E-04	-6.95	2.90E-04	-15.76	3.37E-04	-2.06
	0.1	2.01E-03	2.17E-03	7.81	1.88E-03	-6.67	1.76E-03	-12.78	2.04E-03	1.32
	0.15	5.59E-03	5.99E-03	7.09	5.26E-03	-5.92	4.97E-03	-11.03	5.78E-03	3.31
	0.2	1.12E-02	1.19E-02	5.90	1.05E-02	-6.39	1.00E-02	-10.92	1.16E-02	3.45
	0.25	1.85E-02	1.95E-02	5.86	1.73E-02	-6.12	1.66E-02	-10.32	1.92E-02	4.09
	0.3	2.64E-02	2.83E-02	7.02	2.51E-02	-4.90	2.41E-02	-8.91	2.79E-02	5.52
	0.35	3.62E-02	3.76E-02	3.84	3.35E-02	-7.59	3.21E-02	-11.31	3.71E-02	2.38
	0.4	4.46E-02	4.71E-02	5.60	4.20E-02	-5.91	4.03E-02	-9.55	4.63E-02	3.79
	0.45	5.38E-02	5.64E-02	4.71	5.03E-02	-6.60	4.84E-02	-10.10	5.51E-02	2.30
0.5	6.26E-02	6.52E-02	4.24	5.82E-02	-6.92	5.61E-02	-10.30	6.33E-02	1.13	
		μ_ε %	16.50	μ_ε %	-1.702	μ_ε %	-7.81	μ_ε %	0.93	
		σ_ε %	28.88	σ_ε %	10.09	σ_ε %	6.86	σ_ε %	2.74	
		ε_{\max} %	129.44	ε_{\max} %	34.90	ε_{\max} %	14.16	ε_{\max} %	10.91	
		ε_{\min} %	-2.22	ε_{\min} %	-12.44	ε_{\min} %	-17.46	ε_{\min} %	-4.11	
		$\mu_{ \varepsilon }$ %	16.90	$\mu_{ \varepsilon }$ %	7.72	$\mu_{ \varepsilon }$ %	8.85	$\mu_{ \varepsilon }$ %	2.10	

D.1.3 Kanai-Tajimi and Unit-step Time-modulating Function, $T = 0.5s$

Table D.3 - Proposed #5: Time-variant FFPF computed at $t = 5.0s$ for linear elastic SDOF system with $T = 0.5s$ subjected to KT base excitation from at-rest initial conditions.

ζ	ξ	ISEE	P	ε [%]	cVM	ε [%]	mVM	ε [%]	#5	ε [%]
1.5	0.01	3.86E-01	8.41E-01	117.86	4.93E-01	27.68	3.91E-01	1.27	3.27E-01	-15.17
	0.02	6.72E-01	9.71E-01	44.52	7.61E-01	13.31	6.56E-01	-2.30	5.97E-01	-11.17
	0.05	9.15E-01	9.95E-01	8.69	9.30E-01	1.68	8.77E-01	-4.10	8.87E-01	-3.08
	0.1	9.83E-01	9.97E-01	1.45	9.74E-01	-0.85	9.53E-01	-3.04	9.76E-01	-0.69
	0.15	9.95E-01	9.97E-01	0.28	9.85E-01	-0.92	9.74E-01	-2.09	9.91E-01	-0.32
	0.2	1.00E+00	9.97E-01	-0.26	9.90E-01	-1.02	9.82E-01	-1.76	9.96E-01	-0.43
	0.25	9.96E-01	9.97E-01	0.11	9.92E-01	-0.43	9.87E-01	-0.96	9.97E-01	0.11
	0.3	9.88E-01	9.97E-01	0.89	9.93E-01	0.47	9.89E-01	0.07	9.98E-01	0.96
	0.35	1.00E+00	9.97E-01	-0.29	9.94E-01	-0.61	9.91E-01	-0.94	9.98E-01	-0.17
	0.4	9.93E-01	9.97E-01	0.37	9.94E-01	0.12	9.92E-01	-0.16	9.98E-01	0.52
	0.45	9.88E-01	9.97E-01	0.87	9.95E-01	0.66	9.92E-01	0.42	9.98E-01	1.04
0.5	9.95E-01	9.96E-01	0.15	9.95E-01	-0.02	9.93E-01	-0.24	9.98E-01	0.34	
2	0.01	1.16E-01	3.34E-01	187.19	1.47E-01	26.45	1.10E-01	-5.37	8.64E-02	-25.84
	0.02	3.07E-01	6.75E-01	119.68	3.68E-01	19.86	2.91E-01	-5.21	2.45E-01	-20.20
	0.05	5.96E-01	8.61E-01	44.57	6.29E-01	5.52	5.46E-01	-8.39	5.43E-01	-8.83
	0.1	7.51E-01	8.97E-01	19.41	7.49E-01	-0.19	6.90E-01	-8.16	7.44E-01	-0.94
	0.15	8.15E-01	9.03E-01	10.82	7.94E-01	-2.48	7.49E-01	-8.03	8.23E-01	0.98
	0.2	8.73E-01	9.03E-01	3.43	8.17E-01	-6.46	7.80E-01	-10.59	8.60E-01	-1.45
	0.25	8.71E-01	9.01E-01	3.43	8.28E-01	-4.86	7.99E-01	-8.29	8.80E-01	1.00
	0.3	8.83E-01	8.97E-01	1.61	8.35E-01	-5.44	8.09E-01	-8.35	8.89E-01	0.66
	0.35	8.88E-01	8.93E-01	0.55	8.38E-01	-5.65	8.16E-01	-8.17	8.92E-01	0.43
	0.4	9.04E-01	8.89E-01	-1.75	8.39E-01	-7.21	8.19E-01	-9.42	8.92E-01	-1.41
	0.45	9.01E-01	8.84E-01	-1.90	8.39E-01	-6.89	8.21E-01	-8.90	8.89E-01	-1.31
0.5	8.87E-01	8.78E-01	-1.01	8.37E-01	-5.66	8.21E-01	-7.52	8.85E-01	-0.22	
2.5	0.01	2.36E-02	6.29E-02	166.63	2.77E-02	17.53	2.05E-02	-13.00	1.65E-02	-30.13
	0.02	9.62E-02	2.40E-01	149.22	1.14E-01	18.32	8.71E-02	-9.42	7.37E-02	-23.34
	0.05	2.49E-01	4.43E-01	78.01	2.67E-01	7.36	2.22E-01	-11.00	2.23E-01	-10.48
	0.1	3.62E-01	5.00E-01	38.16	3.57E-01	-1.34	3.15E-01	-12.95	3.55E-01	-1.83
	0.15	4.21E-01	5.08E-01	20.64	3.92E-01	-6.82	3.57E-01	-15.22	4.20E-01	-0.32
	0.2	4.39E-01	5.05E-01	15.07	4.09E-01	-6.88	3.79E-01	-13.68	4.53E-01	3.22
	0.25	4.66E-01	4.98E-01	7.04	4.16E-01	-10.63	3.91E-01	-16.11	4.69E-01	0.71
	0.3	4.69E-01	4.90E-01	4.55	4.18E-01	-10.72	3.96E-01	-15.42	4.74E-01	1.11
	0.35	4.69E-01	4.81E-01	2.37	4.17E-01	-11.07	3.98E-01	-15.18	4.72E-01	0.50
	0.4	4.60E-01	4.71E-01	2.32	4.14E-01	-9.91	3.97E-01	-13.61	4.66E-01	1.22
	0.45	4.58E-01	4.61E-01	0.50	4.10E-01	-10.55	3.95E-01	-13.85	4.57E-01	-0.23
0.5	4.53E-01	4.51E-01	-0.55	4.05E-01	-10.69	3.91E-01	-13.68	4.49E-01	-1.05	

ζ	ξ	ISEE	P	ε [%]	cVM	ε [%]	mVM	ε [%]	#5	ε [%]
3	0.01	3.30E-03	7.43E-03	125.12	3.56E-03	8.00	2.65E-03	-19.67	2.28E-03	-30.99
	0.02	2.18E-02	5.01E-02	129.96	2.45E-02	12.65	1.87E-02	-14.09	1.68E-02	-22.98
	0.05	7.21E-02	1.26E-01	75.42	7.50E-02	4.08	6.16E-02	-14.60	6.48E-02	-10.16
	0.1	1.13E-01	1.51E-01	34.30	1.06E-01	-5.81	9.27E-02	-17.65	1.09E-01	-3.45
	0.15	1.28E-01	1.54E-01	19.74	1.17E-01	-8.73	1.06E-01	-17.53	1.29E-01	0.32
	0.2	1.36E-01	1.51E-01	10.75	1.21E-01	-11.20	1.12E-01	-18.10	1.37E-01	0.58
	0.25	1.38E-01	1.46E-01	6.06	1.22E-01	-11.98	1.14E-01	-17.67	1.39E-01	0.61
	0.3	1.37E-01	1.41E-01	3.57	1.20E-01	-11.86	1.14E-01	-16.70	1.37E-01	0.52
	0.35	1.32E-01	1.36E-01	3.54	1.18E-01	-10.19	1.13E-01	-14.45	1.34E-01	1.63
	0.4	1.29E-01	1.31E-01	1.50	1.15E-01	-10.62	1.11E-01	-14.35	1.29E-01	0.13
	0.45	1.23E-01	1.26E-01	2.65	1.12E-01	-8.51	1.08E-01	-11.89	1.24E-01	1.46
0.5	1.21E-01	1.21E-01	0.01	1.09E-01	-9.97	1.05E-01	-12.94	1.20E-01	-1.06	
3.5	0.01	3.11E-04	6.14E-04	97.41	3.21E-04	3.31	2.41E-04	-22.50	2.23E-04	-28.18
	0.02	3.68E-03	7.37E-03	100.01	3.89E-03	5.65	2.99E-03	-18.93	2.88E-03	-21.81
	0.05	1.50E-02	2.40E-02	60.31	1.51E-02	0.71	1.25E-02	-16.90	1.39E-02	-7.48
	0.1	2.35E-02	2.97E-02	26.19	2.18E-02	-7.20	1.92E-02	-18.34	2.32E-02	-1.20
	0.15	2.62E-02	2.99E-02	13.84	2.37E-02	-9.49	2.16E-02	-17.66	2.66E-02	1.21
	0.2	2.71E-02	2.89E-02	6.44	2.40E-02	-11.32	2.23E-02	-17.65	2.72E-02	0.46
	0.25	2.65E-02	2.75E-02	3.88	2.37E-02	-10.69	2.23E-02	-15.90	2.67E-02	0.87
	0.3	2.51E-02	2.61E-02	3.85	2.29E-02	-8.67	2.18E-02	-13.12	2.57E-02	2.18
	0.35	2.46E-02	2.47E-02	0.43	2.21E-02	-10.16	2.11E-02	-13.89	2.44E-02	-0.63
	0.4	2.29E-02	2.33E-02	1.72	2.11E-02	-7.79	2.04E-02	-11.10	2.31E-02	0.87
	0.45	2.16E-02	2.20E-02	2.24	2.02E-02	-6.33	1.96E-02	-9.27	2.19E-02	1.43
0.5	2.07E-02	2.08E-02	0.54	1.93E-02	-7.10	1.87E-02	-9.68	2.07E-02	-0.28	
4	0.01	2.04E-05	3.63E-05	77.85	2.05E-05	0.38	1.55E-05	-23.96	1.54E-05	-24.71
	0.02	4.55E-04	8.17E-04	79.78	4.65E-04	2.27	3.60E-04	-20.83	3.71E-04	-18.32
	0.05	2.43E-03	3.40E-03	39.86	2.28E-03	-6.15	1.90E-03	-21.77	2.23E-03	-8.39
	0.1	3.72E-03	4.28E-03	14.98	3.32E-03	-10.71	2.96E-03	-20.60	3.64E-03	-2.15
	0.15	3.93E-03	4.25E-03	8.14	3.54E-03	-9.92	3.25E-03	-17.23	3.98E-03	1.16
	0.2	3.89E-03	4.03E-03	3.67	3.50E-03	-10.02	3.28E-03	-15.67	3.92E-03	0.72
	0.25	3.71E-03	3.77E-03	1.56	3.36E-03	-9.45	3.19E-03	-14.01	3.72E-03	0.20
	0.3	3.44E-03	3.50E-03	1.78	3.18E-03	-7.51	3.05E-03	-11.33	3.47E-03	1.04
	0.35	3.27E-03	3.25E-03	-0.83	2.99E-03	-8.60	2.89E-03	-11.76	3.23E-03	-1.32
	0.4	2.99E-03	3.01E-03	0.61	2.81E-03	-6.26	2.72E-03	-9.02	3.00E-03	0.17
	0.45	2.80E-03	2.80E-03	-0.05	2.63E-03	-6.08	2.56E-03	-8.47	2.78E-03	-0.51
0.5	2.54E-03	2.60E-03	2.22	2.46E-03	-3.29	2.41E-03	-5.43	2.59E-03	1.70	

ζ	ξ	ISEE	P	ε [%]	cVM	ε [%]	mVM	ε [%]	#5	ε [%]
4.5	0.01	9.72E-07	1.53E-06	57.66	9.23E-07	-5.05	7.06E-07	-27.35	7.36E-07	-24.26
	0.02	4.25E-05	6.93E-05	62.99	4.21E-05	-1.08	3.29E-05	-22.70	3.58E-05	-15.84
	0.05	2.83E-04	3.72E-04	31.27	2.65E-04	-6.66	2.23E-04	-21.34	2.70E-04	-4.56
	0.1	4.36E-04	4.74E-04	8.72	3.85E-04	-11.56	3.46E-04	-20.51	4.28E-04	-1.76
	0.15	4.41E-04	4.62E-04	4.78	4.00E-04	-9.29	3.71E-04	-15.83	4.46E-04	1.10
	0.2	4.21E-04	4.29E-04	1.80	3.85E-04	-8.70	3.64E-04	-13.67	4.23E-04	0.40
	0.25	3.87E-04	3.92E-04	1.17	3.59E-04	-7.18	3.44E-04	-11.15	3.89E-04	0.55
	0.3	3.53E-04	3.56E-04	0.93	3.32E-04	-5.94	3.20E-04	-9.19	3.55E-04	0.58
	0.35	3.16E-04	3.23E-04	2.24	3.04E-04	-3.62	2.96E-04	-6.36	3.22E-04	1.98
	0.4	2.86E-04	2.93E-04	2.49	2.79E-04	-2.54	2.72E-04	-4.87	2.93E-04	2.23
	0.45	2.61E-04	2.67E-04	2.31	2.56E-04	-2.06	2.50E-04	-4.05	2.66E-04	2.00
0.5	2.42E-04	2.44E-04	0.67	2.35E-04	-3.12	2.30E-04	-4.81	2.43E-04	0.29	
5	0.01	3.12E-08	4.62E-08	47.95	2.94E-08	-5.76	2.28E-08	-27.17	2.47E-08	-20.91
	0.02	3.04E-06	4.50E-06	48.23	2.89E-06	-4.87	2.28E-06	-24.94	2.59E-06	-14.89
	0.05	2.61E-05	3.16E-05	20.93	2.36E-05	-9.71	2.01E-05	-23.10	2.48E-05	-4.97
	0.1	3.83E-05	4.06E-05	5.80	3.43E-05	-10.65	3.11E-05	-18.88	3.80E-05	-0.89
	0.15	3.76E-05	3.87E-05	2.90	3.46E-05	-8.19	3.24E-05	-14.05	3.79E-05	0.79
	0.2	3.52E-05	3.51E-05	-0.34	3.23E-05	-8.34	3.07E-05	-12.65	3.48E-05	-1.11
	0.25	3.10E-05	3.12E-05	0.73	2.93E-05	-5.58	2.82E-05	-8.99	3.11E-05	0.37
	0.3	2.72E-05	2.77E-05	1.78	2.63E-05	-3.37	2.55E-05	-6.13	2.76E-05	1.55
	0.35	2.41E-05	2.45E-05	1.61	2.35E-05	-2.64	2.29E-05	-4.90	2.44E-05	1.40
	0.4	2.17E-05	2.17E-05	0.12	2.10E-05	-3.41	2.06E-05	-5.26	2.17E-05	-0.12
	0.45	1.91E-05	1.93E-05	1.05	1.88E-05	-2.00	1.85E-05	-3.57	1.93E-05	0.73
0.5	1.69E-05	1.73E-05	2.32	1.68E-05	-0.36	1.66E-05	-1.71	1.72E-05	1.90	
		μ_ε %	24.10	μ_ε %	-3.423	μ_ε %	-11.89	μ_ε %	-4.02	
		σ_ε %	41.33	σ_ε %	8.08	σ_ε %	6.81	σ_ε %	8.65	
		ε_{\max} %	187.19	ε_{\max} %	27.68	ε_{\max} %	1.27	ε_{\max} %	3.22	
		ε_{\min} %	-1.90	ε_{\min} %	-11.98	ε_{\min} %	-27.35	ε_{\min} %	-30.99	
		$\mu_{ \varepsilon }$ %	24.25	$\mu_{ \varepsilon }$ %	7.09	$\mu_{ \varepsilon }$ %	11.92	$\mu_{ \varepsilon }$ %	4.97	

D.1.4 Kanai-Tajimi and Unit-step Time-modulating Function, $T = 1.0s$

Table D.4 - Proposed #5: Time-variant FPDF computed at $t = 10.0s$ for linear elastic SDOF system with $T = 1.0s$ subjected to KT base excitation from at-rest initial conditions.

ζ	ξ	ISEE	P	ε [%]	cVM	ε [%]	mVM	ε [%]	#5	ε [%]
1.5	0.01	4.03E-01	8.45E-01	109.56	5.35E-01	32.74	4.38E-01	8.67	3.88E-01	-3.72
	0.02	6.91E-01	9.72E-01	40.68	8.02E-01	15.99	7.11E-01	2.92	6.72E-01	-2.73
	0.05	9.18E-01	9.95E-01	8.37	9.51E-01	3.58	9.13E-01	-0.52	9.23E-01	0.48
	0.1	9.89E-01	9.97E-01	0.81	9.85E-01	-0.48	9.72E-01	-1.76	9.86E-01	-0.37
	0.15	1.00E+00	9.98E-01	-0.20	9.92E-01	-0.77	9.86E-01	-1.36	9.95E-01	-0.46
	0.2	9.93E-01	9.98E-01	0.49	9.95E-01	0.19	9.92E-01	-0.15	9.98E-01	0.46
	0.25	1.00E+00	9.98E-01	-0.16	9.97E-01	-0.34	9.95E-01	-0.55	9.99E-01	-0.12
	0.3	1.00E+00	9.98E-01	-0.16	9.97E-01	-0.26	9.96E-01	-0.40	9.99E-01	-0.08
	0.35	9.94E-01	9.98E-01	0.50	9.98E-01	0.44	9.97E-01	0.34	9.99E-01	0.59
	0.4	1.00E+00	9.99E-01	-0.15	9.98E-01	-0.17	9.97E-01	-0.26	9.99E-01	-0.05
	0.45	1.00E+00	9.99E-01	-0.15	9.98E-01	-0.15	9.98E-01	-0.22	1.00E+00	-0.05
0.5	1.00E+00	9.99E-01	-0.15	9.99E-01	-0.14	9.98E-01	-0.19	1.00E+00	-0.05	
2	0.01	1.22E-01	3.40E-01	179.36	1.65E-01	35.31	1.27E-01	4.52	1.06E-01	-12.57
	0.02	3.15E-01	6.82E-01	116.81	4.05E-01	28.62	3.30E-01	4.94	2.93E-01	-6.78
	0.05	6.24E-01	8.70E-01	39.44	6.75E-01	8.22	6.02E-01	-3.47	6.03E-01	-3.24
	0.1	7.91E-01	9.09E-01	14.91	7.96E-01	0.66	7.48E-01	-5.37	7.93E-01	0.20
	0.15	8.62E-01	9.19E-01	6.62	8.42E-01	-2.32	8.09E-01	-6.21	8.63E-01	0.11
	0.2	8.98E-01	9.24E-01	2.95	8.67E-01	-3.45	8.42E-01	-6.26	8.97E-01	-0.06
	0.25	9.26E-01	9.27E-01	0.16	8.82E-01	-4.70	8.62E-01	-6.86	9.16E-01	-1.05
	0.3	9.22E-01	9.29E-01	0.71	8.92E-01	-3.25	8.76E-01	-5.02	9.26E-01	0.47
	0.35	9.37E-01	9.30E-01	-0.81	8.99E-01	-4.05	8.85E-01	-5.52	9.32E-01	-0.51
	0.4	9.12E-01	9.30E-01	1.97	9.04E-01	-0.85	8.93E-01	-2.14	9.36E-01	2.58
	0.45	9.31E-01	9.30E-01	-0.03	9.08E-01	-2.40	8.98E-01	-3.52	9.37E-01	0.72
0.5	9.28E-01	9.30E-01	0.20	9.11E-01	-1.86	9.02E-01	-2.85	9.38E-01	1.08	
2.5	0.01	2.45E-02	6.45E-02	163.20	3.13E-02	27.63	2.39E-02	-2.44	2.04E-02	-16.66
	0.02	9.72E-02	2.45E-01	152.43	1.28E-01	31.40	1.01E-01	3.80	9.00E-02	-7.43
	0.05	2.58E-01	4.58E-01	77.19	2.98E-01	15.54	2.55E-01	-1.39	2.58E-01	-0.22
	0.1	3.98E-01	5.27E-01	32.34	4.02E-01	0.84	3.64E-01	-8.77	4.01E-01	0.57
	0.15	4.64E-01	5.49E-01	18.24	4.49E-01	-3.30	4.17E-01	-10.05	4.73E-01	1.88
	0.2	5.09E-01	5.59E-01	9.83	4.76E-01	-6.41	4.50E-01	-11.51	5.14E-01	1.06
	0.25	5.36E-01	5.64E-01	5.21	4.94E-01	-7.88	4.72E-01	-11.96	5.39E-01	0.51
	0.3	5.54E-01	5.68E-01	2.52	5.07E-01	-8.49	4.88E-01	-11.89	5.54E-01	0.07
	0.35	5.68E-01	5.69E-01	0.28	5.16E-01	-9.20	4.99E-01	-12.09	5.63E-01	-0.94
	0.4	5.72E-01	5.70E-01	-0.33	5.22E-01	-8.74	5.08E-01	-11.28	5.67E-01	-0.92
	0.45	5.64E-01	5.70E-01	1.21	5.27E-01	-6.52	5.14E-01	-8.82	5.69E-01	0.91
0.5	5.73E-01	5.70E-01	-0.55	5.30E-01	-7.49	5.19E-01	-9.53	5.69E-01	-0.65	

ζ	ξ	ISEE	P	ε [%]	cVM	ε [%]	mVM	ε [%]	#5	ε [%]
3	0.01	3.45E-03	7.69E-03	122.87	4.04E-03	17.15	3.10E-03	-9.96	2.81E-03	-18.46
	0.02	2.27E-02	5.18E-02	128.11	2.78E-02	22.29	2.19E-02	-3.72	2.05E-02	-9.85
	0.05	7.91E-02	1.34E-01	69.19	8.58E-02	8.50	7.25E-02	-8.31	7.61E-02	-3.72
	0.1	1.29E-01	1.67E-01	29.51	1.25E-01	-3.31	1.12E-01	-13.29	1.28E-01	-1.25
	0.15	1.51E-01	1.78E-01	18.04	1.43E-01	-5.18	1.32E-01	-12.40	1.54E-01	2.13
	0.2	1.67E-01	1.83E-01	9.39	1.53E-01	-8.23	1.44E-01	-13.70	1.69E-01	0.96
	0.25	1.76E-01	1.86E-01	5.43	1.60E-01	-8.97	1.52E-01	-13.38	1.77E-01	0.75
	0.3	1.83E-01	1.87E-01	2.24	1.65E-01	-9.89	1.58E-01	-13.53	1.82E-01	-0.46
	0.35	1.84E-01	1.88E-01	1.89	1.68E-01	-8.82	1.62E-01	-11.96	1.85E-01	0.14
	0.4	1.86E-01	1.88E-01	1.06	1.70E-01	-8.48	1.65E-01	-11.21	1.86E-01	-0.24
	0.45	1.89E-01	1.88E-01	-0.63	1.72E-01	-9.16	1.67E-01	-11.54	1.86E-01	-1.74
0.5	1.84E-01	1.87E-01	2.00	1.73E-01	-6.05	1.69E-01	-8.24	1.85E-01	0.93	
3.5	0.01	3.35E-04	6.42E-04	91.53	3.66E-04	9.31	2.84E-04	-15.22	2.75E-04	-18.06
	0.02	3.91E-03	7.71E-03	97.18	4.44E-03	13.50	3.52E-03	-10.04	3.50E-03	-10.44
	0.05	1.71E-02	2.60E-02	52.24	1.76E-02	2.85	1.49E-02	-12.58	1.64E-02	-3.87
	0.1	2.79E-02	3.43E-02	23.01	2.67E-02	-4.34	2.41E-02	-13.70	2.81E-02	0.64
	0.15	3.32E-02	3.69E-02	11.07	3.07E-02	-7.64	2.85E-02	-14.18	3.35E-02	0.75
	0.2	3.58E-02	3.81E-02	6.44	3.29E-02	-7.97	3.11E-02	-12.97	3.62E-02	1.25
	0.25	3.75E-02	3.87E-02	3.28	3.43E-02	-8.39	3.28E-02	-12.37	3.76E-02	0.51
	0.3	3.77E-02	3.90E-02	3.43	3.52E-02	-6.60	3.39E-02	-9.94	3.83E-02	1.76
	0.35	3.89E-02	3.91E-02	0.54	3.58E-02	-8.00	3.47E-02	-10.76	3.87E-02	-0.60
	0.4	3.81E-02	3.91E-02	2.71	3.61E-02	-5.06	3.52E-02	-7.50	3.87E-02	1.73
	0.45	3.83E-02	3.90E-02	1.76	3.63E-02	-5.19	3.55E-02	-7.31	3.86E-02	0.82
0.5	3.85E-02	3.88E-02	0.81	3.64E-02	-5.47	3.57E-02	-7.33	3.85E-02	-0.14	
4	0.01	2.25E-05	3.84E-05	70.21	2.35E-05	4.29	1.84E-05	-18.29	1.88E-05	-16.49
	0.02	5.02E-04	8.65E-04	72.39	5.34E-04	6.38	4.27E-04	-14.91	4.50E-04	-10.43
	0.05	2.74E-03	3.77E-03	37.59	2.70E-03	-1.27	2.32E-03	-15.23	2.66E-03	-2.99
	0.1	4.48E-03	5.18E-03	15.61	4.22E-03	-5.67	3.85E-03	-14.06	4.54E-03	1.42
	0.15	5.23E-03	5.61E-03	7.31	4.86E-03	-7.12	4.55E-03	-12.92	5.31E-03	1.51
	0.2	5.51E-03	5.80E-03	5.16	5.19E-03	-5.89	4.94E-03	-10.30	5.65E-03	2.49
	0.25	5.66E-03	5.88E-03	3.88	5.38E-03	-5.03	5.18E-03	-8.52	5.80E-03	2.52
	0.3	5.82E-03	5.92E-03	1.59	5.49E-03	-5.74	5.33E-03	-8.54	5.87E-03	0.79
	0.35	5.89E-03	5.92E-03	0.60	5.56E-03	-5.66	5.42E-03	-7.98	5.89E-03	0.01
	0.4	5.81E-03	5.91E-03	1.68	5.59E-03	-3.87	5.47E-03	-5.86	5.88E-03	1.14
	0.45	5.81E-03	5.89E-03	1.31	5.60E-03	-3.62	5.50E-03	-5.33	5.85E-03	0.73
0.5	5.81E-03	5.85E-03	0.66	5.59E-03	-3.76	5.50E-03	-5.24	5.81E-03	0.04	

ζ	ξ	ISEE	P	ε [%]	cVM	ε [%]	mVM	ε [%]	#5	ε [%]
4.5	0.01	1.06E-06	1.64E-06	54.96	1.07E-06	0.87	8.45E-07	-20.14	9.01E-07	-14.85
	0.02	4.67E-05	7.44E-05	59.24	4.87E-05	4.37	3.94E-05	-15.69	4.33E-05	-7.34
	0.05	3.31E-04	4.22E-04	27.76	3.19E-04	-3.37	2.77E-04	-16.15	3.26E-04	-1.43
	0.1	5.49E-04	6.01E-04	9.43	5.11E-04	-7.00	4.70E-04	-14.44	5.54E-04	0.89
	0.15	6.44E-04	6.55E-04	1.78	5.86E-04	-8.95	5.54E-04	-13.91	6.36E-04	-1.22
	0.2	6.69E-04	6.77E-04	1.22	6.23E-04	-6.87	5.98E-04	-10.57	6.69E-04	-0.05
	0.25	6.85E-04	6.86E-04	0.10	6.42E-04	-6.27	6.23E-04	-9.13	6.82E-04	-0.53
	0.3	6.92E-04	6.89E-04	-0.50	6.52E-04	-5.72	6.37E-04	-8.00	6.86E-04	-0.89
	0.35	6.82E-04	6.88E-04	0.76	6.57E-04	-3.71	6.44E-04	-5.60	6.85E-04	0.44
	0.4	6.82E-04	6.84E-04	0.41	6.58E-04	-3.44	6.47E-04	-5.02	6.82E-04	0.09
	0.45	6.83E-04	6.80E-04	-0.43	6.57E-04	-3.79	6.48E-04	-5.12	6.77E-04	-0.80
0.5	6.76E-04	6.73E-04	-0.45	6.53E-04	-3.44	6.45E-04	-4.59	6.70E-04	-0.89	
5	0.01	3.53E-08	5.02E-08	42.00	3.44E-08	-2.66	2.75E-08	-22.13	3.03E-08	-14.22
	0.02	3.43E-06	4.90E-06	42.96	3.38E-06	-1.34	2.76E-06	-19.53	3.13E-06	-8.70
	0.05	3.04E-05	3.69E-05	21.41	2.91E-05	-4.07	2.55E-05	-15.89	3.04E-05	0.09
	0.1	5.16E-05	5.43E-05	5.22	4.77E-05	-7.64	4.43E-05	-14.24	5.16E-05	-0.07
	0.15	5.77E-05	5.95E-05	3.10	5.46E-05	-5.40	5.20E-05	-9.85	5.84E-05	1.34
	0.2	6.09E-05	6.14E-05	0.82	5.77E-05	-5.28	5.58E-05	-8.46	6.10E-05	0.10
	0.25	6.21E-05	6.21E-05	-0.01	5.92E-05	-4.71	5.77E-05	-7.10	6.19E-05	-0.38
	0.3	6.04E-05	6.21E-05	2.83	5.98E-05	-1.07	5.86E-05	-3.00	6.20E-05	2.56
	0.35	6.23E-05	6.19E-05	-0.73	5.99E-05	-3.86	5.90E-05	-5.36	6.17E-05	-0.97
	0.4	6.14E-05	6.14E-05	0.03	5.97E-05	-2.65	5.90E-05	-3.90	6.12E-05	-0.25
	0.45	6.01E-05	6.08E-05	1.08	5.93E-05	-1.27	5.87E-05	-2.32	6.05E-05	0.72
0.5	6.07E-05	6.00E-05	-1.19	5.88E-05	-3.21	5.83E-05	-4.08	5.98E-05	-1.62	
		μ_ε %	22.46	μ_ε %	-0.652	μ_ε %	-7.95	μ_ε %	-1.78	
		σ_ε %	40.08	σ_ε %	9.67	σ_ε %	5.92	σ_ε %	4.80	
		ε_{\max} %	179.36	ε_{\max} %	35.31	ε_{\max} %	8.67	ε_{\max} %	2.58	
		ε_{\min} %	-1.19	ε_{\min} %	-9.89	ε_{\min} %	-22.13	ε_{\min} %	-18.46	
		$\mu_{ \varepsilon }$ %	22.60	$\mu_{ \varepsilon }$ %	6.71	$\mu_{ \varepsilon }$ %	8.48	$\mu_{ \varepsilon }$ %	2.63	

D.1.5 Kanai-Tajimi and Shinozuka-Sato Time-modulating Function, $T = 0.1s$

Table D.5 - Proposed #5: Time-variant FFPF computed at $t = 20s$ for linear elastic SDOF system with $T = 0.1s$ subjected to KT base excitation time modulated by a Shinozuka-Sato function.

ζ	ξ	ISEE	P	ε [%]	cVM	ε [%]	mVM	ε [%]	#5	ε [%]
1.5	0.01	9.88E-01	1.00E+00	1.22	1.00E+00	1.22	1.00E+00	1.22	1.00E+00	1.19
	0.02	9.97E-01	1.00E+00	0.31	1.00E+00	0.31	1.00E+00	0.31	1.00E+00	0.31
	0.05	9.98E-01	1.00E+00	0.24	1.00E+00	0.24	1.00E+00	0.24	1.00E+00	0.24
	0.1	1.00E+00	1.00E+00	0.00	1.00E+00	0.00	1.00E+00	0.00	1.00E+00	0.00
	0.15	1.00E+00	1.00E+00	0.00	1.00E+00	0.00	1.00E+00	0.00	1.00E+00	0.00
	0.2	1.00E+00	1.00E+00	0.00	1.00E+00	0.00	1.00E+00	0.00	1.00E+00	0.00
	0.25	1.00E+00	1.00E+00	0.00	1.00E+00	0.00	1.00E+00	0.00	1.00E+00	0.00
	0.3	9.98E-01	1.00E+00	0.24	1.00E+00	0.24	1.00E+00	0.24	1.00E+00	0.24
	0.35	9.96E-01	1.00E+00	0.39	1.00E+00	0.39	1.00E+00	0.39	1.00E+00	0.39
	0.4	1.00E+00	1.00E+00	0.00	1.00E+00	0.00	1.00E+00	0.00	1.00E+00	0.00
	0.45	1.00E+00	1.00E+00	0.00	1.00E+00	0.00	1.00E+00	0.00	1.00E+00	0.00
0.5	9.98E-01	1.00E+00	0.24	1.00E+00	0.24	1.00E+00	0.24	1.00E+00	0.24	
2	0.01	8.74E-01	1.00E+00	14.45	9.93E-01	13.67	9.73E-01	11.35	9.37E-01	7.22
	0.02	9.75E-01	1.00E+00	2.55	9.98E-01	2.31	9.91E-01	1.65	9.85E-01	1.00
	0.05	9.92E-01	1.00E+00	0.80	9.99E-01	0.75	9.98E-01	0.62	9.99E-01	0.66
	0.1	9.90E-01	1.00E+00	1.05	1.00E+00	1.02	9.99E-01	0.97	1.00E+00	1.02
	0.15	9.92E-01	1.00E+00	0.82	1.00E+00	0.79	9.99E-01	0.75	1.00E+00	0.80
	0.2	1.00E+00	1.00E+00	-0.01	1.00E+00	-0.05	9.99E-01	-0.08	1.00E+00	-0.02
	0.25	9.79E-01	1.00E+00	2.18	9.99E-01	2.13	9.99E-01	2.09	1.00E+00	2.17
	0.3	9.88E-01	1.00E+00	1.19	9.99E-01	1.13	9.99E-01	1.09	1.00E+00	1.18
	0.35	9.95E-01	1.00E+00	0.43	9.99E-01	0.37	9.99E-01	0.32	1.00E+00	0.43
	0.4	9.96E-01	1.00E+00	0.41	9.99E-01	0.33	9.99E-01	0.28	1.00E+00	0.41
	0.45	9.91E-01	1.00E+00	0.87	9.99E-01	0.79	9.98E-01	0.73	1.00E+00	0.88
0.5	9.93E-01	1.00E+00	0.64	9.99E-01	0.55	9.98E-01	0.49	1.00E+00	0.65	
2.5	0.01	4.87E-01	9.74E-01	99.93	7.68E-01	57.55	6.57E-01	34.82	5.78E-01	18.61
	0.02	6.84E-01	9.69E-01	41.62	8.28E-01	20.94	7.50E-01	9.65	7.19E-01	5.08
	0.05	8.58E-01	9.61E-01	12.12	8.78E-01	2.40	8.36E-01	-2.52	8.50E-01	-0.85
	0.1	9.17E-01	9.50E-01	3.53	8.89E-01	-3.03	8.62E-01	-5.98	8.93E-01	-2.67
	0.15	9.28E-01	9.38E-01	1.11	8.86E-01	-4.53	8.64E-01	-6.89	9.02E-01	-2.83
	0.2	9.23E-01	9.28E-01	0.52	8.79E-01	-4.77	8.60E-01	-6.86	9.04E-01	-2.12
	0.25	9.22E-01	9.18E-01	-0.48	8.71E-01	-5.54	8.53E-01	-7.47	9.03E-01	-2.15
	0.3	9.04E-01	9.09E-01	0.53	8.63E-01	-4.49	8.47E-01	-6.35	8.99E-01	-0.51
	0.35	9.10E-01	9.00E-01	-1.07	8.55E-01	-5.96	8.39E-01	-7.72	8.94E-01	-1.68
	0.4	8.89E-01	8.92E-01	0.32	8.48E-01	-4.60	8.32E-01	-6.34	8.88E-01	-0.06
	0.45	8.70E-01	8.84E-01	1.55	8.41E-01	-3.41	8.26E-01	-5.14	8.82E-01	1.29
0.5	8.83E-01	8.76E-01	-0.70	8.34E-01	-5.53	8.19E-01	-7.19	8.75E-01	-0.86	

ζ	ξ	ISEE	P	ε [%]	cVM	ε [%]	mVM	ε [%]	#5	ε [%]
3	0.01	1.67E-01	5.46E-01	226.13	2.94E-01	75.81	2.28E-01	36.07	2.02E-01	20.57
	0.02	2.60E-01	5.28E-01	102.78	3.39E-01	30.27	2.82E-01	8.32	2.74E-01	5.34
	0.05	3.86E-01	5.04E-01	30.35	3.85E-01	-0.50	3.45E-01	-10.85	3.66E-01	-5.36
	0.1	4.45E-01	4.74E-01	6.51	3.94E-01	-11.59	3.66E-01	-17.74	4.03E-01	-9.44
	0.15	4.26E-01	4.51E-01	5.96	3.87E-01	-9.06	3.66E-01	-14.11	4.09E-01	-3.93
	0.2	4.24E-01	4.32E-01	1.94	3.78E-01	-10.93	3.60E-01	-15.18	4.07E-01	-4.07
	0.25	4.18E-01	4.16E-01	-0.43	3.68E-01	-12.01	3.52E-01	-15.78	4.01E-01	-4.03
	0.3	3.93E-01	4.03E-01	2.50	3.59E-01	-8.70	3.45E-01	-12.30	3.94E-01	0.20
	0.35	3.90E-01	3.91E-01	0.23	3.50E-01	-10.20	3.37E-01	-13.51	3.85E-01	-1.25
	0.4	3.86E-01	3.80E-01	-1.58	3.42E-01	-11.41	3.30E-01	-14.50	3.76E-01	-2.66
	0.45	3.68E-01	3.71E-01	0.84	3.35E-01	-8.89	3.24E-01	-11.92	3.67E-01	-0.12
0.5	3.59E-01	3.63E-01	1.01	3.29E-01	-8.45	3.18E-01	-11.37	3.59E-01	0.12	
3.5	0.01	3.97E-02	1.26E-01	217.81	6.36E-02	60.10	4.81E-02	21.11	4.55E-02	14.53
	0.02	6.12E-02	1.20E-01	96.96	7.42E-02	21.35	6.05E-02	-0.99	6.20E-02	1.45
	0.05	9.00E-02	1.13E-01	25.56	8.49E-02	-5.66	7.52E-02	-16.44	8.31E-02	-7.70
	0.1	9.83E-02	1.04E-01	6.03	8.63E-02	-12.20	7.99E-02	-18.79	9.05E-02	-7.93
	0.15	9.67E-02	9.76E-02	0.95	8.40E-02	-13.13	7.91E-02	-18.21	9.03E-02	-6.58
	0.2	9.18E-02	9.24E-02	0.66	8.11E-02	-11.56	7.71E-02	-15.93	8.84E-02	-3.69
	0.25	8.63E-02	8.80E-02	2.02	7.84E-02	-9.18	7.50E-02	-13.14	8.59E-02	-0.51
	0.3	8.20E-02	8.44E-02	2.92	7.58E-02	-7.55	7.28E-02	-11.21	8.32E-02	1.36
	0.35	8.02E-02	8.13E-02	1.47	7.36E-02	-8.24	7.09E-02	-11.60	8.05E-02	0.42
	0.4	7.89E-02	7.87E-02	-0.34	7.15E-02	-9.40	6.91E-02	-12.51	7.80E-02	-1.19
	0.45	7.84E-02	7.63E-02	-2.72	6.96E-02	-11.19	6.74E-02	-14.06	7.57E-02	-3.51
0.5	7.34E-02	7.42E-02	1.05	6.80E-02	-7.42	6.59E-02	-10.27	7.36E-02	0.20	
4	0.01	6.87E-03	1.81E-02	163.96	9.66E-03	40.61	7.34E-03	6.85	7.41E-03	7.90
	0.02	1.03E-02	1.72E-02	67.23	1.12E-02	8.45	9.18E-03	-10.99	9.88E-03	-4.20
	0.05	1.40E-02	1.61E-02	15.02	1.26E-02	-9.87	1.13E-02	-19.60	1.28E-02	-8.88
	0.1	1.44E-02	1.48E-02	3.12	1.27E-02	-11.61	1.18E-02	-17.67	1.35E-02	-6.02
	0.15	1.37E-02	1.38E-02	1.17	1.23E-02	-10.22	1.16E-02	-14.91	1.32E-02	-3.29
	0.2	1.29E-02	1.30E-02	1.50	1.18E-02	-8.27	1.13E-02	-12.25	1.27E-02	-0.84
	0.25	1.24E-02	1.24E-02	-0.19	1.13E-02	-8.76	1.09E-02	-12.21	1.23E-02	-1.42
	0.3	1.18E-02	1.19E-02	0.41	1.09E-02	-7.49	1.06E-02	-10.63	1.18E-02	-0.33
	0.35	1.16E-02	1.14E-02	-1.13	1.06E-02	-8.38	1.03E-02	-11.24	1.14E-02	-1.66
	0.4	1.11E-02	1.10E-02	-0.66	1.03E-02	-7.53	9.98E-03	-10.22	1.10E-02	-1.14
	0.45	1.07E-02	1.07E-02	-0.14	9.99E-03	-6.72	9.72E-03	-9.26	1.06E-02	-0.66
0.5	1.03E-02	1.04E-02	0.52	9.74E-03	-5.81	9.48E-03	-8.24	1.03E-02	-0.06	

ζ	ξ	ISEE	P	ε [%]	cVM	ε [%]	mVM	ε [%]	#5	ε [%]
4.5	0.01	8.78E-04	1.95E-03	122.49	1.12E-03	27.06	8.57E-04	-2.47	9.10E-04	3.64
	0.02	1.24E-03	1.86E-03	50.34	1.28E-03	3.41	1.06E-03	-14.20	1.18E-03	-4.31
	0.05	1.57E-03	1.74E-03	10.31	1.42E-03	-9.72	1.28E-03	-18.64	1.47E-03	-6.64
	0.1	1.56E-03	1.59E-03	2.14	1.41E-03	-9.51	1.33E-03	-14.98	1.51E-03	-3.48
	0.15	1.50E-03	1.49E-03	-0.78	1.36E-03	-9.46	1.30E-03	-13.54	1.45E-03	-3.17
	0.2	1.36E-03	1.40E-03	3.35	1.30E-03	-4.23	1.25E-03	-7.76	1.39E-03	2.16
	0.25	1.33E-03	1.33E-03	0.44	1.25E-03	-6.04	1.21E-03	-9.02	1.33E-03	-0.16
	0.3	1.30E-03	1.28E-03	-1.62	1.20E-03	-7.38	1.17E-03	-10.00	1.27E-03	-1.99
	0.35	1.24E-03	1.23E-03	-0.75	1.16E-03	-6.13	1.13E-03	-8.54	1.22E-03	-1.04
	0.4	1.18E-03	1.19E-03	0.19	1.13E-03	-4.89	1.10E-03	-7.15	1.18E-03	-0.10
	0.45	1.14E-03	1.15E-03	0.58	1.09E-03	-4.25	1.07E-03	-6.37	1.14E-03	0.21
0.5	1.11E-03	1.12E-03	0.68	1.07E-03	-3.92	1.04E-03	-5.93	1.11E-03	0.22	
5	0.01	8.64E-05	1.65E-04	90.50	1.00E-04	15.83	7.76E-05	-10.13	8.58E-05	-0.66
	0.02	1.17E-04	1.56E-04	33.84	1.13E-04	-3.08	9.50E-05	-18.69	1.09E-04	-7.10
	0.05	1.37E-04	1.46E-04	6.93	1.24E-04	-9.26	1.13E-04	-17.42	1.30E-04	-5.09
	0.1	1.32E-04	1.34E-04	1.68	1.22E-04	-7.52	1.16E-04	-12.41	1.30E-04	-1.83
	0.15	1.23E-04	1.25E-04	1.70	1.17E-04	-5.16	1.12E-04	-8.80	1.23E-04	0.29
	0.2	1.18E-04	1.18E-04	0.44	1.12E-04	-5.13	1.08E-04	-8.07	1.17E-04	-0.21
	0.25	1.13E-04	1.12E-04	-0.29	1.07E-04	-5.09	1.04E-04	-7.59	1.12E-04	-0.65
	0.3	1.07E-04	1.08E-04	0.17	1.03E-04	-4.16	1.01E-04	-6.38	1.07E-04	-0.08
	0.35	1.03E-04	1.03E-04	0.78	9.93E-05	-3.22	9.73E-05	-5.24	1.03E-04	0.54
	0.4	9.94E-05	9.99E-05	0.52	9.62E-05	-3.19	9.43E-05	-5.05	9.96E-05	0.24
	0.45	9.74E-05	9.67E-05	-0.69	9.34E-05	-4.14	9.17E-05	-5.85	9.64E-05	-1.08
0.5	9.48E-05	9.40E-05	-0.92	9.09E-05	-4.17	8.94E-05	-5.78	9.35E-05	-1.44	
		μ_ε %	15.50	μ_ε %	-0.450	μ_ε %	-5.94	μ_ε %	-0.42	
		σ_ε %	42.05	σ_ε %	14.87	σ_ε %	9.66	σ_ε %	4.46	
		ε_{\max} %	226.13	ε_{\max} %	75.81	ε_{\max} %	36.07	ε_{\max} %	20.57	
		ε_{\min} %	-2.72	ε_{\min} %	-13.13	ε_{\min} %	-19.60	ε_{\min} %	-9.44	
		$\mu_{ \varepsilon }$ %	15.81	$\mu_{ \varepsilon }$ %	8.58	$\mu_{ \varepsilon }$ %	8.85	$\mu_{ \varepsilon }$ %	2.57	

D.1.6 Kanai-Tajimi and Shinozuka-Sato Time-modulating Function, $T = 0.5s$

Table D.6 - Proposed #5: Time-variant FFPF computed at $t = 20s$ for linear elastic SDOF system with $T = 0.5s$ subjected to KT base excitation time modulated by a Shinozuka-Sato function.

ζ	ξ	ISEE	P	ε [%]	cVM	ε [%]	mVM	ε [%]	#5	ε [%]
1.5	0.01	8.23E-01	1.00E+00	21.55	9.38E-01	14.02	8.36E-01	1.68	7.02E-01	-14.69
	0.02	8.78E-01	1.00E+00	13.83	9.58E-01	9.04	8.92E-01	1.52	8.28E-01	-5.71
	0.05	9.62E-01	1.00E+00	3.96	9.83E-01	2.19	9.57E-01	-0.49	9.61E-01	-0.06
	0.1	9.77E-01	1.00E+00	2.32	9.94E-01	1.70	9.85E-01	0.82	9.94E-01	1.75
	0.15	1.00E+00	1.00E+00	-0.03	9.97E-01	-0.33	9.93E-01	-0.72	9.98E-01	-0.16
	0.2	1.00E+00	1.00E+00	-0.03	9.98E-01	-0.20	9.96E-01	-0.42	9.99E-01	-0.06
	0.25	1.00E+00	1.00E+00	-0.02	9.99E-01	-0.14	9.97E-01	-0.28	1.00E+00	-0.03
	0.3	9.80E-01	1.00E+00	2.02	9.99E-01	1.93	9.98E-01	1.84	1.00E+00	2.02
	0.35	1.00E+00	1.00E+00	-0.03	9.99E-01	-0.09	9.98E-01	-0.16	1.00E+00	-0.02
	0.4	1.00E+00	1.00E+00	-0.03	9.99E-01	-0.07	9.99E-01	-0.13	1.00E+00	-0.01
	0.45	9.90E-01	1.00E+00	1.03	9.99E-01	0.99	9.99E-01	0.95	1.00E+00	1.04
0.5	1.00E+00	1.00E+00	-0.03	9.99E-01	-0.06	9.99E-01	-0.09	1.00E+00	-0.01	
2	0.01	4.56E-01	9.80E-01	114.93	6.23E-01	36.55	4.73E-01	3.74	3.41E-01	-25.19
	0.02	5.23E-01	9.60E-01	83.38	6.64E-01	26.86	5.39E-01	3.04	4.49E-01	-14.29
	0.05	6.80E-01	9.40E-01	38.16	7.44E-01	9.35	6.57E-01	-3.37	6.53E-01	-4.05
	0.1	8.12E-01	9.36E-01	15.23	8.11E-01	-0.14	7.55E-01	-7.08	8.06E-01	-0.82
	0.15	8.65E-01	9.36E-01	8.12	8.44E-01	-2.42	8.03E-01	-7.15	8.69E-01	0.41
	0.2	8.86E-01	9.36E-01	5.61	8.64E-01	-2.48	8.32E-01	-6.06	9.01E-01	1.66
	0.25	9.15E-01	9.35E-01	2.20	8.77E-01	-4.23	8.51E-01	-7.03	9.18E-01	0.30
	0.3	9.11E-01	9.35E-01	2.69	8.85E-01	-2.78	8.64E-01	-5.14	9.28E-01	1.88
	0.35	9.39E-01	9.35E-01	-0.43	8.92E-01	-5.02	8.73E-01	-6.98	9.33E-01	-0.60
	0.4	9.24E-01	9.34E-01	1.08	8.96E-01	-3.03	8.80E-01	-4.77	9.36E-01	1.24
	0.45	9.35E-01	9.33E-01	-0.15	9.00E-01	-3.76	8.85E-01	-5.29	9.37E-01	0.20
0.5	9.45E-01	9.33E-01	-1.36	9.02E-01	-4.58	8.89E-01	-5.94	9.37E-01	-0.88	
2.5	0.01	1.74E-01	6.51E-01	274.06	2.53E-01	45.35	1.76E-01	1.12	1.25E-01	-28.02
	0.02	2.05E-01	5.79E-01	182.36	2.75E-01	34.17	2.06E-01	0.72	1.70E-01	-17.30
	0.05	2.95E-01	5.30E-01	79.98	3.25E-01	10.24	2.69E-01	-8.77	2.70E-01	-8.43
	0.1	3.85E-01	5.22E-01	35.79	3.76E-01	-2.18	3.32E-01	-13.64	3.74E-01	-2.71
	0.15	4.33E-01	5.22E-01	20.33	4.06E-01	-6.36	3.70E-01	-14.70	4.34E-01	0.04
	0.2	4.71E-01	5.21E-01	10.60	4.25E-01	-9.85	3.95E-01	-16.31	4.70E-01	-0.36
	0.25	4.85E-01	5.21E-01	7.43	4.38E-01	-9.66	4.12E-01	-15.06	4.92E-01	1.36
	0.3	4.97E-01	5.21E-01	4.72	4.48E-01	-9.94	4.25E-01	-14.54	5.04E-01	1.45
	0.35	5.05E-01	5.20E-01	2.86	4.55E-01	-10.02	4.34E-01	-14.03	5.11E-01	1.11
	0.4	5.19E-01	5.19E-01	-0.10	4.60E-01	-11.42	4.42E-01	-14.91	5.14E-01	-1.06
	0.45	5.13E-01	5.17E-01	0.79	4.64E-01	-9.66	4.47E-01	-12.85	5.14E-01	0.18
0.5	5.13E-01	5.16E-01	0.54	4.66E-01	-9.08	4.51E-01	-11.98	5.14E-01	0.17	

ζ	ξ	ISEE	P	ε [%]	cVM	ε [%]	mVM	ε [%]	#5	ε [%]
3	0.01	4.83E-02	2.03E-01	319.65	6.84E-02	41.54	4.64E-02	-4.05	3.56E-02	-26.27
	0.02	5.97E-02	1.70E-01	184.66	7.42E-02	24.31	5.45E-02	-8.63	4.77E-02	-20.12
	0.05	8.21E-02	1.50E-01	82.93	8.82E-02	7.39	7.18E-02	-12.50	7.56E-02	-7.88
	0.1	1.09E-01	1.47E-01	35.21	1.03E-01	-5.02	9.01E-02	-17.09	1.06E-01	-2.65
	0.15	1.24E-01	1.47E-01	18.05	1.12E-01	-9.78	1.01E-01	-18.51	1.23E-01	-0.83
	0.2	1.34E-01	1.47E-01	9.33	1.18E-01	-12.13	1.09E-01	-18.96	1.33E-01	-0.53
	0.25	1.34E-01	1.47E-01	9.23	1.22E-01	-9.19	1.14E-01	-15.06	1.39E-01	3.72
	0.3	1.40E-01	1.46E-01	4.72	1.25E-01	-10.81	1.18E-01	-15.71	1.42E-01	1.69
	0.35	1.44E-01	1.46E-01	1.61	1.27E-01	-11.85	1.21E-01	-16.05	1.43E-01	-0.22
	0.4	1.43E-01	1.46E-01	1.68	1.28E-01	-10.51	1.23E-01	-14.26	1.44E-01	0.35
	0.45	1.43E-01	1.45E-01	1.67	1.29E-01	-9.48	1.24E-01	-12.86	1.43E-01	0.53
0.5	1.45E-01	1.45E-01	-0.47	1.30E-01	-10.54	1.26E-01	-13.55	1.43E-01	-1.50	
3.5	0.01	1.03E-02	3.81E-02	268.59	1.35E-02	30.76	9.16E-03	-11.34	7.79E-03	-24.56
	0.02	1.22E-02	3.14E-02	158.35	1.45E-02	19.40	1.07E-02	-11.99	1.02E-02	-16.14
	0.05	1.71E-02	2.75E-02	60.33	1.70E-02	-0.67	1.39E-02	-18.61	1.56E-02	-9.07
	0.1	2.15E-02	2.68E-02	25.09	1.97E-02	-7.98	1.73E-02	-19.15	2.10E-02	-1.99
	0.15	2.36E-02	2.68E-02	13.33	2.13E-02	-9.81	1.94E-02	-18.00	2.39E-02	0.87
	0.2	2.50E-02	2.68E-02	7.12	2.23E-02	-10.73	2.07E-02	-17.13	2.53E-02	1.15
	0.25	2.61E-02	2.68E-02	2.70	2.30E-02	-11.78	2.16E-02	-16.96	2.60E-02	-0.28
	0.3	2.62E-02	2.67E-02	2.10	2.35E-02	-10.37	2.23E-02	-14.80	2.63E-02	0.43
	0.35	2.62E-02	2.67E-02	1.68	2.38E-02	-9.30	2.28E-02	-13.13	2.64E-02	0.58
	0.4	2.63E-02	2.66E-02	1.18	2.40E-02	-8.61	2.31E-02	-11.97	2.63E-02	0.29
	0.45	2.63E-02	2.65E-02	0.69	2.42E-02	-8.15	2.34E-02	-11.13	2.63E-02	-0.16
0.5	2.59E-02	2.64E-02	1.65	2.42E-02	-6.52	2.35E-02	-9.21	2.61E-02	0.77	
4	0.01	1.68E-03	5.25E-03	212.60	2.04E-03	21.30	1.39E-03	-17.13	1.30E-03	-22.57
	0.02	1.95E-03	4.32E-03	121.48	2.16E-03	11.05	1.61E-03	-17.36	1.66E-03	-14.72
	0.05	2.58E-03	3.77E-03	46.12	2.50E-03	-3.21	2.07E-03	-19.82	2.43E-03	-5.62
	0.1	3.17E-03	3.68E-03	16.13	2.86E-03	-9.89	2.54E-03	-19.97	3.13E-03	-1.17
	0.15	3.38E-03	3.67E-03	8.72	3.06E-03	-9.49	2.81E-03	-16.88	3.44E-03	1.71
	0.2	3.56E-03	3.67E-03	3.29	3.18E-03	-10.48	2.98E-03	-16.15	3.57E-03	0.32
	0.25	3.57E-03	3.67E-03	2.95	3.27E-03	-8.41	3.10E-03	-13.08	3.62E-03	1.53
	0.3	3.54E-03	3.66E-03	3.45	3.32E-03	-6.28	3.18E-03	-10.23	3.64E-03	2.65
	0.35	3.61E-03	3.66E-03	1.26	3.36E-03	-7.02	3.24E-03	-10.34	3.64E-03	0.72
	0.4	3.66E-03	3.64E-03	-0.33	3.38E-03	-7.54	3.28E-03	-10.38	3.63E-03	-0.81
	0.45	3.64E-03	3.63E-03	-0.15	3.39E-03	-6.63	3.30E-03	-9.12	3.61E-03	-0.67
0.5	3.60E-03	3.61E-03	0.44	3.40E-03	-5.46	3.32E-03	-7.69	3.59E-03	-0.15	

ζ	ξ	ISEE	P	ε [%]	cVM	ε [%]	mVM	ε [%]	#5	ε [%]
4.5	0.01	2.10E-04	5.62E-04	167.43	2.38E-04	13.08	1.64E-04	-22.03	1.65E-04	-21.48
	0.02	2.36E-04	4.62E-04	96.15	2.50E-04	6.08	1.88E-04	-20.22	2.07E-04	-12.29
	0.05	3.06E-04	4.03E-04	31.78	2.84E-04	-7.37	2.38E-04	-22.38	2.90E-04	-5.23
	0.1	3.58E-04	3.94E-04	9.98	3.20E-04	-10.68	2.87E-04	-19.82	3.56E-04	-0.68
	0.15	3.79E-04	3.93E-04	3.78	3.40E-04	-10.30	3.15E-04	-16.83	3.79E-04	0.10
	0.2	3.90E-04	3.93E-04	0.78	3.52E-04	-9.81	3.33E-04	-14.80	3.88E-04	-0.64
	0.25	3.89E-04	3.93E-04	1.03	3.60E-04	-7.57	3.44E-04	-11.61	3.91E-04	0.37
	0.3	3.87E-04	3.92E-04	1.40	3.64E-04	-5.82	3.52E-04	-9.17	3.91E-04	1.02
	0.35	3.92E-04	3.91E-04	-0.20	3.68E-04	-6.28	3.57E-04	-9.06	3.90E-04	-0.49
	0.4	3.87E-04	3.90E-04	0.74	3.69E-04	-4.61	3.60E-04	-7.01	3.89E-04	0.44
	0.45	3.84E-04	3.89E-04	1.19	3.70E-04	-3.57	3.62E-04	-5.66	3.87E-04	0.82
0.5	3.83E-04	3.87E-04	1.03	3.71E-04	-3.22	3.64E-04	-5.05	3.85E-04	0.58	
5	0.01	1.96E-05	4.73E-05	141.54	2.16E-05	10.20	1.50E-05	-23.32	1.61E-05	-17.87
	0.02	2.22E-05	3.89E-05	75.17	2.25E-05	1.17	1.71E-05	-23.10	1.97E-05	-11.27
	0.05	2.75E-05	3.40E-05	23.50	2.51E-05	-8.72	2.13E-05	-22.66	2.65E-05	-3.77
	0.1	3.10E-05	3.32E-05	6.92	2.80E-05	-9.88	2.53E-05	-18.29	3.10E-05	0.09
	0.15	3.26E-05	3.31E-05	1.58	2.95E-05	-9.55	2.76E-05	-15.40	3.24E-05	-0.55
	0.2	3.24E-05	3.31E-05	2.19	3.04E-05	-6.25	2.89E-05	-10.75	3.28E-05	1.36
	0.25	3.32E-05	3.31E-05	-0.46	3.09E-05	-6.97	2.98E-05	-10.43	3.30E-05	-0.86
	0.3	3.25E-05	3.30E-05	1.54	3.13E-05	-3.91	3.03E-05	-6.77	3.29E-05	1.27
	0.35	3.27E-05	3.29E-05	0.65	3.15E-05	-3.90	3.07E-05	-6.25	3.29E-05	0.41
	0.4	3.29E-05	3.28E-05	-0.10	3.16E-05	-3.98	3.09E-05	-5.94	3.28E-05	-0.39
	0.45	3.17E-05	3.27E-05	3.11	3.16E-05	-0.38	3.11E-05	-2.12	3.26E-05	2.71
0.5	3.21E-05	3.26E-05	1.59	3.16E-05	-1.46	3.11E-05	-2.93	3.24E-05	1.08	
		μ_ε %	32.63	μ_ε %	-1.049	μ_ε %	-10.45	μ_ε %	-3.29	
		σ_ε %	65.77	σ_ε %	12.29	σ_ε %	7.09	σ_ε %	7.46	
		ε_{\max} %	319.65	ε_{\max} %	45.35	ε_{\max} %	3.74	ε_{\max} %	3.72	
		ε_{\min} %	-1.36	ε_{\min} %	-12.13	ε_{\min} %	-23.32	ε_{\min} %	-28.02	
		$\mu_{ \varepsilon }$ %	32.71	$\mu_{ \varepsilon }$ %	8.94	$\mu_{ \varepsilon }$ %	10.77	$\mu_{ \varepsilon }$ %	4.17	

D.1.7 Kanai-Tajimi and Shinozuka-Sato Time-modulating Function, $T=1.0s$

Table D.7 - Proposed #5: Time-variant FFPF computed at $t = 20s$ for linear elastic SDOF system with $T = 1.0s$ subjected to KT base excitation time modulated by a Shinozuka-Sato function.

ζ	ξ	ISEE	P	ε [%]	cVM	ε [%]	mVM	ε [%]	#5	ε [%]
1.5	0.01	7.62E-01	9.99E-01	31.20	8.54E-01	12.07	7.27E-01	-4.51	6.11E-01	-19.73
	0.02	7.81E-01	9.97E-01	27.65	8.80E-01	12.60	7.84E-01	0.38	7.22E-01	-7.60
	0.05	8.81E-01	9.90E-01	12.41	9.13E-01	3.69	8.58E-01	-2.59	8.69E-01	-1.32
	0.1	9.40E-01	9.86E-01	4.88	9.43E-01	0.29	9.13E-01	-2.87	9.46E-01	0.59
	0.15	9.60E-01	9.85E-01	2.57	9.58E-01	-0.25	9.39E-01	-2.19	9.70E-01	0.97
	0.2	9.81E-01	9.85E-01	0.43	9.67E-01	-1.42	9.54E-01	-2.74	9.80E-01	-0.08
	0.25	9.62E-01	9.85E-01	2.35	9.72E-01	1.03	9.63E-01	0.04	9.85E-01	2.37
	0.3	9.87E-01	9.85E-01	-0.24	9.76E-01	-1.16	9.69E-01	-1.91	9.88E-01	0.05
	0.35	1.00E+00	9.85E-01	-1.48	9.79E-01	-2.13	9.73E-01	-2.73	9.90E-01	-1.05
	0.4	9.98E-01	9.85E-01	-1.26	9.81E-01	-1.72	9.76E-01	-2.22	9.90E-01	-0.76
	0.45	9.95E-01	9.85E-01	-0.95	9.82E-01	-1.27	9.78E-01	-1.69	9.91E-01	-0.40
0.5	1.00E+00	9.85E-01	-1.46	9.83E-01	-1.66	9.80E-01	-2.02	9.91E-01	-0.88	
2	0.01	3.94E-01	9.21E-01	133.80	4.96E-01	25.79	3.72E-01	-5.54	2.79E-01	-29.14
	0.02	4.14E-01	8.59E-01	107.56	5.18E-01	25.16	4.15E-01	0.12	3.51E-01	-15.12
	0.05	4.94E-01	7.85E-01	58.96	5.59E-01	13.11	4.85E-01	-1.92	4.85E-01	-1.90
	0.1	6.03E-01	7.57E-01	25.52	6.07E-01	0.59	5.55E-01	-8.05	6.03E-01	-0.10
	0.15	6.53E-01	7.52E-01	15.08	6.39E-01	-2.17	5.99E-01	-8.30	6.66E-01	1.92
	0.2	7.00E-01	7.51E-01	7.25	6.62E-01	-5.54	6.29E-01	-10.16	7.04E-01	0.51
	0.25	7.22E-01	7.52E-01	4.12	6.78E-01	-6.09	6.51E-01	-9.82	7.28E-01	0.87
	0.3	7.32E-01	7.52E-01	2.76	6.90E-01	-5.73	6.67E-01	-8.87	7.43E-01	1.56
	0.35	7.56E-01	7.53E-01	-0.39	7.00E-01	-7.46	6.80E-01	-10.10	7.53E-01	-0.40
	0.4	7.59E-01	7.54E-01	-0.71	7.07E-01	-6.84	6.89E-01	-9.16	7.58E-01	-0.08
	0.45	7.55E-01	7.54E-01	-0.17	7.13E-01	-5.58	6.97E-01	-7.66	7.62E-01	0.82
0.5	7.64E-01	7.54E-01	-1.25	7.18E-01	-6.00	7.04E-01	-7.86	7.64E-01	-0.01	
2.5	0.01	1.45E-01	4.96E-01	242.66	1.86E-01	28.71	1.32E-01	-8.89	9.89E-02	-31.64
	0.02	1.53E-01	4.10E-01	167.17	1.94E-01	26.21	1.48E-01	-3.77	1.25E-01	-18.28
	0.05	1.87E-01	3.39E-01	81.08	2.09E-01	11.80	1.75E-01	-6.28	1.77E-01	-5.21
	0.1	2.31E-01	3.17E-01	36.82	2.31E-01	-0.32	2.06E-01	-11.06	2.30E-01	-0.62
	0.15	2.58E-01	3.13E-01	21.21	2.46E-01	-4.49	2.26E-01	-12.17	2.62E-01	1.49
	0.2	2.81E-01	3.12E-01	11.22	2.58E-01	-8.18	2.41E-01	-14.00	2.82E-01	0.51
	0.25	2.89E-01	3.12E-01	8.07	2.66E-01	-7.95	2.52E-01	-12.74	2.95E-01	2.06
	0.3	2.92E-01	3.13E-01	6.94	2.72E-01	-6.85	2.60E-01	-10.94	3.03E-01	3.60
	0.35	3.04E-01	3.13E-01	2.95	2.78E-01	-8.81	2.67E-01	-12.25	3.08E-01	1.15
	0.4	3.15E-01	3.14E-01	-0.48	2.82E-01	-10.68	2.72E-01	-13.64	3.11E-01	-1.50
	0.45	3.12E-01	3.14E-01	0.64	2.85E-01	-8.72	2.77E-01	-11.40	3.12E-01	-0.03
0.5	3.15E-01	3.14E-01	-0.16	2.88E-01	-8.67	2.80E-01	-11.07	3.13E-01	-0.59	

ζ	ξ	ISEE	P	ε [%]	cVM	ε [%]	mVM	ε [%]	#5	ε [%]
3	0.01	4.00E-02	1.37E-01	242.28	4.89E-02	22.37	3.41E-02	-14.59	2.75E-02	-31.23
	0.02	4.15E-02	1.07E-01	158.73	5.02E-02	20.98	3.79E-02	-8.53	3.42E-02	-17.61
	0.05	4.89E-02	8.53E-02	74.40	5.34E-02	9.16	4.47E-02	-8.70	4.70E-02	-3.90
	0.1	6.02E-02	7.86E-02	30.57	5.83E-02	-3.21	5.21E-02	-13.57	5.96E-02	-1.06
	0.15	6.71E-02	7.75E-02	15.43	6.20E-02	-7.59	5.72E-02	-14.84	6.69E-02	-0.27
	0.2	7.00E-02	7.73E-02	10.53	6.47E-02	-7.45	6.08E-02	-13.11	7.14E-02	2.00
	0.25	7.33E-02	7.74E-02	5.57	6.68E-02	-8.97	6.35E-02	-13.48	7.40E-02	0.89
	0.3	7.50E-02	7.76E-02	3.48	6.83E-02	-8.89	6.55E-02	-12.66	7.55E-02	0.73
	0.35	7.57E-02	7.77E-02	2.69	6.95E-02	-8.18	6.71E-02	-11.41	7.64E-02	0.90
	0.4	7.58E-02	7.79E-02	2.67	7.05E-02	-7.09	6.83E-02	-9.92	7.68E-02	1.32
	0.45	7.60E-02	7.80E-02	2.60	7.12E-02	-6.27	6.93E-02	-8.78	7.71E-02	1.41
0.5	7.82E-02	7.80E-02	-0.14	7.18E-02	-8.07	7.01E-02	-10.26	7.72E-02	-1.22	
3.5	0.01	8.32E-03	2.48E-02	198.02	9.57E-03	14.96	6.70E-03	-19.46	5.91E-03	-29.03
	0.02	8.63E-03	1.92E-02	123.13	9.68E-03	12.27	7.37E-03	-14.54	7.16E-03	-17.02
	0.05	1.00E-02	1.52E-02	51.65	1.01E-02	1.08	8.53E-03	-14.69	9.42E-03	-5.81
	0.1	1.18E-02	1.39E-02	17.90	1.09E-02	-8.08	9.78E-03	-17.15	1.14E-02	-3.25
	0.15	1.24E-02	1.37E-02	10.34	1.15E-02	-7.83	1.06E-02	-14.33	1.25E-02	0.45
	0.2	1.29E-02	1.37E-02	6.32	1.19E-02	-7.64	1.12E-02	-12.61	1.30E-02	1.39
	0.25	1.34E-02	1.37E-02	2.06	1.22E-02	-9.08	1.17E-02	-12.97	1.34E-02	-0.51
	0.3	1.35E-02	1.37E-02	1.75	1.24E-02	-7.76	1.20E-02	-11.00	1.35E-02	0.21
	0.35	1.37E-02	1.38E-02	0.43	1.26E-02	-7.78	1.23E-02	-10.50	1.36E-02	-0.64
	0.4	1.40E-02	1.38E-02	-1.83	1.28E-02	-8.97	1.25E-02	-11.26	1.37E-02	-2.70
	0.45	1.36E-02	1.38E-02	1.79	1.29E-02	-4.89	1.26E-02	-6.97	1.37E-02	0.91
0.5	1.36E-02	1.38E-02	1.93	1.30E-02	-4.18	1.27E-02	-6.02	1.37E-02	1.03	
4	0.01	1.34E-03	3.39E-03	153.24	1.44E-03	7.35	1.02E-03	-24.13	9.72E-04	-27.43
	0.02	1.33E-03	2.63E-03	97.46	1.44E-03	7.83	1.10E-03	-17.05	1.15E-03	-13.75
	0.05	1.51E-03	2.07E-03	37.03	1.47E-03	-2.66	1.25E-03	-16.89	1.44E-03	-4.39
	0.1	1.69E-03	1.90E-03	12.40	1.55E-03	-8.00	1.41E-03	-16.20	1.67E-03	-1.09
	0.15	1.77E-03	1.87E-03	5.32	1.62E-03	-8.46	1.52E-03	-14.13	1.77E-03	-0.12
	0.2	1.83E-03	1.86E-03	2.10	1.68E-03	-8.25	1.60E-03	-12.48	1.82E-03	-0.33
	0.25	1.86E-03	1.87E-03	0.31	1.71E-03	-7.95	1.65E-03	-11.26	1.84E-03	-0.91
	0.3	1.84E-03	1.87E-03	1.84	1.74E-03	-5.21	1.69E-03	-7.95	1.86E-03	1.09
	0.35	1.86E-03	1.88E-03	0.62	1.76E-03	-5.38	1.72E-03	-7.64	1.86E-03	0.07
	0.4	1.84E-03	1.88E-03	2.06	1.78E-03	-3.28	1.74E-03	-5.23	1.87E-03	1.56
	0.45	1.86E-03	1.88E-03	1.24	1.79E-03	-3.48	1.76E-03	-5.15	1.87E-03	0.71
0.5	1.84E-03	1.88E-03	2.34	1.80E-03	-1.97	1.78E-03	-3.44	1.87E-03	1.74	

ζ	ξ	ISEE	P	ε [%]	cVM	ε [%]	mVM	ε [%]	#5	ε [%]
4.5	0.01	1.62E-04	3.62E-04	123.41	1.67E-04	3.19	1.19E-04	-26.35	1.22E-04	-24.78
	0.02	1.64E-04	2.82E-04	71.83	1.65E-04	0.91	1.29E-04	-21.49	1.41E-04	-13.89
	0.05	1.74E-04	2.21E-04	27.54	1.66E-04	-4.35	1.43E-04	-17.39	1.70E-04	-2.32
	0.1	1.87E-04	2.03E-04	8.36	1.73E-04	-7.71	1.59E-04	-15.10	1.88E-04	0.09
	0.15	1.93E-04	2.00E-04	3.79	1.79E-04	-6.88	1.70E-04	-11.90	1.94E-04	0.87
	0.2	1.95E-04	2.00E-04	2.11	1.84E-04	-5.79	1.77E-04	-9.48	1.97E-04	0.91
	0.25	2.00E-04	2.00E-04	-0.19	1.88E-04	-6.31	1.82E-04	-9.11	1.99E-04	-0.78
	0.3	1.99E-04	2.00E-04	0.63	1.90E-04	-4.45	1.86E-04	-6.70	2.00E-04	0.27
	0.35	1.96E-04	2.01E-04	2.23	1.92E-04	-2.14	1.88E-04	-4.02	2.00E-04	1.93
	0.4	1.99E-04	2.01E-04	0.99	1.94E-04	-2.74	1.90E-04	-4.30	2.00E-04	0.68
	0.45	1.97E-04	2.01E-04	1.98	1.95E-04	-1.34	1.92E-04	-2.67	2.01E-04	1.62
0.5	2.05E-04	2.02E-04	-1.91	1.96E-04	-4.75	1.93E-04	-5.86	2.01E-04	-2.32	
5	0.01	1.53E-05	3.05E-05	99.24	1.52E-05	-0.82	1.09E-05	-28.52	1.18E-05	-23.00
	0.02	1.50E-05	2.37E-05	57.59	1.48E-05	-1.49	1.17E-05	-22.52	1.33E-05	-11.54
	0.05	1.55E-05	1.86E-05	20.01	1.46E-05	-5.85	1.28E-05	-17.79	1.53E-05	-1.59
	0.1	1.63E-05	1.71E-05	5.12	1.50E-05	-7.59	1.40E-05	-14.20	1.63E-05	-0.05
	0.15	1.64E-05	1.68E-05	2.84	1.55E-05	-5.45	1.47E-05	-9.87	1.65E-05	1.16
	0.2	1.64E-05	1.68E-05	2.15	1.58E-05	-3.87	1.53E-05	-7.04	1.67E-05	1.46
	0.25	1.66E-05	1.68E-05	1.25	1.61E-05	-3.36	1.57E-05	-5.75	1.68E-05	0.89
	0.3	1.70E-05	1.69E-05	-1.04	1.62E-05	-4.68	1.59E-05	-6.50	1.68E-05	-1.29
	0.35	1.69E-05	1.69E-05	-0.17	1.64E-05	-3.22	1.61E-05	-4.70	1.68E-05	-0.40
	0.4	1.66E-05	1.69E-05	1.81	1.65E-05	-0.83	1.63E-05	-2.07	1.69E-05	1.55
	0.45	1.68E-05	1.69E-05	0.91	1.66E-05	-1.36	1.64E-05	-2.39	1.69E-05	0.57
0.5	1.66E-05	1.70E-05	1.92	1.66E-05	-0.10	1.65E-05	-0.99	1.69E-05	1.50	
		μ_ε %	28.31	μ_ε %	-1.356	μ_ε %	-9.69	μ_ε %	-3.46	
		σ_ε %	53.52	σ_ε %	8.85	σ_ε %	5.94	σ_ε %	8.43	
		ε_{\max} %	242.66	ε_{\max} %	28.71	ε_{\max} %	0.38	ε_{\max} %	3.60	
		ε_{\min} %	-1.91	ε_{\min} %	-10.68	ε_{\min} %	-28.52	ε_{\min} %	-31.64	
		$\mu_{ \varepsilon }$ %	28.59	$\mu_{ \varepsilon }$ %	6.80	$\mu_{ \varepsilon }$ %	9.70	$\mu_{ \varepsilon }$ %	4.47	

D.2 PROPOSED #6- WITHOUT THE PROPOSED MODIFICATIONS

The results in this section are obtained using the newly proposed hazard function without the modifications for non-white spectrum and time-modulating functions (see Section 2.3), referred to as #6 NM.

D.2.1 White Noise and Shinozuka-Sato Time-modulating Function, $T = 1.0s$

Table D.8 - Proposed #6 NM: Time-variant FPDF computed at $t = 20s$ for linear elastic SDOF systems with $T = 1.0s$ subjected to WN base excitation time modulated by a Shinozuka-Sato function.

ζ	ξ	ISEE	P	ε [%]	cVM	ε [%]	mVM	ε [%]	#6 NM	ε [%]
1.5	0.01	7.45E-01	9.99E-01	34.15	8.57E-01	15.04	7.33E-01	-1.62	6.11E-01	-17.95
	0.02	7.89E-01	9.97E-01	26.34	8.83E-01	11.81	7.89E-01	-0.04	7.22E-01	-8.56
	0.05	8.81E-01	9.90E-01	12.41	9.15E-01	3.89	8.61E-01	-2.21	8.70E-01	-1.17
	0.1	9.38E-01	9.85E-01	5.08	9.43E-01	0.59	9.14E-01	-2.47	9.45E-01	0.83
	0.15	9.71E-01	9.84E-01	1.30	9.58E-01	-1.40	9.40E-01	-3.25	9.68E-01	-0.28
	0.2	9.80E-01	9.83E-01	0.34	9.66E-01	-1.44	9.53E-01	-2.71	9.78E-01	-0.18
	0.25	9.80E-01	9.83E-01	0.35	9.71E-01	-0.87	9.62E-01	-1.80	9.83E-01	0.36
	0.3	9.60E-01	9.83E-01	2.40	9.75E-01	1.54	9.68E-01	0.80	9.86E-01	2.71
	0.35	9.70E-01	9.83E-01	1.30	9.77E-01	0.72	9.72E-01	0.13	9.88E-01	1.76
	0.4	9.90E-01	9.83E-01	-0.70	9.79E-01	-1.07	9.75E-01	-1.54	9.88E-01	-0.16
	0.45	9.84E-01	9.83E-01	-0.12	9.81E-01	-0.34	9.77E-01	-0.74	9.88E-01	0.44
0.5	9.92E-01	9.83E-01	-0.88	9.82E-01	-0.98	9.79E-01	-1.32	9.88E-01	-0.32	
2	0.01	3.90E-01	9.21E-01	136.15	5.00E-01	28.16	3.77E-01	-3.38	2.90E-01	-25.72
	0.02	4.13E-01	8.59E-01	108.08	5.22E-01	26.48	4.19E-01	1.55	3.59E-01	-12.94
	0.05	4.99E-01	7.83E-01	56.83	5.61E-01	12.37	4.88E-01	-2.24	4.87E-01	-2.42
	0.1	5.95E-01	7.53E-01	26.53	6.07E-01	2.02	5.56E-01	-6.47	5.99E-01	0.73
	0.15	6.46E-01	7.45E-01	15.38	6.37E-01	-1.35	5.99E-01	-7.29	6.58E-01	1.89
	0.2	6.92E-01	7.43E-01	7.36	6.58E-01	-4.91	6.28E-01	-9.34	6.93E-01	0.16
	0.25	7.26E-01	7.42E-01	2.16	6.73E-01	-7.35	6.48E-01	-10.83	7.15E-01	-1.58
	0.3	7.29E-01	7.42E-01	1.75	6.84E-01	-6.14	6.63E-01	-9.06	7.28E-01	-0.10
	0.35	7.39E-01	7.41E-01	0.29	6.93E-01	-6.30	6.74E-01	-8.78	7.36E-01	-0.47
	0.4	7.48E-01	7.41E-01	-0.88	6.99E-01	-6.47	6.83E-01	-8.61	7.39E-01	-1.12
	0.45	7.49E-01	7.41E-01	-1.09	7.05E-01	-5.91	6.91E-01	-7.80	7.41E-01	-1.15
0.5	7.50E-01	7.41E-01	-1.23	7.09E-01	-5.43	6.97E-01	-7.11	7.41E-01	-1.24	

ζ	ξ	ISEE	P	ε [%]	cVM	ε [%]	mVM	ε [%]	#6 NM	ε [%]
2.5	0.01	1.46E-01	4.95E-01	238.92	1.88E-01	28.78	1.34E-01	-8.49	1.02E-01	-30.08
	0.02	1.55E-01	4.09E-01	163.23	1.95E-01	25.72	1.49E-01	-3.78	1.28E-01	-17.76
	0.05	1.85E-01	3.37E-01	81.89	2.10E-01	13.45	1.77E-01	-4.53	1.78E-01	-3.93
	0.1	2.30E-01	3.13E-01	36.33	2.30E-01	0.30	2.06E-01	-10.17	2.28E-01	-0.59
	0.15	2.56E-01	3.08E-01	20.24	2.45E-01	-4.35	2.26E-01	-11.70	2.58E-01	0.80
	0.2	2.72E-01	3.06E-01	12.49	2.55E-01	-6.25	2.40E-01	-11.88	2.76E-01	1.48
	0.25	2.86E-01	3.05E-01	6.73	2.62E-01	-8.24	2.50E-01	-12.70	2.87E-01	0.31
	0.3	2.96E-01	3.05E-01	3.16	2.68E-01	-9.32	2.57E-01	-12.99	2.93E-01	-0.85
	0.35	2.93E-01	3.05E-01	4.17	2.72E-01	-6.88	2.63E-01	-10.09	2.96E-01	1.27
	0.4	2.98E-01	3.05E-01	2.17	2.76E-01	-7.48	2.68E-01	-10.23	2.97E-01	-0.24
	0.45	2.99E-01	3.05E-01	1.89	2.79E-01	-6.76	2.71E-01	-9.19	2.97E-01	-0.48
0.5	3.02E-01	3.05E-01	0.98	2.81E-01	-6.80	2.75E-01	-8.95	2.97E-01	-1.45	
3	0.01	4.01E-02	1.37E-01	240.73	4.94E-02	23.33	3.46E-02	-13.59	2.80E-02	-30.25
	0.02	4.17E-02	1.07E-01	156.43	5.06E-02	21.32	3.84E-02	-7.91	3.45E-02	-17.35
	0.05	4.95E-02	8.47E-02	71.03	5.36E-02	8.21	4.50E-02	-9.12	4.70E-02	-5.05
	0.1	5.87E-02	7.76E-02	32.32	5.81E-02	-0.91	5.21E-02	-11.15	5.93E-02	1.00
	0.15	6.50E-02	7.61E-02	17.13	6.15E-02	-5.31	5.69E-02	-12.39	6.61E-02	1.72
	0.2	6.94E-02	7.56E-02	8.98	6.39E-02	-7.88	6.02E-02	-13.17	6.98E-02	0.69
	0.25	7.16E-02	7.54E-02	5.26	6.56E-02	-8.40	6.26E-02	-12.60	7.18E-02	0.29
	0.3	7.19E-02	7.53E-02	4.68	6.69E-02	-7.00	6.44E-02	-10.50	7.28E-02	1.24
	0.35	7.25E-02	7.53E-02	3.77	6.79E-02	-6.39	6.57E-02	-9.35	7.32E-02	0.96
	0.4	7.44E-02	7.52E-02	1.18	6.87E-02	-7.65	6.68E-02	-10.15	7.32E-02	-1.49
	0.45	7.32E-02	7.52E-02	2.78	6.93E-02	-5.31	6.77E-02	-7.53	7.30E-02	-0.18
0.5	7.43E-02	7.52E-02	1.27	6.98E-02	-6.00	6.84E-02	-7.93	7.28E-02	-1.95	
3.5	0.01	8.28E-03	2.48E-02	199.02	9.67E-03	16.77	6.80E-03	-17.86	6.00E-03	-27.53
	0.02	8.63E-03	1.92E-02	122.33	9.77E-03	13.16	7.46E-03	-13.52	7.22E-03	-16.31
	0.05	1.00E-02	1.51E-02	50.24	1.01E-02	1.17	8.59E-03	-14.26	9.43E-03	-5.89
	0.1	1.14E-02	1.37E-02	20.81	1.08E-02	-4.93	9.78E-03	-13.96	1.14E-02	-0.09
	0.15	1.23E-02	1.35E-02	8.97	1.13E-02	-8.18	1.06E-02	-14.32	1.23E-02	-0.37
	0.2	1.27E-02	1.34E-02	5.56	1.17E-02	-7.54	1.11E-02	-12.19	1.27E-02	0.68
	0.25	1.29E-02	1.33E-02	3.01	1.20E-02	-7.51	1.15E-02	-11.15	1.30E-02	0.06
	0.3	1.31E-02	1.33E-02	1.87	1.22E-02	-6.95	1.18E-02	-9.90	1.30E-02	-0.31
	0.35	1.32E-02	1.33E-02	1.03	1.23E-02	-6.55	1.20E-02	-9.00	1.30E-02	-0.98
	0.4	1.30E-02	1.33E-02	2.24	1.24E-02	-4.52	1.21E-02	-6.63	1.30E-02	0.00
	0.45	1.31E-02	1.33E-02	1.53	1.25E-02	-4.48	1.23E-02	-6.29	1.29E-02	-1.16
0.5	1.29E-02	1.33E-02	2.75	1.26E-02	-2.76	1.24E-02	-4.35	1.29E-02	-0.45	

ζ	ξ	ISEE	P	ε [%]	cVM	ε [%]	mVM	ε [%]	#6 NM	ε [%]	
4	0.01	1.33E-03	3.38E-03	154.94	1.45E-03	9.36	1.03E-03	-22.39	1.00E-03	-24.53	
	0.02	1.32E-03	2.62E-03	98.75	1.45E-03	9.73	1.12E-03	-15.24	1.17E-03	-11.29	
	0.05	1.51E-03	2.05E-03	36.22	1.47E-03	-2.32	1.26E-03	-16.25	1.45E-03	-3.95	
	0.1	1.65E-03	1.87E-03	13.42	1.55E-03	-6.40	1.41E-03	-14.41	1.66E-03	0.36	
	0.15	1.74E-03	1.83E-03	5.25	1.61E-03	-7.83	1.51E-03	-13.21	1.74E-03	-0.03	
	0.2	1.79E-03	1.82E-03	1.72	1.65E-03	-7.96	1.58E-03	-11.90	1.78E-03	-0.87	
	0.25	1.82E-03	1.82E-03	-0.21	1.68E-03	-7.84	1.62E-03	-10.86	1.79E-03	-1.81	
	0.3	1.78E-03	1.81E-03	2.12	1.70E-03	-4.37	1.66E-03	-6.85	1.79E-03	0.77	
	0.35	1.80E-03	1.81E-03	0.95	1.72E-03	-4.52	1.68E-03	-6.53	1.79E-03	-0.49	
	0.4	1.80E-03	1.81E-03	0.54	1.73E-03	-4.19	1.70E-03	-5.87	1.78E-03	-1.28	
	0.45	1.82E-03	1.81E-03	-0.41	1.74E-03	-4.55	1.71E-03	-5.96	1.77E-03	-2.82	
0.5	1.80E-03	1.81E-03	0.62	1.74E-03	-3.12	1.72E-03	-4.35	1.76E-03	-2.40		
4.5	0.01	1.61E-04	3.62E-04	124.53	1.69E-04	4.92	1.21E-04	-24.81	1.28E-04	-20.83	
	0.02	1.60E-04	2.81E-04	75.51	1.67E-04	4.15	1.30E-04	-18.64	1.45E-04	-9.45	
	0.05	1.72E-04	2.20E-04	27.58	1.66E-04	-3.49	1.44E-04	-16.31	1.70E-04	-1.26	
	0.1	1.85E-04	2.00E-04	8.53	1.72E-04	-6.90	1.59E-04	-14.02	1.86E-04	0.56	
	0.15	1.93E-04	1.96E-04	1.41	1.77E-04	-8.43	1.68E-04	-13.07	1.91E-04	-1.46	
	0.2	1.94E-04	1.95E-04	0.22	1.81E-04	-7.00	1.74E-04	-10.35	1.92E-04	-1.15	
	0.25	1.93E-04	1.94E-04	0.89	1.83E-04	-4.80	1.78E-04	-7.37	1.93E-04	-0.02	
	0.3	1.91E-04	1.94E-04	1.57	1.85E-04	-3.09	1.81E-04	-5.12	1.93E-04	0.71	
	0.35	1.91E-04	1.94E-04	1.74	1.87E-04	-2.17	1.83E-04	-3.80	1.92E-04	0.65	
	0.4	1.95E-04	1.94E-04	-0.55	1.88E-04	-3.81	1.85E-04	-5.13	1.91E-04	-2.10	
	0.45	1.92E-04	1.94E-04	1.24	1.88E-04	-1.66	1.86E-04	-2.78	1.90E-04	-1.05	
0.5	1.93E-04	1.94E-04	0.65	1.89E-04	-1.89	1.87E-04	-2.84	1.88E-04	-2.20		
5	0.01	1.53E-05	3.04E-05	99.11	1.53E-05	0.22	1.11E-05	-27.46	1.21E-05	-20.84	
	0.02	1.50E-05	2.36E-05	57.34	1.49E-05	-0.67	1.18E-05	-21.54	1.35E-05	-10.28	
	0.05	1.57E-05	1.85E-05	17.71	1.46E-05	-6.93	1.28E-05	-18.40	1.52E-05	-3.00	
	0.1	1.63E-05	1.69E-05	3.22	1.49E-05	-8.69	1.39E-05	-14.91	1.61E-05	-1.66	
	0.15	1.62E-05	1.65E-05	2.12	1.53E-05	-5.61	1.46E-05	-9.73	1.62E-05	0.47	
	0.2	1.64E-05	1.64E-05	0.29	1.55E-05	-5.17	1.50E-05	-8.03	1.63E-05	-0.46	
	0.25	1.61E-05	1.64E-05	1.31	1.57E-05	-2.89	1.53E-05	-5.04	1.63E-05	0.79	
	0.3	1.63E-05	1.63E-05	0.25	1.58E-05	-3.06	1.55E-05	-4.69	1.63E-05	-0.30	
	0.35	1.63E-05	1.63E-05	0.11	1.59E-05	-2.60	1.57E-05	-3.89	1.62E-05	-0.69	
	0.4	1.60E-05	1.63E-05	1.89	1.60E-05	-0.43	1.58E-05	-1.49	1.61E-05	0.60	
	0.45	1.60E-05	1.63E-05	2.21	1.60E-05	0.21	1.59E-05	-0.66	1.60E-05	0.30	
0.5	1.63E-05	1.63E-05	0.38	1.60E-05	-1.33	1.59E-05	-2.05	1.60E-05	-1.86		
				μ_ε %	28.27	μ_ε %	-0.673	μ_ε %	-8.81	μ_ε %	-3.58
				σ_ε %	53.27	σ_ε %	8.93	σ_ε %	5.74	σ_ε %	7.57
				ε_{\max} %	240.73	ε_{\max} %	28.78	ε_{\max} %	1.55	ε_{\max} %	2.71
				ε_{\min} %	-1.23	ε_{\min} %	-9.32	ε_{\min} %	-27.46	ε_{\min} %	-30.25
				$\mu_{ \varepsilon }$ %	28.39	$\mu_{ \varepsilon }$ %	6.58	$\mu_{ \varepsilon }$ %	8.86	$\mu_{ \varepsilon }$ %	4.09

D.2.2 Kanai-Tajimi and Unit-step Time-modulating Function, $T = 0.1$ s

Table D.9 - Proposed #6 NM: Time-variant FFP computed at $t = 1.0$ s for linear elastic SDOF system with $T = 0.1$ s subjected to KT base excitation from at-rest initial conditions.

ζ	ξ	ISEE	P	ε [%]	cVM	ε [%]	mVM	ε [%]	#6 NM	ε [%]
1.5	0.01	5.15E-01	8.88E-01	72.41	6.71E-01	30.18	5.88E-01	14.16	6.17E-01	19.68
	0.02	8.17E-01	9.84E-01	20.54	9.01E-01	10.36	8.47E-01	3.72	8.69E-01	6.47
	0.05	9.76E-01	9.98E-01	2.25	9.86E-01	1.04	9.73E-01	-0.31	9.84E-01	0.80
	0.1	1.00E+00	9.99E-01	-0.08	9.97E-01	-0.26	9.94E-01	-0.56	9.98E-01	-0.18
	0.15	9.97E-01	9.99E-01	0.24	9.99E-01	0.21	9.98E-01	0.09	1.00E+00	0.26
	0.2	1.00E+00	9.99E-01	-0.05	1.00E+00	-0.05	9.99E-01	-0.10	1.00E+00	-0.01
	0.25	9.79E-01	1.00E+00	2.13	1.00E+00	2.15	9.99E-01	2.12	1.00E+00	2.18
	0.3	9.94E-01	9.99E-01	0.60	1.00E+00	0.64	1.00E+00	0.61	1.00E+00	0.65
	0.35	1.00E+00	9.99E-01	-0.05	1.00E+00	-0.01	1.00E+00	-0.03	1.00E+00	0.00
	0.4	1.00E+00	9.99E-01	-0.06	1.00E+00	-0.01	1.00E+00	-0.03	1.00E+00	0.00
	0.45	1.00E+00	9.99E-01	-0.06	1.00E+00	-0.01	1.00E+00	-0.02	1.00E+00	0.00
	0.5	1.00E+00	9.99E-01	-0.06	1.00E+00	0.00	1.00E+00	-0.01	1.00E+00	0.00
2	0.01	1.82E-01	4.17E-01	129.44	2.45E-01	34.90	2.02E-01	11.34	2.33E-01	28.54
	0.02	4.40E-01	7.73E-01	75.49	5.52E-01	25.38	4.81E-01	9.27	5.28E-01	20.00
	0.05	8.22E-01	9.43E-01	14.75	8.39E-01	2.03	7.89E-01	-4.05	8.34E-01	1.39
	0.1	9.54E-01	9.78E-01	2.48	9.39E-01	-1.56	9.15E-01	-4.06	9.45E-01	-0.90
	0.15	9.93E-01	9.86E-01	-0.63	9.68E-01	-2.46	9.54E-01	-3.84	9.76E-01	-1.64
	0.2	9.99E-01	9.90E-01	-0.87	9.80E-01	-1.84	9.71E-01	-2.73	9.88E-01	-1.03
	0.25	9.92E-01	9.92E-01	-0.03	9.86E-01	-0.57	9.80E-01	-1.22	9.94E-01	0.19
	0.3	9.99E-01	9.93E-01	-0.66	9.90E-01	-0.95	9.85E-01	-1.44	9.96E-01	-0.29
	0.35	1.00E+00	9.93E-01	-0.68	9.92E-01	-0.82	9.88E-01	-1.22	9.98E-01	-0.24
	0.4	1.00E+00	9.93E-01	-0.65	9.93E-01	-0.69	9.90E-01	-1.02	9.98E-01	-0.19
	0.45	1.00E+00	9.94E-01	-0.64	9.94E-01	-0.60	9.91E-01	-0.89	9.98E-01	-0.16
	0.5	1.00E+00	9.94E-01	-0.64	9.95E-01	-0.53	9.92E-01	-0.79	9.98E-01	-0.15
2.5	0.01	4.14E-02	9.31E-02	124.83	5.36E-02	29.44	4.37E-02	5.44	5.40E-02	30.41
	0.02	1.71E-01	3.40E-01	98.60	2.10E-01	22.79	1.76E-01	3.18	2.06E-01	20.33
	0.05	4.85E-01	6.59E-01	35.96	4.99E-01	2.93	4.49E-01	-7.44	5.02E-01	3.54
	0.1	7.33E-01	8.16E-01	11.35	7.03E-01	-4.04	6.62E-01	-9.74	7.20E-01	-1.71
	0.15	8.45E-01	8.79E-01	3.99	8.00E-01	-5.32	7.68E-01	-9.19	8.27E-01	-2.11
	0.2	9.17E-01	9.11E-01	-0.63	8.54E-01	-6.79	8.28E-01	-9.66	8.88E-01	-3.14
	0.25	9.38E-01	9.29E-01	-0.89	8.87E-01	-5.36	8.66E-01	-7.68	9.24E-01	-1.40
	0.3	9.53E-01	9.40E-01	-1.26	9.08E-01	-4.63	8.90E-01	-6.56	9.45E-01	-0.74
	0.35	9.45E-01	9.48E-01	0.30	9.23E-01	-2.34	9.07E-01	-4.04	9.58E-01	1.34
	0.4	9.67E-01	9.53E-01	-1.49	9.33E-01	-3.54	9.18E-01	-5.02	9.64E-01	-0.27
	0.45	9.75E-01	9.56E-01	-1.99	9.40E-01	-3.62	9.27E-01	-4.95	9.68E-01	-0.75
	0.5	9.76E-01	9.58E-01	-1.81	9.45E-01	-3.13	9.33E-01	-4.35	9.70E-01	-0.59

ζ	ξ	ISEE	P	ε [%]	cVM	ε [%]	mVM	ε [%]	#6 NM	ε [%]
3	0.01	6.54E-03	1.30E-02	98.28	7.96E-03	21.77	6.52E-03	-0.33	8.47E-03	29.45
	0.02	4.62E-02	8.76E-02	89.81	5.44E-02	17.76	4.54E-02	-1.69	5.54E-02	19.91
	0.05	1.97E-01	2.81E-01	43.03	2.00E-01	1.56	1.76E-01	-10.33	2.07E-01	5.27
	0.1	3.96E-01	4.70E-01	18.67	3.72E-01	-5.89	3.43E-01	-13.35	3.93E-01	-0.71
	0.15	5.44E-01	5.90E-01	8.34	4.95E-01	-9.12	4.64E-01	-14.67	5.30E-01	-2.59
	0.2	6.32E-01	6.70E-01	6.02	5.82E-01	-7.83	5.53E-01	-12.45	6.32E-01	0.00
	0.25	7.06E-01	7.24E-01	2.51	6.46E-01	-8.62	6.18E-01	-12.53	7.06E-01	-0.10
	0.3	7.60E-01	7.62E-01	0.33	6.92E-01	-8.91	6.66E-01	-12.33	7.57E-01	-0.41
	0.35	7.91E-01	7.89E-01	-0.20	7.27E-01	-8.12	7.02E-01	-11.22	7.91E-01	-0.05
	0.4	8.25E-01	8.09E-01	-1.91	7.53E-01	-8.72	7.30E-01	-11.52	8.12E-01	-1.53
	0.45	8.18E-01	8.24E-01	0.72	7.73E-01	-5.47	7.51E-01	-8.15	8.25E-01	0.90
0.5	8.50E-01	8.35E-01	-1.76	7.89E-01	-7.16	7.68E-01	-9.61	8.33E-01	-1.91	
3.5	0.01	7.25E-04	1.28E-03	76.95	8.45E-04	16.64	6.98E-04	-3.64	9.43E-04	30.13
	0.02	9.32E-03	1.59E-02	70.19	1.04E-02	11.60	8.73E-03	-6.33	1.10E-02	18.44
	0.05	5.72E-02	7.94E-02	38.72	5.75E-02	0.46	5.08E-02	-11.30	6.17E-02	7.75
	0.1	1.54E-01	1.81E-01	17.53	1.42E-01	-7.75	1.30E-01	-15.45	1.54E-01	0.13
	0.15	2.47E-01	2.75E-01	11.45	2.25E-01	-9.09	2.09E-01	-15.26	2.48E-01	0.27
	0.2	3.41E-01	3.57E-01	4.75	2.98E-01	-12.34	2.81E-01	-17.46	3.34E-01	-2.02
	0.25	4.13E-01	4.23E-01	2.61	3.61E-01	-12.44	3.42E-01	-17.00	4.07E-01	-1.33
	0.3	4.65E-01	4.77E-01	2.62	4.13E-01	-11.07	3.94E-01	-15.27	4.65E-01	0.13
	0.35	5.07E-01	5.20E-01	2.40	4.56E-01	-10.14	4.36E-01	-14.06	5.09E-01	0.36
	0.4	5.42E-01	5.54E-01	2.05	4.91E-01	-9.50	4.71E-01	-13.18	5.40E-01	-0.40
	0.45	5.72E-01	5.81E-01	1.47	5.19E-01	-9.21	5.00E-01	-12.69	5.61E-01	-2.05
0.5	6.16E-01	6.02E-01	-2.22	5.43E-01	-11.85	5.23E-01	-15.05	5.74E-01	-6.79	
4	0.01	5.59E-05	9.26E-05	65.64	6.49E-05	16.05	5.42E-05	-3.14	7.53E-05	34.72
	0.02	1.45E-03	2.19E-03	51.44	1.53E-03	5.35	1.29E-03	-10.80	1.68E-03	16.01
	0.05	1.34E-02	1.68E-02	25.32	1.27E-02	-5.00	1.13E-02	-15.52	1.40E-02	4.70
	0.1	4.58E-02	5.13E-02	11.88	4.14E-02	-9.64	3.81E-02	-16.82	4.57E-02	-0.29
	0.15	8.79E-02	9.49E-02	7.92	7.86E-02	-10.64	7.34E-02	-16.54	8.77E-02	-0.29
	0.2	1.32E-01	1.42E-01	6.90	1.19E-01	-10.16	1.12E-01	-15.39	1.34E-01	1.18
	0.25	1.76E-01	1.87E-01	5.97	1.59E-01	-9.95	1.50E-01	-14.72	1.80E-01	1.91
	0.3	2.18E-01	2.28E-01	4.71	1.96E-01	-10.21	1.86E-01	-14.62	2.21E-01	1.24
	0.35	2.51E-01	2.65E-01	5.54	2.29E-01	-8.80	2.18E-01	-13.01	2.55E-01	1.58
	0.4	2.86E-01	2.97E-01	3.66	2.58E-01	-9.82	2.47E-01	-13.77	2.81E-01	-1.73
	0.45	3.15E-01	3.24E-01	2.84	2.84E-01	-9.99	2.72E-01	-13.75	3.00E-01	-4.88
0.5	3.38E-01	3.47E-01	2.86	3.06E-01	-9.48	2.93E-01	-13.11	3.13E-01	-7.29	

ζ	ξ	ISEE	P	ε [%]	cVM	ε [%]	mVM	ε [%]	#6 NM	ε [%]
4.5	0.01	3.19E-06	4.91E-06	53.90	3.62E-06	13.48	3.05E-06	-4.31	4.32E-06	35.39
	0.02	1.68E-04	2.37E-04	41.20	1.74E-04	3.44	1.49E-04	-11.59	1.97E-04	16.95
	0.05	2.44E-03	2.83E-03	16.26	2.25E-03	-7.78	2.02E-03	-17.25	2.52E-03	3.26
	0.1	1.07E-02	1.16E-02	8.88	9.72E-03	-8.79	9.02E-03	-15.41	1.08E-02	1.06
	0.15	2.44E-02	2.61E-02	6.73	2.23E-02	-8.97	2.09E-02	-14.48	2.48E-02	1.30
	0.2	4.17E-02	4.48E-02	7.53	3.86E-02	-7.46	3.65E-02	-12.45	4.31E-02	3.40
	0.25	6.27E-02	6.59E-02	4.98	5.70E-02	-9.14	5.42E-02	-13.65	6.38E-02	1.65
	0.3	8.37E-02	8.75E-02	4.53	7.61E-02	-9.14	7.25E-02	-13.37	8.46E-02	0.99
	0.35	1.01E-01	1.09E-01	7.39	9.48E-02	-6.31	9.06E-02	-10.45	1.04E-01	2.48
	0.4	1.23E-01	1.29E-01	4.85	1.13E-01	-8.24	1.08E-01	-12.12	1.20E-01	-2.42
	0.45	1.39E-01	1.47E-01	5.67	1.29E-01	-7.24	1.24E-01	-11.02	1.32E-01	-5.19
0.5	1.58E-01	1.63E-01	3.32	1.44E-01	-9.04	1.38E-01	-12.62	1.42E-01	-10.49	
5	0.01	1.27E-07	1.90E-07	49.83	1.46E-07	15.32	1.25E-07	-1.77	1.77E-07	39.37
	0.02	1.50E-05	2.02E-05	34.95	1.55E-05	3.29	1.33E-05	-10.90	1.77E-05	18.23
	0.05	3.44E-04	3.88E-04	12.86	3.20E-04	-6.95	2.90E-04	-15.76	3.61E-04	4.76
	0.1	2.01E-03	2.17E-03	7.81	1.88E-03	-6.67	1.76E-03	-12.78	2.07E-03	2.95
	0.15	5.59E-03	5.99E-03	7.09	5.26E-03	-5.92	4.97E-03	-11.03	5.79E-03	3.62
	0.2	1.12E-02	1.19E-02	5.90	1.05E-02	-6.39	1.00E-02	-10.92	1.16E-02	3.14
	0.25	1.85E-02	1.95E-02	5.86	1.73E-02	-6.12	1.66E-02	-10.32	1.91E-02	3.32
	0.3	2.64E-02	2.83E-02	7.02	2.51E-02	-4.90	2.41E-02	-8.91	2.75E-02	3.86
	0.35	3.62E-02	3.76E-02	3.84	3.35E-02	-7.59	3.21E-02	-11.31	3.60E-02	-0.80
	0.4	4.46E-02	4.71E-02	5.60	4.20E-02	-5.91	4.03E-02	-9.55	4.37E-02	-1.99
	0.45	5.38E-02	5.64E-02	4.71	5.03E-02	-6.60	4.84E-02	-10.10	5.03E-02	-6.53
	0.5	6.26E-02	6.52E-02	4.24	5.82E-02	-6.92	5.61E-02	-10.30	5.64E-02	-9.78
		μ_ε %	16.50	μ_ε %	-1.702	μ_ε %	-7.81	μ_ε %	3.84	
		σ_ε %	28.88	σ_ε %	10.09	σ_ε %	6.86	σ_ε %	10.09	
		ε_{\max} %	129.44	ε_{\max} %	34.90	ε_{\max} %	14.16	ε_{\max} %	39.37	
		ε_{\min} %	-2.22	ε_{\min} %	-12.44	ε_{\min} %	-17.46	ε_{\min} %	-10.49	
		$\mu_{ \varepsilon }$ %	16.90	$\mu_{ \varepsilon }$ %	7.72	$\mu_{ \varepsilon }$ %	8.85	$\mu_{ \varepsilon }$ %	5.65	

D.2.3 Kanai-Tajimi and Unit-step Time-modulating Function, $T = 0.5s$

Table D.10 - Proposed #6 NM: Time-variant FFP computed at $t = 5.0s$ for linear elastic SDOF system with $T = 0.5s$ subjected to KT base excitation from at-rest initial conditions.

ζ	ξ	ISEE	P	ε [%]	cVM	ε [%]	mVM	ε [%]	#6 NM	ε [%]
1.5	0.01	3.86E-01	8.41E-01	117.86	4.93E-01	27.68	3.91E-01	1.27	3.28E-01	-15.13
	0.02	6.72E-01	9.71E-01	44.52	7.61E-01	13.31	6.56E-01	-2.30	5.90E-01	-12.14
	0.05	9.15E-01	9.95E-01	8.69	9.30E-01	1.68	8.77E-01	-4.10	8.83E-01	-3.47
	0.1	9.83E-01	9.97E-01	1.45	9.74E-01	-0.85	9.53E-01	-3.04	9.75E-01	-0.76
	0.15	9.95E-01	9.97E-01	0.28	9.85E-01	-0.92	9.74E-01	-2.09	9.91E-01	-0.36
	0.2	1.00E+00	9.97E-01	-0.26	9.90E-01	-1.02	9.82E-01	-1.76	9.95E-01	-0.46
	0.25	9.96E-01	9.97E-01	0.11	9.92E-01	-0.43	9.87E-01	-0.96	9.97E-01	0.08
	0.3	9.88E-01	9.97E-01	0.89	9.93E-01	0.47	9.89E-01	0.07	9.98E-01	0.95
	0.35	1.00E+00	9.97E-01	-0.29	9.94E-01	-0.61	9.91E-01	-0.94	9.98E-01	-0.19
	0.4	9.93E-01	9.97E-01	0.37	9.94E-01	0.12	9.92E-01	-0.16	9.98E-01	0.50
	0.45	9.88E-01	9.97E-01	0.87	9.95E-01	0.66	9.92E-01	0.42	9.98E-01	1.01
	0.5	9.95E-01	9.96E-01	0.15	9.95E-01	-0.02	9.93E-01	-0.24	9.98E-01	0.30
2	0.01	1.16E-01	3.34E-01	187.19	1.47E-01	26.45	1.10E-01	-5.37	9.03E-02	-22.43
	0.02	3.07E-01	6.75E-01	119.68	3.68E-01	19.86	2.91E-01	-5.21	2.45E-01	-20.22
	0.05	5.96E-01	8.61E-01	44.57	6.29E-01	5.52	5.46E-01	-8.39	5.37E-01	-9.89
	0.1	7.51E-01	8.97E-01	19.41	7.49E-01	-0.19	6.90E-01	-8.16	7.37E-01	-1.86
	0.15	8.15E-01	9.03E-01	10.82	7.94E-01	-2.48	7.49E-01	-8.03	8.16E-01	0.18
	0.2	8.73E-01	9.03E-01	3.43	8.17E-01	-6.46	7.80E-01	-10.59	8.54E-01	-2.15
	0.25	8.71E-01	9.01E-01	3.43	8.28E-01	-4.86	7.99E-01	-8.29	8.74E-01	0.33
	0.3	8.83E-01	8.97E-01	1.61	8.35E-01	-5.44	8.09E-01	-8.35	8.83E-01	-0.02
	0.35	8.88E-01	8.93E-01	0.55	8.38E-01	-5.65	8.16E-01	-8.17	8.86E-01	-0.30
	0.4	9.04E-01	8.89E-01	-1.75	8.39E-01	-7.21	8.19E-01	-9.42	8.84E-01	-2.23
	0.45	9.01E-01	8.84E-01	-1.90	8.39E-01	-6.89	8.21E-01	-8.90	8.80E-01	-2.30
	0.5	8.87E-01	8.78E-01	-1.01	8.37E-01	-5.66	8.21E-01	-7.52	8.75E-01	-1.44
2.5	0.01	2.36E-02	6.29E-02	166.63	2.77E-02	17.53	2.05E-02	-13.00	1.72E-02	-26.94
	0.02	9.62E-02	2.40E-01	149.22	1.14E-01	18.32	8.71E-02	-9.42	7.28E-02	-24.38
	0.05	2.49E-01	4.43E-01	78.01	2.67E-01	7.36	2.22E-01	-11.00	2.18E-01	-12.38
	0.1	3.62E-01	5.00E-01	38.16	3.57E-01	-1.34	3.15E-01	-12.95	3.50E-01	-3.14
	0.15	4.21E-01	5.08E-01	20.64	3.92E-01	-6.82	3.57E-01	-15.22	4.15E-01	-1.30
	0.2	4.39E-01	5.05E-01	15.07	4.09E-01	-6.88	3.79E-01	-13.68	4.49E-01	2.28
	0.25	4.66E-01	4.98E-01	7.04	4.16E-01	-10.63	3.91E-01	-16.11	4.64E-01	-0.31
	0.3	4.69E-01	4.90E-01	4.55	4.18E-01	-10.72	3.96E-01	-15.42	4.68E-01	-0.10
	0.35	4.69E-01	4.81E-01	2.37	4.17E-01	-11.07	3.98E-01	-15.18	4.65E-01	-0.93
	0.4	4.60E-01	4.71E-01	2.32	4.14E-01	-9.91	3.97E-01	-13.61	4.58E-01	-0.54
	0.45	4.58E-01	4.61E-01	0.50	4.10E-01	-10.55	3.95E-01	-13.85	4.48E-01	-2.36
	0.5	4.53E-01	4.51E-01	-0.55	4.05E-01	-10.69	3.91E-01	-13.68	4.37E-01	-3.57

ζ	ξ	ISEE	P	ε [%]	cVM	ε [%]	mVM	ε [%]	#6 NM	ε [%]
3	0.01	3.30E-03	7.43E-03	125.12	3.56E-03	8.00	2.65E-03	-19.67	2.36E-03	-28.50
	0.02	2.18E-02	5.01E-02	129.96	2.45E-02	12.65	1.87E-02	-14.09	1.63E-02	-25.02
	0.05	7.21E-02	1.26E-01	75.42	7.50E-02	4.08	6.16E-02	-14.60	6.32E-02	-12.36
	0.1	1.13E-01	1.51E-01	34.30	1.06E-01	-5.81	9.27E-02	-17.65	1.08E-01	-4.36
	0.15	1.28E-01	1.54E-01	19.74	1.17E-01	-8.73	1.06E-01	-17.53	1.28E-01	-0.13
	0.2	1.36E-01	1.51E-01	10.75	1.21E-01	-11.20	1.12E-01	-18.10	1.36E-01	0.07
	0.25	1.38E-01	1.46E-01	6.06	1.22E-01	-11.98	1.14E-01	-17.67	1.38E-01	-0.17
	0.3	1.37E-01	1.41E-01	3.57	1.20E-01	-11.86	1.14E-01	-16.70	1.36E-01	-0.58
	0.35	1.32E-01	1.36E-01	3.54	1.18E-01	-10.19	1.13E-01	-14.45	1.32E-01	0.17
	0.4	1.29E-01	1.31E-01	1.50	1.15E-01	-10.62	1.11E-01	-14.35	1.27E-01	-1.74
	0.45	1.23E-01	1.26E-01	2.65	1.12E-01	-8.51	1.08E-01	-11.89	1.21E-01	-1.01
0.5	1.21E-01	1.21E-01	0.01	1.09E-01	-9.97	1.05E-01	-12.94	1.16E-01	-4.01	
3.5	0.01	3.11E-04	6.14E-04	97.41	3.21E-04	3.31	2.41E-04	-22.50	2.32E-04	-25.48
	0.02	3.68E-03	7.37E-03	100.01	3.89E-03	5.65	2.99E-03	-18.93	2.81E-03	-23.80
	0.05	1.50E-02	2.40E-02	60.31	1.51E-02	0.71	1.25E-02	-16.90	1.36E-02	-9.35
	0.1	2.35E-02	2.97E-02	26.19	2.18E-02	-7.20	1.92E-02	-18.34	2.31E-02	-1.72
	0.15	2.62E-02	2.99E-02	13.84	2.37E-02	-9.49	2.16E-02	-17.66	2.65E-02	1.00
	0.2	2.71E-02	2.89E-02	6.44	2.40E-02	-11.32	2.23E-02	-17.65	2.71E-02	0.03
	0.25	2.65E-02	2.75E-02	3.88	2.37E-02	-10.69	2.23E-02	-15.90	2.65E-02	0.14
	0.3	2.51E-02	2.61E-02	3.85	2.29E-02	-8.67	2.18E-02	-13.12	2.54E-02	1.14
	0.35	2.46E-02	2.47E-02	0.43	2.21E-02	-10.16	2.11E-02	-13.89	2.41E-02	-1.99
	0.4	2.29E-02	2.33E-02	1.72	2.11E-02	-7.79	2.04E-02	-11.10	2.27E-02	-1.04
	0.45	2.16E-02	2.20E-02	2.24	2.02E-02	-6.33	1.96E-02	-9.27	2.13E-02	-1.24
0.5	2.07E-02	2.08E-02	0.54	1.93E-02	-7.10	1.87E-02	-9.68	2.00E-02	-3.62	
4	0.01	2.04E-05	3.63E-05	77.85	2.05E-05	0.38	1.55E-05	-23.96	1.61E-05	-20.84
	0.02	4.55E-04	8.17E-04	79.78	4.65E-04	2.27	3.60E-04	-20.83	3.66E-04	-19.39
	0.05	2.43E-03	3.40E-03	39.86	2.28E-03	-6.15	1.90E-03	-21.77	2.20E-03	-9.58
	0.1	3.72E-03	4.28E-03	14.98	3.32E-03	-10.71	2.96E-03	-20.60	3.63E-03	-2.53
	0.15	3.93E-03	4.25E-03	8.14	3.54E-03	-9.92	3.25E-03	-17.23	3.96E-03	0.85
	0.2	3.89E-03	4.03E-03	3.67	3.50E-03	-10.02	3.28E-03	-15.67	3.90E-03	0.21
	0.25	3.71E-03	3.77E-03	1.56	3.36E-03	-9.45	3.19E-03	-14.01	3.69E-03	-0.51
	0.3	3.44E-03	3.50E-03	1.78	3.18E-03	-7.51	3.05E-03	-11.33	3.44E-03	0.10
	0.35	3.27E-03	3.25E-03	-0.83	2.99E-03	-8.60	2.89E-03	-11.76	3.19E-03	-2.60
	0.4	2.99E-03	3.01E-03	0.61	2.81E-03	-6.26	2.72E-03	-9.02	2.94E-03	-1.78
	0.45	2.80E-03	2.80E-03	-0.05	2.63E-03	-6.08	2.56E-03	-8.47	2.70E-03	-3.42
0.5	2.54E-03	2.60E-03	2.22	2.46E-03	-3.29	2.41E-03	-5.43	2.49E-03	-2.23	

ζ	ξ	ISEE	P	ε [%]	cVM	ε [%]	mVM	ε [%]	#6 NM	ε [%]
4.5	0.01	9.72E-07	1.53E-06	57.66	9.23E-07	-5.05	7.06E-07	-27.35	7.83E-07	-19.48
	0.02	4.25E-05	6.93E-05	62.99	4.21E-05	-1.08	3.29E-05	-22.70	3.57E-05	-16.05
	0.05	2.83E-04	3.72E-04	31.27	2.65E-04	-6.66	2.23E-04	-21.34	2.68E-04	-5.38
	0.1	4.36E-04	4.74E-04	8.72	3.85E-04	-11.56	3.46E-04	-20.51	4.26E-04	-2.14
	0.15	4.41E-04	4.62E-04	4.78	4.00E-04	-9.29	3.71E-04	-15.83	4.44E-04	0.74
	0.2	4.21E-04	4.29E-04	1.80	3.85E-04	-8.70	3.64E-04	-13.67	4.21E-04	-0.06
	0.25	3.87E-04	3.92E-04	1.17	3.59E-04	-7.18	3.44E-04	-11.15	3.87E-04	-0.03
	0.3	3.53E-04	3.56E-04	0.93	3.32E-04	-5.94	3.20E-04	-9.19	3.52E-04	-0.20
	0.35	3.16E-04	3.23E-04	2.24	3.04E-04	-3.62	2.96E-04	-6.36	3.18E-04	0.76
	0.4	2.86E-04	2.93E-04	2.49	2.79E-04	-2.54	2.72E-04	-4.87	2.87E-04	0.20
	0.45	2.61E-04	2.67E-04	2.31	2.56E-04	-2.06	2.50E-04	-4.05	2.58E-04	-1.21
0.5	2.42E-04	2.44E-04	0.67	2.35E-04	-3.12	2.30E-04	-4.81	2.33E-04	-3.88	
5	0.01	3.12E-08	4.62E-08	47.95	2.94E-08	-5.76	2.28E-08	-27.17	2.59E-08	-17.07
	0.02	3.04E-06	4.50E-06	48.23	2.89E-06	-4.87	2.28E-06	-24.94	2.55E-06	-16.01
	0.05	2.61E-05	3.16E-05	20.93	2.36E-05	-9.71	2.01E-05	-23.10	2.45E-05	-6.12
	0.1	3.83E-05	4.06E-05	5.80	3.43E-05	-10.65	3.11E-05	-18.88	3.79E-05	-1.20
	0.15	3.76E-05	3.87E-05	2.90	3.46E-05	-8.19	3.24E-05	-14.05	3.79E-05	0.61
	0.2	3.52E-05	3.51E-05	-0.34	3.23E-05	-8.34	3.07E-05	-12.65	3.47E-05	-1.35
	0.25	3.10E-05	3.12E-05	0.73	2.93E-05	-5.58	2.82E-05	-8.99	3.10E-05	0.02
	0.3	2.72E-05	2.77E-05	1.78	2.63E-05	-3.37	2.55E-05	-6.13	2.74E-05	1.00
	0.35	2.41E-05	2.45E-05	1.61	2.35E-05	-2.64	2.29E-05	-4.90	2.42E-05	0.44
	0.4	2.17E-05	2.17E-05	0.12	2.10E-05	-3.41	2.06E-05	-5.26	2.13E-05	-1.83
	0.45	1.91E-05	1.93E-05	1.05	1.88E-05	-2.00	1.85E-05	-3.57	1.87E-05	-2.05
	0.5	1.69E-05	1.73E-05	2.32	1.68E-05	-0.36	1.66E-05	-1.71	1.66E-05	-1.57
		μ_ε %	24.10	μ_ε %	-3.423	μ_ε %	-11.89	μ_ε %	-4.82	
		σ_ε %	41.33	σ_ε %	8.08	σ_ε %	6.81	σ_ε %	7.87	
		ε_{\max} %	187.19	ε_{\max} %	27.68	ε_{\max} %	1.27	ε_{\max} %	2.28	
		ε_{\min} %	-1.90	ε_{\min} %	-11.98	ε_{\min} %	-27.35	ε_{\min} %	-28.50	
		$\mu_{ \varepsilon }$ %	24.25	$\mu_{ \varepsilon }$ %	7.09	$\mu_{ \varepsilon }$ %	11.92	$\mu_{ \varepsilon }$ %	5.09	

D.2.4 Kanai-Tajimi and Unit-step Time-modulating Function, $T = 1.0s$

Table D.11 - Proposed #6 NM: Time-variant FPDF computed at $t = 10s$ for linear elastic SDOF system with $T = 1.0s$ subjected to KT base excitation from at-rest initial conditions.

ζ	ξ	ISEE	P	ε [%]	cVM	ε [%]	mVM	ε [%]	#6 NM	ε [%]
1.5	0.01	4.03E-01	8.45E-01	109.56	5.35E-01	32.74	4.38E-01	8.67	3.99E-01	-1.00
	0.02	6.91E-01	9.72E-01	40.68	8.02E-01	15.99	7.11E-01	2.92	6.77E-01	-2.03
	0.05	9.18E-01	9.95E-01	8.37	9.51E-01	3.58	9.13E-01	-0.52	9.22E-01	0.42
	0.1	9.89E-01	9.97E-01	0.81	9.85E-01	-0.48	9.72E-01	-1.76	9.86E-01	-0.39
	0.15	1.00E+00	9.98E-01	-0.20	9.92E-01	-0.77	9.86E-01	-1.36	9.95E-01	-0.48
	0.2	9.93E-01	9.98E-01	0.49	9.95E-01	0.19	9.92E-01	-0.15	9.98E-01	0.45
	0.25	1.00E+00	9.98E-01	-0.16	9.97E-01	-0.34	9.95E-01	-0.55	9.99E-01	-0.13
	0.3	1.00E+00	9.98E-01	-0.16	9.97E-01	-0.26	9.96E-01	-0.40	9.99E-01	-0.09
	0.35	9.94E-01	9.98E-01	0.50	9.98E-01	0.44	9.97E-01	0.34	9.99E-01	0.58
	0.4	1.00E+00	9.99E-01	-0.15	9.98E-01	-0.17	9.97E-01	-0.26	9.99E-01	-0.06
	0.45	1.00E+00	9.99E-01	-0.15	9.98E-01	-0.15	9.98E-01	-0.22	9.99E-01	-0.06
	0.5	1.00E+00	9.99E-01	-0.15	9.99E-01	-0.14	9.98E-01	-0.19	9.99E-01	-0.06
2	0.01	1.22E-01	3.40E-01	179.36	1.65E-01	35.31	1.27E-01	4.52	1.17E-01	-3.97
	0.02	3.15E-01	6.82E-01	116.81	4.05E-01	28.62	3.30E-01	4.94	3.05E-01	-3.06
	0.05	6.24E-01	8.70E-01	39.44	6.75E-01	8.22	6.02E-01	-3.47	6.03E-01	-3.25
	0.1	7.91E-01	9.09E-01	14.91	7.96E-01	0.66	7.48E-01	-5.37	7.89E-01	-0.29
	0.15	8.62E-01	9.19E-01	6.62	8.42E-01	-2.32	8.09E-01	-6.21	8.59E-01	-0.37
	0.2	8.98E-01	9.24E-01	2.95	8.67E-01	-3.45	8.42E-01	-6.26	8.93E-01	-0.49
	0.25	9.26E-01	9.27E-01	0.16	8.82E-01	-4.70	8.62E-01	-6.86	9.12E-01	-1.45
	0.3	9.22E-01	9.29E-01	0.71	8.92E-01	-3.25	8.76E-01	-5.02	9.23E-01	0.07
	0.35	9.37E-01	9.30E-01	-0.81	8.99E-01	-4.05	8.85E-01	-5.52	9.29E-01	-0.92
	0.4	9.12E-01	9.30E-01	1.97	9.04E-01	-0.85	8.93E-01	-2.14	9.31E-01	2.11
	0.45	9.31E-01	9.30E-01	-0.03	9.08E-01	-2.40	8.98E-01	-3.52	9.32E-01	0.19
	0.5	9.28E-01	9.30E-01	0.20	9.11E-01	-1.86	9.02E-01	-2.85	9.32E-01	0.44
2.5	0.01	2.45E-02	6.45E-02	163.20	3.13E-02	27.63	2.39E-02	-2.44	2.27E-02	-7.25
	0.02	9.72E-02	2.45E-01	152.43	1.28E-01	31.40	1.01E-01	3.80	9.37E-02	-3.66
	0.05	2.58E-01	4.58E-01	77.19	2.98E-01	15.54	2.55E-01	-1.39	2.56E-01	-0.74
	0.1	3.98E-01	5.27E-01	32.34	4.02E-01	0.84	3.64E-01	-8.77	3.98E-01	-0.21
	0.15	4.64E-01	5.49E-01	18.24	4.49E-01	-3.30	4.17E-01	-10.05	4.70E-01	1.23
	0.2	5.09E-01	5.59E-01	9.83	4.76E-01	-6.41	4.50E-01	-11.51	5.11E-01	0.44
	0.25	5.36E-01	5.64E-01	5.21	4.94E-01	-7.88	4.72E-01	-11.96	5.35E-01	-0.20
	0.3	5.54E-01	5.68E-01	2.52	5.07E-01	-8.49	4.88E-01	-11.89	5.49E-01	-0.77
	0.35	5.68E-01	5.69E-01	0.28	5.16E-01	-9.20	4.99E-01	-12.09	5.57E-01	-1.94
	0.4	5.72E-01	5.70E-01	-0.33	5.22E-01	-8.74	5.08E-01	-11.28	5.60E-01	-2.13
	0.45	5.64E-01	5.70E-01	1.21	5.27E-01	-6.52	5.14E-01	-8.82	5.60E-01	-0.59
	0.5	5.73E-01	5.70E-01	-0.55	5.30E-01	-7.49	5.19E-01	-9.53	5.59E-01	-2.43

ζ	ξ	ISEE	P	ε [%]	cVM	ε [%]	mVM	ε [%]	#6 NM	ε [%]
3	0.01	3.45E-03	7.69E-03	122.87	4.04E-03	17.15	3.10E-03	-9.96	3.12E-03	-9.66
	0.02	2.27E-02	5.18E-02	128.11	2.78E-02	22.29	2.19E-02	-3.72	2.11E-02	-7.07
	0.05	7.91E-02	1.34E-01	69.19	8.58E-02	8.50	7.25E-02	-8.31	7.54E-02	-4.62
	0.1	1.29E-01	1.67E-01	29.51	1.25E-01	-3.31	1.12E-01	-13.29	1.27E-01	-1.76
	0.15	1.51E-01	1.78E-01	18.04	1.43E-01	-5.18	1.32E-01	-12.40	1.54E-01	1.88
	0.2	1.67E-01	1.83E-01	9.39	1.53E-01	-8.23	1.44E-01	-13.70	1.68E-01	0.62
	0.25	1.76E-01	1.86E-01	5.43	1.60E-01	-8.97	1.52E-01	-13.38	1.76E-01	0.18
	0.3	1.83E-01	1.87E-01	2.24	1.65E-01	-9.89	1.58E-01	-13.53	1.81E-01	-1.28
	0.35	1.84E-01	1.88E-01	1.89	1.68E-01	-8.82	1.62E-01	-11.96	1.83E-01	-0.96
	0.4	1.86E-01	1.88E-01	1.06	1.70E-01	-8.48	1.65E-01	-11.21	1.83E-01	-1.67
	0.45	1.89E-01	1.88E-01	-0.63	1.72E-01	-9.16	1.67E-01	-11.54	1.82E-01	-3.57
0.5	1.84E-01	1.87E-01	2.00	1.73E-01	-6.05	1.69E-01	-8.24	1.81E-01	-1.37	
3.5	0.01	3.35E-04	6.42E-04	91.53	3.66E-04	9.31	2.84E-04	-15.22	3.04E-04	-9.22
	0.02	3.91E-03	7.71E-03	97.18	4.44E-03	13.50	3.52E-03	-10.04	3.60E-03	-7.88
	0.05	1.71E-02	2.60E-02	52.24	1.76E-02	2.85	1.49E-02	-12.58	1.63E-02	-4.66
	0.1	2.79E-02	3.43E-02	23.01	2.67E-02	-4.34	2.41E-02	-13.70	2.80E-02	0.39
	0.15	3.32E-02	3.69E-02	11.07	3.07E-02	-7.64	2.85E-02	-14.18	3.35E-02	0.65
	0.2	3.58E-02	3.81E-02	6.44	3.29E-02	-7.97	3.11E-02	-12.97	3.61E-02	0.95
	0.25	3.75E-02	3.87E-02	3.28	3.43E-02	-8.39	3.28E-02	-12.37	3.74E-02	-0.05
	0.3	3.77E-02	3.90E-02	3.43	3.52E-02	-6.60	3.39E-02	-9.94	3.80E-02	0.94
	0.35	3.89E-02	3.91E-02	0.54	3.58E-02	-8.00	3.47E-02	-10.76	3.82E-02	-1.68
	0.4	3.81E-02	3.91E-02	2.71	3.61E-02	-5.06	3.52E-02	-7.50	3.81E-02	0.21
	0.45	3.83E-02	3.90E-02	1.76	3.63E-02	-5.19	3.55E-02	-7.31	3.79E-02	-1.24
0.5	3.85E-02	3.88E-02	0.81	3.64E-02	-5.47	3.57E-02	-7.33	3.75E-02	-2.71	
4	0.01	2.25E-05	3.84E-05	70.21	2.35E-05	4.29	1.84E-05	-18.29	2.10E-05	-6.78
	0.02	5.02E-04	8.65E-04	72.39	5.34E-04	6.38	4.27E-04	-14.91	4.65E-04	-7.32
	0.05	2.74E-03	3.77E-03	37.59	2.70E-03	-1.27	2.32E-03	-15.23	2.65E-03	-3.41
	0.1	4.48E-03	5.18E-03	15.61	4.22E-03	-5.67	3.85E-03	-14.06	4.53E-03	1.23
	0.15	5.23E-03	5.61E-03	7.31	4.86E-03	-7.12	4.55E-03	-12.92	5.30E-03	1.31
	0.2	5.51E-03	5.80E-03	5.16	5.19E-03	-5.89	4.94E-03	-10.30	5.63E-03	2.10
	0.25	5.66E-03	5.88E-03	3.88	5.38E-03	-5.03	5.18E-03	-8.52	5.77E-03	1.94
	0.3	5.82E-03	5.92E-03	1.59	5.49E-03	-5.74	5.33E-03	-8.54	5.83E-03	0.03
	0.35	5.89E-03	5.92E-03	0.60	5.56E-03	-5.66	5.42E-03	-7.98	5.83E-03	-1.04
	0.4	5.81E-03	5.91E-03	1.68	5.59E-03	-3.87	5.47E-03	-5.86	5.79E-03	-0.41
	0.45	5.81E-03	5.89E-03	1.31	5.60E-03	-3.62	5.50E-03	-5.33	5.72E-03	-1.50
0.5	5.81E-03	5.85E-03	0.66	5.59E-03	-3.76	5.50E-03	-5.24	5.64E-03	-2.83	

ζ	ξ	ISEE	P	ε [%]	cVM	ε [%]	mVM	ε [%]	#6 NM	ε [%]
4.5	0.01	1.06E-06	1.64E-06	54.96	1.07E-06	0.87	8.45E-07	-20.14	1.01E-06	-4.42
	0.02	4.67E-05	7.44E-05	59.24	4.87E-05	4.37	3.94E-05	-15.69	4.50E-05	-3.68
	0.05	3.31E-04	4.22E-04	27.76	3.19E-04	-3.37	2.77E-04	-16.15	3.25E-04	-1.66
	0.1	5.49E-04	6.01E-04	9.43	5.11E-04	-7.00	4.70E-04	-14.44	5.53E-04	0.66
	0.15	6.44E-04	6.55E-04	1.78	5.86E-04	-8.95	5.54E-04	-13.91	6.34E-04	-1.46
	0.2	6.69E-04	6.77E-04	1.22	6.23E-04	-6.87	5.98E-04	-10.57	6.66E-04	-0.39
	0.25	6.85E-04	6.86E-04	0.10	6.42E-04	-6.27	6.23E-04	-9.13	6.79E-04	-1.00
	0.3	6.92E-04	6.89E-04	-0.50	6.52E-04	-5.72	6.37E-04	-8.00	6.82E-04	-1.52
	0.35	6.82E-04	6.88E-04	0.76	6.57E-04	-3.71	6.44E-04	-5.60	6.79E-04	-0.51
	0.4	6.82E-04	6.84E-04	0.41	6.58E-04	-3.44	6.47E-04	-5.02	6.72E-04	-1.41
	0.45	6.83E-04	6.80E-04	-0.43	6.57E-04	-3.79	6.48E-04	-5.12	6.62E-04	-3.06
0.5	6.76E-04	6.73E-04	-0.45	6.53E-04	-3.44	6.45E-04	-4.59	6.51E-04	-3.79	
5	0.01	3.53E-08	5.02E-08	42.00	3.44E-08	-2.66	2.75E-08	-22.13	3.36E-08	-5.00
	0.02	3.43E-06	4.90E-06	42.96	3.38E-06	-1.34	2.76E-06	-19.53	3.22E-06	-6.20
	0.05	3.04E-05	3.69E-05	21.41	2.91E-05	-4.07	2.55E-05	-15.89	3.02E-05	-0.53
	0.1	5.16E-05	5.43E-05	5.22	4.77E-05	-7.64	4.43E-05	-14.24	5.15E-05	-0.26
	0.15	5.77E-05	5.95E-05	3.10	5.46E-05	-5.40	5.20E-05	-9.85	5.84E-05	1.21
	0.2	6.09E-05	6.14E-05	0.82	5.77E-05	-5.28	5.58E-05	-8.46	6.09E-05	-0.08
	0.25	6.21E-05	6.21E-05	-0.01	5.92E-05	-4.71	5.77E-05	-7.10	6.17E-05	-0.66
	0.3	6.04E-05	6.21E-05	2.83	5.98E-05	-1.07	5.86E-05	-3.00	6.17E-05	2.11
	0.35	6.23E-05	6.19E-05	-0.73	5.99E-05	-3.86	5.90E-05	-5.36	6.13E-05	-1.69
	0.4	6.14E-05	6.14E-05	0.03	5.97E-05	-2.65	5.90E-05	-3.90	6.05E-05	-1.48
	0.45	6.01E-05	6.08E-05	1.08	5.93E-05	-1.27	5.87E-05	-2.32	5.94E-05	-1.18
	0.5	6.07E-05	6.00E-05	-1.19	5.88E-05	-3.21	5.83E-05	-4.08	5.84E-05	-3.83
		μ_ε %	22.46	μ_ε %	-0.652	μ_ε %	-7.95	μ_ε %	-1.48	
		σ_ε %	40.08	σ_ε %	9.67	σ_ε %	5.92	σ_ε %	2.49	
		ε_{\max} %	179.36	ε_{\max} %	35.31	ε_{\max} %	8.67	ε_{\max} %	2.11	
		ε_{\min} %	-1.19	ε_{\min} %	-9.89	ε_{\min} %	-22.13	ε_{\min} %	-9.66	
		$\mu_{ \varepsilon }$ %	22.60	$\mu_{ \varepsilon }$ %	6.71	$\mu_{ \varepsilon }$ %	8.48	$\mu_{ \varepsilon }$ %	1.95	

D.2.5 Kanai-Tajimi and Shinozuka-Sato Time-modulating Function, $T = 0.1s$

Table D.12 - Proposed #6 NM: FFP computed at $t = 20s$ for linear elastic SDOF system with $T = 0.1s$ subjected to KT base excitation time modulated by a Shinozuka-Sato function.

ζ	ξ	ISEE	P	ε [%]	cVM	ε [%]	mVM	ε [%]	#6 NM	ε [%]
1.5	0.01	9.88E-01	1.00E+00	1.22	1.00E+00	1.22	1.00E+00	1.22	1.00E+00	1.18
	0.02	9.97E-01	1.00E+00	0.31	1.00E+00	0.31	1.00E+00	0.31	1.00E+00	0.31
	0.05	9.98E-01	1.00E+00	0.24	1.00E+00	0.24	1.00E+00	0.24	1.00E+00	0.24
	0.1	1.00E+00	1.00E+00	0.00	1.00E+00	0.00	1.00E+00	0.00	1.00E+00	0.00
	0.15	1.00E+00	1.00E+00	0.00	1.00E+00	0.00	1.00E+00	0.00	1.00E+00	0.00
	0.2	1.00E+00	1.00E+00	0.00	1.00E+00	0.00	1.00E+00	0.00	1.00E+00	0.00
	0.25	1.00E+00	1.00E+00	0.00	1.00E+00	0.00	1.00E+00	0.00	1.00E+00	0.00
	0.3	9.98E-01	1.00E+00	0.24	1.00E+00	0.24	1.00E+00	0.24	1.00E+00	0.24
	0.35	9.96E-01	1.00E+00	0.39	1.00E+00	0.39	1.00E+00	0.39	1.00E+00	0.39
	0.4	1.00E+00	1.00E+00	0.00	1.00E+00	0.00	1.00E+00	0.00	1.00E+00	0.00
	0.45	1.00E+00	1.00E+00	0.00	1.00E+00	0.00	1.00E+00	0.00	1.00E+00	0.00
	0.5	9.98E-01	1.00E+00	0.24	1.00E+00	0.24	1.00E+00	0.24	1.00E+00	0.24
2	0.01	8.74E-01	1.00E+00	14.45	9.93E-01	13.67	9.73E-01	11.35	9.43E-01	7.97
	0.02	9.75E-01	1.00E+00	2.55	9.98E-01	2.31	9.91E-01	1.65	9.88E-01	1.33
	0.05	9.92E-01	1.00E+00	0.80	9.99E-01	0.75	9.98E-01	0.62	9.99E-01	0.70
	0.1	9.90E-01	1.00E+00	1.05	1.00E+00	1.02	9.99E-01	0.97	1.00E+00	1.02
	0.15	9.92E-01	1.00E+00	0.82	1.00E+00	0.79	9.99E-01	0.75	1.00E+00	0.80
	0.2	1.00E+00	1.00E+00	-0.01	1.00E+00	-0.05	9.99E-01	-0.08	1.00E+00	-0.02
	0.25	9.79E-01	1.00E+00	2.18	9.99E-01	2.13	9.99E-01	2.09	1.00E+00	2.17
	0.3	9.88E-01	1.00E+00	1.19	9.99E-01	1.13	9.99E-01	1.09	1.00E+00	1.18
	0.35	9.95E-01	1.00E+00	0.43	9.99E-01	0.37	9.99E-01	0.32	1.00E+00	0.43
	0.4	9.96E-01	1.00E+00	0.41	9.99E-01	0.33	9.99E-01	0.28	1.00E+00	0.40
	0.45	9.91E-01	1.00E+00	0.87	9.99E-01	0.79	9.98E-01	0.73	1.00E+00	0.87
	0.5	9.93E-01	1.00E+00	0.64	9.99E-01	0.55	9.98E-01	0.49	1.00E+00	0.64
2.5	0.01	4.87E-01	9.74E-01	99.93	7.68E-01	57.55	6.57E-01	34.82	5.97E-01	22.54
	0.02	6.84E-01	9.69E-01	41.62	8.28E-01	20.94	7.50E-01	9.65	7.45E-01	8.78
	0.05	8.58E-01	9.61E-01	12.12	8.78E-01	2.40	8.36E-01	-2.52	8.66E-01	1.00
	0.1	9.17E-01	9.50E-01	3.53	8.89E-01	-3.03	8.62E-01	-5.98	8.97E-01	-2.21
	0.15	9.28E-01	9.38E-01	1.11	8.86E-01	-4.53	8.64E-01	-6.89	9.02E-01	-2.85
	0.2	9.23E-01	9.28E-01	0.52	8.79E-01	-4.77	8.60E-01	-6.86	9.01E-01	-2.36
	0.25	9.22E-01	9.18E-01	-0.48	8.71E-01	-5.54	8.53E-01	-7.47	9.00E-01	-2.44
	0.3	9.04E-01	9.09E-01	0.53	8.63E-01	-4.49	8.47E-01	-6.35	8.96E-01	-0.89
	0.35	9.10E-01	9.00E-01	-1.07	8.55E-01	-5.96	8.39E-01	-7.72	8.90E-01	-2.18
	0.4	8.89E-01	8.92E-01	0.32	8.48E-01	-4.60	8.32E-01	-6.34	8.82E-01	-0.74
	0.45	8.70E-01	8.84E-01	1.55	8.41E-01	-3.41	8.26E-01	-5.14	8.74E-01	0.37
	0.5	8.83E-01	8.76E-01	-0.70	8.34E-01	-5.53	8.19E-01	-7.19	8.65E-01	-2.01

ζ	ξ	ISEE	P	ε [%]	cVM	ε [%]	mVM	ε [%]	#6 NM	ε [%]
3	0.01	1.67E-01	5.46E-01	226.13	2.94E-01	75.81	2.28E-01	36.07	2.12E-01	26.68
	0.02	2.60E-01	5.28E-01	102.78	3.39E-01	30.27	2.82E-01	8.32	2.93E-01	12.49
	0.05	3.86E-01	5.04E-01	30.35	3.85E-01	-0.50	3.45E-01	-10.85	3.84E-01	-0.55
	0.1	4.45E-01	4.74E-01	6.51	3.94E-01	-11.59	3.66E-01	-17.74	4.10E-01	-7.91
	0.15	4.26E-01	4.51E-01	5.96	3.87E-01	-9.06	3.66E-01	-14.11	4.10E-01	-3.61
	0.2	4.24E-01	4.32E-01	1.94	3.78E-01	-10.93	3.60E-01	-15.18	4.05E-01	-4.37
	0.25	4.18E-01	4.16E-01	-0.43	3.68E-01	-12.01	3.52E-01	-15.78	3.99E-01	-4.54
	0.3	3.93E-01	4.03E-01	2.50	3.59E-01	-8.70	3.45E-01	-12.30	3.90E-01	-0.62
	0.35	3.90E-01	3.91E-01	0.23	3.50E-01	-10.20	3.37E-01	-13.51	3.81E-01	-2.40
	0.4	3.86E-01	3.80E-01	-1.58	3.42E-01	-11.41	3.30E-01	-14.50	3.70E-01	-4.24
	0.45	3.68E-01	3.71E-01	0.84	3.35E-01	-8.89	3.24E-01	-11.92	3.59E-01	-2.34
0.5	3.59E-01	3.63E-01	1.01	3.29E-01	-8.45	3.18E-01	-11.37	3.49E-01	-2.74	
3.5	0.01	3.97E-02	1.26E-01	217.81	6.36E-02	60.10	4.81E-02	21.11	4.85E-02	22.09
	0.02	6.12E-02	1.20E-01	96.96	7.42E-02	21.35	6.05E-02	-0.99	6.73E-02	10.10
	0.05	9.00E-02	1.13E-01	25.56	8.49E-02	-5.66	7.52E-02	-16.44	8.84E-02	-1.78
	0.1	9.83E-02	1.04E-01	6.03	8.63E-02	-12.20	7.99E-02	-18.79	9.24E-02	-5.98
	0.15	9.67E-02	9.76E-02	0.95	8.40E-02	-13.13	7.91E-02	-18.21	9.08E-02	-6.14
	0.2	9.18E-02	9.24E-02	0.66	8.11E-02	-11.56	7.71E-02	-15.93	8.81E-02	-3.98
	0.25	8.63E-02	8.80E-02	2.02	7.84E-02	-9.18	7.50E-02	-13.14	8.54E-02	-1.09
	0.3	8.20E-02	8.44E-02	2.92	7.58E-02	-7.55	7.28E-02	-11.21	8.24E-02	0.45
	0.35	8.02E-02	8.13E-02	1.47	7.36E-02	-8.24	7.09E-02	-11.60	7.94E-02	-0.90
	0.4	7.89E-02	7.87E-02	-0.34	7.15E-02	-9.40	6.91E-02	-12.51	7.65E-02	-3.10
	0.45	7.84E-02	7.63E-02	-2.72	6.96E-02	-11.19	6.74E-02	-14.06	7.35E-02	-6.24
0.5	7.34E-02	7.42E-02	1.05	6.80E-02	-7.42	6.59E-02	-10.27	7.08E-02	-3.60	
4	0.01	6.87E-03	1.81E-02	163.96	9.66E-03	40.61	7.34E-03	6.85	8.05E-03	17.14
	0.02	1.03E-02	1.72E-02	67.23	1.12E-02	8.45	9.18E-03	-10.99	1.08E-02	5.09
	0.05	1.40E-02	1.61E-02	15.02	1.26E-02	-9.87	1.13E-02	-19.60	1.36E-02	-2.89
	0.1	1.44E-02	1.48E-02	3.12	1.27E-02	-11.61	1.18E-02	-17.67	1.38E-02	-4.24
	0.15	1.37E-02	1.38E-02	1.17	1.23E-02	-10.22	1.16E-02	-14.91	1.33E-02	-2.97
	0.2	1.29E-02	1.30E-02	1.50	1.18E-02	-8.27	1.13E-02	-12.25	1.27E-02	-1.20
	0.25	1.24E-02	1.24E-02	-0.19	1.13E-02	-8.76	1.09E-02	-12.21	1.22E-02	-2.00
	0.3	1.18E-02	1.19E-02	0.41	1.09E-02	-7.49	1.06E-02	-10.63	1.17E-02	-1.19
	0.35	1.16E-02	1.14E-02	-1.13	1.06E-02	-8.38	1.03E-02	-11.24	1.12E-02	-2.94
	0.4	1.11E-02	1.10E-02	-0.66	1.03E-02	-7.53	9.98E-03	-10.22	1.08E-02	-3.19
	0.45	1.07E-02	1.07E-02	-0.14	9.99E-03	-6.72	9.72E-03	-9.26	1.03E-02	-3.92
0.5	1.03E-02	1.04E-02	0.52	9.74E-03	-5.81	9.48E-03	-8.24	9.85E-03	-4.67	

ζ	ξ	ISEE	P	ε [%]	cVM	ε [%]	mVM	ε [%]	#6 NM	ε [%]
4.5	0.01	8.78E-04	1.95E-03	122.49	1.12E-03	27.06	8.57E-04	-2.47	1.00E-03	13.99
	0.02	1.24E-03	1.86E-03	50.34	1.28E-03	3.41	1.06E-03	-14.20	1.30E-03	5.47
	0.05	1.57E-03	1.74E-03	10.31	1.42E-03	-9.72	1.28E-03	-18.64	1.56E-03	-0.79
	0.1	1.56E-03	1.59E-03	2.14	1.41E-03	-9.51	1.33E-03	-14.98	1.53E-03	-1.96
	0.15	1.50E-03	1.49E-03	-0.78	1.36E-03	-9.46	1.30E-03	-13.54	1.45E-03	-2.94
	0.2	1.36E-03	1.40E-03	3.35	1.30E-03	-4.23	1.25E-03	-7.76	1.38E-03	1.82
	0.25	1.33E-03	1.33E-03	0.44	1.25E-03	-6.04	1.21E-03	-9.02	1.32E-03	-0.64
	0.3	1.30E-03	1.28E-03	-1.62	1.20E-03	-7.38	1.17E-03	-10.00	1.26E-03	-2.70
	0.35	1.24E-03	1.23E-03	-0.75	1.16E-03	-6.13	1.13E-03	-8.54	1.21E-03	-2.24
	0.4	1.18E-03	1.19E-03	0.19	1.13E-03	-4.89	1.10E-03	-7.15	1.16E-03	-2.23
	0.45	1.14E-03	1.15E-03	0.58	1.09E-03	-4.25	1.07E-03	-6.37	1.10E-03	-3.39
0.5	1.11E-03	1.12E-03	0.68	1.07E-03	-3.92	1.04E-03	-5.93	1.05E-03	-4.88	
5	0.01	8.64E-05	1.65E-04	90.50	1.00E-04	15.83	7.76E-05	-10.13	9.33E-05	8.04
	0.02	1.17E-04	1.56E-04	33.84	1.13E-04	-3.08	9.50E-05	-18.69	1.19E-04	1.55
	0.05	1.37E-04	1.46E-04	6.93	1.24E-04	-9.26	1.13E-04	-17.42	1.37E-04	0.45
	0.1	1.32E-04	1.34E-04	1.68	1.22E-04	-7.52	1.16E-04	-12.41	1.31E-04	-0.40
	0.15	1.23E-04	1.25E-04	1.70	1.17E-04	-5.16	1.12E-04	-8.80	1.24E-04	0.58
	0.2	1.18E-04	1.18E-04	0.44	1.12E-04	-5.13	1.08E-04	-8.07	1.17E-04	-0.39
	0.25	1.13E-04	1.12E-04	-0.29	1.07E-04	-5.09	1.04E-04	-7.59	1.12E-04	-0.94
	0.3	1.07E-04	1.08E-04	0.17	1.03E-04	-4.16	1.01E-04	-6.38	1.07E-04	-0.58
	0.35	1.03E-04	1.03E-04	0.78	9.93E-05	-3.22	9.73E-05	-5.24	1.02E-04	-0.41
	0.4	9.94E-05	9.99E-05	0.52	9.62E-05	-3.19	9.43E-05	-5.05	9.78E-05	-1.60
	0.45	9.74E-05	9.67E-05	-0.69	9.34E-05	-4.14	9.17E-05	-5.85	9.33E-05	-4.23
	0.5	9.48E-05	9.40E-05	-0.92	9.09E-05	-4.17	8.94E-05	-5.78	8.95E-05	-5.65
		μ_ε %	15.50	μ_ε %	-0.450	μ_ε %	-5.94	μ_ε %	0.33	
		σ_ε %	42.05	σ_ε %	14.87	σ_ε %	9.66	σ_ε %	5.88	
		ε_{\max} %	226.13	ε_{\max} %	75.81	ε_{\max} %	36.07	ε_{\max} %	26.68	
		ε_{\min} %	-2.72	ε_{\min} %	-13.13	ε_{\min} %	-19.60	ε_{\min} %	-7.91	
		$\mu_{ \varepsilon }$ %	15.81	$\mu_{ \varepsilon }$ %	8.58	$\mu_{ \varepsilon }$ %	8.85	$\mu_{ \varepsilon }$ %	3.39	

D.2.6 Kanai-Tajimi and Shinozuka-Sato Time-modulating Function, $T = 0.5s$

Table D.13 - Proposed #6 NM: Time-variant FPDF computed at $t = 20s$ for linear elastic SDOF system with $T = 0.5s$ subjected to KT base excitation time modulated by a Shinozuka-Sato function.

ζ	ξ	ISEE	P	ε [%]	cVM	ε [%]	mVM	ε [%]	#6 NM	ε [%]
1.5	0.01	8.23E-01	1.00E+00	21.55	9.38E-01	14.02	8.36E-01	1.68	6.76E-01	-17.79
	0.02	8.78E-01	1.00E+00	13.83	9.58E-01	9.04	8.92E-01	1.52	8.12E-01	-7.56
	0.05	9.62E-01	1.00E+00	3.96	9.83E-01	2.19	9.57E-01	-0.49	9.58E-01	-0.38
	0.1	9.77E-01	1.00E+00	2.32	9.94E-01	1.70	9.85E-01	0.82	9.94E-01	1.72
	0.15	1.00E+00	1.00E+00	-0.03	9.97E-01	-0.33	9.93E-01	-0.72	9.98E-01	-0.17
	0.2	1.00E+00	1.00E+00	-0.03	9.98E-01	-0.20	9.96E-01	-0.42	9.99E-01	-0.07
	0.25	1.00E+00	1.00E+00	-0.02	9.99E-01	-0.14	9.97E-01	-0.28	1.00E+00	-0.03
	0.3	9.80E-01	1.00E+00	2.02	9.99E-01	1.93	9.98E-01	1.84	1.00E+00	2.02
	0.35	1.00E+00	1.00E+00	-0.03	9.99E-01	-0.09	9.98E-01	-0.16	1.00E+00	-0.02
	0.4	1.00E+00	1.00E+00	-0.03	9.99E-01	-0.07	9.99E-01	-0.13	1.00E+00	-0.02
	0.45	9.90E-01	1.00E+00	1.03	9.99E-01	0.99	9.99E-01	0.95	1.00E+00	1.04
0.5	1.00E+00	1.00E+00	-0.03	9.99E-01	-0.06	9.99E-01	-0.09	1.00E+00	-0.02	
2	0.01	4.56E-01	9.80E-01	114.93	6.23E-01	36.55	4.73E-01	3.74	3.31E-01	-27.39
	0.02	5.23E-01	9.60E-01	83.38	6.64E-01	26.86	5.39E-01	3.04	4.37E-01	-16.51
	0.05	6.80E-01	9.40E-01	38.16	7.44E-01	9.35	6.57E-01	-3.37	6.43E-01	-5.54
	0.1	8.12E-01	9.36E-01	15.23	8.11E-01	-0.14	7.55E-01	-7.08	7.98E-01	-1.71
	0.15	8.65E-01	9.36E-01	8.12	8.44E-01	-2.42	8.03E-01	-7.15	8.63E-01	-0.27
	0.2	8.86E-01	9.36E-01	5.61	8.64E-01	-2.48	8.32E-01	-6.06	8.95E-01	1.07
	0.25	9.15E-01	9.35E-01	2.20	8.77E-01	-4.23	8.51E-01	-7.03	9.13E-01	-0.23
	0.3	9.11E-01	9.35E-01	2.69	8.85E-01	-2.78	8.64E-01	-5.14	9.23E-01	1.36
	0.35	9.39E-01	9.35E-01	-0.43	8.92E-01	-5.02	8.73E-01	-6.98	9.28E-01	-1.12
	0.4	9.24E-01	9.34E-01	1.08	8.96E-01	-3.03	8.80E-01	-4.77	9.30E-01	0.64
	0.45	9.35E-01	9.33E-01	-0.15	9.00E-01	-3.76	8.85E-01	-5.29	9.30E-01	-0.50
0.5	9.45E-01	9.33E-01	-1.36	9.02E-01	-4.58	8.89E-01	-5.94	9.29E-01	-1.69	
2.5	0.01	1.74E-01	6.51E-01	274.06	2.53E-01	45.35	1.76E-01	1.12	1.20E-01	-31.13
	0.02	2.05E-01	5.79E-01	182.36	2.75E-01	34.17	2.06E-01	0.72	1.63E-01	-20.60
	0.05	2.95E-01	5.30E-01	79.98	3.25E-01	10.24	2.69E-01	-8.77	2.63E-01	-10.84
	0.1	3.85E-01	5.22E-01	35.79	3.76E-01	-2.18	3.32E-01	-13.64	3.69E-01	-4.11
	0.15	4.33E-01	5.22E-01	20.33	4.06E-01	-6.36	3.70E-01	-14.70	4.29E-01	-0.96
	0.2	4.71E-01	5.21E-01	10.60	4.25E-01	-9.85	3.95E-01	-16.31	4.65E-01	-1.29
	0.25	4.85E-01	5.21E-01	7.43	4.38E-01	-9.66	4.12E-01	-15.06	4.87E-01	0.33
	0.3	4.97E-01	5.21E-01	4.72	4.48E-01	-9.94	4.25E-01	-14.54	4.98E-01	0.26
	0.35	5.05E-01	5.20E-01	2.86	4.55E-01	-10.02	4.34E-01	-14.03	5.04E-01	-0.31
	0.4	5.19E-01	5.19E-01	-0.10	4.60E-01	-11.42	4.42E-01	-14.91	5.05E-01	-2.75
	0.45	5.13E-01	5.17E-01	0.79	4.64E-01	-9.66	4.47E-01	-12.85	5.03E-01	-1.91
0.5	5.13E-01	5.16E-01	0.54	4.66E-01	-9.08	4.51E-01	-11.98	5.01E-01	-2.30	

ζ	ξ	ISEE	P	ε [%]	cVM	ε [%]	mVM	ε [%]	#6 NM	ε [%]
3	0.01	4.83E-02	2.03E-01	319.65	6.84E-02	41.54	4.64E-02	-4.05	3.37E-02	-30.36
	0.02	5.97E-02	1.70E-01	184.66	7.42E-02	24.31	5.45E-02	-8.63	4.54E-02	-23.98
	0.05	8.21E-02	1.50E-01	82.93	8.82E-02	7.39	7.18E-02	-12.50	7.35E-02	-10.48
	0.1	1.09E-01	1.47E-01	35.21	1.03E-01	-5.02	9.01E-02	-17.09	1.05E-01	-3.63
	0.15	1.24E-01	1.47E-01	18.05	1.12E-01	-9.78	1.01E-01	-18.51	1.23E-01	-1.29
	0.2	1.34E-01	1.47E-01	9.33	1.18E-01	-12.13	1.09E-01	-18.96	1.33E-01	-1.05
	0.25	1.34E-01	1.47E-01	9.23	1.22E-01	-9.19	1.14E-01	-15.06	1.38E-01	2.88
	0.3	1.40E-01	1.46E-01	4.72	1.25E-01	-10.81	1.18E-01	-15.71	1.41E-01	0.54
	0.35	1.44E-01	1.46E-01	1.61	1.27E-01	-11.85	1.21E-01	-16.05	1.41E-01	-1.72
	0.4	1.43E-01	1.46E-01	1.68	1.28E-01	-10.51	1.23E-01	-14.26	1.41E-01	-1.62
	0.45	1.43E-01	1.45E-01	1.67	1.29E-01	-9.48	1.24E-01	-12.86	1.40E-01	-2.05
0.5	1.45E-01	1.45E-01	-0.47	1.30E-01	-10.54	1.26E-01	-13.55	1.39E-01	-4.57	
3.5	0.01	1.03E-02	3.81E-02	268.59	1.35E-02	30.76	9.16E-03	-11.34	7.42E-03	-28.18
	0.02	1.22E-02	3.14E-02	158.35	1.45E-02	19.40	1.07E-02	-11.99	9.77E-03	-19.62
	0.05	1.71E-02	2.75E-02	60.33	1.70E-02	-0.67	1.39E-02	-18.61	1.52E-02	-11.11
	0.1	2.15E-02	2.68E-02	25.09	1.97E-02	-7.98	1.73E-02	-19.15	2.09E-02	-2.54
	0.15	2.36E-02	2.68E-02	13.33	2.13E-02	-9.81	1.94E-02	-18.00	2.38E-02	0.65
	0.2	2.50E-02	2.68E-02	7.12	2.23E-02	-10.73	2.07E-02	-17.13	2.52E-02	0.71
	0.25	2.61E-02	2.68E-02	2.70	2.30E-02	-11.78	2.16E-02	-16.96	2.58E-02	-1.03
	0.3	2.62E-02	2.67E-02	2.10	2.35E-02	-10.37	2.23E-02	-14.80	2.60E-02	-0.64
	0.35	2.62E-02	2.67E-02	1.68	2.38E-02	-9.30	2.28E-02	-13.13	2.60E-02	-0.90
	0.4	2.63E-02	2.66E-02	1.18	2.40E-02	-8.61	2.31E-02	-11.97	2.58E-02	-1.76
	0.45	2.63E-02	2.65E-02	0.69	2.42E-02	-8.15	2.34E-02	-11.13	2.55E-02	-3.01
0.5	2.59E-02	2.64E-02	1.65	2.42E-02	-6.52	2.35E-02	-9.21	2.52E-02	-2.89	
4	0.01	1.68E-03	5.25E-03	212.60	2.04E-03	21.30	1.39E-03	-17.13	1.27E-03	-24.34
	0.02	1.95E-03	4.32E-03	121.48	2.16E-03	11.05	1.61E-03	-17.36	1.62E-03	-16.69
	0.05	2.58E-03	3.77E-03	46.12	2.50E-03	-3.21	2.07E-03	-19.82	2.40E-03	-6.94
	0.1	3.17E-03	3.68E-03	16.13	2.86E-03	-9.89	2.54E-03	-19.97	3.12E-03	-1.57
	0.15	3.38E-03	3.67E-03	8.72	3.06E-03	-9.49	2.81E-03	-16.88	3.43E-03	1.40
	0.2	3.56E-03	3.67E-03	3.29	3.18E-03	-10.48	2.98E-03	-16.15	3.55E-03	-0.20
	0.25	3.57E-03	3.67E-03	2.95	3.27E-03	-8.41	3.10E-03	-13.08	3.59E-03	0.78
	0.3	3.54E-03	3.66E-03	3.45	3.32E-03	-6.28	3.18E-03	-10.23	3.60E-03	1.63
	0.35	3.61E-03	3.66E-03	1.26	3.36E-03	-7.02	3.24E-03	-10.34	3.58E-03	-0.72
	0.4	3.66E-03	3.64E-03	-0.33	3.38E-03	-7.54	3.28E-03	-10.38	3.55E-03	-2.96
	0.45	3.64E-03	3.63E-03	-0.15	3.39E-03	-6.63	3.30E-03	-9.12	3.49E-03	-3.89
0.5	3.60E-03	3.61E-03	0.44	3.40E-03	-5.46	3.32E-03	-7.69	3.44E-03	-4.41	

ζ	ξ	ISEE	P	ε [%]	cVM	ε [%]	mVM	ε [%]	#6 NM	ε [%]
4.5	0.01	2.10E-04	5.62E-04	167.43	2.38E-04	13.08	1.64E-04	-22.03	1.65E-04	-21.47
	0.02	2.36E-04	4.62E-04	96.15	2.50E-04	6.08	1.88E-04	-20.22	2.05E-04	-12.99
	0.05	3.06E-04	4.03E-04	31.78	2.84E-04	-7.37	2.38E-04	-22.38	2.87E-04	-6.09
	0.1	3.58E-04	3.94E-04	9.98	3.20E-04	-10.68	2.87E-04	-19.82	3.54E-04	-1.07
	0.15	3.79E-04	3.93E-04	3.78	3.40E-04	-10.30	3.15E-04	-16.83	3.78E-04	-0.26
	0.2	3.90E-04	3.93E-04	0.78	3.52E-04	-9.81	3.33E-04	-14.80	3.86E-04	-1.11
	0.25	3.89E-04	3.93E-04	1.03	3.60E-04	-7.57	3.44E-04	-11.61	3.88E-04	-0.24
	0.3	3.87E-04	3.92E-04	1.40	3.64E-04	-5.82	3.52E-04	-9.17	3.88E-04	0.16
	0.35	3.92E-04	3.91E-04	-0.20	3.68E-04	-6.28	3.57E-04	-9.06	3.85E-04	-1.82
	0.4	3.87E-04	3.90E-04	0.74	3.69E-04	-4.61	3.60E-04	-7.01	3.80E-04	-1.79
	0.45	3.84E-04	3.89E-04	1.19	3.70E-04	-3.57	3.62E-04	-5.66	3.74E-04	-2.73
0.5	3.83E-04	3.87E-04	1.03	3.71E-04	-3.22	3.64E-04	-5.05	3.67E-04	-4.09	
5	0.01	1.96E-05	4.73E-05	141.54	2.16E-05	10.20	1.50E-05	-23.32	1.58E-05	-19.10
	0.02	2.22E-05	3.89E-05	75.17	2.25E-05	1.17	1.71E-05	-23.10	1.94E-05	-12.93
	0.05	2.75E-05	3.40E-05	23.50	2.51E-05	-8.72	2.13E-05	-22.66	2.61E-05	-4.99
	0.1	3.10E-05	3.32E-05	6.92	2.80E-05	-9.88	2.53E-05	-18.29	3.09E-05	-0.24
	0.15	3.26E-05	3.31E-05	1.58	2.95E-05	-9.55	2.76E-05	-15.40	3.24E-05	-0.73
	0.2	3.24E-05	3.31E-05	2.19	3.04E-05	-6.25	2.89E-05	-10.75	3.28E-05	1.10
	0.25	3.32E-05	3.31E-05	-0.46	3.09E-05	-6.97	2.98E-05	-10.43	3.28E-05	-1.23
	0.3	3.25E-05	3.30E-05	1.54	3.13E-05	-3.91	3.03E-05	-6.77	3.27E-05	0.67
	0.35	3.27E-05	3.29E-05	0.65	3.15E-05	-3.90	3.07E-05	-6.25	3.25E-05	-0.66
	0.4	3.29E-05	3.28E-05	-0.10	3.16E-05	-3.98	3.09E-05	-5.94	3.21E-05	-2.31
	0.45	3.17E-05	3.27E-05	3.11	3.16E-05	-0.38	3.11E-05	-2.12	3.16E-05	-0.48
	0.5	3.21E-05	3.26E-05	1.59	3.16E-05	-1.46	3.11E-05	-2.93	3.12E-05	-2.81
		μ_ε %	32.63	μ_ε %	-1.049	μ_ε %	-10.45	μ_ε %	-4.70	
		σ_ε %	65.77	σ_ε %	12.29	σ_ε %	7.09	σ_ε %	8.02	
		ε_{\max} %	319.65	ε_{\max} %	45.35	ε_{\max} %	3.74	ε_{\max} %	2.88	
		ε_{\min} %	-1.36	ε_{\min} %	-12.13	ε_{\min} %	-23.32	ε_{\min} %	-31.13	
		$\mu_{ \varepsilon }$ %	32.71	$\mu_{ \varepsilon }$ %	8.94	$\mu_{ \varepsilon }$ %	10.77	$\mu_{ \varepsilon }$ %	5.10	

D.2.7 Kanai-Tajimi and Shinozuka-Sato Time-modulating Function, $T = 1.0s$

Table D.14 - Proposed #6 NM: Time-variant FPDF computed at $t = 20s$ for linear elastic SDOF system with $T = 1.0s$ subjected to KT base excitation time modulated by a Shinozuka-Sato function.

ζ	ξ	ISEE	P	ε [%]	cVM	ε [%]	mVM	ε [%]	#6 NM	ε [%]
1.5	0.01	7.62E-01	9.99E-01	31.20	8.54E-01	12.07	7.27E-01	-4.51	6.02E-01	-20.97
	0.02	7.81E-01	9.97E-01	27.65	8.80E-01	12.60	7.84E-01	0.38	7.14E-01	-8.65
	0.05	8.81E-01	9.90E-01	12.41	9.13E-01	3.69	8.58E-01	-2.59	8.66E-01	-1.66
	0.1	9.40E-01	9.86E-01	4.88	9.43E-01	0.29	9.13E-01	-2.87	9.45E-01	0.48
	0.15	9.60E-01	9.85E-01	2.57	9.58E-01	-0.25	9.39E-01	-2.19	9.69E-01	0.88
	0.2	9.81E-01	9.85E-01	0.43	9.67E-01	-1.42	9.54E-01	-2.74	9.79E-01	-0.16
	0.25	9.62E-01	9.85E-01	2.35	9.72E-01	1.03	9.63E-01	0.04	9.84E-01	2.29
	0.3	9.87E-01	9.85E-01	-0.24	9.76E-01	-1.16	9.69E-01	-1.91	9.87E-01	-0.02
	0.35	1.00E+00	9.85E-01	-1.48	9.79E-01	-2.13	9.73E-01	-2.73	9.89E-01	-1.11
	0.4	9.98E-01	9.85E-01	-1.26	9.81E-01	-1.72	9.76E-01	-2.22	9.90E-01	-0.82
	0.45	9.95E-01	9.85E-01	-0.95	9.82E-01	-1.27	9.78E-01	-1.69	9.90E-01	-0.49
0.5	1.00E+00	9.85E-01	-1.46	9.83E-01	-1.66	9.80E-01	-2.02	9.90E-01	-1.00	
2	0.01	3.94E-01	9.21E-01	133.80	4.96E-01	25.79	3.72E-01	-5.54	2.83E-01	-28.11
	0.02	4.14E-01	8.59E-01	107.56	5.18E-01	25.16	4.15E-01	0.12	3.52E-01	-14.89
	0.05	4.94E-01	7.85E-01	58.96	5.59E-01	13.11	4.85E-01	-1.92	4.82E-01	-2.53
	0.1	6.03E-01	7.57E-01	25.52	6.07E-01	0.59	5.55E-01	-8.05	5.97E-01	-0.98
	0.15	6.53E-01	7.52E-01	15.08	6.39E-01	-2.17	5.99E-01	-8.30	6.60E-01	1.01
	0.2	7.00E-01	7.51E-01	7.25	6.62E-01	-5.54	6.29E-01	-10.16	6.98E-01	-0.38
	0.25	7.22E-01	7.52E-01	4.12	6.78E-01	-6.09	6.51E-01	-9.82	7.22E-01	-0.01
	0.3	7.32E-01	7.52E-01	2.76	6.90E-01	-5.73	6.67E-01	-8.87	7.37E-01	0.65
	0.35	7.56E-01	7.53E-01	-0.39	7.00E-01	-7.46	6.80E-01	-10.10	7.46E-01	-1.37
	0.4	7.59E-01	7.54E-01	-0.71	7.07E-01	-6.84	6.89E-01	-9.16	7.50E-01	-1.17
	0.45	7.55E-01	7.54E-01	-0.17	7.13E-01	-5.58	6.97E-01	-7.66	7.52E-01	-0.47
0.5	7.64E-01	7.54E-01	-1.25	7.18E-01	-6.00	7.04E-01	-7.86	7.53E-01	-1.51	
2.5	0.01	1.45E-01	4.96E-01	242.66	1.86E-01	28.71	1.32E-01	-8.89	9.97E-02	-31.12
	0.02	1.53E-01	4.10E-01	167.17	1.94E-01	26.21	1.48E-01	-3.77	1.25E-01	-18.55
	0.05	1.87E-01	3.39E-01	81.08	2.09E-01	11.80	1.75E-01	-6.28	1.76E-01	-6.25
	0.1	2.31E-01	3.17E-01	36.82	2.31E-01	-0.32	2.06E-01	-11.06	2.28E-01	-1.60
	0.15	2.58E-01	3.13E-01	21.21	2.46E-01	-4.49	2.26E-01	-12.17	2.60E-01	0.66
	0.2	2.81E-01	3.12E-01	11.22	2.58E-01	-8.18	2.41E-01	-14.00	2.80E-01	-0.30
	0.25	2.89E-01	3.12E-01	8.07	2.66E-01	-7.95	2.52E-01	-12.74	2.92E-01	1.12
	0.3	2.92E-01	3.13E-01	6.94	2.72E-01	-6.85	2.60E-01	-10.94	3.00E-01	2.46
	0.35	3.04E-01	3.13E-01	2.95	2.78E-01	-8.81	2.67E-01	-12.25	3.04E-01	-0.19
	0.4	3.15E-01	3.14E-01	-0.48	2.82E-01	-10.68	2.72E-01	-13.64	3.06E-01	-3.09
	0.45	3.12E-01	3.14E-01	0.64	2.85E-01	-8.72	2.77E-01	-11.40	3.06E-01	-1.99
0.5	3.15E-01	3.14E-01	-0.16	2.88E-01	-8.67	2.80E-01	-11.07	3.06E-01	-2.88	

ζ	ξ	ISEE	P	ε [%]	cVM	ε [%]	mVM	ε [%]	#6 NM	ε [%]
3	0.01	4.00E-02	1.37E-01	242.28	4.89E-02	22.37	3.41E-02	-14.59	2.73E-02	-31.74
	0.02	4.15E-02	1.07E-01	158.73	5.02E-02	20.98	3.79E-02	-8.53	3.37E-02	-18.65
	0.05	4.89E-02	8.53E-02	74.40	5.34E-02	9.16	4.47E-02	-8.70	4.64E-02	-5.10
	0.1	6.02E-02	7.86E-02	30.57	5.83E-02	-3.21	5.21E-02	-13.57	5.93E-02	-1.63
	0.15	6.71E-02	7.75E-02	15.43	6.20E-02	-7.59	5.72E-02	-14.84	6.67E-02	-0.56
	0.2	7.00E-02	7.73E-02	10.53	6.47E-02	-7.45	6.08E-02	-13.11	7.11E-02	1.60
	0.25	7.33E-02	7.74E-02	5.57	6.68E-02	-8.97	6.35E-02	-13.48	7.35E-02	0.25
	0.3	7.50E-02	7.76E-02	3.48	6.83E-02	-8.89	6.55E-02	-12.66	7.48E-02	-0.19
	0.35	7.57E-02	7.77E-02	2.69	6.95E-02	-8.18	6.71E-02	-11.41	7.54E-02	-0.33
	0.4	7.58E-02	7.79E-02	2.67	7.05E-02	-7.09	6.83E-02	-9.92	7.56E-02	-0.31
	0.45	7.60E-02	7.80E-02	2.60	7.12E-02	-6.27	6.93E-02	-8.78	7.55E-02	-0.68
0.5	7.82E-02	7.80E-02	-0.14	7.18E-02	-8.07	7.01E-02	-10.26	7.53E-02	-3.67	
3.5	0.01	8.32E-03	2.48E-02	198.02	9.57E-03	14.96	6.70E-03	-19.46	5.86E-03	-29.52
	0.02	8.63E-03	1.92E-02	123.13	9.68E-03	12.27	7.37E-03	-14.54	7.08E-03	-17.92
	0.05	1.00E-02	1.52E-02	51.65	1.01E-02	1.08	8.53E-03	-14.69	9.33E-03	-6.68
	0.1	1.18E-02	1.39E-02	17.90	1.09E-02	-8.08	9.78E-03	-17.15	1.14E-02	-3.50
	0.15	1.24E-02	1.37E-02	10.34	1.15E-02	-7.83	1.06E-02	-14.33	1.25E-02	0.33
	0.2	1.29E-02	1.37E-02	6.32	1.19E-02	-7.64	1.12E-02	-12.61	1.30E-02	1.07
	0.25	1.34E-02	1.37E-02	2.06	1.22E-02	-9.08	1.17E-02	-12.97	1.33E-02	-1.08
	0.3	1.35E-02	1.37E-02	1.75	1.24E-02	-7.76	1.20E-02	-11.00	1.34E-02	-0.63
	0.35	1.37E-02	1.38E-02	0.43	1.26E-02	-7.78	1.23E-02	-10.50	1.35E-02	-1.78
	0.4	1.40E-02	1.38E-02	-1.83	1.28E-02	-8.97	1.25E-02	-11.26	1.34E-02	-4.25
	0.45	1.36E-02	1.38E-02	1.79	1.29E-02	-4.89	1.26E-02	-6.97	1.34E-02	-1.26
0.5	1.36E-02	1.38E-02	1.93	1.30E-02	-4.18	1.27E-02	-6.02	1.33E-02	-1.68	
4	0.01	1.34E-03	3.39E-03	153.24	1.44E-03	7.35	1.02E-03	-24.13	9.81E-04	-26.70
	0.02	1.33E-03	2.63E-03	97.46	1.44E-03	7.83	1.10E-03	-17.05	1.15E-03	-13.67
	0.05	1.51E-03	2.07E-03	37.03	1.47E-03	-2.66	1.25E-03	-16.89	1.44E-03	-4.79
	0.1	1.69E-03	1.90E-03	12.40	1.55E-03	-8.00	1.41E-03	-16.20	1.67E-03	-1.27
	0.15	1.77E-03	1.87E-03	5.32	1.62E-03	-8.46	1.52E-03	-14.13	1.77E-03	-0.33
	0.2	1.83E-03	1.86E-03	2.10	1.68E-03	-8.25	1.60E-03	-12.48	1.81E-03	-0.71
	0.25	1.86E-03	1.87E-03	0.31	1.71E-03	-7.95	1.65E-03	-11.26	1.83E-03	-1.47
	0.3	1.84E-03	1.87E-03	1.84	1.74E-03	-5.21	1.69E-03	-7.95	1.84E-03	0.31
	0.35	1.86E-03	1.88E-03	0.62	1.76E-03	-5.38	1.72E-03	-7.64	1.84E-03	-1.03
	0.4	1.84E-03	1.88E-03	2.06	1.78E-03	-3.28	1.74E-03	-5.23	1.84E-03	-0.08
	0.45	1.86E-03	1.88E-03	1.24	1.79E-03	-3.48	1.76E-03	-5.15	1.83E-03	-1.63
0.5	1.84E-03	1.88E-03	2.34	1.80E-03	-1.97	1.78E-03	-3.44	1.82E-03	-1.27	

ζ	ξ	ISEE	P	ε [%]	cVM	ε [%]	mVM	ε [%]	#6 NM	ε [%]
4.5	0.01	1.62E-04	3.62E-04	123.41	1.67E-04	3.19	1.19E-04	-26.35	1.25E-04	-22.84
	0.02	1.64E-04	2.82E-04	71.83	1.65E-04	0.91	1.29E-04	-21.49	1.43E-04	-12.98
	0.05	1.74E-04	2.21E-04	27.54	1.66E-04	-4.35	1.43E-04	-17.39	1.69E-04	-2.48
	0.1	1.87E-04	2.03E-04	8.36	1.73E-04	-7.71	1.59E-04	-15.10	1.87E-04	-0.12
	0.15	1.93E-04	2.00E-04	3.79	1.79E-04	-6.88	1.70E-04	-11.90	1.94E-04	0.62
	0.2	1.95E-04	2.00E-04	2.11	1.84E-04	-5.79	1.77E-04	-9.48	1.97E-04	0.56
	0.25	2.00E-04	2.00E-04	-0.19	1.88E-04	-6.31	1.82E-04	-9.11	1.98E-04	-1.24
	0.3	1.99E-04	2.00E-04	0.63	1.90E-04	-4.45	1.86E-04	-6.70	1.98E-04	-0.39
	0.35	1.96E-04	2.01E-04	2.23	1.92E-04	-2.14	1.88E-04	-4.02	1.98E-04	0.92
	0.4	1.99E-04	2.01E-04	0.99	1.94E-04	-2.74	1.90E-04	-4.30	1.97E-04	-0.90
	0.45	1.97E-04	2.01E-04	1.98	1.95E-04	-1.34	1.92E-04	-2.67	1.96E-04	-0.80
0.5	2.05E-04	2.02E-04	-1.91	1.96E-04	-4.75	1.93E-04	-5.86	1.95E-04	-5.28	
5	0.01	1.53E-05	3.05E-05	99.24	1.52E-05	-0.82	1.09E-05	-28.52	1.19E-05	-22.32
	0.02	1.50E-05	2.37E-05	57.59	1.48E-05	-1.49	1.17E-05	-22.52	1.33E-05	-11.65
	0.05	1.55E-05	1.86E-05	20.01	1.46E-05	-5.85	1.28E-05	-17.79	1.52E-05	-2.12
	0.1	1.63E-05	1.71E-05	5.12	1.50E-05	-7.59	1.40E-05	-14.20	1.62E-05	-0.22
	0.15	1.64E-05	1.68E-05	2.84	1.55E-05	-5.45	1.47E-05	-9.87	1.65E-05	1.03
	0.2	1.64E-05	1.68E-05	2.15	1.58E-05	-3.87	1.53E-05	-7.04	1.66E-05	1.27
	0.25	1.66E-05	1.68E-05	1.25	1.61E-05	-3.36	1.57E-05	-5.75	1.67E-05	0.61
	0.3	1.70E-05	1.69E-05	-1.04	1.62E-05	-4.68	1.59E-05	-6.50	1.67E-05	-1.72
	0.35	1.69E-05	1.69E-05	-0.17	1.64E-05	-3.22	1.61E-05	-4.70	1.67E-05	-1.15
	0.4	1.66E-05	1.69E-05	1.81	1.65E-05	-0.83	1.63E-05	-2.07	1.67E-05	0.23
	0.45	1.68E-05	1.69E-05	0.91	1.66E-05	-1.36	1.64E-05	-2.39	1.66E-05	-1.42
0.5	1.66E-05	1.70E-05	1.92	1.66E-05	-0.10	1.65E-05	-0.99	1.65E-05	-0.92	
		μ_ε %	28.31	μ_ε %	-1.356	μ_ε %	-9.69	μ_ε %	-4.23	
		σ_ε %	53.52	σ_ε %	8.85	σ_ε %	5.94	σ_ε %	8.08	
		ε_{\max} %	242.66	ε_{\max} %	28.71	ε_{\max} %	0.38	ε_{\max} %	2.46	
		ε_{\min} %	-1.91	ε_{\min} %	-10.68	ε_{\min} %	-28.52	ε_{\min} %	-31.74	
		$\mu_{ \varepsilon }$ %	28.59	$\mu_{ \varepsilon }$ %	6.80	$\mu_{ \varepsilon }$ %	9.70	$\mu_{ \varepsilon }$ %	4.62	

D.3 COMPARISON OF THE PROPOSED #5 AND #6 NM

It is found that the Proposed #5 (see Table C.4) for the case of white noise base excitation from at-rest initial conditions also present significant improvements compared to other analytical approximations. Therefore, in this section the summary of the time-variant FPDF obtained using proposed #5 and proposed #6 NM (without proposed modifications see Section 2.3) are compared to determine the better approximation. It is found that for the case of Shinozuka-Sato time-modulating function, the proposed #5 and for the case of unit-step time-modulating function proposed #6 present smaller error values compared to analytical approximations (see

Section 2.3 for modification imposed when the modulating function present discontinuity at $t=0$).

Table D.15 - Summary of time-variant FPF obtained using the Proposed #5 and #6 NM.

PSD	Time Modulation	$T_0(s)$	ε [%]	P	cVM	mVM	#5	#6 NM
WN	Step	1	ε_{\max} %	176.24	35.26	9.10	4.78	3.83
			ε_{\min} %	-0.75	-9.23	-21.38	-17.99	-8.35
			$\mu_{ \varepsilon }$ %	22.48	6.32	7.70	2.46	4.09
	Shinozuka-Sato	1	ε_{\max} %	240.73	28.78	1.55	2.77	2.71
			ε_{\min} %	-1.23	-9.32	-27.46	-30.93	-30.25
			$\mu_{ \varepsilon }$ %	28.39	6.58	8.86	4.09	4.09
KT	Step	0.1	ε_{\max} %	129.44	34.90	14.16	10.91	39.37
			ε_{\min} %	-2.22	-12.44	-17.46	-4.11	-10.49
			$\mu_{ \varepsilon }$ %	16.90	7.72	8.85	2.10	5.65
		0.5	ε_{\max} %	187.19	27.68	1.27	3.22	2.28
			ε_{\min} %	-1.90	-11.98	-27.35	-30.99	-28.50
			$\mu_{ \varepsilon }$ %	24.25	7.09	11.92	4.97	5.09
		1	ε_{\max} %	179.36	35.31	8.67	2.58	2.11
			ε_{\min} %	-1.19	-9.89	-22.13	-18.46	-9.66
			$\mu_{ \varepsilon }$ %	22.60	6.71	8.48	2.63	1.95
	Shinozuka-Sato	0.1	ε_{\max} %	226.13	75.81	36.07	20.57	26.68
			ε_{\min} %	-2.72	-13.13	-19.60	-9.44	-7.91
			$\mu_{ \varepsilon }$ %	15.81	8.58	8.85	2.57	3.39
		0.5	ε_{\max} %	319.65	45.35	3.74	3.72	2.88
			ε_{\min} %	-1.36	-12.13	-23.32	-28.02	-31.13
			$\mu_{ \varepsilon }$ %	32.71	8.94	10.77	4.17	5.10
		1	ε_{\max} %	242.66	28.71	0.38	3.60	2.46
			ε_{\min} %	-1.91	-10.68	-28.52	-31.64	-31.74
			$\mu_{ \varepsilon }$ %	28.59	6.80	9.70	4.47	4.62

D.4 NEWLY PROPOSED APPROXIMATION

The parametric study results for the FPDF obtained using the Newly proposed approximation (see Section 2.2 and 2.3) and considering the corresponding modifications are presented in Tables D.4.1 through D.4.7.

D.4.1 White noise and Shinozuka-Sato Time-modulating Function, $T=1.0s$

Table D.16 - New: Time-variant FPDF computed at $t = 20s$ for SDOF systems with $T = 1.0s$ subjected to WN base excitation time modulated by a Shinozuka-Sato function.

ζ	ξ	ISEE	P	ε [%]	cVM	ε [%]	mVM	ε [%]	New	ε [%]
1.5	0.01	7.45E-01	9.99E-01	34.15	8.57E-01	15.04	7.33E-01	-1.62	6.37E-01	-14.44
	0.02	7.89E-01	9.97E-01	26.34	8.83E-01	11.81	7.89E-01	-0.04	7.26E-01	-7.97
	0.05	8.81E-01	9.90E-01	12.41	9.15E-01	3.89	8.61E-01	-2.21	8.63E-01	-1.97
	0.1	9.38E-01	9.85E-01	5.08	9.43E-01	0.59	9.14E-01	-2.47	9.42E-01	0.49
	0.15	9.71E-01	9.84E-01	1.30	9.58E-01	-1.40	9.40E-01	-3.25	9.67E-01	-0.41
	0.2	9.80E-01	9.83E-01	0.34	9.66E-01	-1.44	9.53E-01	-2.71	9.78E-01	-0.23
	0.25	9.80E-01	9.83E-01	0.35	9.71E-01	-0.87	9.62E-01	-1.80	9.83E-01	0.35
	0.3	9.60E-01	9.83E-01	2.40	9.75E-01	1.54	9.68E-01	0.80	9.86E-01	2.71
	0.35	9.70E-01	9.83E-01	1.30	9.77E-01	0.72	9.72E-01	0.13	9.88E-01	1.77
	0.4	9.90E-01	9.83E-01	-0.70	9.79E-01	-1.07	9.75E-01	-1.54	9.88E-01	-0.15
	0.45	9.84E-01	9.83E-01	-0.12	9.81E-01	-0.34	9.77E-01	-0.74	9.89E-01	0.45
0.5	9.92E-01	9.83E-01	-0.88	9.82E-01	-0.98	9.79E-01	-1.32	9.89E-01	-0.31	
2	0.01	3.90E-01	9.21E-01	136.15	5.00E-01	28.16	3.77E-01	-3.38	3.21E-01	-17.62
	0.02	4.13E-01	8.59E-01	108.08	5.22E-01	26.48	4.19E-01	1.55	3.73E-01	-9.53
	0.05	4.99E-01	7.83E-01	56.83	5.61E-01	12.37	4.88E-01	-2.24	4.87E-01	-2.48
	0.1	5.95E-01	7.53E-01	26.53	6.07E-01	2.02	5.56E-01	-6.47	5.99E-01	0.69
	0.15	6.46E-01	7.45E-01	15.38	6.37E-01	-1.35	5.99E-01	-7.29	6.59E-01	2.02
	0.2	6.92E-01	7.43E-01	7.36	6.58E-01	-4.91	6.28E-01	-9.34	6.95E-01	0.34
	0.25	7.26E-01	7.42E-01	2.16	6.73E-01	-7.35	6.48E-01	-10.83	7.16E-01	-1.42
	0.3	7.29E-01	7.42E-01	1.75	6.84E-01	-6.14	6.63E-01	-9.06	7.29E-01	0.03
	0.35	7.39E-01	7.41E-01	0.29	6.93E-01	-6.30	6.74E-01	-8.78	7.36E-01	-0.39
	0.4	7.48E-01	7.41E-01	-0.88	6.99E-01	-6.47	6.83E-01	-8.61	7.40E-01	-1.10
	0.45	7.49E-01	7.41E-01	-1.09	7.05E-01	-5.91	6.91E-01	-7.80	7.40E-01	-1.18
0.5	7.50E-01	7.41E-01	-1.23	7.09E-01	-5.43	6.97E-01	-7.11	7.40E-01	-1.30	

ζ	ξ	ISEE	P	ε [%]	cVM	ε [%]	mVM	ε [%]	New	ε [%]
2.5	0.01	1.46E-01	4.95E-01	238.92	1.88E-01	28.78	1.34E-01	-8.49	1.20E-01	-17.75
	0.02	1.55E-01	4.09E-01	163.23	1.95E-01	25.72	1.49E-01	-3.78	1.38E-01	-11.03
	0.05	1.85E-01	3.37E-01	81.89	2.10E-01	13.45	1.77E-01	-4.53	1.81E-01	-2.32
	0.1	2.30E-01	3.13E-01	36.33	2.30E-01	0.30	2.06E-01	-10.17	2.30E-01	0.17
	0.15	2.56E-01	3.08E-01	20.24	2.45E-01	-4.35	2.26E-01	-11.70	2.59E-01	1.38
	0.2	2.72E-01	3.06E-01	12.49	2.55E-01	-6.25	2.40E-01	-11.88	2.77E-01	1.89
	0.25	2.86E-01	3.05E-01	6.73	2.62E-01	-8.24	2.50E-01	-12.70	2.88E-01	0.56
	0.3	2.96E-01	3.05E-01	3.16	2.68E-01	-9.32	2.57E-01	-12.99	2.93E-01	-0.73
	0.35	2.93E-01	3.05E-01	4.17	2.72E-01	-6.88	2.63E-01	-10.09	2.96E-01	1.27
	0.4	2.98E-01	3.05E-01	2.17	2.76E-01	-7.48	2.68E-01	-10.23	2.97E-01	-0.35
	0.45	2.99E-01	3.05E-01	1.89	2.79E-01	-6.76	2.71E-01	-9.19	2.97E-01	-0.69
0.5	3.02E-01	3.05E-01	0.98	2.81E-01	-6.80	2.75E-01	-8.95	2.96E-01	-1.72	
3	0.01	4.01E-02	1.37E-01	240.73	4.94E-02	23.33	3.46E-02	-13.59	3.36E-02	-16.12
	0.02	4.17E-02	1.07E-01	156.43	5.06E-02	21.32	3.84E-02	-7.91	3.82E-02	-8.47
	0.05	4.95E-02	8.47E-02	71.03	5.36E-02	8.21	4.50E-02	-9.12	4.84E-02	-2.38
	0.1	5.87E-02	7.76E-02	32.32	5.81E-02	-0.91	5.21E-02	-11.15	5.99E-02	2.07
	0.15	6.50E-02	7.61E-02	17.13	6.15E-02	-5.31	5.69E-02	-12.39	6.65E-02	2.31
	0.2	6.94E-02	7.56E-02	8.98	6.39E-02	-7.88	6.02E-02	-13.17	7.01E-02	0.99
	0.25	7.16E-02	7.54E-02	5.26	6.56E-02	-8.40	6.26E-02	-12.60	7.19E-02	0.40
	0.3	7.19E-02	7.53E-02	4.68	6.69E-02	-7.00	6.44E-02	-10.50	7.28E-02	1.22
	0.35	7.25E-02	7.53E-02	3.77	6.79E-02	-6.39	6.57E-02	-9.35	7.31E-02	0.84
	0.4	7.44E-02	7.52E-02	1.18	6.87E-02	-7.65	6.68E-02	-10.15	7.31E-02	-1.72
	0.45	7.32E-02	7.52E-02	2.78	6.93E-02	-5.31	6.77E-02	-7.53	7.28E-02	-0.51
0.5	7.43E-02	7.52E-02	1.27	6.98E-02	-6.00	6.84E-02	-7.93	7.25E-02	-2.33	
3.5	0.01	8.28E-03	2.48E-02	199.02	9.67E-03	16.77	6.80E-03	-17.86	7.01E-03	-15.31
	0.02	8.63E-03	1.92E-02	122.33	9.77E-03	13.16	7.46E-03	-13.52	7.95E-03	-7.89
	0.05	1.00E-02	1.51E-02	50.24	1.01E-02	1.17	8.59E-03	-14.26	9.70E-03	-3.16
	0.1	1.14E-02	1.37E-02	20.81	1.08E-02	-4.93	9.78E-03	-13.96	1.15E-02	0.78
	0.15	1.23E-02	1.35E-02	8.97	1.13E-02	-8.18	1.06E-02	-14.32	1.23E-02	0.00
	0.2	1.27E-02	1.34E-02	5.56	1.17E-02	-7.54	1.11E-02	-12.19	1.28E-02	0.81
	0.25	1.29E-02	1.33E-02	3.01	1.20E-02	-7.51	1.15E-02	-11.15	1.29E-02	0.05
	0.3	1.31E-02	1.33E-02	1.87	1.22E-02	-6.95	1.18E-02	-9.90	1.30E-02	-0.41
	0.35	1.32E-02	1.33E-02	1.03	1.23E-02	-6.55	1.20E-02	-9.00	1.30E-02	-1.16
	0.4	1.30E-02	1.33E-02	2.24	1.24E-02	-4.52	1.21E-02	-6.63	1.30E-02	-0.28
	0.45	1.31E-02	1.33E-02	1.53	1.25E-02	-4.48	1.23E-02	-6.29	1.29E-02	-1.53
0.5	1.29E-02	1.33E-02	2.75	1.26E-02	-2.76	1.24E-02	-4.35	1.28E-02	-0.87	

ζ	ξ	ISEE	P	ε [%]	cVM	ε [%]	mVM	ε [%]	New	ε [%]	
4	0.01	1.33E-03	3.38E-03	154.94	1.45E-03	9.36	1.03E-03	-22.39	1.09E-03	-17.68	
	0.02	1.32E-03	2.62E-03	98.75	1.45E-03	9.73	1.12E-03	-15.24	1.24E-03	-5.73	
	0.05	1.51E-03	2.05E-03	36.22	1.47E-03	-2.32	1.26E-03	-16.25	1.48E-03	-1.95	
	0.1	1.65E-03	1.87E-03	13.42	1.55E-03	-6.40	1.41E-03	-14.41	1.67E-03	0.90	
	0.15	1.74E-03	1.83E-03	5.25	1.61E-03	-7.83	1.51E-03	-13.21	1.74E-03	0.14	
	0.2	1.79E-03	1.82E-03	1.72	1.65E-03	-7.96	1.58E-03	-11.90	1.78E-03	-0.86	
	0.25	1.82E-03	1.82E-03	-0.21	1.68E-03	-7.84	1.62E-03	-10.86	1.79E-03	-1.89	
	0.3	1.78E-03	1.81E-03	2.12	1.70E-03	-4.37	1.66E-03	-6.85	1.79E-03	0.63	
	0.35	1.80E-03	1.81E-03	0.95	1.72E-03	-4.52	1.68E-03	-6.53	1.78E-03	-0.68	
	0.4	1.80E-03	1.81E-03	0.54	1.73E-03	-4.19	1.70E-03	-5.87	1.77E-03	-1.55	
	0.45	1.82E-03	1.81E-03	-0.41	1.74E-03	-4.55	1.71E-03	-5.96	1.76E-03	-3.17	
	0.5	1.80E-03	1.81E-03	0.62	1.74E-03	-3.12	1.72E-03	-4.35	1.75E-03	-2.78	
4.5	0.01	1.61E-04	3.62E-04	124.53	1.69E-04	4.92	1.21E-04	-24.81	1.29E-04	-19.90	
	0.02	1.60E-04	2.81E-04	75.51	1.67E-04	4.15	1.30E-04	-18.64	1.47E-04	-8.33	
	0.05	1.72E-04	2.20E-04	27.58	1.66E-04	-3.49	1.44E-04	-16.31	1.71E-04	-0.58	
	0.1	1.85E-04	2.00E-04	8.53	1.72E-04	-6.90	1.59E-04	-14.02	1.86E-04	0.76	
	0.15	1.93E-04	1.96E-04	1.41	1.77E-04	-8.43	1.68E-04	-13.07	1.91E-04	-1.42	
	0.2	1.94E-04	1.95E-04	0.22	1.81E-04	-7.00	1.74E-04	-10.35	1.92E-04	-1.20	
	0.25	1.93E-04	1.94E-04	0.89	1.83E-04	-4.80	1.78E-04	-7.37	1.92E-04	-0.12	
	0.3	1.91E-04	1.94E-04	1.57	1.85E-04	-3.09	1.81E-04	-5.12	1.92E-04	0.58	
	0.35	1.91E-04	1.94E-04	1.74	1.87E-04	-2.17	1.83E-04	-3.80	1.92E-04	0.48	
	0.4	1.95E-04	1.94E-04	-0.55	1.88E-04	-3.81	1.85E-04	-5.13	1.90E-04	-2.32	
	0.45	1.92E-04	1.94E-04	1.24	1.88E-04	-1.66	1.86E-04	-2.78	1.89E-04	-1.32	
	0.5	1.93E-04	1.94E-04	0.65	1.89E-04	-1.89	1.87E-04	-2.84	1.88E-04	-2.46	
5	0.01	1.53E-05	3.04E-05	99.11	1.53E-05	0.22	1.11E-05	-27.46	1.18E-05	-22.94	
	0.02	1.50E-05	2.36E-05	57.34	1.49E-05	-0.67	1.18E-05	-21.54	1.32E-05	-11.93	
	0.05	1.57E-05	1.85E-05	17.71	1.46E-05	-6.93	1.28E-05	-18.40	1.51E-05	-3.71	
	0.1	1.63E-05	1.69E-05	3.22	1.49E-05	-8.69	1.39E-05	-14.91	1.60E-05	-1.83	
	0.15	1.62E-05	1.65E-05	2.12	1.53E-05	-5.61	1.46E-05	-9.73	1.62E-05	0.40	
	0.2	1.64E-05	1.64E-05	0.29	1.55E-05	-5.17	1.50E-05	-8.03	1.63E-05	-0.53	
	0.25	1.61E-05	1.64E-05	1.31	1.57E-05	-2.89	1.53E-05	-5.04	1.63E-05	0.70	
	0.3	1.63E-05	1.63E-05	0.25	1.58E-05	-3.06	1.55E-05	-4.69	1.62E-05	-0.40	
	0.35	1.63E-05	1.63E-05	0.11	1.59E-05	-2.60	1.57E-05	-3.89	1.62E-05	-0.79	
	0.4	1.60E-05	1.63E-05	1.89	1.60E-05	-0.43	1.58E-05	-1.49	1.61E-05	0.48	
	0.45	1.60E-05	1.63E-05	2.21	1.60E-05	0.21	1.59E-05	-0.66	1.60E-05	0.17	
	0.5	1.63E-05	1.63E-05	0.38	1.60E-05	-1.33	1.59E-05	-2.05	1.59E-05	-1.99	
				μ_ε %	28.27	μ_ε %	-0.673	μ_ε %	-8.81	μ_ε %	-2.57
				σ_ε %	53.27	σ_ε %	8.93	σ_ε %	5.74	σ_ε %	5.38
				ε_{\max} %	240.73	ε_{\max} %	28.78	ε_{\max} %	1.55	ε_{\max} %	2.71
				ε_{\min} %	-1.23	ε_{\min} %	-9.32	ε_{\min} %	-27.46	ε_{\min} %	-22.94
				$\mu_{ \varepsilon }$ %	28.39	$\mu_{ \varepsilon }$ %	6.58	$\mu_{ \varepsilon }$ %	8.86	$\mu_{ \varepsilon }$ %	3.17

D.4.2 Kanai-Tajimi and Unit-step Time-modulating Function, $T = 0.1s$

Table D.17 - New: Time-variant FFP computed at $t = 1.0s$ for linear elastic SDOF system with $T = 0.1s$ subjected to KT base excitation from at-rest initial conditions.

ζ	ξ	ISEE	P	ε [%]	cVM	ε [%]	mVM	ε [%]	New	ε [%]
1.5	0.01	4.87E-01	8.66E-01	77.82	6.39E-01	31.17	5.57E-01	14.32	5.64E-01	15.72
	0.02	7.77E-01	9.74E-01	25.42	8.67E-01	11.61	8.06E-01	3.70	8.17E-01	5.21
	0.05	9.41E-01	9.93E-01	5.50	9.63E-01	2.27	9.38E-01	-0.35	9.58E-01	1.75
	0.1	9.95E-01	9.94E-01	-0.13	9.79E-01	-1.61	9.66E-01	-2.90	9.84E-01	-1.11
	0.15	9.88E-01	9.92E-01	0.41	9.81E-01	-0.71	9.71E-01	-1.71	9.88E-01	0.00
	0.2	9.90E-01	9.90E-01	0.00	9.81E-01	-0.95	9.72E-01	-1.85	9.89E-01	-0.13
	0.25	9.98E-01	9.88E-01	-1.02	9.79E-01	-1.87	9.71E-01	-2.71	9.89E-01	-0.94
	0.3	9.95E-01	9.85E-01	-1.00	9.78E-01	-1.78	9.69E-01	-2.61	9.88E-01	-0.75
	0.35	9.94E-01	9.83E-01	-1.07	9.76E-01	-1.80	9.68E-01	-2.62	9.87E-01	-0.67
	0.4	9.86E-01	9.81E-01	-0.60	9.74E-01	-1.28	9.66E-01	-2.11	9.86E-01	-0.05
	0.45	9.79E-01	9.78E-01	-0.15	9.72E-01	-0.78	9.63E-01	-1.63	9.85E-01	0.54
	0.5	9.95E-01	9.75E-01	-1.95	9.70E-01	-2.53	9.61E-01	-3.38	9.83E-01	-1.15
2	0.01	1.60E-01	3.74E-01	133.71	2.18E-01	36.11	1.79E-01	12.05	1.78E-01	11.16
	0.02	3.88E-01	6.97E-01	79.72	4.79E-01	23.34	4.13E-01	6.45	4.18E-01	7.77
	0.05	6.84E-01	8.55E-01	25.04	7.06E-01	3.26	6.50E-01	-5.01	6.92E-01	1.12
	0.1	8.05E-01	8.72E-01	8.31	7.71E-01	-4.22	7.30E-01	-9.25	7.90E-01	-1.86
	0.15	8.41E-01	8.63E-01	2.68	7.81E-01	-7.16	7.47E-01	-11.13	8.11E-01	-3.59
	0.2	8.31E-01	8.52E-01	2.50	7.78E-01	-6.30	7.49E-01	-9.86	8.14E-01	-2.06
	0.25	8.50E-01	8.39E-01	-1.29	7.72E-01	-9.18	7.45E-01	-12.37	8.10E-01	-4.67
	0.3	8.06E-01	8.27E-01	2.57	7.64E-01	-5.21	7.39E-01	-8.37	8.04E-01	-0.21
	0.35	8.21E-01	8.15E-01	-0.72	7.56E-01	-7.96	7.32E-01	-10.90	7.97E-01	-2.89
	0.4	8.01E-01	8.04E-01	0.47	7.47E-01	-6.63	7.24E-01	-9.52	7.90E-01	-1.32
	0.45	8.02E-01	7.94E-01	-0.99	7.39E-01	-7.80	7.17E-01	-10.59	7.82E-01	-2.42
	0.5	7.97E-01	7.84E-01	-1.56	7.32E-01	-8.17	7.10E-01	-10.88	7.75E-01	-2.71
2.5	0.01	3.30E-02	7.61E-02	130.61	4.41E-02	33.48	3.59E-02	8.74	3.50E-02	6.00
	0.02	1.31E-01	2.60E-01	98.44	1.59E-01	21.65	1.33E-01	1.88	1.34E-01	2.07
	0.05	3.15E-01	4.44E-01	40.87	3.20E-01	1.58	2.84E-01	-9.82	3.09E-01	-1.78
	0.1	4.16E-01	4.79E-01	15.19	3.80E-01	-8.54	3.50E-01	-15.77	3.95E-01	-5.04
	0.15	4.26E-01	4.73E-01	10.93	3.90E-01	-8.45	3.65E-01	-14.38	4.14E-01	-2.85
	0.2	4.34E-01	4.60E-01	5.96	3.88E-01	-10.66	3.66E-01	-15.73	4.15E-01	-4.29
	0.25	4.29E-01	4.46E-01	4.04	3.81E-01	-11.06	3.62E-01	-15.65	4.11E-01	-4.26
	0.3	4.16E-01	4.33E-01	4.19	3.74E-01	-10.07	3.56E-01	-14.38	4.03E-01	-2.94
	0.35	4.12E-01	4.21E-01	2.30	3.66E-01	-11.05	3.49E-01	-15.07	3.96E-01	-3.88
	0.4	4.03E-01	4.10E-01	1.72	3.58E-01	-11.05	3.43E-01	-14.88	3.87E-01	-3.86
	0.45	3.81E-01	4.00E-01	5.04	3.51E-01	-7.72	3.37E-01	-11.53	3.80E-01	-0.13
	0.5	3.78E-01	3.91E-01	3.29	3.45E-01	-8.89	3.31E-01	-12.52	3.74E-01	-1.22

ζ	ξ	ISEE	P	ε [%]	cVM	ε [%]	mVM	ε [%]	New	ε [%]
3	0.01	5.02E-03	9.68E-03	93.05	6.00E-03	19.73	4.92E-03	-1.89	4.75E-03	-5.33
	0.02	3.08E-02	5.66E-02	83.73	3.56E-02	15.49	2.97E-02	-3.51	2.95E-02	-4.23
	0.05	9.30E-02	1.30E-01	39.45	9.27E-02	-0.27	8.18E-02	-12.05	8.93E-02	-4.00
	0.1	1.29E-01	1.49E-01	15.32	1.17E-01	-9.19	1.07E-01	-16.74	1.22E-01	-5.61
	0.15	1.36E-01	1.48E-01	9.07	1.21E-01	-10.49	1.13E-01	-16.52	1.29E-01	-4.89
	0.2	1.34E-01	1.44E-01	7.18	1.21E-01	-9.95	1.14E-01	-15.19	1.29E-01	-3.50
	0.25	1.31E-01	1.39E-01	6.12	1.18E-01	-9.45	1.12E-01	-14.18	1.27E-01	-2.63
	0.3	1.27E-01	1.34E-01	4.86	1.15E-01	-9.53	1.10E-01	-13.87	1.24E-01	-2.73
	0.35	1.22E-01	1.29E-01	5.74	1.12E-01	-8.01	1.07E-01	-12.12	1.21E-01	-1.00
	0.4	1.18E-01	1.25E-01	5.61	1.09E-01	-7.52	1.05E-01	-11.42	1.18E-01	-0.27
	0.45	1.18E-01	1.21E-01	2.49	1.06E-01	-9.78	1.02E-01	-13.40	1.15E-01	-2.48
0.5	1.12E-01	1.17E-01	4.40	1.04E-01	-7.68	9.98E-02	-11.23	1.12E-01	-0.04	
3.5	0.01	4.97E-04	8.67E-04	74.25	5.77E-04	16.05	4.78E-04	-3.98	4.58E-04	-7.83
	0.02	5.30E-03	8.67E-03	63.67	5.80E-03	9.43	4.88E-03	-7.91	4.81E-03	-9.16
	0.05	1.99E-02	2.54E-02	27.67	1.90E-02	-4.37	1.69E-02	-15.13	1.83E-02	-7.92
	0.1	2.76E-02	3.05E-02	10.79	2.50E-02	-9.32	2.31E-02	-16.31	2.59E-02	-6.13
	0.15	2.86E-02	3.08E-02	7.62	2.62E-02	-8.55	2.46E-02	-14.16	2.76E-02	-3.55
	0.2	2.80E-02	3.00E-02	7.05	2.60E-02	-7.08	2.47E-02	-11.93	2.76E-02	-1.38
	0.25	2.71E-02	2.89E-02	6.50	2.54E-02	-6.26	2.43E-02	-10.60	2.70E-02	-0.50
	0.3	2.60E-02	2.78E-02	6.97	2.47E-02	-4.92	2.37E-02	-8.92	2.63E-02	1.04
	0.35	2.53E-02	2.68E-02	5.87	2.40E-02	-5.19	2.31E-02	-8.88	2.56E-02	1.00
	0.4	2.43E-02	2.58E-02	6.21	2.33E-02	-4.34	2.24E-02	-7.83	2.49E-02	2.15
	0.45	2.39E-02	2.50E-02	4.48	2.26E-02	-5.46	2.18E-02	-8.71	2.42E-02	1.11
0.5	2.30E-02	2.42E-02	5.44	2.20E-02	-4.21	2.13E-02	-7.35	2.35E-02	2.51	
4	0.01	3.44E-05	5.60E-05	62.90	3.96E-05	15.26	3.31E-05	-3.62	3.17E-05	-7.69
	0.02	6.81E-04	1.00E-03	47.20	7.11E-04	4.46	6.04E-04	-11.26	5.94E-04	-12.79
	0.05	3.13E-03	3.71E-03	18.32	2.92E-03	-6.72	2.62E-03	-16.41	2.82E-03	-10.00
	0.1	4.35E-03	4.65E-03	6.90	3.97E-03	-8.72	3.69E-03	-14.98	4.09E-03	-5.97
	0.15	4.49E-03	4.75E-03	5.74	4.19E-03	-6.73	3.96E-03	-11.71	4.38E-03	-2.48
	0.2	4.32E-03	4.65E-03	7.63	4.18E-03	-3.35	3.99E-03	-7.68	4.38E-03	1.31
	0.25	4.24E-03	4.49E-03	6.03	4.08E-03	-3.66	3.92E-03	-7.44	4.28E-03	1.09
	0.3	4.10E-03	4.32E-03	5.38	3.96E-03	-3.45	3.82E-03	-6.86	4.17E-03	1.58
	0.35	3.89E-03	4.16E-03	6.82	3.83E-03	-1.52	3.71E-03	-4.72	4.04E-03	3.84
	0.4	3.79E-03	4.01E-03	5.69	3.71E-03	-2.10	3.60E-03	-5.06	3.92E-03	3.36
	0.45	3.67E-03	3.87E-03	5.55	3.60E-03	-1.86	3.50E-03	-4.64	3.80E-03	3.65
0.5	3.56E-03	3.75E-03	5.37	3.49E-03	-1.72	3.40E-03	-4.35	3.69E-03	3.74	

ζ	ξ	ISEE	P	ε [%]	cVM	ε [%]	mVM	ε [%]	New	ε [%]
4.5	0.01	1.68E-06	2.61E-06	55.51	1.94E-06	15.73	1.64E-06	-2.21	1.57E-06	-6.36
	0.02	6.54E-05	8.90E-05	36.01	6.64E-05	1.54	5.70E-05	-12.89	5.59E-05	-14.58
	0.05	3.67E-04	4.19E-04	14.10	3.45E-04	-6.05	3.12E-04	-14.97	3.34E-04	-9.10
	0.1	5.09E-04	5.45E-04	7.18	4.82E-04	-5.25	4.53E-04	-10.96	4.94E-04	-2.83
	0.15	5.21E-04	5.64E-04	8.26	5.13E-04	-1.60	4.89E-04	-6.12	5.32E-04	2.09
	0.2	5.19E-04	5.56E-04	7.09	5.13E-04	-1.19	4.94E-04	-4.95	5.32E-04	2.53
	0.25	5.08E-04	5.39E-04	6.02	5.02E-04	-1.22	4.85E-04	-4.46	5.22E-04	2.79
	0.3	4.80E-04	5.18E-04	7.98	4.86E-04	1.29	4.72E-04	-1.67	5.07E-04	5.67
	0.35	4.53E-04	4.99E-04	9.98	4.70E-04	3.68	4.57E-04	0.92	4.91E-04	8.30
	0.4	4.46E-04	4.80E-04	7.70	4.54E-04	1.92	4.43E-04	-0.59	4.74E-04	6.46
	0.45	4.37E-04	4.63E-04	5.84	4.39E-04	0.47	4.29E-04	-1.84	4.59E-04	4.86
0.5	4.13E-04	4.48E-04	8.36	4.26E-04	3.12	4.17E-04	0.89	4.44E-04	7.48	
5	0.01	5.81E-08	8.81E-08	51.50	6.84E-08	17.62	5.84E-08	0.41	5.59E-08	-3.75
	0.02	4.58E-06	6.07E-06	32.60	4.73E-06	3.28	4.10E-06	-10.54	4.01E-06	-12.36
	0.05	3.36E-05	3.69E-05	9.83	3.15E-05	-6.32	2.88E-05	-14.42	3.06E-05	-9.11
	0.1	4.68E-05	4.98E-05	6.36	4.52E-05	-3.39	4.28E-05	-8.48	4.62E-05	-1.32
	0.15	4.86E-05	5.22E-05	7.29	4.85E-05	-0.23	4.66E-05	-4.15	4.99E-05	2.55
	0.2	4.83E-05	5.18E-05	7.26	4.88E-05	0.98	4.72E-05	-2.24	5.03E-05	4.09
	0.25	4.66E-05	5.03E-05	7.84	4.77E-05	2.35	4.64E-05	-0.44	4.93E-05	5.83
	0.3	4.47E-05	4.84E-05	8.19	4.62E-05	3.26	4.51E-05	0.77	4.78E-05	6.93
	0.35	4.35E-05	4.65E-05	6.84	4.46E-05	2.38	4.36E-05	0.16	4.62E-05	6.03
	0.4	4.08E-05	4.47E-05	9.54	4.30E-05	5.29	4.21E-05	3.19	4.45E-05	8.95
	0.45	4.01E-05	4.31E-05	7.55	4.15E-05	3.62	4.08E-05	1.70	4.29E-05	7.07
	0.5	3.95E-05	4.16E-05	5.36	4.02E-05	1.71	3.95E-05	-0.05	4.15E-05	4.93
		μ_ε %	17.68	μ_ε %	-0.593	μ_ε %	-6.96	μ_ε %	-0.67	
		σ_ε %	28.17	σ_ε %	9.86	σ_ε %	6.67	σ_ε %	5.26	
		ε_{\max} %	133.71	ε_{\max} %	36.11	ε_{\max} %	14.32	ε_{\max} %	15.72	
		ε_{\min} %	-1.95	ε_{\min} %	-11.06	ε_{\min} %	-16.74	ε_{\min} %	-14.58	
		$\mu_{ \varepsilon }$ %	17.90	$\mu_{ \varepsilon }$ %	7.12	$\mu_{ \varepsilon }$ %	8.11	$\mu_{ \varepsilon }$ %	4.09	

D.4.3 Kanai-Tajimi and Unit-step Time-modulating Function, $T = 0.5s$

Table D.18 - New: Time-variant FFP computed at $t = 1.0s$ for linear elastic SDOF system with $T = 0.5s$ subjected to KT base excitation from at-rest initial conditions.

ζ	ξ	ISEE	P	ε [%]	cVM	ε [%]	mVM	ε [%]	New	ε [%]
1.5	0.01	3.97E-01	8.44E-01	112.50	4.96E-01	24.93	3.94E-01	-0.85	3.67E-01	-7.46
	0.02	6.74E-01	9.72E-01	44.26	7.64E-01	13.44	6.60E-01	-2.10	6.17E-01	-8.40
	0.05	9.13E-01	9.95E-01	8.96	9.34E-01	2.24	8.82E-01	-3.40	9.13E-01	-0.03
	0.1	9.94E-01	9.97E-01	0.39	9.77E-01	-1.62	9.58E-01	-3.62	9.67E-01	-2.71
	0.15	1.00E+00	9.98E-01	-0.68	9.88E-01	-1.64	9.78E-01	-2.64	9.88E-01	-1.69
	0.2	1.00E+00	9.98E-01	-0.53	9.93E-01	-1.09	9.87E-01	-1.68	9.94E-01	-0.92
	0.25	1.01E+00	9.98E-01	-1.13	9.95E-01	-1.48	9.91E-01	-1.87	9.97E-01	-1.27
	0.3	9.91E-01	9.98E-01	0.79	9.96E-01	0.54	9.93E-01	0.26	9.98E-01	0.76
	0.35	9.93E-01	9.98E-01	0.50	9.97E-01	0.34	9.95E-01	0.13	9.99E-01	0.53
	0.4	9.97E-01	9.98E-01	0.15	9.97E-01	0.03	9.96E-01	-0.13	9.99E-01	0.21
	0.45	1.01E+00	9.98E-01	-0.78	9.98E-01	-0.86	9.96E-01	-0.99	9.99E-01	-0.70
0.5	9.91E-01	9.98E-01	0.73	9.98E-01	0.68	9.97E-01	0.56	9.99E-01	0.83	
2	0.01	1.20E-01	3.39E-01	182.15	1.49E-01	24.35	1.12E-01	-6.92	1.09E-01	-9.49
	0.02	3.06E-01	6.80E-01	122.13	3.72E-01	21.55	2.94E-01	-3.82	2.77E-01	-9.61
	0.05	5.94E-01	8.69E-01	46.43	6.39E-01	7.66	5.56E-01	-6.37	6.31E-01	6.30
	0.1	7.91E-01	9.09E-01	14.92	7.68E-01	-2.92	7.09E-01	-10.40	7.41E-01	-6.29
	0.15	8.62E-01	9.20E-01	6.73	8.19E-01	-4.91	7.76E-01	-9.98	8.25E-01	-4.30
	0.2	8.81E-01	9.25E-01	4.90	8.47E-01	-3.84	8.13E-01	-7.70	8.68E-01	-1.50
	0.25	9.12E-01	9.27E-01	1.62	8.65E-01	-5.19	8.37E-01	-8.21	8.93E-01	-2.09
	0.3	9.22E-01	9.29E-01	0.70	8.77E-01	-4.90	8.54E-01	-7.40	9.09E-01	-1.45
	0.35	9.04E-01	9.29E-01	2.84	8.85E-01	-2.04	8.65E-01	-4.22	9.18E-01	1.64
	0.4	9.44E-01	9.29E-01	-1.49	8.91E-01	-5.54	8.74E-01	-7.37	9.25E-01	-2.01
	0.45	9.46E-01	9.29E-01	-1.73	8.96E-01	-5.28	8.80E-01	-6.90	9.28E-01	-1.83
0.5	9.23E-01	9.29E-01	0.63	8.99E-01	-2.61	8.85E-01	-4.09	9.31E-01	0.80	
2.5	0.01	2.40E-02	6.43E-02	168.01	2.83E-02	18.05	2.10E-02	-12.61	2.22E-02	-7.27
	0.02	9.74E-02	2.44E-01	150.46	1.16E-01	18.95	8.87E-02	-8.92	8.93E-02	-8.31
	0.05	2.58E-01	4.57E-01	77.30	2.77E-01	7.26	2.30E-01	-11.01	2.90E-01	12.23
	0.1	3.94E-01	5.29E-01	34.13	3.80E-01	-3.68	3.36E-01	-14.88	3.78E-01	-4.21
	0.15	4.58E-01	5.51E-01	20.29	4.29E-01	-6.43	3.91E-01	-14.69	4.51E-01	-1.49
	0.2	5.01E-01	5.62E-01	12.08	4.58E-01	-8.57	4.26E-01	-15.06	4.96E-01	-1.15
	0.25	5.32E-01	5.68E-01	6.72	4.78E-01	-10.12	4.50E-01	-15.44	5.23E-01	-1.66
	0.3	5.44E-01	5.72E-01	4.97	4.92E-01	-9.55	4.68E-01	-14.12	5.41E-01	-0.62
	0.35	5.58E-01	5.74E-01	2.82	5.03E-01	-9.85	4.81E-01	-13.82	5.52E-01	-1.00
	0.4	5.61E-01	5.75E-01	2.36	5.11E-01	-9.03	4.91E-01	-12.57	5.59E-01	-0.41
	0.45	5.67E-01	5.75E-01	1.40	5.16E-01	-8.89	4.98E-01	-12.07	5.63E-01	-0.74
0.5	5.80E-01	5.74E-01	-1.00	5.21E-01	-10.25	5.04E-01	-13.09	5.64E-01	-2.81	

ζ	ξ	ISEE	P	ε [%]	cVM	ε [%]	mVM	ε [%]	New	ε [%]
3	0.01	3.34E-03	7.66E-03	129.25	3.67E-03	9.85	2.73E-03	-18.30	3.20E-03	-4.38
	0.02	2.23E-02	5.15E-02	130.52	2.52E-02	12.80	1.92E-02	-13.97	2.12E-02	-4.94
	0.05	7.56E-02	1.34E-01	77.18	7.94E-02	4.97	6.51E-02	-13.87	8.89E-02	17.49
	0.1	1.26E-01	1.69E-01	34.14	1.18E-01	-6.12	1.03E-01	-17.93	1.25E-01	-0.92
	0.15	1.50E-01	1.80E-01	19.92	1.37E-01	-8.84	1.24E-01	-17.65	1.51E-01	0.72
	0.2	1.67E-01	1.86E-01	11.20	1.49E-01	-11.13	1.37E-01	-18.07	1.67E-01	-0.20
	0.25	1.80E-01	1.89E-01	4.85	1.56E-01	-13.31	1.46E-01	-18.95	1.76E-01	-2.39
	0.3	1.85E-01	1.91E-01	3.61	1.62E-01	-12.20	1.53E-01	-17.08	1.82E-01	-1.52
	0.35	1.87E-01	1.92E-01	2.91	1.66E-01	-11.14	1.58E-01	-15.43	1.85E-01	-1.02
	0.4	1.91E-01	1.93E-01	1.25	1.69E-01	-11.28	1.62E-01	-15.05	1.87E-01	-2.01
	0.45	1.91E-01	1.93E-01	1.21	1.71E-01	-10.26	1.65E-01	-13.67	1.88E-01	-1.82
0.5	1.92E-01	1.93E-01	0.75	1.73E-01	-9.80	1.67E-01	-12.88	1.87E-01	-2.32	
3.5	0.01	3.24E-04	6.41E-04	97.98	3.35E-04	3.47	2.51E-04	-22.38	3.12E-04	-3.50
	0.02	3.80E-03	7.66E-03	101.26	4.04E-03	6.15	3.10E-03	-18.55	3.64E-03	-4.38
	0.05	1.66E-02	2.61E-02	56.91	1.64E-02	-1.73	1.35E-02	-18.95	1.91E-02	14.63
	0.1	2.83E-02	3.48E-02	22.71	2.55E-02	-10.20	2.24E-02	-21.05	2.79E-02	-1.73
	0.15	3.31E-02	3.77E-02	14.08	2.98E-02	-9.87	2.71E-02	-18.10	3.35E-02	1.37
	0.2	3.59E-02	3.92E-02	9.25	3.24E-02	-9.64	3.01E-02	-16.22	3.66E-02	1.87
	0.25	3.83E-02	4.00E-02	4.53	3.42E-02	-10.85	3.21E-02	-16.19	3.83E-02	-0.16
	0.3	3.95E-02	4.06E-02	2.86	3.54E-02	-10.32	3.36E-02	-14.86	3.92E-02	-0.55
	0.35	4.00E-02	4.09E-02	2.37	3.63E-02	-9.25	3.47E-02	-13.19	3.98E-02	-0.42
	0.4	4.17E-02	4.11E-02	-1.37	3.69E-02	-11.43	3.55E-02	-14.79	4.01E-02	-3.85
	0.45	4.04E-02	4.12E-02	1.96	3.74E-02	-7.49	3.62E-02	-10.58	4.02E-02	-0.66
0.5	4.07E-02	4.12E-02	1.34	3.77E-02	-7.28	3.66E-02	-10.04	4.01E-02	-1.54	
4	0.01	2.21E-05	3.83E-05	73.04	2.16E-05	-2.46	1.64E-05	-26.13	2.02E-05	-8.59
	0.02	4.78E-04	8.59E-04	79.49	4.88E-04	1.95	3.77E-04	-21.09	4.41E-04	-7.80
	0.05	2.65E-03	3.80E-03	43.07	2.54E-03	-4.31	2.12E-03	-20.28	2.97E-03	12.02
	0.1	4.48E-03	5.28E-03	18.06	4.08E-03	-8.80	3.63E-03	-19.00	4.44E-03	-0.71
	0.15	5.33E-03	5.79E-03	8.64	4.79E-03	-10.09	4.40E-03	-17.51	5.32E-03	-0.23
	0.2	5.86E-03	6.05E-03	3.22	5.21E-03	-11.08	4.87E-03	-16.81	5.77E-03	-1.57
	0.25	6.06E-03	6.19E-03	2.16	5.48E-03	-9.64	5.19E-03	-14.36	6.01E-03	-0.86
	0.3	6.08E-03	6.28E-03	3.37	5.66E-03	-6.84	5.42E-03	-10.89	6.15E-03	1.16
	0.35	6.16E-03	6.34E-03	2.94	5.80E-03	-5.95	5.58E-03	-9.40	6.23E-03	1.13
	0.4	6.32E-03	6.38E-03	0.94	5.89E-03	-6.78	5.71E-03	-9.73	6.28E-03	-0.70
	0.45	6.35E-03	6.40E-03	0.91	5.96E-03	-6.02	5.80E-03	-8.62	6.30E-03	-0.78
0.5	6.33E-03	6.41E-03	1.37	6.01E-03	-4.96	5.87E-03	-7.27	6.29E-03	-0.55	

ζ	ξ	ISEE	P	ε [%]	cVM	ε [%]	mVM	ε [%]	New	ε [%]
4.5	0.01	1.02E-06	1.64E-06	61.04	9.87E-07	-3.13	7.55E-07	-25.90	9.26E-07	-9.09
	0.02	4.59E-05	7.37E-05	60.57	4.47E-05	-2.69	3.49E-05	-23.97	4.04E-05	-11.96
	0.05	3.24E-04	4.27E-04	31.93	3.03E-04	-6.48	2.55E-04	-21.25	3.54E-04	9.48
	0.1	5.59E-04	6.18E-04	10.62	5.01E-04	-10.45	4.49E-04	-19.62	5.39E-04	-3.50
	0.15	6.43E-04	6.84E-04	6.35	5.89E-04	-8.47	5.45E-04	-15.21	6.43E-04	-0.06
	0.2	6.97E-04	7.17E-04	2.78	6.39E-04	-8.41	6.03E-04	-13.56	6.94E-04	-0.50
	0.25	7.23E-04	7.36E-04	1.75	6.70E-04	-7.29	6.40E-04	-11.43	7.21E-04	-0.22
	0.3	7.38E-04	7.47E-04	1.28	6.92E-04	-6.28	6.66E-04	-9.70	7.37E-04	-0.08
	0.35	7.55E-04	7.55E-04	-0.02	7.07E-04	-6.43	6.85E-04	-9.28	7.47E-04	-1.09
	0.4	7.46E-04	7.60E-04	1.88	7.18E-04	-3.83	6.99E-04	-6.32	7.53E-04	0.88
	0.45	7.61E-04	7.64E-04	0.35	7.26E-04	-4.63	7.09E-04	-6.76	7.56E-04	-0.66
0.5	7.49E-04	7.65E-04	2.16	7.31E-04	-2.39	7.17E-04	-4.30	7.56E-04	0.98	
5	0.01	3.40E-08	5.02E-08	47.87	3.20E-08	-5.92	2.47E-08	-27.31	3.01E-08	-11.46
	0.02	3.26E-06	4.86E-06	49.11	3.11E-06	-4.43	2.46E-06	-24.62	2.82E-06	-13.39
	0.05	3.06E-05	3.74E-05	22.20	2.78E-05	-9.02	2.37E-05	-22.57	3.26E-05	6.58
	0.1	5.27E-05	5.63E-05	6.96	4.74E-05	-10.05	4.29E-05	-18.44	5.06E-05	-3.96
	0.15	5.86E-05	6.28E-05	7.21	5.58E-05	-4.84	5.21E-05	-11.05	6.00E-05	2.45
	0.2	6.43E-05	6.61E-05	2.84	6.04E-05	-5.94	5.75E-05	-10.52	6.46E-05	0.59
	0.25	6.57E-05	6.80E-05	3.36	6.33E-05	-3.67	6.09E-05	-7.33	6.71E-05	2.07
	0.3	6.80E-05	6.91E-05	1.69	6.52E-05	-4.02	6.32E-05	-6.95	6.85E-05	0.84
	0.35	6.99E-05	6.99E-05	-0.02	6.66E-05	-4.75	6.49E-05	-7.15	6.94E-05	-0.67
	0.4	7.07E-05	7.04E-05	-0.44	6.75E-05	-4.50	6.61E-05	-6.52	7.00E-05	-1.02
	0.45	6.94E-05	7.07E-05	1.86	6.82E-05	-1.77	6.70E-05	-3.54	7.03E-05	1.25
0.5	7.10E-05	7.09E-05	-0.03	6.87E-05	-3.19	6.76E-05	-4.69	7.05E-05	-0.71	
		μ_ε %	24.12	μ_ε %	-3.466	μ_ε %	-11.93	μ_ε %	-1.16	
		σ_ε %	41.20	σ_ε %	7.98	σ_ε %	6.75	σ_ε %	4.88	
		ε_{\max} %	182.15	ε_{\max} %	24.93	ε_{\max} %	0.56	ε_{\max} %	17.49	
		ε_{\min} %	-1.73	ε_{\min} %	-13.31	ε_{\min} %	-27.31	ε_{\min} %	-13.39	
		$\mu_{ \varepsilon }$ %	24.31	$\mu_{ \varepsilon }$ %	7.20	$\mu_{ \varepsilon }$ %	11.94	$\mu_{ \varepsilon }$ %	3.22	

D.4.4 Kanai-Tajimi and Unit-step Time-modulating Function, $T=1.0s$

Table D.19 - New: Time-variant FFP computed at $t = 1.0s$ for linear elastic SDOF system with $T=1.0s$ subjected to KT base excitation from at-rest initial conditions.

ζ	ξ	ISEE	P	ε [%]	cVM	ε [%]	mVM	ε [%]	New	ε [%]
1.5	0.01	4.08E-01	8.46E-01	107.47	5.37E-01	31.60	4.40E-01	7.77	4.09E-01	0.20
	0.02	6.80E-01	9.72E-01	43.02	8.02E-01	17.96	7.12E-01	4.69	6.82E-01	0.30
	0.05	9.28E-01	9.95E-01	7.19	9.51E-01	2.49	9.14E-01	-1.55	9.20E-01	-0.91
	0.1	9.70E-01	9.98E-01	2.80	9.85E-01	1.51	9.73E-01	0.23	9.84E-01	1.44
	0.15	9.94E-01	9.98E-01	0.36	9.93E-01	-0.19	9.87E-01	-0.77	9.95E-01	0.03
	0.2	9.95E-01	9.98E-01	0.30	9.95E-01	0.01	9.92E-01	-0.31	9.98E-01	0.23
	0.25	1.00E+00	9.98E-01	-0.36	9.97E-01	-0.52	9.95E-01	-0.72	9.99E-01	-0.34
	0.3	9.64E-01	9.99E-01	3.54	9.98E-01	3.44	9.96E-01	3.30	9.99E-01	3.60
	0.35	1.00E+00	9.99E-01	-0.17	9.98E-01	-0.22	9.97E-01	-0.32	9.99E-01	-0.10
	0.4	9.95E-01	9.99E-01	0.32	9.98E-01	0.30	9.98E-01	0.23	9.99E-01	0.40
	0.45	9.98E-01	9.99E-01	0.11	9.99E-01	0.11	9.98E-01	0.05	1.00E+00	0.20
0.5	9.85E-01	9.99E-01	1.38	9.99E-01	1.39	9.98E-01	1.34	1.00E+00	1.46	
2	0.01	1.22E-01	3.42E-01	180.89	1.66E-01	36.11	1.28E-01	5.15	1.21E-01	-0.56
	0.02	3.10E-01	6.83E-01	120.26	4.05E-01	30.71	3.31E-01	6.65	3.11E-01	0.33
	0.05	6.12E-01	8.71E-01	42.32	6.76E-01	10.55	6.03E-01	-1.37	6.06E-01	-0.95
	0.1	8.00E-01	9.10E-01	13.76	7.98E-01	-0.23	7.51E-01	-6.17	7.89E-01	-1.47
	0.15	8.49E-01	9.22E-01	8.51	8.45E-01	-0.45	8.12E-01	-4.38	8.60E-01	1.24
	0.2	8.91E-01	9.27E-01	3.99	8.71E-01	-2.33	8.46E-01	-5.13	8.95E-01	0.38
	0.25	9.18E-01	9.30E-01	1.32	8.86E-01	-3.46	8.67E-01	-5.60	9.14E-01	-0.43
	0.3	9.24E-01	9.32E-01	0.96	8.97E-01	-2.87	8.81E-01	-4.60	9.26E-01	0.23
	0.35	9.29E-01	9.34E-01	0.50	9.05E-01	-2.63	8.91E-01	-4.07	9.33E-01	0.35
	0.4	9.37E-01	9.35E-01	-0.26	9.11E-01	-2.86	8.99E-01	-4.08	9.37E-01	-0.09
	0.45	9.35E-01	9.36E-01	0.13	9.15E-01	-2.09	9.05E-01	-3.16	9.39E-01	0.45
0.5	9.50E-01	9.36E-01	-1.46	9.19E-01	-3.34	9.10E-01	-4.27	9.40E-01	-1.09	
2.5	0.01	2.47E-02	6.52E-02	164.34	3.16E-02	28.14	2.42E-02	-2.05	2.39E-02	-3.14
	0.02	1.01E-01	2.46E-01	143.53	1.28E-01	26.77	1.01E-01	0.15	9.71E-02	-3.86
	0.05	2.64E-01	4.59E-01	74.07	3.00E-01	13.55	2.56E-01	-3.07	2.62E-01	-0.74
	0.1	3.99E-01	5.31E-01	33.11	4.05E-01	1.49	3.67E-01	-8.16	4.03E-01	1.02
	0.15	4.76E-01	5.55E-01	16.46	4.54E-01	-4.68	4.22E-01	-11.31	4.76E-01	-0.03
	0.2	5.20E-01	5.67E-01	9.05	4.83E-01	-6.98	4.57E-01	-12.02	5.18E-01	-0.23
	0.25	5.37E-01	5.74E-01	6.94	5.03E-01	-6.26	4.81E-01	-10.39	5.44E-01	1.38
	0.3	5.65E-01	5.79E-01	2.49	5.18E-01	-8.41	4.99E-01	-11.79	5.60E-01	-0.87
	0.35	5.73E-01	5.83E-01	1.78	5.29E-01	-7.72	5.12E-01	-10.63	5.70E-01	-0.46
	0.4	5.84E-01	5.86E-01	0.36	5.37E-01	-7.99	5.22E-01	-10.52	5.76E-01	-1.33
	0.45	5.83E-01	5.88E-01	0.79	5.43E-01	-6.78	5.30E-01	-9.04	5.79E-01	-0.74
0.5	5.93E-01	5.89E-01	-0.65	5.49E-01	-7.44	5.37E-01	-9.45	5.80E-01	-2.21	

ζ	ξ	ISEE	P	ε [%]	cVM	ε [%]	mVM	ε [%]	New	ε [%]
3	0.01	3.55E-03	7.80E-03	119.71	4.10E-03	15.43	3.15E-03	-11.30	3.32E-03	-6.41
	0.02	2.30E-02	5.20E-02	126.01	2.79E-02	21.15	2.20E-02	-4.62	2.23E-02	-3.33
	0.05	7.83E-02	1.35E-01	72.10	8.64E-02	10.35	7.30E-02	-6.75	7.85E-02	0.16
	0.1	1.31E-01	1.70E-01	29.23	1.27E-01	-3.54	1.14E-01	-13.50	1.31E-01	-0.53
	0.15	1.51E-01	1.82E-01	20.07	1.46E-01	-3.58	1.35E-01	-10.93	1.58E-01	4.31
	0.2	1.73E-01	1.88E-01	8.69	1.58E-01	-8.85	1.48E-01	-14.28	1.73E-01	0.20
	0.25	1.77E-01	1.92E-01	8.39	1.66E-01	-6.45	1.58E-01	-10.98	1.83E-01	3.00
	0.3	1.91E-01	1.95E-01	1.99	1.72E-01	-10.15	1.65E-01	-13.79	1.88E-01	-1.57
	0.35	1.92E-01	1.97E-01	2.36	1.76E-01	-8.43	1.70E-01	-11.59	1.91E-01	-0.51
	0.4	1.95E-01	1.99E-01	1.63	1.80E-01	-8.01	1.74E-01	-10.76	1.93E-01	-1.02
	0.45	2.01E-01	2.00E-01	-0.79	1.82E-01	-9.35	1.78E-01	-11.74	1.94E-01	-3.51
0.5	1.99E-01	2.00E-01	0.69	1.85E-01	-7.30	1.80E-01	-9.47	1.94E-01	-2.42	
3.5	0.01	3.42E-04	6.55E-04	91.76	3.74E-04	9.37	2.90E-04	-15.17	3.28E-04	-3.94
	0.02	3.89E-03	7.75E-03	99.32	4.46E-03	14.71	3.54E-03	-9.08	3.83E-03	-1.43
	0.05	1.72E-02	2.63E-02	53.18	1.78E-02	3.45	1.51E-02	-12.08	1.71E-02	-0.36
	0.1	2.86E-02	3.50E-02	22.59	2.72E-02	-4.72	2.46E-02	-14.05	2.91E-02	1.69
	0.15	3.46E-02	3.81E-02	10.11	3.17E-02	-8.51	2.94E-02	-15.00	3.47E-02	0.42
	0.2	3.65E-02	3.97E-02	8.86	3.43E-02	-5.96	3.24E-02	-11.08	3.77E-02	3.43
	0.25	3.91E-02	4.07E-02	4.08	3.61E-02	-7.77	3.45E-02	-11.80	3.94E-02	0.73
	0.3	4.05E-02	4.14E-02	2.39	3.74E-02	-7.64	3.60E-02	-10.96	4.04E-02	-0.12
	0.35	4.12E-02	4.20E-02	2.01	3.84E-02	-6.75	3.72E-02	-9.57	4.11E-02	-0.24
	0.4	4.08E-02	4.24E-02	3.79	3.91E-02	-4.17	3.81E-02	-6.65	4.14E-02	1.36
	0.45	4.23E-02	4.27E-02	0.92	3.97E-02	-6.08	3.88E-02	-8.20	4.15E-02	-1.84
0.5	4.36E-02	4.29E-02	-1.67	4.02E-02	-7.90	3.94E-02	-9.73	4.15E-02	-4.94	
4	0.01	2.32E-05	3.94E-05	69.97	2.41E-05	4.08	1.89E-05	-18.46	2.27E-05	-2.11
	0.02	4.96E-04	8.71E-04	75.75	5.37E-04	8.43	4.30E-04	-13.27	4.94E-04	-0.38
	0.05	2.71E-03	3.82E-03	41.17	2.74E-03	1.26	2.35E-03	-13.07	2.78E-03	2.51
	0.1	4.67E-03	5.32E-03	14.03	4.34E-03	-7.02	3.95E-03	-15.30	4.72E-03	1.09
	0.15	5.45E-03	5.85E-03	7.24	5.06E-03	-7.25	4.74E-03	-13.07	5.54E-03	1.64
	0.2	5.78E-03	6.12E-03	5.91	5.48E-03	-5.30	5.22E-03	-9.76	5.95E-03	2.92
	0.25	6.03E-03	6.30E-03	4.40	5.75E-03	-4.65	5.54E-03	-8.17	6.18E-03	2.43
	0.3	6.31E-03	6.42E-03	1.73	5.95E-03	-5.70	5.77E-03	-8.53	6.32E-03	0.15
	0.35	6.38E-03	6.51E-03	2.03	6.10E-03	-4.42	5.95E-03	-6.79	6.41E-03	0.40
	0.4	6.54E-03	6.58E-03	0.63	6.22E-03	-4.97	6.09E-03	-6.96	6.46E-03	-1.29
	0.45	6.60E-03	6.64E-03	0.54	6.31E-03	-4.46	6.19E-03	-6.18	6.47E-03	-1.94
0.5	6.65E-03	6.68E-03	0.38	6.38E-03	-4.13	6.28E-03	-5.64	6.46E-03	-2.82	

ζ	ξ	ISEE	P	ε [%]	cVM	ε [%]	mVM	ε [%]	New	ε [%]
4.5	0.01	1.09E-06	1.70E-06	55.51	1.10E-06	1.16	8.73E-07	-19.92	1.08E-06	-1.21
	0.02	4.77E-05	7.50E-05	57.06	4.91E-05	2.93	3.97E-05	-16.86	4.69E-05	-1.79
	0.05	3.37E-04	4.30E-04	27.68	3.25E-04	-3.47	2.82E-04	-16.24	3.38E-04	0.30
	0.1	5.75E-04	6.23E-04	8.25	5.29E-04	-8.06	4.87E-04	-15.42	5.76E-04	0.19
	0.15	6.65E-04	6.91E-04	3.82	6.17E-04	-7.19	5.84E-04	-12.26	6.70E-04	0.67
	0.2	7.10E-04	7.26E-04	2.25	6.68E-04	-5.99	6.41E-04	-9.75	7.15E-04	0.64
	0.25	7.37E-04	7.48E-04	1.44	7.00E-04	-5.09	6.78E-04	-8.00	7.40E-04	0.34
	0.3	7.62E-04	7.64E-04	0.22	7.23E-04	-5.12	7.05E-04	-7.43	7.56E-04	-0.77
	0.35	7.82E-04	7.75E-04	-0.87	7.40E-04	-5.35	7.26E-04	-7.24	7.67E-04	-1.99
	0.4	7.72E-04	7.84E-04	1.64	7.54E-04	-2.34	7.41E-04	-3.96	7.73E-04	0.12
	0.45	7.78E-04	7.91E-04	1.68	7.64E-04	-1.84	7.53E-04	-3.22	7.75E-04	-0.43
0.5	7.83E-04	7.97E-04	1.77	7.72E-04	-1.37	7.63E-04	-2.57	7.75E-04	-1.01	
5	0.01	3.63E-08	5.22E-08	43.75	3.58E-08	-1.51	2.86E-08	-21.22	3.51E-08	-3.48
	0.02	3.34E-06	4.95E-06	48.13	3.42E-06	2.21	2.79E-06	-16.63	3.27E-06	-2.29
	0.05	3.16E-05	3.77E-05	19.18	2.98E-05	-5.86	2.61E-05	-17.47	3.09E-05	-2.45
	0.1	5.38E-05	5.67E-05	5.49	4.98E-05	-7.45	4.62E-05	-14.07	5.36E-05	-0.35
	0.15	6.13E-05	6.34E-05	3.55	5.82E-05	-5.04	5.54E-05	-9.53	6.22E-05	1.44
	0.2	6.62E-05	6.69E-05	1.08	6.28E-05	-5.09	6.07E-05	-8.29	6.63E-05	0.09
	0.25	6.88E-05	6.91E-05	0.42	6.58E-05	-4.36	6.41E-05	-6.78	6.87E-05	-0.24
	0.3	6.90E-05	7.06E-05	2.36	6.79E-05	-1.59	6.65E-05	-3.53	7.02E-05	1.75
	0.35	7.05E-05	7.17E-05	1.76	6.94E-05	-1.51	6.83E-05	-3.07	7.12E-05	1.06
	0.4	7.16E-05	7.26E-05	1.51	7.06E-05	-1.28	6.97E-05	-2.56	7.19E-05	0.55
	0.45	7.30E-05	7.33E-05	0.51	7.16E-05	-1.89	7.08E-05	-2.96	7.23E-05	-0.85
0.5	7.42E-05	7.39E-05	-0.50	7.23E-05	-2.59	7.17E-05	-3.49	7.25E-05	-2.32	
		μ_ε %	22.79	μ_ε %	-0.352	μ_ε %	-7.67	μ_ε %	-0.34	
		σ_ε %	39.82	σ_ε %	9.57	σ_ε %	5.96	σ_ε %	1.80	
		ε_{\max} %	180.89	ε_{\max} %	36.11	ε_{\max} %	7.77	ε_{\max} %	4.31	
		ε_{\min} %	-1.67	ε_{\min} %	-10.15	ε_{\min} %	-21.22	ε_{\min} %	-6.41	
		$\mu_{ \varepsilon }$ %	22.93	$\mu_{ \varepsilon }$ %	6.62	$\mu_{ \varepsilon }$ %	8.28	$\mu_{ \varepsilon }$ %	1.32	

D.4.5 Kanai-Tajimi and Shinozuka-Sato Time-modulating Function, $T = 0.1s$

Table D.20 - New: FPDF computed at $t = 20s$ for linear elastic SDOF system with $T = 0.1s$ subjected to KT base excitation time modulated by a Shinozuka-Sato function.

ζ	ξ	ISEE	P	ε [%]	cVM	ε [%]	mVM	ε [%]	New	ε [%]
1.5	0.01	9.88E-01	1	1.22	1	1.22	1.00E+00	1.22	1.00E+00	1.17
	0.02	9.97E-01	1	0.31	1	0.31	1.00E+00	0.31	1.00E+00	0.31
	0.05	9.98E-01	1	0.24	1	0.24	1.00E+00	0.24	1.00E+00	0.24
	0.1	1	1	0.00	1	0.00	1.00E+00	0.00	1.00E+00	0.00
	0.15	1	1	0.00	1	0.00	1.00E+00	0.00	1.00E+00	0.00
	0.2	1	1	0.00	1	0.00	1.00E+00	0.00	1.00E+00	0.00
	0.25	1	1	0.00	1	0.00	1.00E+00	0.00	1.00E+00	0.00
	0.3	9.98E-01	1	0.24	1	0.24	1.00E+00	0.24	1.00E+00	0.24
	0.35	9.96E-01	1	0.39	1	0.39	1.00E+00	0.39	1.00E+00	0.39
	0.4	1	1	0.00	1	0.00	1.00E+00	0.00	1.00E+00	0.00
	0.45	1	1	0.00	1	0.00	1.00E+00	0.00	1.00E+00	0.00
	0.5	9.98E-01	1	0.24	1	0.24	1.00E+00	0.24	1.00E+00	0.24
2	0.01	8.74E-01	1	14.45	9.93E-01	13.67	9.73E-01	11.35	9.31E-01	6.52
	0.02	9.75E-01	1	2.55	9.98E-01	2.31	9.91E-01	1.65	9.86E-01	1.10
	0.05	9.92E-01	1	0.80	9.99E-01	0.75	9.98E-01	0.62	9.99E-01	0.71
	0.1	9.90E-01	1	1.05	1	1.02	9.99E-01	0.97	1.00E+00	1.03
	0.15	9.92E-01	1	0.82	1	0.79	9.99E-01	0.75	1.00E+00	0.81
	0.2	1	1	-0.01	1	-0.05	9.99E-01	-0.08	1.00E+00	-0.02
	0.25	9.79E-01	1	2.18	9.99E-01	2.13	9.99E-01	2.09	1.00E+00	2.17
	0.3	9.88E-01	1	1.19	9.99E-01	1.13	9.99E-01	1.09	1.00E+00	1.17
	0.35	9.95E-01	1	0.43	9.99E-01	0.37	9.99E-01	0.32	1.00E+00	0.42
	0.4	9.96E-01	1	0.41	9.99E-01	0.33	9.99E-01	0.28	1.00E+00	0.39
	0.45	9.91E-01	1	0.87	9.99E-01	0.79	9.98E-01	0.73	1.00E+00	0.86
	0.5	9.93E-01	1	0.64	9.99E-01	0.55	9.98E-01	0.49	9.99E-01	0.63
2.5	0.01	4.87E-01	9.74E-01	99.93	7.68E-01	57.55	6.57E-01	34.82	5.49E-01	12.71
	0.02	6.84E-01	9.69E-01	41.62	8.28E-01	20.94	7.50E-01	9.65	7.14E-01	4.38
	0.05	8.58E-01	9.61E-01	12.12	8.78E-01	2.40	8.36E-01	-2.52	8.61E-01	0.42
	0.1	9.17E-01	9.50E-01	3.53	8.89E-01	-3.03	8.62E-01	-5.98	8.99E-01	-1.94
	0.15	9.28E-01	9.38E-01	1.11	8.86E-01	-4.53	8.64E-01	-6.89	9.03E-01	-2.72
	0.2	9.23E-01	9.28E-01	0.52	8.79E-01	-4.77	8.60E-01	-6.86	8.99E-01	-2.59
	0.25	9.22E-01	9.18E-01	-0.48	8.71E-01	-5.54	8.53E-01	-7.47	8.93E-01	-3.15
	0.3	9.04E-01	9.09E-01	0.53	8.63E-01	-4.49	8.47E-01	-6.35	8.87E-01	-1.89
	0.35	9.10E-01	9.00E-01	-1.07	8.55E-01	-5.96	8.39E-01	-7.72	8.80E-01	-3.26
	0.4	8.89E-01	8.92E-01	0.32	8.48E-01	-4.60	8.32E-01	-6.34	8.73E-01	-1.76
	0.45	8.70E-01	8.84E-01	1.55	8.41E-01	-3.41	8.26E-01	-5.14	8.67E-01	-0.44
	0.5	8.83E-01	8.76E-01	-0.70	8.34E-01	-5.53	8.19E-01	-7.19	8.60E-01	-2.56

ζ	ξ	ISEE	P	ε [%]	cVM	ε [%]	mVM	ε [%]	New	ε [%]
3	0.01	1.67E-01	5.46E-01	226.13	2.94E-01	75.81	2.28E-01	36.07	1.76E-01	5.23
	0.02	2.60E-01	5.28E-01	102.78	3.39E-01	30.27	2.82E-01	8.32	2.59E-01	-0.38
	0.05	3.86E-01	5.04E-01	30.35	3.85E-01	-0.50	3.45E-01	-10.85	3.68E-01	-4.91
	0.1	4.45E-01	4.74E-01	6.51	3.94E-01	-11.59	3.66E-01	-17.74	4.05E-01	-9.08
	0.15	4.26E-01	4.51E-01	5.96	3.87E-01	-9.06	3.66E-01	-14.11	4.05E-01	-4.79
	0.2	4.24E-01	4.32E-01	1.94	3.78E-01	-10.93	3.60E-01	-15.18	3.98E-01	-6.11
	0.25	4.18E-01	4.16E-01	-0.43	3.68E-01	-12.01	3.52E-01	-15.78	3.89E-01	-6.97
	0.3	3.93E-01	4.03E-01	2.50	3.59E-01	-8.70	3.45E-01	-12.30	3.80E-01	-3.34
	0.35	3.90E-01	3.91E-01	0.23	3.50E-01	-10.20	3.37E-01	-13.51	3.71E-01	-4.86
	0.4	3.86E-01	3.80E-01	-1.58	3.42E-01	-11.41	3.30E-01	-14.50	3.63E-01	-6.13
	0.45	3.68E-01	3.71E-01	0.84	3.35E-01	-8.89	3.24E-01	-11.92	3.55E-01	-3.48
0.5	3.59E-01	3.63E-01	1.01	3.29E-01	-8.45	3.18E-01	-11.37	3.48E-01	-3.04	
3.5	0.01	3.97E-02	1.26E-01	217.81	6.36E-02	60.10	4.81E-02	21.11	3.65E-02	-8.05
	0.02	6.12E-02	1.20E-01	96.96	7.42E-02	21.35	6.05E-02	-0.99	5.52E-02	-9.67
	0.05	9.00E-02	1.13E-01	25.56	8.49E-02	-5.66	7.52E-02	-16.44	8.08E-02	-10.29
	0.1	9.83E-02	1.04E-01	6.03	8.63E-02	-12.20	7.99E-02	-18.79	8.89E-02	-9.54
	0.15	9.67E-02	9.76E-02	0.95	8.40E-02	-13.13	7.91E-02	-18.21	8.81E-02	-8.90
	0.2	9.18E-02	9.24E-02	0.66	8.11E-02	-11.56	7.71E-02	-15.93	8.56E-02	-6.75
	0.25	8.63E-02	8.80E-02	2.02	7.84E-02	-9.18	7.50E-02	-13.14	8.28E-02	-4.06
	0.3	8.20E-02	8.44E-02	2.92	7.58E-02	-7.55	7.28E-02	-11.21	8.01E-02	-2.31
	0.35	8.02E-02	8.13E-02	1.47	7.36E-02	-8.24	7.09E-02	-11.60	7.77E-02	-3.06
	0.4	7.89E-02	7.87E-02	-0.34	7.15E-02	-9.40	6.91E-02	-12.51	7.55E-02	-4.35
	0.45	7.84E-02	7.63E-02	-2.72	6.96E-02	-11.19	6.74E-02	-14.06	7.35E-02	-6.30
0.5	7.34E-02	7.42E-02	1.05	6.80E-02	-7.42	6.59E-02	-10.27	7.16E-02	-2.40	
4	0.01	6.87E-03	1.81E-02	163.96	9.66E-03	40.61	7.34E-03	6.85	5.58E-03	-18.83
	0.02	1.03E-02	1.72E-02	67.23	1.12E-02	8.45	9.18E-03	-10.99	8.38E-03	-18.76
	0.05	1.40E-02	1.61E-02	15.02	1.26E-02	-9.87	1.13E-02	-19.60	1.20E-02	-14.10
	0.1	1.44E-02	1.48E-02	3.12	1.27E-02	-11.61	1.18E-02	-17.67	1.30E-02	-9.28
	0.15	1.37E-02	1.38E-02	1.17	1.23E-02	-10.22	1.16E-02	-14.91	1.28E-02	-6.50
	0.2	1.29E-02	1.30E-02	1.50	1.18E-02	-8.27	1.13E-02	-12.25	1.23E-02	-4.10
	0.25	1.24E-02	1.24E-02	-0.19	1.13E-02	-8.76	1.09E-02	-12.21	1.19E-02	-4.54
	0.3	1.18E-02	1.19E-02	0.41	1.09E-02	-7.49	1.06E-02	-10.63	1.15E-02	-3.24
	0.35	1.16E-02	1.14E-02	-1.13	1.06E-02	-8.38	1.03E-02	-11.24	1.11E-02	-4.24
	0.4	1.11E-02	1.10E-02	-0.66	1.03E-02	-7.53	9.98E-03	-10.22	1.07E-02	-3.44
	0.45	1.07E-02	1.07E-02	-0.14	9.99E-03	-6.72	9.72E-03	-9.26	1.04E-02	-2.67
0.5	1.03E-02	1.04E-02	0.52	9.74E-03	-5.81	9.48E-03	-8.24	1.01E-02	-1.82	

ζ	ξ	ISEE	P	ε [%]	cVM	ε [%]	mVM	ε [%]	New	ε [%]
4.5	0.01	8.78E-04	1.95E-03	122.49	1.12E-03	27.06	8.57E-04	-2.47	6.51E-04	-25.90
	0.02	1.24E-03	1.86E-03	50.34	1.28E-03	3.41	1.06E-03	-14.20	9.60E-04	-22.28
	0.05	1.57E-03	1.74E-03	10.31	1.42E-03	-9.72	1.28E-03	-18.64	1.35E-03	-14.45
	0.1	1.56E-03	1.59E-03	2.14	1.41E-03	-9.51	1.33E-03	-14.98	1.44E-03	-7.98
	0.15	1.50E-03	1.49E-03	-0.78	1.36E-03	-9.46	1.30E-03	-13.54	1.40E-03	-6.64
	0.2	1.36E-03	1.40E-03	3.35	1.30E-03	-4.23	1.25E-03	-7.76	1.35E-03	-0.89
	0.25	1.33E-03	1.33E-03	0.44	1.25E-03	-6.04	1.21E-03	-9.02	1.29E-03	-2.70
	0.3	1.30E-03	1.28E-03	-1.62	1.20E-03	-7.38	1.17E-03	-10.00	1.24E-03	-4.12
	0.35	1.24E-03	1.23E-03	-0.75	1.16E-03	-6.13	1.13E-03	-8.54	1.20E-03	-2.88
	0.4	1.18E-03	1.19E-03	0.19	1.13E-03	-4.89	1.10E-03	-7.15	1.16E-03	-1.68
	0.45	1.14E-03	1.15E-03	0.58	1.09E-03	-4.25	1.07E-03	-6.37	1.13E-03	-1.10
0.5	1.11E-03	1.12E-03	0.68	1.07E-03	-3.92	1.04E-03	-5.93	1.10E-03	-0.85	
5	0.01	8.64E-05	1.65E-04	90.50	1.00E-04	15.83	7.76E-05	-10.13	5.92E-05	-31.43
	0.02	1.17E-04	1.56E-04	33.84	1.13E-04	-3.08	9.50E-05	-18.69	8.57E-05	-26.67
	0.05	1.37E-04	1.46E-04	6.93	1.24E-04	-9.26	1.13E-04	-17.42	1.17E-04	-14.28
	0.1	1.32E-04	1.34E-04	1.68	1.22E-04	-7.52	1.16E-04	-12.41	1.23E-04	-6.56
	0.15	1.23E-04	1.25E-04	1.70	1.17E-04	-5.16	1.12E-04	-8.80	1.20E-04	-2.91
	0.2	1.18E-04	1.18E-04	0.44	1.12E-04	-5.13	1.08E-04	-8.07	1.15E-04	-2.57
	0.25	1.13E-04	1.12E-04	-0.29	1.07E-04	-5.09	1.04E-04	-7.59	1.10E-04	-2.48
	0.3	1.07E-04	1.08E-04	0.17	1.03E-04	-4.16	1.01E-04	-6.38	1.06E-04	-1.55
	0.35	1.03E-04	1.03E-04	0.78	9.93E-05	-3.22	9.73E-05	-5.24	1.02E-04	-0.65
	0.4	9.94E-05	9.99E-05	0.52	9.62E-05	-3.19	9.43E-05	-5.05	9.87E-05	-0.69
	0.45	9.74E-05	9.67E-05	-0.69	9.34E-05	-4.14	9.17E-05	-5.85	9.57E-05	-1.74
	0.5	9.48E-05	9.40E-05	-0.92	9.09E-05	-4.17	8.94E-05	-5.78	9.31E-05	-1.86
		μ_ε %	15.50	μ_ε %	-0.450	μ_ε %	-5.94	μ_ε %	-4.00	
		σ_ε %	42.05	σ_ε %	14.87	σ_ε %	9.66	σ_ε %	6.71	
		ε_{\max} %	226.13	ε_{\max} %	75.81	ε_{\max} %	36.07	ε_{\max} %	12.71	
		ε_{\min} %	-2.72	ε_{\min} %	-13.13	ε_{\min} %	-19.60	ε_{\min} %	-31.43	
		$\mu_{ \varepsilon }$ %	15.81	$\mu_{ \varepsilon }$ %	8.58	$\mu_{ \varepsilon }$ %	8.85	$\mu_{ \varepsilon }$ %	4.67	

D.4.6 Kanai-Tajimi and Shinozuka-Sato Time-modulating Function, $T = 0.5s$

Table D.21 - New: FFPF computed at $t = 20s$ for linear elastic SDOF system with $T = 0.5s$ subjected to KT base excitation time modulated by a Shinozuka-Sato function.

ζ	ξ	ISEE	P	ε [%]	cVM	ε [%]	mVM	ε [%]	New	ε [%]
1.5	0.01	8.23E-01	1.00E+00	21.55	9.38E-01	14.02	8.36E-01	1.68	7.42E-01	-9.85
	0.02	8.78E-01	1.00E+00	13.83	9.58E-01	9.04	8.92E-01	1.52	8.20E-01	-6.68
	0.05	9.62E-01	1.00E+00	3.96	9.83E-01	2.19	9.57E-01	-0.49	9.41E-01	-2.11
	0.1	9.77E-01	1.00E+00	2.32	9.94E-01	1.70	9.85E-01	0.82	9.89E-01	1.20
	0.15	1.00E+00	1.00E+00	-0.03	9.97E-01	-0.33	9.93E-01	-0.72	9.97E-01	-0.34
	0.2	1.00E+00	1.00E+00	-0.03	9.98E-01	-0.20	9.96E-01	-0.42	9.99E-01	-0.14
	0.25	1.00E+00	1.00E+00	-0.02	9.99E-01	-0.14	9.97E-01	-0.28	9.99E-01	-0.07
	0.3	9.80E-01	1.00E+00	2.02	9.99E-01	1.93	9.98E-01	1.84	1.00E+00	2.00
	0.35	1.00E+00	1.00E+00	-0.03	9.99E-01	-0.09	9.98E-01	-0.16	1.00E+00	-0.03
	0.4	1.00E+00	1.00E+00	-0.03	9.99E-01	-0.07	9.99E-01	-0.13	1.00E+00	-0.02
	0.45	9.90E-01	1.00E+00	1.03	9.99E-01	0.99	9.99E-01	0.95	1.00E+00	1.04
	0.5	1.00E+00	1.00E+00	-0.03	9.99E-01	-0.06	9.99E-01	-0.09	1.00E+00	-0.02
2	0.01	4.56E-01	9.80E-01	114.93	6.23E-01	36.55	4.73E-01	3.74	4.19E-01	-8.12
	0.02	5.23E-01	9.60E-01	83.38	6.64E-01	26.86	5.39E-01	3.04	4.84E-01	-7.47
	0.05	6.80E-01	9.40E-01	38.16	7.44E-01	9.35	6.57E-01	-3.37	6.43E-01	-5.45
	0.1	8.12E-01	9.36E-01	15.23	8.11E-01	-0.14	7.55E-01	-7.08	7.90E-01	-2.72
	0.15	8.65E-01	9.36E-01	8.12	8.44E-01	-2.42	8.03E-01	-7.15	8.53E-01	-1.37
	0.2	8.86E-01	9.36E-01	5.61	8.64E-01	-2.48	8.32E-01	-6.06	8.86E-01	0.05
	0.25	9.15E-01	9.35E-01	2.20	8.77E-01	-4.23	8.51E-01	-7.03	9.05E-01	-1.12
	0.3	9.11E-01	9.35E-01	2.69	8.85E-01	-2.78	8.64E-01	-5.14	9.16E-01	0.63
	0.35	9.39E-01	9.35E-01	-0.43	8.92E-01	-5.02	8.73E-01	-6.98	9.23E-01	-1.63
	0.4	9.24E-01	9.34E-01	1.08	8.96E-01	-3.03	8.80E-01	-4.77	9.28E-01	0.38
	0.45	9.35E-01	9.33E-01	-0.15	9.00E-01	-3.76	8.85E-01	-5.29	9.30E-01	-0.51
	0.5	9.45E-01	9.33E-01	-1.36	9.02E-01	-4.58	8.89E-01	-5.94	9.31E-01	-1.52
2.5	0.01	1.74E-01	6.51E-01	274.06	2.53E-01	45.35	1.76E-01	1.12	1.70E-01	-2.18
	0.02	2.05E-01	5.79E-01	182.36	2.75E-01	34.17	2.06E-01	0.72	2.00E-01	-2.32
	0.05	2.95E-01	5.30E-01	79.98	3.25E-01	10.24	2.69E-01	-8.77	2.79E-01	-5.36
	0.1	3.85E-01	5.22E-01	35.79	3.76E-01	-2.18	3.32E-01	-13.64	3.79E-01	-1.53
	0.15	4.33E-01	5.22E-01	20.33	4.06E-01	-6.36	3.70E-01	-14.70	4.32E-01	-0.39
	0.2	4.71E-01	5.21E-01	10.60	4.25E-01	-9.85	3.95E-01	-16.31	4.63E-01	-1.78
	0.25	4.85E-01	5.21E-01	7.43	4.38E-01	-9.66	4.12E-01	-15.06	4.82E-01	-0.63
	0.3	4.97E-01	5.21E-01	4.72	4.48E-01	-9.94	4.25E-01	-14.54	4.93E-01	-0.73
	0.35	5.05E-01	5.20E-01	2.86	4.55E-01	-10.02	4.34E-01	-14.03	5.00E-01	-1.03
	0.4	5.19E-01	5.19E-01	-0.10	4.60E-01	-11.42	4.42E-01	-14.91	5.03E-01	-3.02
	0.45	5.13E-01	5.17E-01	0.79	4.64E-01	-9.66	4.47E-01	-12.85	5.04E-01	-1.69
	0.5	5.13E-01	5.16E-01	0.54	4.66E-01	-9.08	4.51E-01	-11.98	5.04E-01	-1.76

ζ	ξ	ISEE	P	ε [%]	cVM	ε [%]	mVM	ε [%]	New	ε [%]
3	0.01	4.83E-02	2.03E-01	319.65	6.84E-02	41.54	4.64E-02	-4.05	4.86E-02	0.47
	0.02	5.97E-02	1.70E-01	184.66	7.42E-02	24.31	5.45E-02	-8.63	5.79E-02	-3.05
	0.05	8.21E-02	1.50E-01	82.93	8.82E-02	7.39	7.18E-02	-12.50	8.00E-02	-2.57
	0.1	1.09E-01	1.47E-01	35.21	1.03E-01	-5.02	9.01E-02	-17.09	1.10E-01	1.12
	0.15	1.24E-01	1.47E-01	18.05	1.12E-01	-9.78	1.01E-01	-18.51	1.25E-01	0.31
	0.2	1.34E-01	1.47E-01	9.33	1.18E-01	-12.13	1.09E-01	-18.96	1.33E-01	-1.03
	0.25	1.34E-01	1.47E-01	9.23	1.22E-01	-9.19	1.14E-01	-15.06	1.37E-01	2.26
	0.3	1.40E-01	1.46E-01	4.72	1.25E-01	-10.81	1.18E-01	-15.71	1.40E-01	-0.14
	0.35	1.44E-01	1.46E-01	1.61	1.27E-01	-11.85	1.21E-01	-16.05	1.41E-01	-2.13
	0.4	1.43E-01	1.46E-01	1.68	1.28E-01	-10.51	1.23E-01	-14.26	1.41E-01	-1.59
	0.45	1.43E-01	1.45E-01	1.67	1.29E-01	-9.48	1.24E-01	-12.86	1.41E-01	-1.49
0.5	1.45E-01	1.45E-01	-0.47	1.30E-01	-10.54	1.26E-01	-13.55	1.40E-01	-3.71	
3.5	0.01	1.03E-02	3.81E-02	268.59	1.35E-02	30.76	9.16E-03	-11.34	9.80E-03	-5.14
	0.02	1.22E-02	3.14E-02	158.35	1.45E-02	19.40	1.07E-02	-11.99	1.18E-02	-3.23
	0.05	1.71E-02	2.75E-02	60.33	1.70E-02	-0.67	1.39E-02	-18.61	1.60E-02	-6.51
	0.1	2.15E-02	2.68E-02	25.09	1.97E-02	-7.98	1.73E-02	-19.15	2.16E-02	0.64
	0.15	2.36E-02	2.68E-02	13.33	2.13E-02	-9.81	1.94E-02	-18.00	2.40E-02	1.32
	0.2	2.50E-02	2.68E-02	7.12	2.23E-02	-10.73	2.07E-02	-17.13	2.51E-02	0.38
	0.25	2.61E-02	2.68E-02	2.70	2.30E-02	-11.78	2.16E-02	-16.96	2.57E-02	-1.57
	0.3	2.62E-02	2.67E-02	2.10	2.35E-02	-10.37	2.23E-02	-14.80	2.59E-02	-1.05
	0.35	2.62E-02	2.67E-02	1.68	2.38E-02	-9.30	2.28E-02	-13.13	2.60E-02	-0.95
	0.4	2.63E-02	2.66E-02	1.18	2.40E-02	-8.61	2.31E-02	-11.97	2.59E-02	-1.29
	0.45	2.63E-02	2.65E-02	0.69	2.42E-02	-8.15	2.34E-02	-11.13	2.58E-02	-1.86
0.5	2.59E-02	2.64E-02	1.65	2.42E-02	-6.52	2.35E-02	-9.21	2.56E-02	-1.23	
4	0.01	1.68E-03	5.25E-03	212.60	2.04E-03	21.30	1.39E-03	-17.13	1.48E-03	-11.54
	0.02	1.95E-03	4.32E-03	121.48	2.16E-03	11.05	1.61E-03	-17.36	1.77E-03	-9.38
	0.05	2.58E-03	3.77E-03	46.12	2.50E-03	-3.21	2.07E-03	-19.82	2.36E-03	-8.43
	0.1	3.17E-03	3.68E-03	16.13	2.86E-03	-9.89	2.54E-03	-19.97	3.10E-03	-2.20
	0.15	3.38E-03	3.67E-03	8.72	3.06E-03	-9.49	2.81E-03	-16.88	3.38E-03	0.15
	0.2	3.56E-03	3.67E-03	3.29	3.18E-03	-10.48	2.98E-03	-16.15	3.51E-03	-1.25
	0.25	3.57E-03	3.67E-03	2.95	3.27E-03	-8.41	3.10E-03	-13.08	3.57E-03	0.09
	0.3	3.54E-03	3.66E-03	3.45	3.32E-03	-6.28	3.18E-03	-10.23	3.59E-03	1.37
	0.35	3.61E-03	3.66E-03	1.26	3.36E-03	-7.02	3.24E-03	-10.34	3.59E-03	-0.43
	0.4	3.66E-03	3.64E-03	-0.33	3.38E-03	-7.54	3.28E-03	-10.38	3.59E-03	-1.90
	0.45	3.64E-03	3.63E-03	-0.15	3.39E-03	-6.63	3.30E-03	-9.12	3.57E-03	-1.80
0.5	3.60E-03	3.61E-03	0.44	3.40E-03	-5.46	3.32E-03	-7.69	3.55E-03	-1.45	

ζ	ξ	ISEE	P	ε [%]	cVM	ε [%]	mVM	ε [%]	New	ε [%]
4.5	0.01	2.10E-04	5.62E-04	167.43	2.38E-04	13.08	1.64E-04	-22.03	1.74E-04	-16.99
	0.02	2.36E-04	4.62E-04	96.15	2.50E-04	6.08	1.88E-04	-20.22	2.06E-04	-12.83
	0.05	3.06E-04	4.03E-04	31.78	2.84E-04	-7.37	2.38E-04	-22.38	2.69E-04	-12.03
	0.1	3.58E-04	3.94E-04	9.98	3.20E-04	-10.68	2.87E-04	-19.82	3.44E-04	-4.00
	0.15	3.79E-04	3.93E-04	3.78	3.40E-04	-10.30	3.15E-04	-16.83	3.70E-04	-2.29
	0.2	3.90E-04	3.93E-04	0.78	3.52E-04	-9.81	3.33E-04	-14.80	3.81E-04	-2.29
	0.25	3.89E-04	3.93E-04	1.03	3.60E-04	-7.57	3.44E-04	-11.61	3.86E-04	-0.81
	0.3	3.87E-04	3.92E-04	1.40	3.64E-04	-5.82	3.52E-04	-9.17	3.87E-04	0.10
	0.35	3.92E-04	3.91E-04	-0.20	3.68E-04	-6.28	3.57E-04	-9.06	3.87E-04	-1.24
	0.4	3.87E-04	3.90E-04	0.74	3.69E-04	-4.61	3.60E-04	-7.01	3.86E-04	-0.24
	0.45	3.84E-04	3.89E-04	1.19	3.70E-04	-3.57	3.62E-04	-5.66	3.85E-04	0.15
0.5	3.83E-04	3.87E-04	1.03	3.71E-04	-3.22	3.64E-04	-5.05	3.82E-04	-0.16	
5	0.01	1.96E-05	4.73E-05	141.54	2.16E-05	10.20	1.50E-05	-23.32	1.60E-05	-18.54
	0.02	2.22E-05	3.89E-05	75.17	2.25E-05	1.17	1.71E-05	-23.10	1.86E-05	-16.26
	0.05	2.75E-05	3.40E-05	23.50	2.51E-05	-8.72	2.13E-05	-22.66	2.39E-05	-13.00
	0.1	3.10E-05	3.32E-05	6.92	2.80E-05	-9.88	2.53E-05	-18.29	2.98E-05	-3.98
	0.15	3.26E-05	3.31E-05	1.58	2.95E-05	-9.55	2.76E-05	-15.40	3.17E-05	-2.81
	0.2	3.24E-05	3.31E-05	2.19	3.04E-05	-6.25	2.89E-05	-10.75	3.24E-05	0.05
	0.25	3.32E-05	3.31E-05	-0.46	3.09E-05	-6.97	2.98E-05	-10.43	3.27E-05	-1.65
	0.3	3.25E-05	3.30E-05	1.54	3.13E-05	-3.91	3.03E-05	-6.77	3.28E-05	0.73
	0.35	3.27E-05	3.29E-05	0.65	3.15E-05	-3.90	3.07E-05	-6.25	3.27E-05	0.01
	0.4	3.29E-05	3.28E-05	-0.10	3.16E-05	-3.98	3.09E-05	-5.94	3.26E-05	-0.69
	0.45	3.17E-05	3.27E-05	3.11	3.16E-05	-0.38	3.11E-05	-2.12	3.25E-05	2.46
	0.5	3.21E-05	3.26E-05	1.59	3.16E-05	-1.46	3.11E-05	-2.93	3.23E-05	0.84
	μ_ε %		32.63	μ_ε %	-1.049	μ_ε %	-10.45	μ_ε %	-2.51	
	σ_ε %		65.77	σ_ε %	12.29	σ_ε %	7.09	σ_ε %	4.19	
	ε_{\max} %		319.65	ε_{\max} %	45.35	ε_{\max} %	3.74	ε_{\max} %	2.46	
	ε_{\min} %		-1.36	ε_{\min} %	-12.13	ε_{\min} %	-23.32	ε_{\min} %	-18.54	
	$\mu_{ \varepsilon }$ %		32.71	$\mu_{ \varepsilon }$ %	8.94	$\mu_{ \varepsilon }$ %	10.77	$\mu_{ \varepsilon }$ %	2.80	

D.4.7 Kanai-Tajimi and Shinozuka-Sato Time-modulating Function, $T = 1.0s$

Table D.22 - FPDF computed at $t = 20s$ for linear elastic SDOF system with $T = 1.0s$ subjected to KT base excitation time modulated by a Shinozuka-Sato function.

ζ	ξ	ISEE	P	ε [%]	cVM	ε [%]	mVM	ε [%]	New	ε [%]
1.5	0.01	7.62E-01	9.99E-01	31.20	8.54E-01	12.07	7.27E-01	-4.51	6.38E-01	-16.20
	0.02	7.81E-01	9.97E-01	27.65	8.80E-01	12.60	7.84E-01	0.38	7.23E-01	-7.49
	0.05	8.81E-01	9.90E-01	12.41	9.13E-01	3.69	8.58E-01	-2.59	8.56E-01	-2.84
	0.1	9.40E-01	9.86E-01	4.88	9.43E-01	0.29	9.13E-01	-2.87	9.38E-01	-0.22
	0.15	9.60E-01	9.85E-01	2.57	9.58E-01	-0.25	9.39E-01	-2.19	9.66E-01	0.54
	0.2	9.81E-01	9.85E-01	0.43	9.67E-01	-1.42	9.54E-01	-2.74	9.77E-01	-0.34
	0.25	9.62E-01	9.85E-01	2.35	9.72E-01	1.03	9.63E-01	0.04	9.83E-01	2.19
	0.3	9.87E-01	9.85E-01	-0.24	9.76E-01	-1.16	9.69E-01	-1.91	9.87E-01	-0.07
	0.35	1.00E+00	9.85E-01	-1.48	9.79E-01	-2.13	9.73E-01	-2.73	9.89E-01	-1.13
	0.4	9.98E-01	9.85E-01	-1.26	9.81E-01	-1.72	9.76E-01	-2.22	9.90E-01	-0.82
	0.45	9.95E-01	9.85E-01	-0.95	9.82E-01	-1.27	9.78E-01	-1.69	9.90E-01	-0.45
	0.5	1.00E+00	9.85E-01	-1.46	9.83E-01	-1.66	9.80E-01	-2.02	9.91E-01	-0.95
2	0.01	3.94E-01	9.21E-01	133.80	4.96E-01	25.79	3.72E-01	-5.54	3.26E-01	-17.28
	0.02	4.14E-01	8.59E-01	107.56	5.18E-01	25.16	4.15E-01	0.12	3.76E-01	-9.22
	0.05	4.94E-01	7.85E-01	58.96	5.59E-01	13.11	4.85E-01	-1.92	4.85E-01	-1.87
	0.1	6.03E-01	7.57E-01	25.52	6.07E-01	0.59	5.55E-01	-8.05	5.97E-01	-1.04
	0.15	6.53E-01	7.52E-01	15.08	6.39E-01	-2.17	5.99E-01	-8.30	6.60E-01	0.98
	0.2	7.00E-01	7.51E-01	7.25	6.62E-01	-5.54	6.29E-01	-10.16	6.98E-01	-0.41
	0.25	7.22E-01	7.52E-01	4.12	6.78E-01	-6.09	6.51E-01	-9.82	7.21E-01	-0.07
	0.3	7.32E-01	7.52E-01	2.76	6.90E-01	-5.73	6.67E-01	-8.87	7.36E-01	0.60
	0.35	7.56E-01	7.53E-01	-0.39	7.00E-01	-7.46	6.80E-01	-10.10	7.46E-01	-1.36
	0.4	7.59E-01	7.54E-01	-0.71	7.07E-01	-6.84	6.89E-01	-9.16	7.51E-01	-1.07
	0.45	7.55E-01	7.54E-01	-0.17	7.13E-01	-5.58	6.97E-01	-7.66	7.53E-01	-0.26
	0.5	7.64E-01	7.54E-01	-1.25	7.18E-01	-6.00	7.04E-01	-7.86	7.54E-01	-1.30
2.5	0.01	1.45E-01	4.96E-01	242.66	1.86E-01	28.71	1.32E-01	-8.89	1.23E-01	-14.84
	0.02	1.53E-01	4.10E-01	167.17	1.94E-01	26.21	1.48E-01	-3.77	1.41E-01	-7.89
	0.05	1.87E-01	3.39E-01	81.08	2.09E-01	11.80	1.75E-01	-6.28	1.83E-01	-2.23
	0.1	2.31E-01	3.17E-01	36.82	2.31E-01	-0.32	2.06E-01	-11.06	2.32E-01	0.31
	0.15	2.58E-01	3.13E-01	21.21	2.46E-01	-4.49	2.26E-01	-12.17	2.62E-01	1.80
	0.2	2.81E-01	3.12E-01	11.22	2.58E-01	-8.18	2.41E-01	-14.00	2.81E-01	0.29
	0.25	2.89E-01	3.12E-01	8.07	2.66E-01	-7.95	2.52E-01	-12.74	2.93E-01	1.38
	0.3	2.92E-01	3.13E-01	6.94	2.72E-01	-6.85	2.60E-01	-10.94	3.00E-01	2.54
	0.35	3.04E-01	3.13E-01	2.95	2.78E-01	-8.81	2.67E-01	-12.25	3.04E-01	-0.14
	0.4	3.15E-01	3.14E-01	-0.48	2.82E-01	-10.68	2.72E-01	-13.64	3.06E-01	-3.00
	0.45	3.12E-01	3.14E-01	0.64	2.85E-01	-8.72	2.77E-01	-11.40	3.06E-01	-1.85
	0.5	3.15E-01	3.14E-01	-0.16	2.88E-01	-8.67	2.80E-01	-11.07	3.06E-01	-2.84

ζ	ξ	ISEE	P	ε [%]	cVM	ε [%]	mVM	ε [%]	New	ε [%]
3	0.01	4.00E-02	1.37E-01	242.28	4.89E-02	22.37	3.41E-02	-14.59	3.44E-02	-13.94
	0.02	4.15E-02	1.07E-01	158.73	5.02E-02	20.98	3.79E-02	-8.53	3.93E-02	-5.31
	0.05	4.89E-02	8.53E-02	74.40	5.34E-02	9.16	4.47E-02	-8.70	4.95E-02	1.20
	0.1	6.02E-02	7.86E-02	30.57	5.83E-02	-3.21	5.21E-02	-13.57	6.10E-02	1.27
	0.15	6.71E-02	7.75E-02	15.43	6.20E-02	-7.59	5.72E-02	-14.84	6.77E-02	0.91
	0.2	7.00E-02	7.73E-02	10.53	6.47E-02	-7.45	6.08E-02	-13.11	7.16E-02	2.28
	0.25	7.33E-02	7.74E-02	5.57	6.68E-02	-8.97	6.35E-02	-13.48	7.37E-02	0.48
	0.3	7.50E-02	7.76E-02	3.48	6.83E-02	-8.89	6.55E-02	-12.66	7.49E-02	-0.15
	0.35	7.57E-02	7.77E-02	2.69	6.95E-02	-8.18	6.71E-02	-11.41	7.54E-02	-0.35
	0.4	7.58E-02	7.79E-02	2.67	7.05E-02	-7.09	6.83E-02	-9.92	7.56E-02	-0.31
	0.45	7.60E-02	7.80E-02	2.60	7.12E-02	-6.27	6.93E-02	-8.78	7.55E-02	-0.66
0.5	7.82E-02	7.80E-02	-0.14	7.18E-02	-8.07	7.01E-02	-10.26	7.52E-02	-3.79	
3.5	0.01	8.32E-03	2.48E-02	198.02	9.57E-03	14.96	6.70E-03	-19.46	7.07E-03	-15.03
	0.02	8.63E-03	1.92E-02	123.13	9.68E-03	12.27	7.37E-03	-14.54	8.10E-03	-6.05
	0.05	1.00E-02	1.52E-02	51.65	1.01E-02	1.08	8.53E-03	-14.69	9.95E-03	-0.48
	0.1	1.18E-02	1.39E-02	17.90	1.09E-02	-8.08	9.78E-03	-17.15	1.17E-02	-0.90
	0.15	1.24E-02	1.37E-02	10.34	1.15E-02	-7.83	1.06E-02	-14.33	1.26E-02	1.47
	0.2	1.29E-02	1.37E-02	6.32	1.19E-02	-7.64	1.12E-02	-12.61	1.31E-02	1.49
	0.25	1.34E-02	1.37E-02	2.06	1.22E-02	-9.08	1.17E-02	-12.97	1.33E-02	-0.99
	0.3	1.35E-02	1.37E-02	1.75	1.24E-02	-7.76	1.20E-02	-11.00	1.34E-02	-0.66
	0.35	1.37E-02	1.38E-02	0.43	1.26E-02	-7.78	1.23E-02	-10.50	1.34E-02	-1.84
	0.4	1.40E-02	1.38E-02	-1.83	1.28E-02	-8.97	1.25E-02	-11.26	1.34E-02	-4.27
	0.45	1.36E-02	1.38E-02	1.79	1.29E-02	-4.89	1.26E-02	-6.97	1.34E-02	-1.26
0.5	1.36E-02	1.38E-02	1.93	1.30E-02	-4.18	1.27E-02	-6.02	1.33E-02	-1.83	
4	0.01	1.34E-03	3.39E-03	153.24	1.44E-03	7.35	1.02E-03	-24.13	1.08E-03	-18.98
	0.02	1.33E-03	2.63E-03	97.46	1.44E-03	7.83	1.10E-03	-17.05	1.24E-03	-6.55
	0.05	1.51E-03	2.07E-03	37.03	1.47E-03	-2.66	1.25E-03	-16.89	1.50E-03	-0.46
	0.1	1.69E-03	1.90E-03	12.40	1.55E-03	-8.00	1.41E-03	-16.20	1.70E-03	0.46
	0.15	1.77E-03	1.87E-03	5.32	1.62E-03	-8.46	1.52E-03	-14.13	1.78E-03	0.29
	0.2	1.83E-03	1.86E-03	2.10	1.68E-03	-8.25	1.60E-03	-12.48	1.82E-03	-0.54
	0.25	1.86E-03	1.87E-03	0.31	1.71E-03	-7.95	1.65E-03	-11.26	1.83E-03	-1.46
	0.3	1.84E-03	1.87E-03	1.84	1.74E-03	-5.21	1.69E-03	-7.95	1.84E-03	0.28
	0.35	1.86E-03	1.88E-03	0.62	1.76E-03	-5.38	1.72E-03	-7.64	1.84E-03	-1.04
	0.4	1.84E-03	1.88E-03	2.06	1.78E-03	-3.28	1.74E-03	-5.23	1.84E-03	-0.01
	0.45	1.86E-03	1.88E-03	1.24	1.79E-03	-3.48	1.76E-03	-5.15	1.83E-03	-1.46
0.5	1.84E-03	1.88E-03	2.34	1.80E-03	-1.97	1.78E-03	-3.44	1.82E-03	-1.19	

ζ	ξ	ISEE	P	ε [%]	cVM	ε [%]	mVM	ε [%]	New	ε [%]
4.5	0.01	1.62E-04	3.62E-04	123.41	1.67E-04	3.19	1.19E-04	-26.35	1.27E-04	-21.52
	0.02	1.64E-04	2.82E-04	71.83	1.65E-04	0.91	1.29E-04	-21.49	1.45E-04	-11.64
	0.05	1.74E-04	2.21E-04	27.54	1.66E-04	-4.35	1.43E-04	-17.39	1.71E-04	-1.22
	0.1	1.87E-04	2.03E-04	8.36	1.73E-04	-7.71	1.59E-04	-15.10	1.88E-04	0.46
	0.15	1.93E-04	2.00E-04	3.79	1.79E-04	-6.88	1.70E-04	-11.90	1.94E-04	0.79
	0.2	1.95E-04	2.00E-04	2.11	1.84E-04	-5.79	1.77E-04	-9.48	1.97E-04	0.59
	0.25	2.00E-04	2.00E-04	-0.19	1.88E-04	-6.31	1.82E-04	-9.11	1.98E-04	-1.23
	0.3	1.99E-04	2.00E-04	0.63	1.90E-04	-4.45	1.86E-04	-6.70	1.98E-04	-0.35
	0.35	1.96E-04	2.01E-04	2.23	1.92E-04	-2.14	1.88E-04	-4.02	1.98E-04	1.05
	0.4	1.99E-04	2.01E-04	0.99	1.94E-04	-2.74	1.90E-04	-4.30	1.98E-04	-0.57
	0.45	1.97E-04	2.01E-04	1.98	1.95E-04	-1.34	1.92E-04	-2.67	1.97E-04	-0.20
0.5	2.05E-04	2.02E-04	-1.91	1.96E-04	-4.75	1.93E-04	-5.86	1.96E-04	-4.68	
5	0.01	1.53E-05	3.05E-05	99.24	1.52E-05	-0.82	1.09E-05	-28.52	1.16E-05	-24.07
	0.02	1.50E-05	2.37E-05	57.59	1.48E-05	-1.49	1.17E-05	-22.52	1.30E-05	-13.27
	0.05	1.55E-05	1.86E-05	20.01	1.46E-05	-5.85	1.28E-05	-17.79	1.51E-05	-3.07
	0.1	1.63E-05	1.71E-05	5.12	1.50E-05	-7.59	1.40E-05	-14.20	1.62E-05	-0.66
	0.15	1.64E-05	1.68E-05	2.84	1.55E-05	-5.45	1.47E-05	-9.87	1.65E-05	0.82
	0.2	1.64E-05	1.68E-05	2.15	1.58E-05	-3.87	1.53E-05	-7.04	1.66E-05	1.18
	0.25	1.66E-05	1.68E-05	1.25	1.61E-05	-3.36	1.57E-05	-5.75	1.67E-05	0.60
	0.3	1.70E-05	1.69E-05	-1.04	1.62E-05	-4.68	1.59E-05	-6.50	1.68E-05	-1.64
	0.35	1.69E-05	1.69E-05	-0.17	1.64E-05	-3.22	1.61E-05	-4.70	1.68E-05	-0.89
	0.4	1.66E-05	1.69E-05	1.81	1.65E-05	-0.83	1.63E-05	-2.07	1.67E-05	0.80
	0.45	1.68E-05	1.69E-05	0.91	1.66E-05	-1.36	1.64E-05	-2.39	1.67E-05	-0.53
	0.5	1.66E-05	1.70E-05	1.92	1.66E-05	-0.10	1.65E-05	-0.99	1.66E-05	-0.05
		μ_ε %	28.31	μ_ε %	-1.356	μ_ε %	-9.69	μ_ε %	-2.55	
		σ_ε %	53.52	σ_ε %	8.85	σ_ε %	5.94	σ_ε %	5.40	
		ε_{\max} %	242.66	ε_{\max} %	28.71	ε_{\max} %	0.38	ε_{\max} %	2.54	
		ε_{\min} %	-1.91	ε_{\min} %	-10.68	ε_{\min} %	-28.52	ε_{\min} %	-24.07	
		$\mu_{ \varepsilon }$ %	28.59	$\mu_{ \varepsilon }$ %	6.80	$\mu_{ \varepsilon }$ %	9.70	$\mu_{ \varepsilon }$ %	2.97	

D.4.8 Summary of the Time-variant FPDF Obtained Using the New Proposed Hazard Function

Table D.23 - Summary of FPDF obtained using the New Proposed Hazard Function.

PSD	Time Modulation	T_0 (s)	ε [%]	P	cVM	mVM	New
WN	Step	1	ε_{\max} %	176.24	35.26	9.10	3.83
			ε_{\min} %	-0.75	-9.23	-21.38	-8.35
			$\mu_{ \varepsilon }$ %	22.48	6.32	7.70	1.48
	Shinozuka-Sato	1	ε_{\max} %	240.73	28.78	1.55	2.71
			ε_{\min} %	-1.23	-9.32	-27.46	-22.94
			$\mu_{ \varepsilon }$ %	28.39	6.58	8.86	3.17
KT	Step	0.1	ε_{\max} %	129.44	34.90	14.16	15.72
			ε_{\min} %	-2.22	-12.44	-17.46	-14.58
			$\mu_{ \varepsilon }$ %	16.90	7.72	8.85	4.09
		0.5	ε_{\max} %	187.19	27.68	1.27	17.49
			ε_{\min} %	-1.90	-11.98	-27.35	-13.39
			$\mu_{ \varepsilon }$ %	24.25	7.09	11.92	3.22
		1	ε_{\max} %	179.36	35.31	8.67	4.31
			ε_{\min} %	-1.19	-9.89	-22.13	-6.41
			$\mu_{ \varepsilon }$ %	22.60	6.71	8.48	1.32
	Shinozuka-Sato	0.1	ε_{\max} %	226.13	75.81	36.07	12.71
			ε_{\min} %	-2.72	-13.13	-19.60	-31.43
			$\mu_{ \varepsilon }$ %	15.81	8.58	8.85	4.67
		0.5	ε_{\max} %	319.65	45.35	3.74	2.46
			ε_{\min} %	-1.36	-12.13	-23.32	-18.54
			$\mu_{ \varepsilon }$ %	32.71	8.94	10.77	2.80
		1	ε_{\max} %	242.66	28.71	0.38	2.54
			ε_{\min} %	-1.91	-10.68	-28.52	-24.07
			$\mu_{ \varepsilon }$ %	28.59	6.80	9.70	2.97

APPENDIX E : INPUT PSD FUNCTIONS OF SHEAR-TYPE BUILDINGS

The input PSD functions in correspondence with the circular frequency, to be used in the stochastic dynamic analysis, of the shear-type buildings are presented in this appendix. As it is discussed in Chapter 3, the shear-type buildings are subjected to KT-CP PSD function as the input PSD of the nonstationary processes.

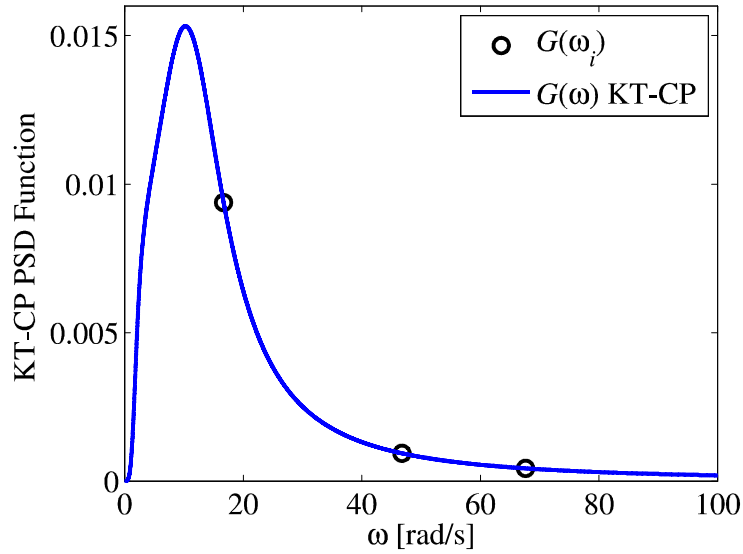


Figure E.1-Input PSD function for the three-story building.

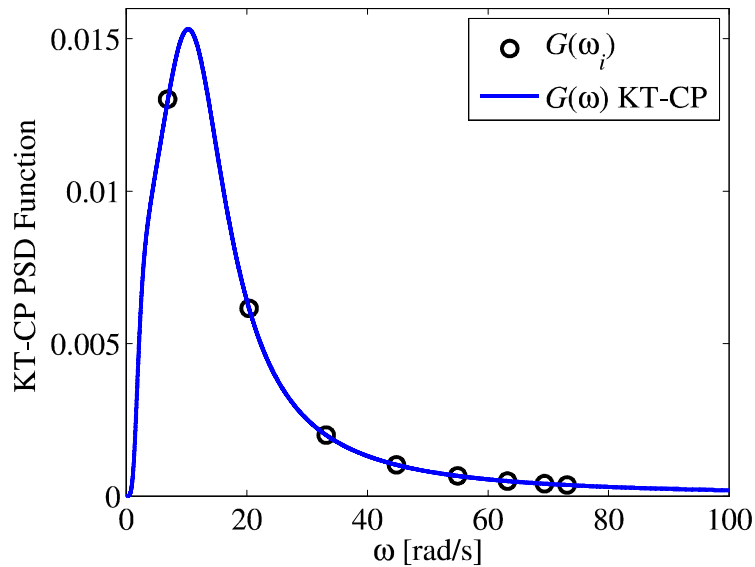


Figure E.2- Input PSD function for the eight-story building.

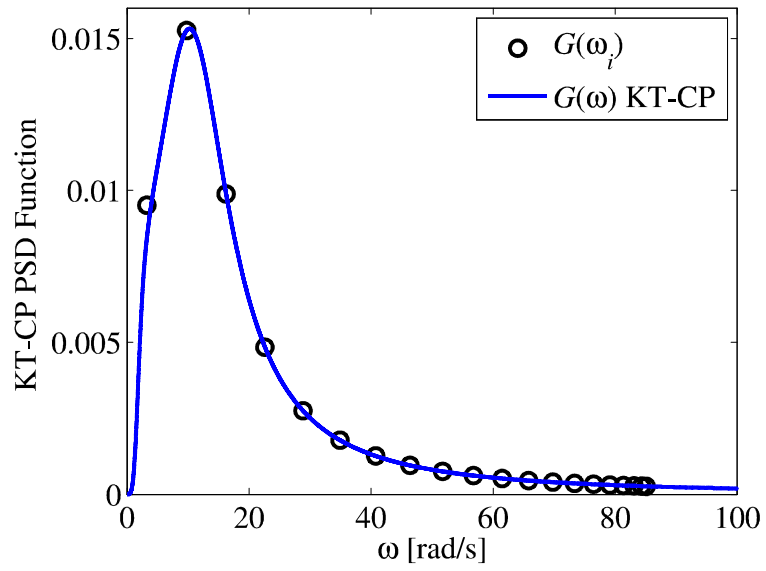


Figure E.3- Input PSD function for the 20-story building.

VITA

Sara Ghazizadeh was born in September 1985 in Shiraz, Iran. She received her secondary and high school education from NODET (National Organization for Development of Exceptional Talents) in Shiraz, Iran. Sara graduated with her bachelor's degree from Shiraz University in civil engineering. After her graduation, she worked in a petrochemical and road design company before she moved to the United States for continuing her education. She got admitted for the master's program in structural engineering in the Department of Civil and Environmental Engineering at Louisiana State University in August 2009. She has been working as a graduate research assistant under the supervision of Dr. Barbato and is a candidate for degree of Master of Science in Civil Engineering to be awarded in December 2011. Her main areas of interests are random vibrations and earthquake engineering.